Open String Field Theory, Unstable D-branes and Open-Closed Duality

Davide Gaiotto Silvano Achille

A Dissertation

Presented to the Faculty

of Princeton University

in Candidacy for the Degree

of Doctor of Philosophy

Recommended for Acceptance

by the Department of

Physics

June, 2004

Abstract

In this thesis we explore different aspects of unstable D-brane dynamics and open-closed dualities. The first chapters focus on the properties of the so-called "tachyon vacuum" for unstable D-branes, that is conjectured to describe the complete decay of the D-brane, using the tool of Open String Field Theory. The first chapter discusses a numerical analysis of this vacuum state, the second discusses and motivates a conjecture on the structure of String Field Theory around the vacuum state and the third presents in more detail some important analytic tools that appeared in chapter two.

We shift the focus in chapter four to a time-dependent version of the tachyon decay process and to the duality between some configurations of D-branes in the imaginary time direction and some purely closed wave-like backgrounds. Similar ideas have an application in noncritical string theories in the context of the identification of D-branes as the basic degrees of freedom of the theory. In chapter five we discuss one particular aspect of this identification in the context of the $(2,1)$ noncritical string ($2d$ topological gravity): we reduce Open String Field Theory on the stable D-branes of the $(2,1)$ model to the Kontsevich matrix integral, that is known to encode the whole closed string theory for the $(2,1)$ model.

Acknowledgements

I would like to thank my advisor, Leonardo Rastelli, whose guidance made this thesis possible. Through the years I spent in Princeton his enthusiasm and patience have been unwavering and extremely invaluable.

I want to thank all my collaborators. Chapters 2 and 6 are the result of collaboration with Leonardo Rastelli. Chapter 3 and 4 are the result of collaboration with Leonardo Rastelli, Ashoke Sen and Barton Zwiebach. Chapter 5 is the result of collaboration with Nissan Itzhaki and Leonardo Rastelli. I want to thank Nissan Itzhaki for invaluable discussions both on string theory and on academic life. I'm also grateful to professor Enrico Arbarello for starting me on the path that brought me to the field of String Theory and to Princeton University.

These years would not have been the same for me without the the focus and intensity of Princeton Shotokan Karate club practices, and the fun and good eating afterwards.

I want to thank Adriana for greatly enriching my life and for the love and support that she gave me in these years. I also need to thank her for the help and patience she offered during the final days of work on this thesis.

Last, I want to thank my family for their unconditional love, for the thousands of times they encouraged me to try harder and learn more, for giving me every tool I needed to become the person I am. I want to thank my mother for teaching me the beauty of arithmetics many years ago, and my father for transmitting me the love for science.

The research in this thesis was supported in part by the National Science Foundation Grant No. PHY-0243680. Any opinions, findings, and conclusions or recommendations

expressed in this material are those of the authors and do not necessarily reflect the views of the National Science Foundation.

Contents

List of Figures

List of Tables

Chapter 1

Introduction and Summary

1.1 Closed string theory and D-branes

The most ambitious dream of physics is to formulate a complete and self-consistent set of basic laws able to describe our universe. String theory is one strong candidate for this role: it appears to be self-contained, to include quantum gravity and interesting low energy field theories, its scope is wide enough to describe not just one, but many different universes. This power becomes even a problem for a seeker of the ultimate laws of the universe: String Theory does not seem to offer many a-priori reasons for our universe to be as it is and not different.

This flexibility makes String Theory a powerful tool to explore and understand several other physical theories, even to produce powerful mathematical statements. If some day String Theory will prove itself unable to offer a proper description of our universe, that would not affect its ability to give powerful and lasting insights on abstract problems. Since it was discovered that it contains a self-consistent theory of quantum gravity, String Theory has radically changed a physicist's perspective on topics like black holes, gauge theories, geometry, topology...

Many of these important advances have become possible after the discovery of a powerful tool to explore non-perturbative string physics: D-branes. D-branes are solitonic objects

that enjoy a very simple description at the level of the perturbative expansion of string theory but at the same time represent non-perturbative degrees of freedom of the theory.

D-branes have two properties (almost) immediately visible from their definition: first, inthe presence of a D-brane the closed string equations of motion acquire a source and second, a new set of degrees of freedom (open strings) is associated with each pair of D-branes and encodes their dynamics. The first property is evident when one evaluates closed string scattering amplitudes: the presence of the D-branes affects the propagation of the closed strings as an added source would do.

A simple physical reasoning then assures that D-branes have to be dynamical objects: closed string theory includes gravity, and a source for the gravitational fields has to obey certain equations of motion, i.e. the conservation of the energy momentum tensor. A D-brane sources the gravitational field and has a certain mass, so it will have to behave properly during physical processes: for example it will have to recoil appropriately during a scattering process, to conserve energy and momentum.

This agrees with the presence of "open strings" degrees of freedom. The recoil of a D-brane will be represented by the emission of a very low energy open string mode associated with the D-brane displacement. Much harder to understand physically is the fact that there is an open string sector associated not to each D-brane, but to each pair of them, so that the "displacements" of a group of N D-branes will be parameterized by $N \times N$ matrix-valued coordinates.

Loosely speaking, D-brane usually appears as a submanifold in space-time on which open string endpoints are attached. The degrees of freedom on such a D-brane are organized, in a low energy limit, into an appropriate quantum field theory living on the D-brane worldsheet, often a gauge theory coupled with some scalars and fermions and endowed with appropriate supersymmetry and possibly non-commutativity.

There is strong link between the degrees of freedom of the D-branes and the properties of the closed string backgrounds sourced by them. In fact, one of the first, surprising, applications of D-branes was to evaluate the entropy of a black hole by counting the degrees

of freedom of a system of D-branes that placed in flat space would source the black hole background.

This link allows, in appropriate limits, to formulate many different dualities, whose prototype is AdS/CFT: an appropriate scaling reduces the degrees of freedom of certain D-branes (N D3-branes in IIB superstring theory) to $\mathcal{N} = 4$ supersymmetric $SU(N)$ Yang-Mills theory; the same scaling turns out to be a near horizon limit of the supergravity background sourced by the D-branes, that is $AdS_5 \times S_5$ with radius $\equiv g_{YM}^2 N$. As the scaling focuses on the part of space-time "due" to the presence of the D-branes it is possible to conjecture that type IIB superstring on $AdS_5 \times S_5$ and $N = 4$ SYM in four dimensions, while apparently very different physical theories, are actually equivalent. [1, 2, 3]

1.2 The string perturbative expansion

String theory is defined perturbatively, and D-branes give access to nonperturbative information. While D-branes are non-perturbative objects in closed string theory, for very small string coupling constant g_s they admit a simple description in perturbation theory as extra "objects" inserted in the closed string theory. As g_s increases they would become lighter and more dynamical, on the same footing as strings.

In closed string theory amplitudes are evaluated through a perturbative sum over closed Riemann surfaces of various topology. [4, 5] The genus of these surfaces corresponds to the number of closed string loops: a diagram associated with a sphere is a tree level contribution, a torus diagram corresponds to 1-loop contributions, etc. A surface of genus g is weighted with a power g_s^{2g-2} of the string coupling.

In presence of one or more D-branes this sum is extended to Riemann surfaces with boundaries, with a choice of boundary conditions for the worldsheet fields at each boundary. Different D-branes corresponds to different boundary conditions. Each boundary added to the surface is weighted with another factor of g_s.

A typical tree level scattering of closed strings from a D-brane corresponds to a disk topology. The diagram can be interpreted as an exchange of a closed string intermediate

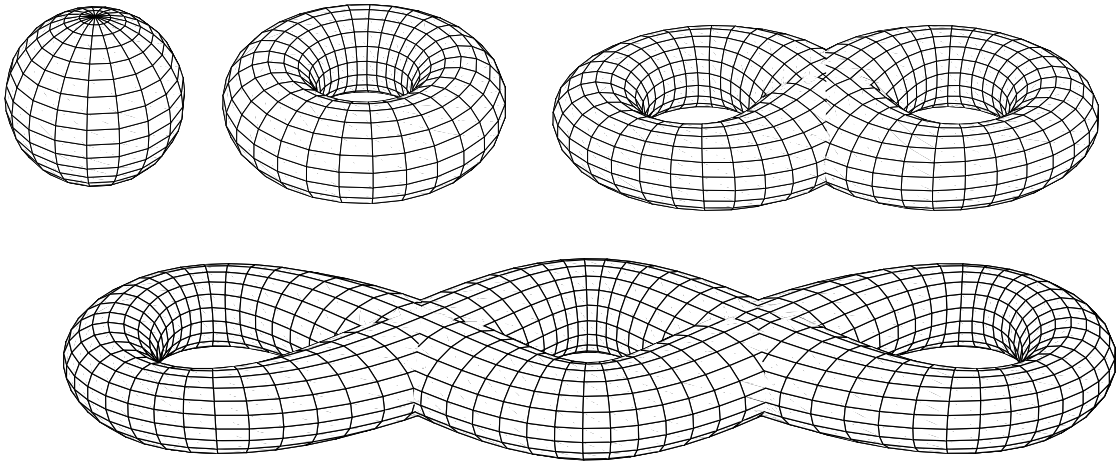

Figure 1.1: Examples of closed Riemann surfaces of genus 0,1,2,3

state between the scattering string and the D-brane, that acts as a fixed source. (see Figure (1.2)) The worldsheet amplitude can in fact be decomposed as a sum over infinitely many field-theoretical Feymann diagrams exchanging different closed string states. The coupling between these states and the D-brane is determined by the boundary condition associated with the D-brane, and the intensity of these sources will be of order g_s, the weight of the disk with respect to the sphere.

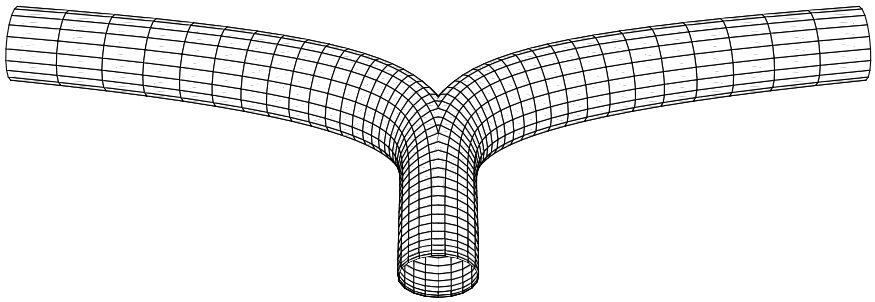

Figure 1.2: "Space time" view of a closed string scattering from a D-brane in t-channel. Time flows to the left.

Diagrams with many boundaries can be similarly related to multiple interactions with the source: the global effect will be as if the D-branes were changing the closed string background, sourcing all the closed string fields with intensity scaling as g_s. In particular

they will source the gravitational field as masses of order $1/g_s$, an indication of the fact that they are non-perturbative objects in the closed string theory.

All of this is already evident in the the disk amplitude that describes scattering of a tachyon from a $D0$ brane at the origin (here the kinematic variables are as usual $s = -4E^2$ and $t = (P_{in} - P_{out})^2$ in appropriate units) :

$$A(P_{in}, P_{out}) \sim \frac{\Gamma(t/4-1)\Gamma(s-1)}{2\,\Gamma(t/4+s-2)} = \sum \frac{c_k(s)}{t/4+k-1} \tag{1.2.1}$$

$$c_k(s) = \prod_{i=1}^{k}(1+\frac{1-s}{i}) \tag{1.2.2}$$

The expansion of the amplitude makes evident the exchange of closed string modes of mass $4k-4$ and spin up to $2k$ between the scattering tachyon and the D-brane. Nevertheless it obscures a very important piece of physics: there are extra s-channel poles in the amplitude, not due to closed string intermediate states, but to other excitations with masses going like $k-1$ and spin up to k:

$$A(P_{in}, P_{out}) \sim \frac{\Gamma(t/4-1)\Gamma(s-1)}{2\,\Gamma(t/4+s-2)} = \sum \frac{d_k(t)}{s+k-1} \tag{1.2.3}$$

$$d_k(s) = \prod_{i=1}^{k}(1+\frac{1-t/4}{i}) \tag{1.2.4}$$

This different expansion singles out string states whose propagation is not described by a cylinder, but a strip: open strings. (see figure (1.3))

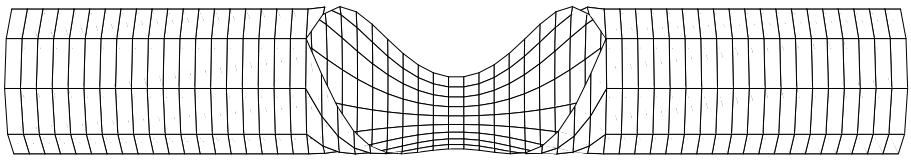

Figure 1.3: "Space time" view of a closed string scattering from a D-brane in s-channel. Time flows to the left.

Open strings arise as these extra poles in closed string amplitudes, and they have an important property: on-shell open strings living on a D-brane are in precise correspondence with all the possible infinitesimal deformations of the boundary condition that defines the

D-brane itself. Open strings attached to two different D-branes correspond to deformations that mix different boundary conditions.

This connection allows one to view the poles and infrared singularities associated to exchange of open strings as appropriate manifestations of the dynamics of the D-brane itself, as required for a consistent coupling to gravity and to the other closed string modes.

1.3 String Field Theories

In the previous sections we used a powerful concept: worldsheet amplitudes may be understood better by cutting the worldsheet along cylinders and strips and reducing amplitudes to sums over field theoretical Feymann diagrams. This can be formalized through the structure of string field theory, that is a field theory of infinite degrees of freedom whose perturbative expansion in terms of Feymann diagrams correctly reproduces the amplitudes from the worldsheet expansion.

The basic principle underlying string field theory is that a cylindrical tube in a Riemann surface can be cut, and the two resulting holes filled by two disks with an insertion of a complete set of intermediate states $\sum |\bar{i}\rangle\langle i|$, summed over all the closed string Hilbert space. The moduli of length and twist of the cylinder may then be reabsorbed into a factor of $b_0\bar{b}_0 e^{-(l+i\theta)L_0-(l-i\theta)\bar{L}_0}$ in the middle of the sum of states. The integral over the moduli of length and twist of the cylinder may then be readily executed to yield a field theoretical propagator.

$$\int dld\theta e^{-(l+i\theta)L_0-(l-i\theta)\bar{L}_0} = \frac{\delta(L_0-\bar{L}_0)}{L_0+\bar{L}_0} \tag{1.3.5}$$

By cutting the right cylinders the surface gets chopped down to a Feymann diagram with vertexes corresponding to the joining of the cylinders. By integrating on lengths and twists of the cylinders we cover a certain patch of the moduli space for that Riemann surface.

If an appropriate decomposition of the moduli space of Riemann surfaces in similar patches is available, such that each patch corresponds to a different Feymann diagram, then the sum over all Feymann diagrams is equivalent to an integral over the whole the

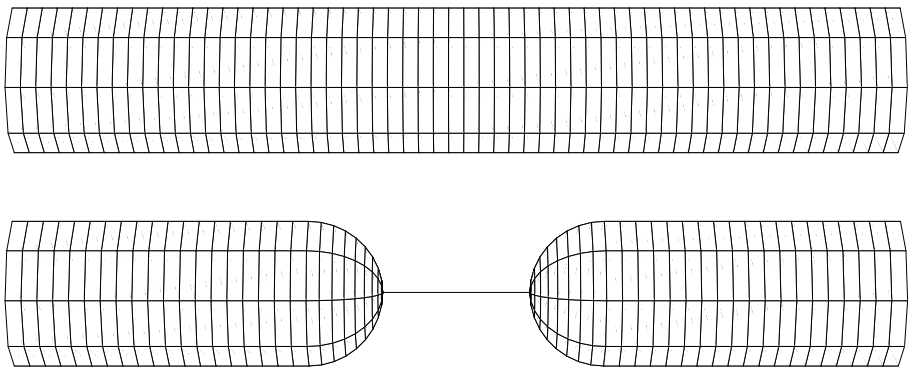

Figure 1.4: a cylinder in a surface may be cut and replaced with a pair of punctures, summed over all possible intermediate states

moduli space. The problem of evaluating amplitudes over Riemann surfaces of various genus and integrating them appropriately over the moduli space is transformed into the evaluation of th perturbative expansion of a "string field theory" involving a field for each intermediate state propagating in the cylinders.

It is actually possible to find such a decomposition, thanks to a beautiful mathematical result. Unfortunately the decomposition for closed string field theory is complicated, as it requires vertexes of all possible orders in the action to build all the relevant Feymann diagrams. Closed string field theory is non-polynomial.

On the other hand a similar reasoning can be applied to Riemann surfaces with at least a boundary [6] and then the story changes dramatically: a very simple decomposition is possible that involves only open string intermediate states and trivalent vertexes. Joining strips is easier than joining cylinders! This procedure works even in presence of external closed string insertions: it is still enough to cut along strips and use open string intermediate states, coupled appropriately with the closed string insertions. This construction is at the hearth of cubic Open String Field Theory, and is one of the main tools used in this thesis.

The OSFT action has a deceptively simple form:

$$\frac{1}{2}\langle\Psi, Q_B\Psi\rangle + \frac{1}{3}\langle\Psi,\Psi,\Psi\rangle \tag{1.3.6}$$

Here Ψ is the string field, a ghost number one element of the Hilbert space of states of

the Boundary CFT (BCFT) associated with the D-brane. Q_B is the usual nilpotent BRST charge associated with fixing the conformal gauge:

$$Q_B = \oint dz \left[c(z) T^m(z) + \frac{1}{2} : b(z) c(z) \partial c(z) : \right] \tag{1.3.7}$$

On-shell open degrees of freedom are defined as the cohomology of Q_B. The two vertex $(,)$ is just the usual BPZ pairing of states, that evaluate the amplitude by putting them at the two ends of a strip. The trilinear vertex $(,,)$ is defined by putting the three arguments at the ends of three half strips glued together as shown in figure ((1.5)))(for a detailed description of the vertexes see for example [12])

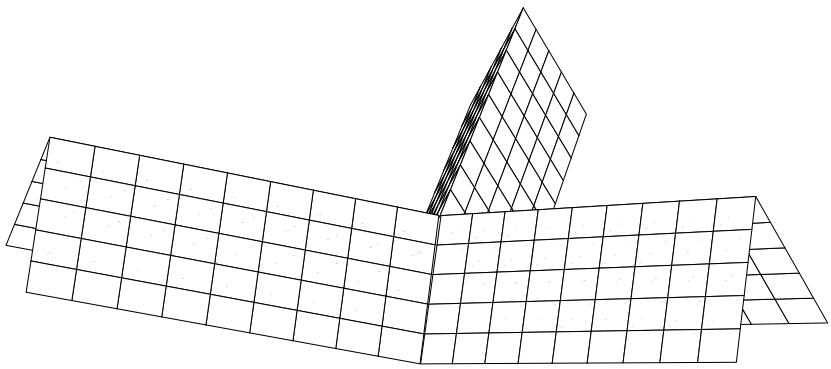

Figure 1.5: How to glue the three half strips to define the OSFT triple product

The equations of motion following from the action (1.3.6) are simply

$$Q_B \Psi + \Psi * \Psi = 0 \tag{1.3.8}$$

The $*$ product is associative and Q_B is a derivation for it. As a consequence the OSFT action has a wide gauge symmetry

$$\delta \Psi = Q_B \Lambda + \Psi * \Lambda - \Lambda * \Psi \tag{1.3.9}$$

The infinitesimal form of the equations of motion and of the gauge symmetry show clearly that infinitesimal solutions are just on-shell open string states. (i.e. BRST cohomology at ghost nr. one) Finite solutions will represent finite deformations of the original D-brane.

A simple way to verify that the perturbative expansion for the action (1.3.6) does reproduce amplitudes for the BCFT on Riemann surfaces of various genus and number of holes is to gauge fix it with the Siegel gauge condition:

$$b_0\Psi = 0 \tag{1.3.10}$$

This gauge fixings requires the introduction of an infinite tower of ghosts and anti-ghosts, but surprisingly they can be repackaged together in a larger string field Ψ by relaxing the ghost number one condition. The action remains the same. The propagator becomes $\frac{b_0}{L_0}$ and can be rewritten as

$$\int_0^\infty e^{-tL_0} b_0 dt \tag{1.3.11}$$

This corresponds in the BCFT to the propagation along a strip of width π and length t. The strips are glued together at appropriate trivalent vertexes and the amplitude is summed over all possible BCFT intermediate states in each strips. The result reproduces by definition the worldsheet amplitude over the Riemann surfaces built by the gluing process.

The measure $b_0 dt$ is the correct one to integrate on the patch of the moduli space for the Riemann surface that is parametrized by the lengths of the propagators. It can be proved that the patches associated to all possible trivalent ribboned Feymann graphs cover the whole moduli space properly.

This works even if there are many D-branes: the string field is replaced with the matrix Ψ^i_j of string fields living in the Hilbert space of open strings between D-brane i and D-brane j. All the products include matrix multiplication.

A less trivial extension allows OSFT to deal with amplitudes that include closed string punctures as well (and at least one boundary). Each closed string puncture is accounted for by a special open-closed vertex $\langle C||\Psi\rangle$: closed strings are attached to the Feymann diagram as sources for the open string field. (see figure for the graphical representation of the open-closed vertex).

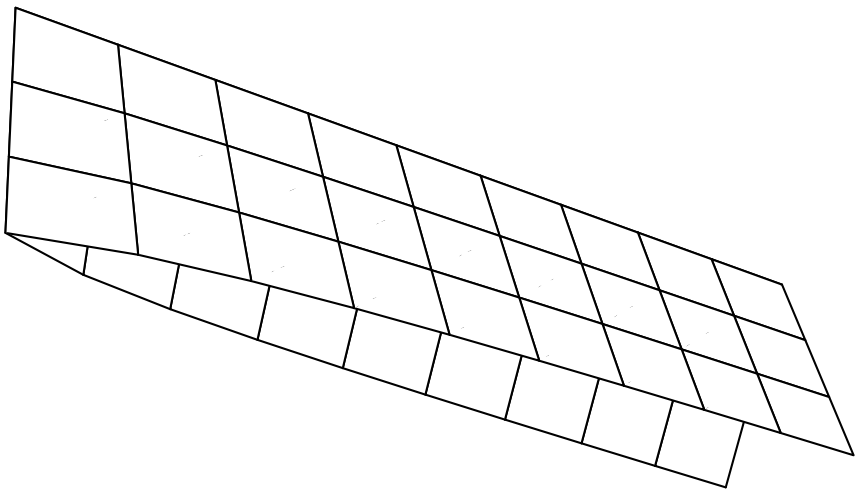

Figure 1.6: The open closed vertex: glue the open string state at the end of the strip, place the on-shell closed string vertex operator at the tip of the cone

This extension allows OSFT to compute the whole correction to closed string amplitudes due to the presence of the D-branes. The only thing that it cannot calculate is the original purely closed (no boundaries) amplitude.

It is very interesting, and almost baffling, that all the information about scattering of closed strings from a D-branes can be evaluated through a purely open string theory, living on the D-brane itself. It is probable that this is one of the facts that makes open-closed duality possible.

1.4 Open-closed duality

Any closed string amplitude that includes at least an interaction with a D-brane can be reproduced by open string field theory. The way such closed string amplitudes are evaluated is quite peculiar: internal cylinders that correspond to closed string exchanges are realized as loops of open string degrees of freedom.

A diagram that looks like a sphere with some boundaries and closed string interactions will be mapped into a loop planar diagram on open string field theory. Handles will result from non-planarity. This correspondence works exactly the same way as the t'Hooft ex-

pansion works for large N Yang Mills theories and is at the hearth of open-closed duality. [7]

The perturbative expansion for closed string theory in presence of N D-branes of the same kind can be written a bit formally as

$$F_{cl}(g_s, N) = F_{cl}(g_s, 0) + \sum_{g=0}^{\infty}\sum_{b=1}^{\infty} F_{g,b} g_s^{2g-2} (g_s N)^b \qquad F_{cl}(g_s, 0) = \sum_{g=0}^{\infty} F_g^{cl} g_s^{2g-2} \tag{1.4.12}$$

Here $F_{g,b}$ are evaluated from the open string field theory. Following t'Hooft intuition we can recollect the sum as

$$F_{cl}(g_s, N) = \sum_{g=0}^{\infty} (F_g^{cl} + \delta F_g^{cl}) g_s^{2g-2} \tag{1.4.13}$$

The coefficients $(F_g^{cl} + \delta F_g^{cl})$ should then describe closed string theory on a shifted background, with a shift proportional to $g_s N$

This shift will be quite peculiar, as it will usually involves all closed string field modes, but at least its properties will be available through calculations done in the unshifted background.

As long as we want to keep the perturbative expansion valid and g_s small we will normally need to place many D-branes (of order $1/g_s$) to deform the closed string background at the order 1. The open degrees of freedom living on N D-branes are organized in $N \times N$ matrices, so the open string theory will be the theory of some set of large(but finite) $N \times N$ matrix valued fields.

Appropriate limits allow one to extract many useful information. Typically one seeks a closed string configuration such that the dynamics of the D-branes can be captured by a relatively small amount of degrees of freedom, whose properties are understood. If the closed string theory in this background is trivial or simple then this open degrees of freedom will capture all the nontrivial dynamics of the deformed, possibly complicated closed string theory.

Until now, only some of the known open-closed dualities have been understood fully at the level of the worldsheet, either in the environment of solvable noncritical string theories

or in topological string theories, in which the degrees of freedom of D-branes are necessarily few. Still it does not appear impossible to work out a similar understanding of more complex dualities, as AdS/CFT.

There is also an interesting inverse question: why should some shift in closed string backgrounds admit a realization as boundaries added to the worldsheet? In certain topological cases an understanding has been developed that relates these boundaries to the appearance of a new phase in the worldsheet theory: fluctuating phase boundaries can be expressed as boundaries with fixed boundary conditions. The general story is still unknown.

One possible avenue to understand the relation of D-branes and closed string configurations is to study the processes that can create or destroy a D-brane dynamically. For example certain D-branes or configurations of D-branes are unstable and may decay to different D-branes or just to closed strings. This instability is related to the presence of a tachyonic open string mode, and the final configuration of the "classical" decay is presumably described by a nontrivial vacuum configuration of this tachyon field.

1.5 Tachyon vacuum

Open string tachyons appear often on D-branes that are not protected against decay by some conserved charges, or between D-branes that can annihilate between themselves, or recombine to diminish the total energy of the system.

The case we are most interested in is a pair of D-brane and anti D-brane close enough or, even simpler, a D-brane in bosonic string theory. It is natural to expect that the decay of these D-brane configurations might be described by the dynamics of this open string tachyon, but how should we interpret the endpoint of the tachyon condensation? There are some ways to compute an effective potential for the tachyon field on an unstable D-brane: besides the maximum of the potential at the starting configuration of the brane, this potential has usually also one minimum. The energy of this minimum appears to exactly offset the tension of the D-brane, so this field configuration seems paradoxically to describe the absence of the D-brane. [8, 13, 9] Might some sort of open string theory survive in this

situation and, maybe, know something about the closed string vacuum?

Open string field theory is a natural tool to address these questions. OSFT classical equations of motion are quadratic relations on a "string field", that is a ghost number one element of the full Hilbert space of open string modes. The equation is written with the help of the nilpotent Q_B BRST operator and of a special associative product, Witten's star product.

$$Q_B\Psi + \Psi * \Psi = 0 \tag{1.5.14}$$

The linearized version of this equation is just the condition $Q_B\Psi = 0$, that we recognize as the on-shell condition for open string fluctuations. The space of classical solutions of this equation spans all possible finite deformations of the original D-brane. An on-shell open string state represent an infinitesimal deformation, that often can be completed to a full finite deformation. Besides these solutions that are continuously connected to zero there might be other ones that represent a more drastic change in the D-brane. A nontrivial minimum for the tachyon effective potential manifest itself in OSFT as one of these nontrivial solutions.

Given a classical solution of the equations of motion there is a straightforward way to evaluate the properties of the corresponding D-brane configuration: a shift of Ψ by the solution Ψ_0 makes the equations of motion into

$$Q'\Psi + \Psi * \Psi = 0 \qquad Q'\Psi = Q_B\Psi + \Psi_0 * \Psi + \Psi * \Psi_0 \tag{1.5.15}$$

Q' is still nilpotent and the equations look formally the same. In fact for solutions that are infinitesimally connected to zero is possible to act with a field redefinition that rewrites these equations as the equations of motion for the deformed D-brane.

The same way the solution corresponding to the tachyon vacuum would ideally allow to study all the properties of the D-brane and of the open string theory living on it after the decay. It would even be possible to understand the scattering of closed strings from it, to understand what are the remnants of the D-brane after the decay.

Unfortunately the OFST equations are complicated and no analytic solution has been found for them. Nevertheless they are amenable of numerical analysis through the "level

truncation" scheme. Chapter one of this thesis will cover some of the efforts to set up such a reliable numerical scheme to verify the presence of a true tachyon vacuum and study it's properties.

Even though an analytic study of the original OSFT equations has not been possible yet, solid conjectures have been made about the form Open String Field Theory might assume around the tachyon vacuum. These conjectures basically amount to proper choices for a simple Q' with the right properties. This is assumed to come from the original Q' around the tachyon vacuum through a singular field redefinition. This vacuum string field theory is amenable of analytic treatment. We review in Chapter two how such a description might arise and what should be able to tell us about open-closed duality.

Vacuum String Field Theory assumes a simplified form for Q' around the tachyon vacuum, but still has to handle the intricacies of Witten's star product. Basic analytic tools for this purpose are a family of projectors for the star product, states such that

$$P * A * P = c(A)P \tag{1.5.16}$$

for any string field A and a normalization constant $c(A)$. These states are described in detail in Chapter three.

1.6 Time-dependent D-brane decay

As the endpoint of the decay process is so hard to study it may come as a surprise that the time-dependent process of tachyon decay seems to be amenable of a simpler analysis.

A key fact is that the functional profile of a decaying tachyon, $\lambda \cosh(X^0)$ may be analytically continued to $\lambda \cos(X^1)$. This euclidean tachyon profile happens to be one of the very few examples of a nontrivial infinitesimal deformation of a D-brane that can be exponentiated to a finite deformation in a controllable way.

In fact it turns out that the $\cos(X)$ deformation continuously interpolates between a D-brane extended in the X direction (Neumann condition on X) and an array of localized D-branes at a certain critical distance from each other (Dirichlet condition on X).

This description ideally allows one to compute both the closed string fields sourced by the deformed D-branes and to probe it by string scattering. If a careful analytic continuation of X back to time-like is possible, this will describe the process of tachyon decay in detail, at least classically. In fact it is possble to see the decay of the D-brane as well as the production of closed string radiation with interesting properties.

Analytic continuation of the deformed D-brane at an intermediate step between Neumann and Dirichlet will lead to a configuration in which massive closed string radiation comes together to form a D-brane, that decays again after a certain time. The lifetime goes to zero as the interpolation parameter moves towards the Dirichlet array configuration.

Thus the analytic continuation of the array of D-branes in imaginary time direction yields a background purely consisting of a closed string wave (the D-brane never appears). This equivalence seems to be an interesting sort of open-closed duality and is the main topic of chapter four of this thesis.

1.7 Noncritical string theory and D-branes

One surprising application of the description of the closed string radiation from D-brane decay was the identification of D-branes as the basic degrees of freedom in a wide range of solvable string models. The first example was noncritical string in $c = 1$, that admits a description as double scaling limit of matrix quantum mechanics.

The idea beyond double scaling limit is that the t'Hooft expansion of a matrix model will usually have a finite radius of convergence in the t'Hooft parameter $t = g_s N$ so that the free energy will have a critical behavior.

$$\int dM e^{-\frac{1}{g_s}W(M)} = \exp\left(\sum_g g_s^{2g-2}\mathcal{F}_g(t = g_s N)\right) \qquad \mathcal{F}_g(t) \sim (t - t_c)^{(2-2g)\alpha} \qquad (1.7.17)$$

These non-analytic pieces in the free energy are universal and independent from details of the matrix model itself, and can be recollected in a new expansion in terms of an expansion parameter $\mu = (t - t_c)^\alpha / g_s$. By sending g_s to zero and keeping μ finite one reaches a continuum limit. This limit is traditionally understood as a way to focus on Feymann

diagrams with infinitely many vertexes, that build up a Riemann surface in the continuous limit.

This idea motivates the relation between noncritical string theories (i.e. gravity on the worldsheet coupled to minimal matter theories) and these double scaled matrix models.

On the other hand there is evidence that even without the double scaling limit, the finite N, finite g_s matrix model should describe the dynamics of some D-branes in a topological string setting, so that again the free energy of the matrix model would be the difference of two closed topological string free energies, the one living in the geometry deformed by the D-branes and the one living in the un-deformed one.

In that case the double scaling limit focuses on a particular spot of the deformed geometry at which a singularity occurs as $t \to t_c$ and on the universal geometry around that spot. Details of the original geometry are washed away and one is left with an open-closed duality.

In the $c = 1$ model the closed string theory describes the collective excitations of a Fermi sea built out of the eigenvalues of the matrix. Ripples on the Fermi sea describe closed string excitations, and the closed string radiation produced by an unstable D-brane in the model turned out to be due to a single eigenvalue raised from the Fermi sea. Soon it was realized that D-branes were closely related to the eigenvalues that make up the Fermi sea, so that the whole closed string dynamics may be reformulated in terms of D-brane dynamics. [150]

In a similar way in the topological gravity setting it was shown that the dynamics of a certain class of closed string backgrounds could be more easily understood and solved in terms of D-branes that could source those background.[172]

In order to understand better the open-closed duality on the worldsheet we need a situation in which the theory is well under control. In minimal strings there is a statement known for a long time that has the look of a precise open-closed duality. The partition function for the $(2, n)$ models is a function of an infinite set of closed string deformations t_n and is the tau function for the famous KdV infinite hierarchy of differential equations.

It satisfies an interesting formula (see [180, 181] for a review):

$$\tau\left(t_k + \sum_i^N \frac{g_s}{2k+1} z_i^{-2k-1}\right) = \tau(t_k) \frac{\det[w_i(z_j, t_k)]}{\det[z_j^i]} \tag{1.7.18}$$

The last expression is readily identified in the matrix model as a partition function that includes boundaries on the putative worldsheet: after the double scaling limit it should correspond to the partition function in the presence of N D-branes (so called FZZT branes for the Liouville theory[158, 159]) parametrized by the z_i.

The formula may be rewritten in an even more tantalizing way for the $(2,1)$ minimal model, as the Kontsevich integral ($Z = diag(z_i)$)[160]:

$$\mathcal{Z}\left(g_s, t_k = \sum_i^N \frac{g_s}{2k+1} z_i^{-2k-1}\right) \quad = \quad \rho(Z)^{-1} \int [dX]\, e^{\frac{1}{g_s}\mathrm{Tr}\left[-\frac{1}{2}ZX^2 + \frac{1}{6}X^3\right]}, \tag{1.7.19}$$

The formula is formally similar to a OSFT partition function, and the derivation makes use of the same decomposition of moduli space that is vital for the construction of OSFT. Of course there is a big difference as well: X is a matrix and not a matrix valued string field.

In chapter five of this thesis we will give flesh to this correspondence and show how Open String Field Theory may reduce to a matrix model through topological localization.

Chapter 2

Open String Field Theory and Tachyon condensation

2.1 Introduction and Summary

The realization that solitonic configurations of the open string tachyon [8, 9] may represent lower dimensional branes has triggered a revival of interest in open string field theory. Classical solutions of OSFT should describe in detain such solitonic lumps in the tachyon field, and thus offer insight on the nonperturbative physics of D-branes. As reviewed in the introduction, OSFT around the tachionic vacuum condensate also promises an alternative definition of closed string amplitudes through a purely open construction, so an understanding of this solution is potentially very interesting. Much work has focused on the search of an analytic form for these classical solutions of cubic bosonic open string field theory [6] (OSFT). Despite important technical progress in the understanding of the open string star product, analytic and well defined classical solutions of OSFT are still missing.

On the other hand the OSFT equations of motion can be solved *numerically* in the 'level-truncation' scheme invented by Kostelecky and Samuel [10]. The infinite tower of fields hidden in the open string field is truncated to modes with an L_0 eigenvalue smaller than a prescribed maximum 'level' L. For any finite L the truncated OSFT action can be

evaluated and numerical computations are possible. Remarkably, numerical results [10]-[11] for various classical solutions appear to converge rapidly to the expected answers as the level L is increased. Much of our present intuition about the classical dynamics of OSFT comes from the level truncation scheme, and several exact analytic results were first guessed based on numerical computations

This motivated us to develop efficient algorithms for level-truncation calculations. Our main technical innovations are the systematic use of conservation laws [12] to compute the cubic vertices, and the implementation of our algorithms in a $C{+}{+}$ code.

A considerable simplification is possible by restricting the string field to live in the *universal* subspace [9, 12], which is the space of string fields generated by ghost oscillators and matter Virasoro generators acting on the vacuum. This subspace is called universal because it has always the same structure whatever is the D-brane in consideration, as long as the identity operator is in the BCFT spectrum.

It is reasonable to assume that the process of homogeneous tachyon decay can be captured classically by solutions in the universal subspace: it contains the open string tachyon and is closed under the operation $\frac{b_0}{L_0}(A*B)$ that one would use to build iteratively a solution starting from the open string tachyon and progressively adding corrections to satisfy the equations of motion.

Using conservation laws we determine the classical action directly in the universal basis in a recursive way, with an algorithm whose complexity is linear in the number of vertices (cubic in the number of fields). Some details about the numerical algorithms can be found in the last section of this chapter. The gain in efficiency of our methods compared to previous efforts is of several orders of magnitude, and we are able to obtain the 10^{10} universal cubic vertices at level (18,54). This numerical tool is the main tool in our exploration in this chapter, but is also used for several computations used in the next two chapters.

The tachyon condensate string field, the homogeneous solution of OSFT that we seek, corresponds to the stable vacuum of the open string tachyon. Its (negative) energy per unit volume must exactly cancel the D-brane tension. Sen and Zwiebach's computation [13] of

the tachyon condensate up to level (4,8) gave the first evidence that OSFT reproduces the correct D-brane physics. Moeller and Taylor [14] pushed the computation to level (10,20) finding that 99.91% of the D-brane tension is cancelled in the tachyon vacuum. Given such a remarkable agreement, it may appear quite pointless to extend their results to higher level. Not so. Up to level 10, the individual coefficients of the string field appear to converge much less rapidly than the value of the action. A more precise determination of the coefficients is likely to provide clues for an exact solution. Indeed various surprising patterns obeyed by OSFT solutions were 'experimentally' observed in [11], and can be checked against our calculations. Higher level computations can also be expected to shed light on the nature of the level truncation procedure itself, which still lacks a sound theoretical justification.

The first set of results, described in section 3, is the computation of the Siegel gauge tachyon condensate in level-truncation up to $L = 18$. The procedure is fairly straightforward: at any given level L, there are N_L scalar fields that obey the Siegel condition, and we determine their vev's by solving the N_L equations of motion implied by the gauge-fixed action. There is a potential subtlety here: the full equations of motion before gauge-fixing impose a bigger number of constraints [15] (the extra conditions simply enforce extremality of the action along gauge orbits). Consistency demands that the full set of equations of motion is satisfied as $L \to \infty$, and we systematically check that this indeed happens, with remarkable accuracy. As another consistency check, we verify that the tachyon condensate obeys the quadratic relations analytically derived by Schnabl [16], and we again find excellent agreement.

The values of the vacuum energy as a function of L are shown in Table 2.1. Unexpectedly, at $L = 14$ the energy overshoots the predicted answer of -1 and appears to further decrease at higher levels. As a first reaction, one may wonder whether the level-truncation procedure is breaking down for $L > 10$, as could happen if the approximation was only asymptotic. In this pessimistic scenario, for any OSFT observable there would be a maximum level that gives the estimate closest to the 'exact' value, and beyond this optimal level the procedure would stop converging. However, the data favor a smooth behavior as L increases, since

L	$E_{(L,3L)}$	$E_{(L,2L)}$
2	-0.9593766	-0.9485534
4	-0.9878218	-0.9864034
6	-0.9951771	-0.9947727
8	-0.9979302	-0.9977795
10	-0.9991825	-0.9991161
12	-0.9998223	-0.9997907
14	-1.0001737	-1.0001580
16	-1.0003754	-1.0003678
18	-1.0004937	-1.00049

Table 2.1: Values of the vacuum energy in level-truncation, in the $(L, 3L)$ and $(L, 2L)$ approximation schemes.

the differences between consecutive approximations are getting smaller.

The results in Table 1 may simply indicate that the approach of the energy to -1 as $L \to \infty$ is non-monotonic, contrary to previous naive expectations. Indeed, Taylor has presented convincing evidence [17] for this benign interpretation of our results.[1] He applies a clever extrapolation technique to level-truncation data for $L \leq 10$ to estimate the vacuum energies even for $L > 10$. This procedure reproduces quite accurately our exact values in Table 1 and further predicts that the vacuum energy reaches a minimum for $L \sim 28$, but then turns back to approach asymptotically -1 for $L \to \infty$.

In sections 4 we introduce our second main set of results. We devise an extrapolation technique in the same spirit of Taylor's analysis. We consider the effective tachyon potential $V_L(T)$ around the unstable vacuum, obtained by classically integrating out all the higher scalars up to level L. $V_L(T)$ is computed 'non-perturbatively' by fixing the value of T and solving numerically the equations of motion for the other scalars[2] . We are able to obtain $V_L(T)$ up to $L = 16$. Clearly for each L, the minimum of $V_L(T)$ is just the vacuum energy E_L at level L. However the functional dependence on T contains more information than just the extremal value E_L. The idea is to perform an extrapolation in L of the whole *functions* in T. In practice, we consider a finite interval of values of T around the non-

[1] The data in Table 1 were first announced at the Strings 2002 conference, Cambridge, July 2002 [28] .

[2] In this we differ from Taylor [17], who uses instead a series expansion of the potential in powers of T.

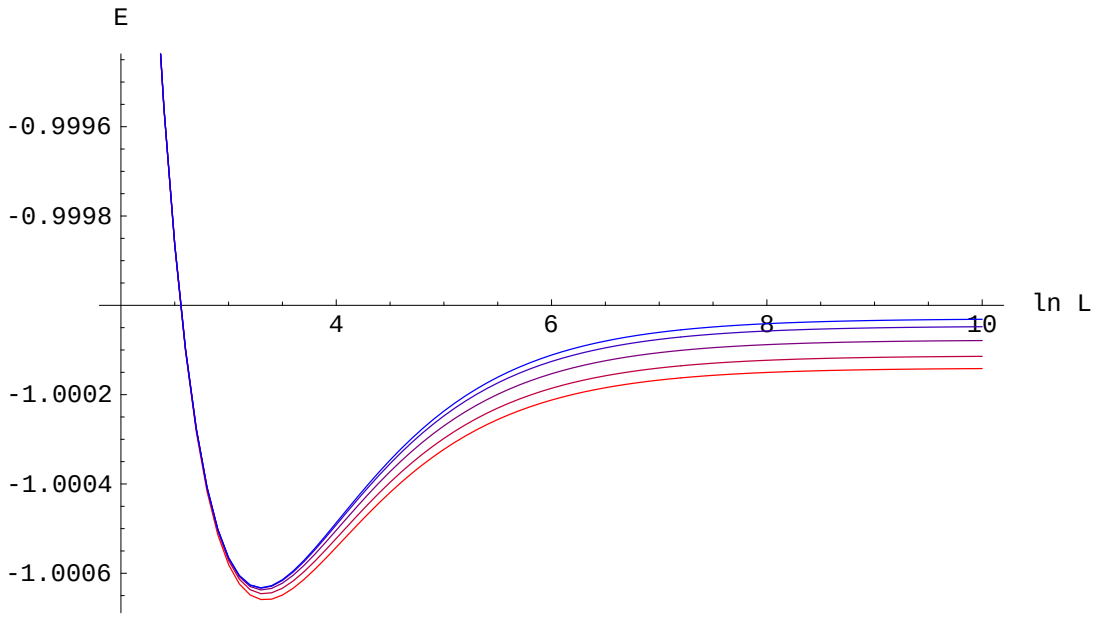

Figure 2.1: Curves of the vacuum energy as a function of level, as predicted by our extrapolation scheme for various values of M (maximum level of the data used in the extrapolation). The figure shows the curves $E^{(M)}(L)$ on a logarithmic plot, for M between 8 (lowermost curve) and 16 (uppermost curve). Data in the $(L, 3L)$ scheme.

perturbative minimum. For a fixed T in this interval we interpolate our data for $V_L(T)$ with a polynomial in $1/L$, and then extrapolate this polynomial to higher levels. To check the stability of this approximation scheme, we vary the maximum level M of the set of data used as input for the extrapolation: for each $M \leq 16$, we apply the extrapolation to the functions $\{V_L(T) \,|\, L \leq M\}$. This gives estimates $T_L^{(M)}$ for the tachyon vev and for the corresponding vacuum energy $E_L^{(M)}$, for any $L > M$.

The predicted power of the method is quite impressive. For example, with $M = 10$, that is using only level-truncation results up to level 10, the estimate $T_{18}^{(10)}$ reproduces with an accuracy of 10^{-5} the exact tachyon vev T_{18}, obtained by straightforward level-truncation at $L = 18$. This is remarkable, since the former computation is over a thousand times faster than the latter.

	L_{min}	E_{min}	E_∞
$M = 6$	41.1	-1.001171	-1.000949
$M = 8$	28.2	-1.000660	-1.000140
$M = 10$	27.8	-1.000646	-1.000113
$M = 12$	27.5	-1.000637	-1.000077
$M = 14$	27.3	-1.000633	-1.000046
$M = 16$	27.3	-1.000632	-1.000030

Table 2.2: Parameters of the curves $E^{(M)}(L)$ (in the $(L, 3L)$ scheme). The energy reaches its minimum E_{min} for $L = L_{min}$, and tends asymptotically to E_∞ as $L \to \infty$.

Figure 2.1 and Table 2.2 summarize the extrapolations of the energy as a function of level, for various values of M. The data completely confirm (with enhanced precision) the conclusions of Taylor [17]. The behavior of the energy as a function of level is non-monotonic, but eventually the asymptotic limit of -1 is reached with spectacular accuracy.

These results greatly reassure us of the validity of the level-truncation scheme. Observables in OSFT have a smooth limit as $L \to \infty$, which (in the absence of an alternative definition) should be identified with their 'exact' value. In all cases where an independent prediction for the observable is available (as for the vacuum energy, or for Schnabl's quadratic identities), the $L \to \infty$ extrapolation gives the correct answer.

A practical lesson of this analysis is that polynomial interpolations in $1/L$ have great predictive power, at least for the $(L, 3L)$ approximation scheme[3] . This observation makes the level-truncation scheme much more efficient, as reliable estimates can be extracted from (relatively) painless numerical work.

In section 5 we describe the results for the individual coefficients of the tachyon string field extrapolated to $L = \infty$. We hope that our accurate data will stimulate new imaginative approaches to the problem of finding an exact solution. It will be straightforward to extend the methods of this chapter to the computation of more general classical solutions of OSFT, which should provide more analytic clues.

To make this chapter self-contained, we begin in the next section with a review of some

[3]In the $(L, 3L)$ scheme, the string field is truncated up to level L and all of its mode are kept in the OSFT action. By contrast, in the $(L, 2L)$ scheme one keeps only the cubic terms in the action whose total level is $\leq 2L$. It turns out that$(L, 3L)$ results display a much smoother dependence on L.

basics.

2.2 OSFT and the Universal Tachyon Condensate

In this section we describe the basic setup for classical equations of motion in OSFT, with an emphasis on the symmetries obeyed by the tachyon condensate string field in Siegel gauge.

2.2.1 The Tachyon Condensate

The action of OSFT takes the well-known (deceptively) simple form [6]

$$S = -\frac{1}{g^2}\left(\frac{1}{2}\langle\Psi, Q_B\Psi\rangle + \frac{1}{3}\langle\Psi, \Psi * \Psi\rangle\right) . \tag{2.2.1}$$

This action describes the worldvolume dynamics of a D-brane specified by some Boundary CFT. The string field Ψ belongs to the full matter+ghost state-space of this BCFT. In classical OSFT, Ψ has ghost number one[4] . According to Sen's conjecture [8], the classical OSFT eom's

$$Q_B\Psi + \Psi * \Psi = 0 \tag{2.2.2}$$

must admit a Poincaré invariant solution $\Psi \equiv \mathcal{T}$ corresponding to the condensation of the open string tachyon to the vacuum with no D-branes. The tachyon potential $\mathcal{V}(\Psi)$ is given by [9]

$$\frac{\mathcal{V}(\Psi)}{2\pi^2 M} \equiv \frac{1}{2\pi^2} f(\Psi) = \frac{1}{2}\langle\Psi, Q_B\Psi\rangle + \frac{1}{3}\langle\,\Psi, \Psi * \Psi\rangle\,, \tag{2.2.3}$$

where M is the brane mass. The normalized potential $f(\Psi)$ is expected to equal minus one at the tachyon vacuum,

$$f(\mathcal{T}) = -1\,. \tag{2.2.4}$$

[4]Our conventions and notations are the same as [12]. In particular we define the SL(2,R) vacuum $|0\rangle$ to have ghost number zero, and the ghost and antighost fields $c(z)$ and $b(z)$ to have ghost number one and minus one, respectively.

Universality

A basic property of the tachyon condensate string field $\mathcal{T}$ is *universality* [9],

$$\mathcal{T} \in \mathcal{H}^{(1)}_{univ}\,, \tag{2.2.5}$$

where

$$\mathcal{H}_{univ} \equiv \mathrm{Span}\{L^m_{-j_1}\ldots L^m_{-j_p}\, b_{-k_1}\ldots b_{-k_q}\, c_{-l_1}\ldots c_{-l_r}|0\rangle\,,\ j_i \geq 2, k_i \geq 2, l_i \geq -1\} \tag{2.2.6}$$

with L^m_k denoting the matter Virasoro generators. The universal space is further decomposed into a direct sum of spaces with definite ghost number

$$\mathcal{H}_{univ} = \oplus_{n\in Z}\mathcal{H}^{(n)}_{univ}\,. \tag{2.2.7}$$

The restriction of the classical action to $\mathcal{H}_{univ}$ can be evaluated using purely combinatorial algorithms that only involve the ghosts and the matter Virasoro algebra with $c = 26$ [9, 12]. It follows that the form of $\mathcal{T}$ does not depend on any of the details of the BCFT that defines the D-brane background before condensation.

Twist

An obvious symmetry of the tachyon condensate is twist symmetry. The twist is a parity that is preserved by the star product, so that OSFT equations of motion admit a consistent truncation to twist even string fields [46], and indeed the tachyon condensate solution turns out to be twist even. In $\mathcal{H}^{(1)}_{univ}$, twist is defined simply as $(-1)^{L_0+1}$, so $\mathcal{T}$ contains only states with *even* level $L \equiv L_0 + 1$.

Siegel gauge and SU(1,1)

The Siegel gauge condition $b_0\Psi = 0$ is particularly natural in level truncation since it is easily imposed level by level by simply omitting all Fock states containing the ghost zero mode c_0.

The Siegel gauge-fixed equations of motion

$$L_0\Psi + b_0(\Psi * \Psi) = 0 \tag{2.2.8}$$

admit a consistent truncation to the subspace of string fields which are singlets of SU(1,1) [47]. The SU(1,1) symmetry in question is generated by

$$\mathcal{G} = \sum_{n=1}^{\infty} (c_{-n} b_n - b_{-n} c_n) \quad X = -\sum_{n=1}^{\infty} (n\, c_{-n} c_n) \quad Y = \sum_{n=1}^{\infty} \left(\frac{1}{n} b_{-n} b_n \right) \tag{2.2.9}$$

and the singlet subspace is defined as

$$\Psi \in \mathcal{H}_{singl} \quad \text{iff } b_0 \Psi = \mathcal{G}\Psi = X\Psi = Y\Psi = 0\,. \tag{2.2.10}$$

Notice that acting on Siegel states $\mathcal{G}$ is just ghost number shifted by one unit, so all states in $\mathcal{H}_{singl}$ have ghost number one. To show consistent truncation of equations (2.2.8) to the singlet subspace, we need to prove that if $\Psi \in \mathcal{H}_{singl}$, then $b_0(\Psi * \Psi) \in \mathcal{H}_{singl}$, so that all components of Ψ outside $\mathcal{H}_{singl}$ can be consistently set to zero. A simple argument is as follows. The generator X is a derivation of the $*$-algebra[5] , and commutes with b_0. Hence if $X\Psi = 0$, $X\, b_0(\Psi * \Psi) = 0$. Clearly $\mathcal{G}$ is also zero on $b_0(\Psi * \Psi)$, since ghost number adds under $*$-product. By the structure of the finite-dimensional[6] representations of SU(1,1), a vector with zero $\mathcal{G}$ and X eigenvalues must also have zero Y eigenvalue, that is, $b_0(\Psi * \Psi) \in \mathcal{H}_{singl}$, as desired.

The SU(1,1) singlet subspace has a simple characterization in terms of the Virasoro generators of the 'twisted' ghost conformal field theory of central charge -2 [24] [7] ,

$$\mathcal{H}_{singl} = \text{Span}\left\{ \mathcal{L}_{-k_1} \ldots \mathcal{L}_{-k_n} c_1 |0\rangle \,, k_i \geq 2 \right\} \otimes \mathcal{H}_{matter} \tag{2.2.11}$$

where

$$\mathcal{L}_k \equiv L^g_k + k j^{gh}_k + \delta_{k,0} = \sum_{n=-\infty}^{+\infty} (k-n) : b_n c_{k-n} : \,. \tag{2.2.12}$$

The statement that

$$\begin{aligned} \mathcal{T}_{Siegel} \quad \in \quad & \mathcal{H}^{(1)}_{univ} \cap \mathcal{H}_{twist+} \cap \mathcal{H}_{singl} = \\ & \text{Span}\left\{ \mathcal{L}_{-k_1} \ldots \mathcal{L}_{-k_n} L^m_{-j_1} \ldots L^m_{-j_l} \, c_1 |0\rangle \,, k_i \geq 2, j_i \geq 2, \, \sum k_i + \sum j_i \in 2\mathbf{N} \right\} \end{aligned} \tag{2.2.13}$$

[5] It is enough to notice that $-2X = \{Q_B, c_0\}$, see (2.2.16) below. Both Q_B and c_0 are derivations [12], and (anti)commutators of (graded) derivations are derivations. On the other hand, the generator Y is *not* a derivation.

[6] Since SU(1,1) commutes with L_0, we can run the argument in the subspaces of $\mathcal{H}_{univ}$ with given L_0, which are finite-dimensional.

[7] A proof of the equivalence of definitions (2.2.10) and (2.2.11) for $\mathcal{H}_{singl}$ can be found in [48], section 3.

L	0	2	4	6	8	10	12	14	16	18	20
$M_{L,1}$	1	2	6	17	43	102	231	496	1027	2060	4010
N_L	1	3	9	26	69	171	402	898	1925	3985	7995
$M_{L,2}$	0	1	4	12	32	79	182	399	839	1700	3342
N'_L	0	1	5	17	49	128	310	709	1548	3248	6590

Table 2.3: Dimensions of some relevant subspaces of $\mathcal{H}_{univ}$.

summarizes all the known *linear* symmetries of the Siegel gauge tachyon condensate. Other exact constraints (quadratic identities [16]) are considered in section 2.3.3.

2.2.2 Level-Truncation and Gauge Invariance

We measure the level L of a Fock state with reference to the zero momentum tachyon $c_1|0\rangle$, which we define to be level zero, in other terms $L \equiv L_0 + 1$. As usual, the level truncation approximation (L, N) is obtained by truncating the string field to level L, and keeping interactions terms in the OSFT action up to total level N, with $2L \leq N \leq 3L$. In our numerical work we have systematically explored both the $(L, 2L)$ scheme, which is (naively) the most efficient, and the $(L, 3L)$ scheme, which is the most natural. In section 2.4.3 we discuss some empirical differences between these two schemes, but in short it appears that the natural $(L, 3L)$ scheme has better convergence properties.

The most economic representation of $\mathcal{T}_{Siegel}$ is using the basis (2.2.13), but unfortunately we have not found a simple algorithm to perform computations within the SU(1,1) singlet subspace[8] . We shall work instead with the universal basis (2.2.6) using fermionic ghost oscillators. In this basis, the number N_L of modes in $\mathcal{T}_{Siegel}$ truncated at level L (with L an even integer) is given by

$$N_L = \sum_{j=0}^{L/2} M_{2j,1}\,, \tag{2.2.14}$$

where $M_{l,g}$ denotes the number of Siegel Fock states in $\mathcal{H}_{univ}$ with level l and ghost number g. $M_{l,g}$ which is computed by the generating function

$$\sum_{l,g} M_{l,g} x^l y^{g-1} = \prod_{p=2}^{\infty} \frac{1}{1-x^p} \prod_{q=1}^{\infty} (1 + x^q y)(1 + \frac{x^q}{y})\,. \tag{2.2.15}$$

[8]The twisted ghost Virasoro's L'^g_n do not have simple conservation laws on the cubic vertex.

The Siegel gauge-fixed eom's (2.2.8) truncated at level L are a system of N_L equations in N_L unknowns. The solution can be found very efficiently using the Newton method. By construction the resulting string field $\mathcal{T}^L_{Siegel}$ solves the truncated Siegel gauge eom's with extremely good accuracy. However the full gauge invariant eom's (2.2.2) impose an extra set of constraints on the solution. Recall that the BRST operator can be written as

$$Q_B = c_0 L_0 - 2b_0 X + \widetilde{Q}\,, \tag{2.2.16}$$

where

$$\widetilde{Q} = \sum_{\substack{m,n\neq 0\\ m+n\neq 0}} \frac{m-n}{2}\, c_m c_n b_{-m-n} + \sum_{n\neq 0} c_{-n} L^m_n\,. \tag{2.2.17}$$

The extra conditions on a Siegel string field are then

$$\widetilde{Q}\Psi + b_0 c_0 (\Psi * \Psi) = 0\,. \tag{2.2.18}$$

At level L, this equation entails N'_L extra constraints on $\mathcal{T}^L_{Siegel}$, with

$$N'_L = \sum_{j=0}^{L/2} M_{2j,2}\,. \tag{2.2.19}$$

Table 2.3 shows the numbers $M_{L,1}$, N_L, $M_{L,2}$ and N'_L up to $L = 20$.

The role of equation (2.2.18) is simply to enforce extremality of the solution along gauge orbits. However, in principle there could be an issue about the non-perturbative validity of the Siegel gauge condition (are gauge orbits non-degenerate at the non-perturbative Siegel gauge vacuum? [44]). Moreover, the level truncation procedure explicitly breaks gauge invariance, which is formally recovered only as $L \to \infty$. Thus equation (2.2.18) gives an independent set of constraints which are not a priori satisfied by the level-truncated solution. If Siegel gauge is a consistent gauge choice and if gauge invariance is truly recovered in the infinite level limit, then we expect (2.2.18) to hold asymptotically as $L \to \infty$. This is a very non-trivial consistency requirement on $\mathcal{T}^L_{Siegel}$. Numerical evidence for this is examined in section 2.3.2.

2.3 The Level-Truncated Tachyon Condensate

Using the numerical methods outlined in appendix A, we have determined $\mathcal{T}_{Siegel}$ up to $L = 18$, both in the $(L, 2L)$ and in the $(L, 3L)$ schemes. $(L, 3L)$ results appear to be better behaved (we come back back to this point in section 2.4.3), and in this section we only consider this scheme. It is clearly impossible to reproduce here all the coefficients of the tachyon condensate up to level 18. We give some sample results in Table 2.4.

In this section we perform some consistency checks of the level-truncation results, verifying some *exact* properties that the tachyon condensate must obey.

2.3.1 SU(1,1) invariance

We have systematically checked that our solutions for the tachyon condensate can be written in the basis (2.2.13), and thus obey the full SU(1,1) invariance. This property holds with perfect accuracy (that is, with the same precision as the number of significant digits that we keep, which is 15 for double-precision variables in C++). This is nice, but not surprising, since the SU(1,1) generators commute with L_0, and thus SU(1,1) is an exact symmetry of the level-truncated theory.

2.3.2 Out-of-Siegel Equations

We now turn to the crucial check of the extra conditions imposed by the full equations of motion before gauge-fixing. We were able to carry out this computation up to $L = 14$. Table 2.5 shows some sample results for the string field (2.2.18) evaluated for $\Psi = \mathcal{T}_{Siegel}$. The extra constraints are satisfied already very well at $L = 6$, and significantly better at $L = 14$[9] . This is happening thanks to large cancellations between the two terms in (2.2.18)[10] , as can be easily checked by applying the operator $\widetilde{Q}$ to the results in Table 2.4.

Even more remarkable are the extrapolations of the data to $L = \infty$, which give values two or three orders of magnitude smaller than the $L = 14$ results! Our extrapolation method

[9] This behavior is common to the higher level modes not reproduced in Table 2.5.

[10] At $L = 14$, each term in (2.2.18) is typically one or two orders of magnitude bigger than their sum.

	$L=4$	$L=6$	$L=8$	$L=10$
$c_1\|0\rangle$	0.548399	0.547932	0.547052	0.546260
$c_{-1}\|0\rangle$	0.205673	0.211815	0.215025	0.216982
$L^m_{-2}c_1\|0\rangle$	0.056923	0.057143	0.057214	0.057241
$c_{-3}\|0\rangle$	-0.056210	-0.057392	-0.057969	-0.058290
$b_{-2}c_{-2}c_1\|0\rangle$	-0.033107	0.034063	0.034626	0.034982
$b_{-3}c_{-1}c_1\|0\rangle$	0.018737	0.019131	0.019323	0.019430
$L^m_{-2}c_{-1}\|0\rangle$	-0.0068607	-0.0074047	-0.0076921	0.0078698
$L^m_{-4}c_1\|0\rangle$	-0.005121	-0.005109	-0.005102	-0.005095
$L^m_{-2}L^m_{-2}c_1\|0\rangle$	-0.00058934	-0.00062206	-0.00063692	-0.00064553

	$L=12$	$L=14$	$L=16$	$L=18$
$c_1\|0\rangle$	0.545608	0.545075	0.544637	0.544272
$c_{-1}\|0\rangle$	0.218296	0.219236	-0.219942	-0.220491
$L^m_{-2}c_1\|0\rangle$	0.057252	0.057256	0.057257	0.057257
$c_{-3}\|0\rangle$	-0.058489	-0.058625	-0.058721	-0.058794
$b_{-2}c_{-2}c_1\|0\rangle$	0.035225	0.035402	0.035535	0.035640
$b_{-3}c_{-1}c_1\|0\rangle$	0.019496	0.019542	0.019574	0.019598
$L^m_{-2}c_{-1}\|0\rangle$	0.0079906	0.0080782	0.0081445	0.0081966
$L^m_{-4}c_1\|0\rangle$	-0.005090	-0.005086	-0.005082	-0.005079
$L^m_{-2}L^m_{-2}c_1\|0\rangle$	-0.00065124	-0.00065532	-0.00065839	-0.00066081

Table 2.4: $(L, 3L)$ level-truncation results for the lowest modes of $\mathcal{T}_{Siegel}$.

	$L=6$	$L=14$	$L=\infty$
$c_{-2}c_1\|0\rangle$	0.00841347	0.00257255	-0.0000400232
$c_{-4}c_1\|0\rangle$	-0.0103276	-0.00307849	0.0000536768
$c_{-1}c_{-2}\|0\rangle$	0.0107901	0.00483115	0.000005367
$L^m_{-2}c_{-2}c_1\|0\rangle$	0.000892329	0.000612637	0.00000877198
$L^m_{-3}c_{-1}c_1\|0\rangle$	-0.00212947	-0.000877716	0.00000163665
$c_{-6}c_1\|0\rangle$	0.0130217	0.00341282	0.0000208782
$c_{-4}c_{-1}\|0\rangle$	-0.0110576	-0.00431119	-0.000160066
$c_{-3}c_{-2}\|0\rangle$	0.00360400	0.00160614	-0.0000134344
$b_{-2}c_{-3}c_{-1}c_1\|0\rangle$	-0.00306293	-0.000919219	-0.0000799493
$b_{-3}c_{-2}c_{-1}c_1\|0\rangle$	-0.00324329	-0.00114819	-0.0000488214
$L^m_{-2}c_{-4}c_1\|0\rangle$	0.000132483	-0.000183042	-0.0000162206
$L^m_{-2}c_{-2}c_{-1}\|0\rangle$	-0.00188148	-0.000811710	-0.0000098375
$L^m_{-3}c_{-3}c_1\|0\rangle$	0.000834397	0.000303847	-0.0000004570
$L^m_{-4}c_{-2}c_1\|0\rangle$	0.000127107	0.0000135260	0.0000021124
$L^m_{-2}L^m_{-2}c_{-2}c_1\|0\rangle$	-0.000179524	-0.0000980000	-0.0000014704
$L^m_{-5}c_{-1}c_1\|0\rangle$	0.000903154	0.000310410	0.0000131051
$L^m_{-3}L^m_{-2}c_{-1}c_1\|0\rangle$	0.000271962	0.000105286	0.0000014747

Table 2.5: Sample $(L, 3L)$ level-truncation results for the out-of-Siegel equations of motion. The table shows data for $L=6$ and $L=14$, and $L=\infty$ extrapolations obtained from the data for $2 \le L \le 14$ with a polynomial fit in $1/L$.

consists in interpolating the data with a polynomial in $1/L$ of *maximum* degree (that is, with as many parameters as the number of data points). For example, for the mode $c_{-4}c_1|0\rangle$ we have six data points ($L = 4, 6, 8, 10, 12, 14$) and we use a polynomial in $1/L$ of degree five. Empirically, this method gives better results ($L=\infty$ extrapolations closer to zero) than making fits with polynomials in $1/L$ of lower degree.

This analysis leaves little doubt that the full equations of motion are satisfied as $L \to \infty$.

2.3.3 Exact Quadratic Identities

As pointed out by Schnabl [16], any solution of the OSFT eom's must obey certain exact quadratic identities that follow from the existence of anomalous derivations of the star product. An infinite set of identities is obtained from the anomalous derivations $K^m_{2n} = L^m_{2n} - L^m_{-2n}$. They are [16]:

$$\langle\Psi|c_0 L^m_{2n}|\Psi\rangle = (-1)^n \frac{65}{54} \langle\Psi|c_0 L_0|\Psi\rangle\,, \tag{2.3.1}$$

	L_2^m	L_4^m	L_6^m	L_8^m	L_{10}^m	L_{12}^m	L_{14}^m	L_{16}^m
2	1.127927							
4	1.069643	1.079864						
6	1.046467	1.051898	1.053517					
8	1.034587	1.037554	1.040767	1.036977				
10	1.027439	1.029304	1.031367	1.033082	1.025628			
12	1.022688	1.023975	1.025369	1.026797	1.027437	1.017346		
14	1.019312	1.020257	1.021261	1.022317	1.023271	1.023102	1.011026	
16	1.016795	1.017520	1.018279	1.019076	1.019875	1.020461	1.019662	1.006039
∞	0.999916	0.999877	1.00429	1.00526				

Table 2.6: $(L, 3L)$ level-truncation results for Schnabl's quadratic matter identities. The table shows the values for the ratios R_n of equ. (2.3.2).

where Ψ is a solution in Siegel gauge.

In Table 2.6 we show the level-truncation results for the ratios

$$R_n \equiv (-1)^n \frac{54}{65} \frac{\langle \mathcal{T}|c_0 L_{2n}^m|\mathcal{T}\rangle}{\langle \mathcal{T}|c_0 L_0|\mathcal{T}\rangle}\,, \tag{2.3.2}$$

which are of course predicted to be exactly one. The quadratic identities are satisfied quite well already at low levels, and the extrapolations to $L = \infty$ (performed again with polynomials in $1/L$ of maximum degree) give really good results.

Both the quadratic identities just analyzed and the out-of-gauge eom's (2.2.18) are exact constraints on the solution that are broken by level-truncation. We have found that the level-truncated answers for this class of observables are very accurately converging to their known exact values as $L \to \infty$. This is strong evidence for the idea that level-truncation is a convergent approximation scheme. We have also learnt that maximal polynomials in $1/L$ give very precise extrapolations. It seems safe to assume that this should be a universal feature, and in the following we shall adopt the same extrapolation technique to quantities whose exact asymptotic value is a priori unknown[11] .

[11] Polynomials in $1/L$ have also been used in the extrapolation procedure of of [17]. It was also noted in [49] that large level results appear to have corrections of order $1/L$, although there the definition of level is somewhat different.

2.4 Extrapolations to Higher Levels

Encouraged by the successful extrapolations to $L = \infty$ described in the previous section, and inspired by Taylor's analysis [17], we have set up a systematic scheme to extrapolate to higher levels the results for the vacuum energy and for the tachyon condensate string field. In this section we focus on the results for the vacuum energy, while in the next we shall examine the results for the individual coefficients of the tachyon condensate.

Unless explicitly stated otherwise, the use of the $(L, 3L)$ scheme is implied in the rest of the chapter. We justify this choice in section 2.4.3, where we briefly contrast $(L, 2L)$ versus $(L, 3L)$ results.

2.4.1 Extrapolations of the Tachyon Effective Action

The basic idea of our method has already been explained in the introduction. The first step is the computation of the tachyon effective action $V_L(T)$, obtained by integrating out the higher modes up to level L. Some details of how this is done numerically are explained in appendix A. Figure 2.4.1 shows the plots of $V_L(T)$ for $0 \leq L \leq 16$. There is good convergence as L increases, indeed the curves for $L \geq 6$ are indistinguishable on the scale of Figure 2.2.

For our extrapolations, we focus on a interval for the tachyon vev around the non-perturbative vacuum. We take $0.54 \leq T \leq 0.55$. The function $V_L^{(M)}(T)$, where M is an even integer ≤ 16, is the extrapolation 'of order M' of the tachyon effective action at level L, and is constructed as follows. We fix the dependence on L by writing

$$V_L^{(M)}(T) = \sum_{n=0}^{M/2+1} \frac{a_n(T)}{(L+1)^n}\,, \tag{2.4.3}$$

for some coefficients functions $a_n(T)$. The functions $a_n(T)$ are determined by imposing the conditions

$$V_L^{(M)}(T) = V_L(T)\,, \qquad \text{for } L = 0, 2, \cdots, M\,, \qquad \forall\, T \in [0.54, 0.55]\,. \tag{2.4.4}$$

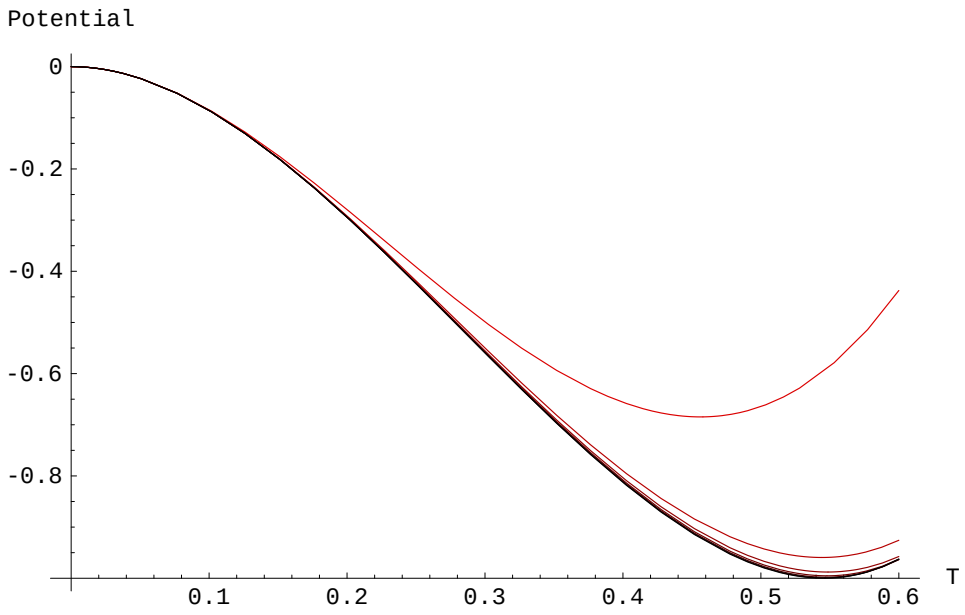

Figure 2.2: Plots of the tachyon effective potential $V_L(T)$ at level L, for L between zero (uppermost curve) and 16 (lowermost curve). The curves for $L = 6, 10, 12, 14, 16$ appear superimposed in the figure.

In other terms, we interpolate the $M/2+1$ values $\{V_L(T)|L = 0, 2, \ldots M\}$ with a polynomial in $1/(L+1)$ that passes through all the data points[12] .

Our best estimate for the tachyon effective action at level L is the function $V_L^{(16)}(T)$. Figure 2.3 shows the plots of $V_L^{(16)}(T)$ for L between ten and infinity. The position of the minimum in each curve defines our order $M = 16$ estimates $T_L^{(16)}$ and $E_L^{(16)}$ for the tachyon vev and vacuum energy at level L. We can follow very clearly the behavior of the minima as L increases. The energy falls below -1, reaches its lowest point in $L = 28$ curve, and then turns back to approach asymptotically the value $E_\infty^{(16)} = -1.00003$! In Figure 2.4 we see the same phenomenon in a plot of $E_L^{(16)}$ as a function of $1/L$.

It is interesting to consider how the extrapolations change as we vary M. Table 2.7 shows the estimates $E_L^{(M)}$ up to $L = 18$, while Table 2.10 (appendix B) shows the analogous estimates for the tachyon vev. By construction, the diagonal entries $E_L^{(L)}$ and $T_L^{(L)}$ are

[12]The rationale for using polynomials in $1/(L+1)$ rather than $1/L$ is that we wish to include also the data for $L = 0$. This works somewhat better than excluding the $L = 0$ point and making extrapolations in $1/L$. Committed readers can find more about this technicality in footnote 13.

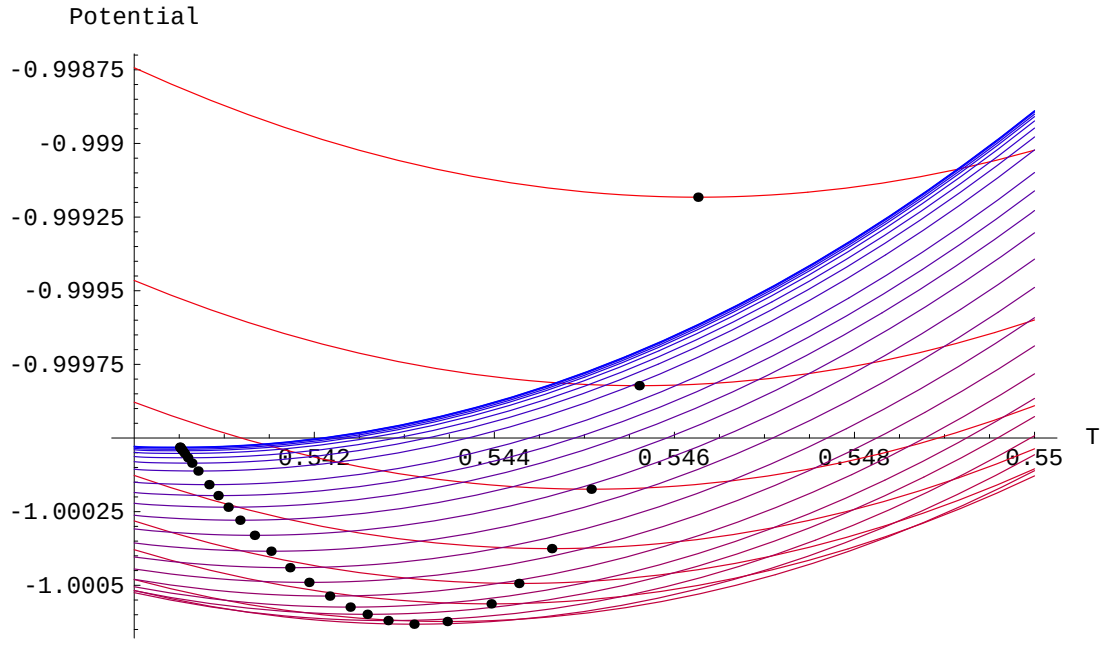

Figure 2.3: Plots of the order 16 estimates $V_L^{(16)}(T)$ for the effective tachyon potential, for some sample values of $L \geq 10$. The minimum of each curve is indicated by a black dot, which by definition has coordinates $(T_L^{(16)}, E_L^{(16)})$. The isolated uppermost plot corresponds to $L = 10$. To follow the curves from $L = 10$ to $L = \infty$, focus on the position of the minima: as L increases, the dot moves from right to left (*i.e.*, the tachyon vev decreases). As $L \to \infty$, the curves crowd towards an asymptotic function with minimum at $(T_\infty^{(16)}, E_\infty^{(16)}) = (0.5405, -1.00003)$.

simply the exact values obtained by direct level-truncation at level L. One can observe from the tables that the method has remarkable predictive power. For example, by only knowing level-truncation results up to level 10, one can obtain the prediction $E_{16}^{(10)} = -1.0003780$ for the energy at level 16, to be compared to the exact value $E_{16} = -1.0003755$. We thus feel quite comfortable in trusting the extrapolations even for L large. Figure 2.1 and Table 2.2 (already discussed in the introduction) illustrate the main features of the larger L results for the vacuum energy, for various M's. It is pleasant to observe that, as M increases, the estimates $L_{min}^{(M)}$ and $E_{min}^{(M)}$ (Table 2.2) quickly reach stable values, while $E_\infty^{(M)}$ steadily approaches minus one[13] .

[13] Finally we would like to comment on how results change if instead of using a polynomial extrapolation

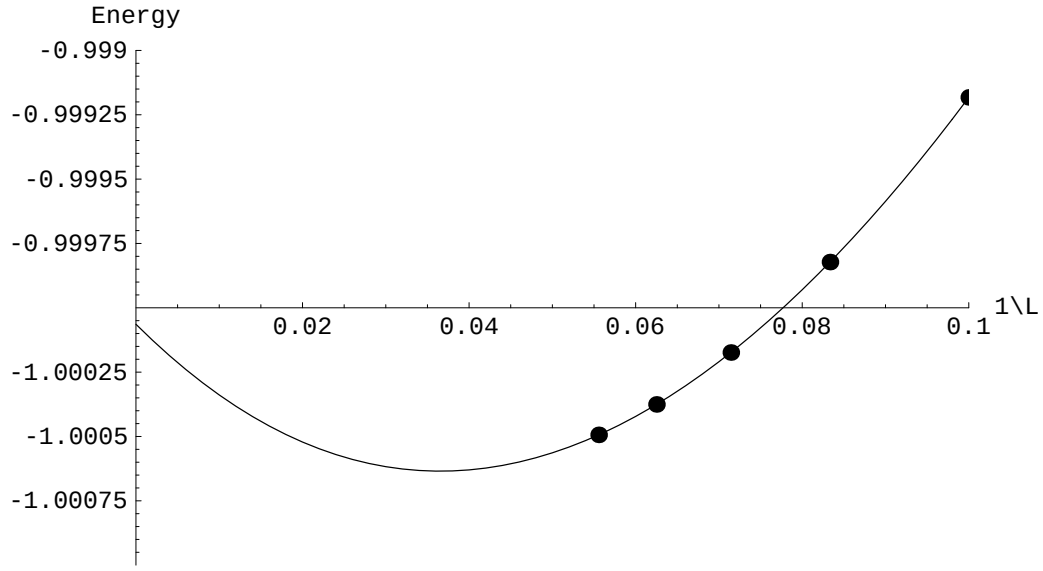

Figure 2.4: Plot of $E_L^{(16)}$ as a function of $1/L$. The black dots represent the exact values up to $L = 18$ computed by direct level-truncation (Table 1, $(L, 3L)$ scheme). To first approximation, the curve in the figure is roughly a parabola: since the energy overshoots -1 at $1/L = 1/14 \simeq 0.07$, we have a visual understanding of the position of the minimum of the energy around $1/L = (1/14)/2 = 1/28 \simeq 0.036$.

It is remarkable that extrapolations to higher levels work so well. The data have a smooth and predictable dependence on L, which is very well captured by polynomials in $1/L$. This property was not *a priori* obvious, and indeed it appears to be true only for $(L, 3L)$ data, as we shall see in section 2.4.3.

2.4.2 Comparison with Straightforward Extrapolations

The method just described appears to work remarkably well. To which extent does the success of the method depend on the sophisticated idea of extrapolating the *functional*

in $1/(L+1)$ we use an extrapolation in $1/L$ (excluding the $L = 0$ point), or alternatively we keep the $L = 0$ point and use a polynomial in $1/(L + a)$ for some other $a > 0$. One finds that for $M = 16$ the differences among all these schemes are very minor, even for a wide range of reasonable values of a (say $0.1 < a < 3$). For $M < 10$, including the $L = 0$ data (and using $1/(L + a)$) works somewhat better than excluding it (and using $1/L$). For example the prediction $E_{16}^{(8)}$ obtained excluding $L = 0$ differs by the exact value by an error of 0.0003, which is 30 times bigger than for the prediction obtained including $L = 0$. All of this scheme-dependence is expected to disappear for M large, and indeed is already irrelevant at $M = 16$.

	$L=4$	$L=6$	$L=8$	$L=10$
$M=4$	-0.98782176	-0.99546179	-0.99850722	-1.0000023
$M=6$		-0.99517712	-0.99798495	-0.99930406
$M=8$			-0.99793018	-0.99918359
$M=10$				-0.99918246
	$L=12$	$L=14$	$L=16$	$L=18$
$M=4$	-1.0008372	-1.0013461	-1.0016765	-1.0019017
$M=6$	-1.0000079	-1.0004169	-1.0006692	-1.0008317
$M=8$	-0.99982545	-1.0001796	-1.0003843	-1.0005057
$M=10$	-0.99982266	-1.0001750	-1.0003780	-1.0004979
$M=12$	-0.99982226	-1.0001739	-1.0003759	-1.0004947
$M=14$		-1.0001737	-1.0003755	-1.0004938
$M=16$			-1.0003755	-1.0004937
$M=18$				-1.0004937

Table 2.7: Estimates $E_L^{(M)}$ for the vacuum energy obtained from extrapolations of the effective tachyon potential, at various orders M and for $L \leq 18$. Data in the $(L, 3L)$ scheme. By definition, the diagonal entries $E_L^{(M=L)}$ coincide with the exact computation from direct level-truncation at level $(L, 3L)$ (Table 1).

form of the tachyon effective action? We can answer this question by considering the more straightforward procedure of simply extrapolating the values of the vacuum energies E_L (as opposed to the full functions $V_L(T)$). We define the 'straightforward' order M estimate $\widetilde{E}_L^{(M)}$ at level L by considering the data $\{E_L | 0 \leq L \leq M\}$, and interpolating them with a polynomial in $1/(L+1)$ of maximum degree. (This is in complete analogy with (2.4.3)). The results for $L \leq 18$ in the $(L, 3L)$ scheme are presented in Table 2.8, while in Table 2.9 we give the extrapolations to $L = \infty$. We see that for $M < 10$, the more sophisticated method gives much more accurate predictions (compare Table 2.7 and Table 2.8: for example $E_{18}^{(8)}$, $\widetilde{E}_{18}^{(8)}$ and the exact value $E_{18}^{(18)}$). However for $M > 10$ there is no significant difference between the two procedures[14] . We also compared the results for the individual coefficients of the tachyon string field obtained with the two procedures, and found a very similar pattern.

We conclude that with the sophisticated procedure one can achieve remarkable accuracy even for small M, where a naive extrapolation would work quite poorly. However if one

[14] A comparison with the results of [17], which in our language correspond to $M = 10$, shows that the accuracy of the perturbative method of [17] seems comparable with the accuracy of the straightforward extrapolation. For $M = 10$ our non-perturbative method based on the tachyon effective action appears to be more accurate.

	$L=4$	$L=6$	$L=8$	$L=10$
$M=4$	-0.98782176	-0.99730348	-1.0020443	-1.0048888
$M=6$		-0.99517712	-0.99845611	-1.0002959
$M=8$			-0.99793018	-0.99921882
$M=10$				-0.99918246
	$L=12$	$L=14$	$L=16$	$L=18$
$M=4$	-1.0067851	-1.0081397	-1.0091556	-1.0099457
$M=6$	-1.0014693	-1.0022814	-1.0028762	-1.0033304
$M=8$	-0.99991100	-1.0003187	-1.0005753	-1.0007448
$M=10$	-0.99982332	-1.0001767	-1.0003811	-1.0005023
$M=12$	-0.99982226	-1.0001738	-1.0003758	-1.0004946
$M=14$		-1.0001737	-1.0003755	-1.0004939
$M=16$			-1.0003755	-1.0004937
$M=18$				-1.0004937

Table 2.8: The estimates $\widetilde{E}_L^{(M)}$ for the vacuum energy in the $(L, 3L)$ scheme, obtained with the 'straightforward' polynomial extrapolation in $1/(L+1)$.

is willing to perform level-truncation up to level 12 or above, the simpler extrapolation procedure is equally effective.

2.4.3 $(L, 3L)$ versus $(L, 2L)$

	$(L, 3L)$	$(L, 2L)$
$M=6$	-0.998698	-0.988625
$M=8$	-0.999784	-1.00261
$M=10$	-1.00010	-0.999316
$M=12$	-1.00008	-1.00048
$M=14$	-1.00004	-0.999655
$M=16$	-1.00003	-1.00057

Table 2.9: The estimates $\widetilde{E}_\infty^{(M)}$ for the asymptotic vacuum energy in the $(L, 3L)$ and $(L, 2L)$ schemes, obtained with the 'straightforward' polynomial extrapolation in $1/(L+1)$.

All the extrapolations described so far are for results in the $(L, 3L)$ scheme. We have investigated the data in the $(L, 2L)$ scheme and concluded that their behavior as a function of L is not nearly as smooth: as a consequence, extrapolations to higher levels are less reliable. A glance at Table 2.9 and Figure 2.5 is sufficient to illustrate our point. We are comparing the 'straightforward' extrapolations of the vacuum energy to $L=\infty$, for various

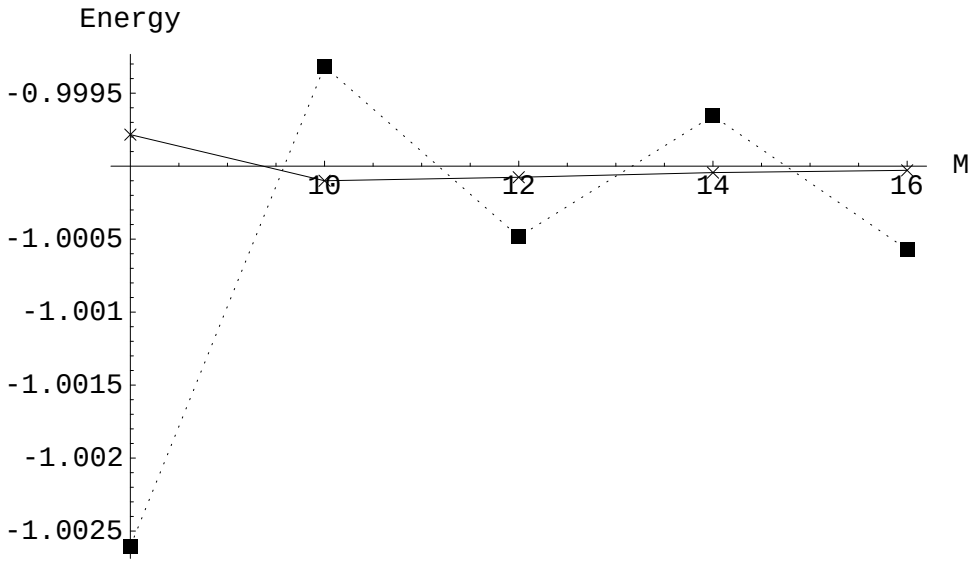

Figure 2.5: Plot of the results in Table 2.9. The continuous line represents the $(L, 3L)$ results, while the dashed line represents the $(L, 2L)$ results.

M's, obtained with data in the $(L, 3L)$ scheme, with the analogous quantities in the $(L, 2L)$ scheme. While the $(L, 3L)$ data have a really smooth dependence on M and converge nicely to -1, the $(L, 2L)$ data have a much more irregular behavior. A similar pattern is observed for extrapolations at finite L: estimates $\widetilde{E}_L^{(M)}$ of exact results at level $L \leq 18$ are not nearly as accurate in the $(L, 2L)$ scheme as they are in the $(L, 3L)$ scheme. An analogous behavior is found in comparing $(L, 3L)$ and $(L, 2L)$ data for the tachyon vev. We have also repeated for $(L, 2L)$ data the full analysis based on extrapolations of the tachyon effective action, and found no improvement with respect to the straightforward extrapolations shown in Table 2.9.

It would be interesting to explain these findings from an analytic point of view. The $(L, 3L)$ scheme can be understood as a cut-off procedure in which only the kinetic term of the OSFT action is changed, such to give an infinite mass to modes with level higher than L. On the other hand, in the $(L, 2L)$ scheme both the kinetic and the cubic term of the action are changed. This may explain why $(L, 3L)$ data have a simpler dependence on L.

2.5 The Numerical Algorithms

In this section we explain some technical details about the algorithms that we have used to compute the universal star products and find the tachyon solution in level truncation.

2.5.1 Star Products from Conservation Laws

The strategy for evaluating star products using conservation laws is explained in detail in [12]. Each Fock state in $\mathcal{H}^{(1)}_{univ}$ can be represented as a string of negatively moded ghost or Virasoro generators acting on the zero-momentum tachyon $c_1|0\rangle$. The triple product of three such states is evaluated recursively by converting a negatively moded generator on one state space to a sum of positively moded generators acting on all three state spaces,

$$\langle A_{-k}\Phi_1, \Psi_2, \Psi_3\rangle = \tag{2.5.1}$$
$$r_k\langle \Phi_1, \Psi_2, \Psi_3\rangle + \langle \sum_{n\geq 0} \alpha_n^k A_n \Phi_1, \Psi_2, \Psi_3\rangle + \langle \Phi_1, \sum_{n\geq 0} \beta_n^k A_n \Psi_2, \Psi_3\rangle + \langle \Phi_1, \Psi_2, \sum_{n\geq 0} \gamma_n^k A_n \Psi_3\rangle\,,$$

where A_{-k} is any constructor symbol and the coefficients appearing in this 'conservation law' are computed from the geometry of the Witten vertex [12]. All triple products in $\mathcal{H}^{(1)}_{univ}$ are thus reduced to the coupling $\langle c_1, c_1, c_1\rangle$ of three tachyons.

Once the triple products are known, star products are easily obtained by inverting the non-degenerate bpz inner product. If $\{\Psi_i\}$ is a Fock basis for $\mathcal{H}^{(1)}_{univ}$, we define the dual basis $\{\Psi^i\}$ of $\mathcal{H}^{(2)}_{univ}$ by the bpz pairing

$$\langle \Psi_i, \Psi^j\rangle = \delta_i^j\,. \tag{2.5.2}$$

Then

$$\Psi_i * \Psi_j \equiv \sum_k \langle \Psi_i, \Psi_j, \Psi_k\rangle\, \Psi^k\,. \tag{2.5.3}$$

We automated this algorithm on a C++ computer code. We briefly highlight some features of our implementation:

- We use the factorization of the star product into matter and ghost sectors. The algorithm to find the triple products is executed separately in the two subsectors.

- We use cyclic and twist symmetry of the vertex to reduce the computation to triple products $\langle \Psi_i, \Psi_j, \Psi_k \rangle$ with a canonical ordering $i \leq j \leq k$.

- While in the matter sector the algorithm can be implemented in a straightforward way, in the ghost sector we need to face a slight complication. We are ultimately interested in triple products of ghost number one states, but the use of fermionic ghost conservation laws necessarily brings us outside the ghost number one subspace. We found it most efficient to use only conservation laws for the b_{-k} oscillators. A single application of a b-ghost conservation law reduces the evaluation of a $\langle 1,1,1 \rangle$ product (ghost number one in all three slots) to a sum of terms of the form $\langle 1,1,1 \rangle$ *and* $\langle 0,1,2 \rangle$. Products of this latter type can be treated by applying a b-conservation law to the first state (of ghost number zero), obtaining a sum of terms $\langle 1,1,1 \rangle$ and again (after cyclic rearrangement) $\langle 0,1,2 \rangle$. It is easy to show that this algorithm always terminates on the product of three tachyons. So we see that we only need to consider triple products of the form $\langle 0,1,2 \rangle$ besides the standard products $\langle 1,1,1 \rangle$.

- After each application of a conservation law, the resulting triple products on the r.h.s of (2.5.1) are processed using the Virasoro algebra or the ghost commutation relations, till all states are reduced to the Fock basis (2.2.6) with the canonical ordering $j_1 \geq \cdots \geq j_p$, $k_1 \geq \cdots \geq k_q$, $l_1 \geq \cdots \geq l_r$. The evaluation of expressions like $L_k L_{-n_1} \cdots L_{-n_i} c_1 |0\rangle$, with $n_1 \geq n_2 \cdots \geq n_i$ (and similarly for the ghosts) is thus a basic elementary operation. There is a critical gain in efficiency in evaluating beforehand all such expressions (up to the desired maximum level) and reading the results from a file, rather then re-computing them each time. The size of such a file grows only linearly with the number of modes, whereas the table of triple products grows cubically, so this strategy is not problematic from the point of view of memory occupation.

This algorithm can be easily extended to evaluate more general star products of string fields belonging to a larger space than $\mathcal{H}_{univ}$, for example the space relevant for tachyon

lump solutions [33] or Wilson line solutions [35]. One needs to enlarge the algebra of matter operators and consider the appropriate conservation laws.

2.5.2 Solving the Equations of Motion

Once all triple products at level L have been computed, the evaluation of the star product of two Siegel gauge string fields at level L involves $O(N_L^3)$ algebraic operations. It is clearly desirable to have an algorithm to solve the classical eom's that requires as few star products as possible. We tried various options, which can all be represented as a recursive procedure $\Psi^{(n+1)} = F(\Psi^{(n)})$, where $\Psi = F(\Psi)$ implies that Ψ is a solution.

The most obvious idea is to invert the kinetic term in Siegel gauge and define

$$F(\Psi) = -\frac{b_0}{L_0}\,(\Psi * \Psi)\,. \tag{2.5.4}$$

Clearly this iteration cannot converge since $F(\lambda\Psi) = \lambda^2 F(\Psi)$. There is a simple way to fix this problem, defining

$$\widetilde{F}(\Psi) = \left(\frac{T[\Psi]}{T[F(\Psi)]}\right)^2 F(\Psi)\,, \tag{2.5.5}$$

where $T[\Phi]$ indicates the coefficient of $c_1|0\rangle$ in the string field Φ. Unfortunately the algorithm based on the recursion $\widetilde{F}$ still fails to converge, and generically falls into stable two-cycles. An improved recursion is

$$F_\alpha(\Psi) = \alpha\,\Psi + (\alpha - 1)\frac{b_0}{L_0}\Psi * \Psi \tag{2.5.6}$$

where α is a real number which is chosen randomly in some reasonable interval (say $0.2 < \alpha < 0.8$) at each iteration step. This randomization breaks the cycles and the algorithm converges to a unique solution in about 20-30 steps. (The algorithm stops when the eom's are satisfied with the same accuracy as the accuracy of double-precision variables in C++, which have 15 significant digits). This algorithm is very robust with respect to the choice of the starting point Ψ_0, in fact at any given level L we found only one non-trivial solution.

A more efficient approach is the standard Newton algorithm. Recall that given a system of N algebraic equations in N variables, $f_i[x_\alpha] = 0$, $1 \le i, \alpha \le N$, the Newton recursion is

$$x_\alpha^{(n+1)} = x_\alpha^{(n)} - M^{-1}_{\alpha i}[x^{(n)}] f_i[x^{(n)}] \tag{2.5.7}$$

where the matrix $M_{i\alpha}[x]$ is defined as

$$M_{i\alpha}[x] \equiv \frac{\partial f_i}{\partial x_\alpha} \,. \tag{2.5.8}$$

In our case, the truncated Siegel equations of motion are a system of N_L algebraic equations in N_L variables (Table 2.3) and this method can be directly applied. It is interesting to write the Newton algorithm as a recursion for the Siegel string field itself. One finds the compact expression

$$\Psi^{(n+1)} = Q^{-1}_{\Psi^{(n)}}(\Psi^{(n)} * \Psi^{(n)}) \,. \tag{2.5.9}$$

Here the operator Q_Ψ is defined by

$$Q_\Psi \, \Phi \equiv Q_B \Psi + \Psi * \Phi + \Phi * \Psi \tag{2.5.10}$$

for any ghost number one string field Φ. The inverse operator Q_Ψ^{-1} is naturally defined by projecting onto the Siegel subspace. In other terms, for any ghost number two string field Σ, we look for the ghost number one string field $Q_\Psi^{-1}\Sigma$ that obeys

$$b_0 \, (Q_\Psi^{-1}\Sigma) = 0 \,, \quad c_0 b_0 \, \Sigma = c_0 b_0 \, Q_\Psi(Q_\Psi^{-1}) \, \Sigma \,. \tag{2.5.11}$$

The operator Q_Ψ has a natural physical interpretation: If Ψ is a solution of the OSFT eom's, then Q_Ψ is the new BRST operator obtained expanding the OSFT action around Ψ. Thus as we approach the fixed point of the Newton recursion, $Q_{\Psi^{(n)}}$ becomes a better and better approximation to the BRST operator around the tachyon vacuum.

In level-truncation, the action of the operator Q_Ψ in the Siegel subspace is represented by an $N_L \times N_L$ matrix. Since there is an order $O(N_L^3)$ algorithm to invert a matrix, the Newton recursion is not significantly more time-expensive than the evaluation of a single star product. The Newton algorithm is very fast, effectively squaring the accuracy at each step, and the solution is reached in four or five iterations. On our pc, the complete algorithm (computing the vertices from scratch and finding the tachyon solution) takes less than 10 seconds at level (10,20), and less than a minute at level (12,36)! There is however a rather critical dependence on the initial conditions: one finds convergence only from a starting point sufficiently close to the solution (it is enough to take *e.g.* $\Psi^{(0)} = 0.5 \, c_1|0\rangle$).

We compared the solution obtained with the Newton method with the solution found with the alternative algorithm described above, finding exact agreement up to level 16. (At level 18 the recursion (2.5.6) runs too slowly on our pc). This gives a strong check on the correctness of the solutions. As another check, we compared our results at level (10,20) with the results of Moeller and Taylor [14][15] , finding agreement to the tenth significant digit.

2.5.3 Tachyon Effective Action

To compute the tachyon effective action, we write the string field as

$$\Psi_L = T\, c_1|0\rangle + \widetilde{\Psi}_L\,, \tag{2.5.12}$$

where $\widetilde{\Psi}_L$ contains all the modes up to level L, except $c_1|0\rangle$. For a given numerical value of of the variable T, we solve the classical OSFT equations of motion for all the higher modes, using the Newton method. This gives $\Psi_L[T] = Tc_1|0\rangle + \widetilde{\Psi}_L[T]$ as a function of T. Plugging $\Psi_L[T]$ into the OSFT action[16] we obtain the effective tachyon potential $V_L(T)$.

The Newton algorithm that finds the solution $\widetilde{\Psi}_L[T]$ fails to converge if the variable T is outside an interval $[T_L^{min}, T_L^{max}]$. We find for example $T_{16}^{min} \sim -0.1$ and $T_{16}^{max} \sim 0.7$ (notice that both the tachyon vacuum and the perturbative vacuum are safely inside the convergence region). The failure of the numerical algorithm can be explicitly traced to the existence of other branches in the tachyon effective action. This phenomenon has been studied in [14, 44], where it has also been related to the non-perturbative failure of the Siegel gauge condition. In this chapter we only need $V_L(T)$ in an interval around the non-perturbative vacuum, which we take to be $0.54 \leq T \leq 0.55$. We postpone a more detailed investigation of the global behavior of the tachyon potential.

[15] We thank the authors of [14] for making their full results available to us.

[16] More precisely, $V_L(T) \equiv f(\Psi_L[T])$, where $f(\Psi)$ is defined in (2.2.3).

2.6 Concluding Remarks

Our results support the idea that level-truncation is a completely reliable approximation scheme for OSFT, with a convergent limit as the level is sent to infinity. All available exact predictions (notably the value of the vacuum energy) are accurately confirmed by the data. No inconsistencies seem to arise from the fact that gauge-invariance is broken at finite level, indeed we found strong evidence that it is smoothly restored as $L \to \infty$. Quantities computed in level-truncation exhibit a predictable dependence on level which is very well approximated by polynomials in $1/L$ (at least for the $(L, 3L)$ scheme). This allows reliable extrapolations to higher levels. Combining this observation with efficient computer algorithms based on conservation laws [12], we have developed very powerful numerical tools to study OSFT.

In this work we have focused on the universal subspace and obtained accurate data for the tachyon condensate. An obvious direction for further research is to use our results to learn about the kinetic term around the tachyon vacuum. The nature of this kinetic term is still rather mysterious. No perturbative open string states are expected to be present, and numerical evidence for this has already been obtained [40].

The most intriguing aspects of the non-perturbative vacuum are related to the elusive closed string states. In OSFT, amplitudes for external closed strings (on a surface with a least one boundary) are given by correlation functions of certain gauge-invariant open string functionals, the "open-closed" vertexes [50, 51, 52, 24]. It would be very interesting to compute such amplitudes in the non-perturbative vacuum. This should shed some light on the mechanism by which open string moduli are frozen in the tachyon vacuum, but closed string moduli are still present. There are promising ideas for how this may come about [24, 53, 54], but the actual mechanism realized in OSFT is still unknown.

Another avenue for future work is the application of our methods to more general classical solutions. It will be straightforward to extend our algorithms to include the matter states necessary to construct non-universal solutions, *e.g.* tachyon lump solutions [33] and Wilson

line solutions [35]. It would also be very nice to investigate numerically time-dependent solutions, and demonstrate the existence of tachyon matter [55] in OSFT. The study of several classical solutions will help to build the intuition that is needed for analytic progress.

2.7 Some Further Numerical Data

	$L=4$	$L=6$	$L=8$	$L=10$
$M=4$	0.54839904	0.54849677	0.54814406	0.54777626
$M=6$		0.54793242	0.54711284	0.54639593
$M=8$			0.54705245	0.54626520
$M=10$				0.54626093
	$L=12$	$L=14$	$L=16$	$L=18$
$M=4$	0.54745869	0.54719393	0.54697362	0.54678893
$M=6$	0.54581507	0.54534684	0.54496539	0.54465027
$M=8$	0.54561932	0.54509452	0.54466463	0.54430807
$M=10$	0.54560864	0.54507682	0.54464004	0.54427703
$M=12$	0.54560809	0.54507524	0.54463714	0.54427267
$M=14$		0.54507515	0.54463683	0.54427204
$M=16$			0.54463682	0.54427198
$M=18$				0.54427196

Table 2.10: Estimates $T_L^{(M)}$ for the tachyon vev obtained from extrapolations of the effective tachyon potential, at various orders M and for $L \leq 18$. Data in the $(L, 3L)$ scheme. By definition, the diagonal entries $T_L^{(M=L)}$ coincide with the exact computation from direct level-truncation at level $(L, 3L)$ (Table 2.4).

Matter	Ghost	$L=\infty$	$L=18$
		.5405	0.5443
	$b_{-1}c_{-1}$	-0.2248	-0.2205
L^m_{-2}		0.05721	0.05726
	$b_{-1}c_{-3}$	0.05928	0.05879
	$b_{-2}c_{-2}$	0.03650	0.03564
	$b_{-3}c_{-1}$	0.01976	0.01960
L^m_{-2}	$b_{-1}c_{-3}$	0.008627	0.008197
L^m_{-4}		-0.005049	-0.005079
$L^m_{-2}L^m_{-2}$		-0.000681	-0.000661
	$b_{-1}c_{-5}$	-0.03091	-0.03076
	$b_{-2}c_{-4}$	-0.01976	-0.01941
	$b_{-3}c_{-3}$	-0.01152	-0.01151
	$b_{-2}b_{-1}c_{-2}c_{-1}$	-0.008626	-0.008316
	$b_{-4}c_{-2}$	-0.00988	-0.009704
	$b_{-5}c_{-1}$	-0.00618	-0.006152
L^m_{-2}	$b_{-1}c_{-3}$	-0.003702	-0.003605
L^m_{-2}	$b_{-2}c_{-2}$	-0.003186	-0.003056
L^m_{-2}	$b_{-1}c_{-1}$	-0.001234	-0.001202
L^m_{-3}	$b_{-1}c_{-2}$	-0.000076	-0.0000775
L^m_{-3}	$b_{-2}c_{-1}$	-0.000038	-0.0000387
L^m_{-4}	$b_{-1}c_{-1}$	-0.0012	-0.001242
$L^m_{-2}L^m_{-2}$	$b_{-1}c_{-2}$	-0.000248	-0.000215
L^m_{-6}		0.001434	0.001446
$L^m_{-3}L^m_{-3}$		0.0000075	0.0000075
$L^m_{-4}L^m_{-2}$		0.000311	0.000310
$L^m_{-2}L^m_{-2}L^m_{-2}$		-0.0000049	-0.0000065

Table 2.11: Asymptotic values for the first coefficients of the tachyon condensate string field, compared with the $L = 18$ data. The $L = \infty$ results are obtained from the $M = 16$ extrapolation procedure based on the effective tachyon potential. Data in the $(L, 3L)$ scheme.

	$L=4$	$L=6$	$L=8$	$L=10$
$M=4$	-0.20567285	-0.21119493	-0.21392087	-0.21552208
$M=6$		-0.21181486	-0.21499106	-0.21690691
$M=8$			-0.21502535	-0.21697620
$M=10$				-0.21698254
	$L=12$	$L=14$	$L=16$	$L=18$
$M=4$	-0.21656852	-0.21730328	-0.21784642	-0.21826369
$M=6$	-0.21818110	-0.21908711	-0.21976325	-0.22028663
$M=8$	-0.21827982	-0.21920964	-0.21990503	-0.22044413
$M=10$	-0.21829559	-0.21923573	-0.21994128	-0.22048993
$M=12$	-0.21829570	-0.21923600	-0.21994171	-0.22049051
$M=14$		-0.21923603	-0.21994180	-0.22049069
$M=16$			-0.21994181	-0.22049069
$M=18$				-0.22049069

Table 2.12: Estimates for the vev of $c_{-1}|0\rangle$, obtained from extrapolations of the effective tachyon potential, at various orders M and for $L \leq 18$. Data in the $(L, 3L)$ scheme. By definition, the diagonal entries coincide with the exact computation from direct level-truncation at level $(L, 3L)$ (Table 2.4).

	$L=4$	$L=6$	$L=8$	$L=10$
$M=4$	0.056923526	0.057062755	0.057068423	0.057045668
$M=6$		0.057143493	0.057209039	0.057229308
$M=8$			0.057214101	0.057239805
$M=10$				0.057241066
	$L=12$	$L=14$	$L=16$	$L=18$
$M=4$	0.057018045	0.056991677	0.056968053	0.056947298
$M=6$	0.057233609	0.057231744	0.057227479	0.057222387
$M=8$	0.057248895	0.057251070	0.057250189	0.057247946
$M=10$	0.057252093	0.057256442	0.057257742	0.057257584
$M=12$	0.057252005	0.057256182	0.057257253	0.057256834
$M=14$		0.057256190	0.057257279	0.057256887
$M=16$			0.057257279	0.057256886
$M=18$				0.057256885

Table 2.13: Estimates for the vev of $L_{-2}^m c_1|0\rangle$, obtained from extrapolations of the effective tachyon potential, at various 'orders' M and for $L \leq 18$. Data in the $(L, 3L)$ scheme. By definition, the diagonal entries coincide with the exact computation from direct level-truncation at level $(L, 3L)$ (Table 2.4).

	$L=10$	$L=12$	$L=14$	$L=16$	$L=18$	$conj$
$r_{9,1}$	0.0259407	0.0261085	0.0262255	0.0263037	0.0263594	0.027063
$r_{7,3}$	0.0104886	0.0104825	0.0104948	0.0105063	0.0105159	0.0105868
$r_{5,5}$	0.00658638	0.0065773	0.00658224	0.00658778	0.00659265	0.0066192
$r_{11,1}$		-0.0200117	-0.0201181	-0.0201948	-0.0202469	-0.0208326
$r_{9,3}$		–0.00818159	-0.00817378	-0.00818	-0.00818657	-0.00824041
$r_{7,5}$		-0.00525767	-0.00524794	-0.00524929	-0.00525185	-0.00526601
$r_{13,1}$			0.0161045	0.0161778	0.0162318	0.0167396
$r_{11,3}$			0.00662999	0.00662276	0.0066262	0.0066689
$r_{9,5}$			0.00431978	0.00431134	0.00431141	0.00431915
$r_{7,7}$			0.00315946	0.00315272	0.00315241	0.0031549
$r_{15,1}$				-0.0133607	-0.0134141	-0.013871
$r_{13,3}$				-0.0055259	-0.00551968	-0.005553
$r_{11,5}$				-0.00363327	-0.00362626	-0.003629

Table 2.14: $(L, 3L)$ numerical results for the pattern coefficients $r_{n,m}$ for the tachyon condensate.

Chapter 3

Vacuum String Field Theory

3.1 Introduction and Summary

As reviewed in the introduction, the possibility of formulating open string field theory directly around the tachyon vacuum by guessing the form of the kynetic term has led to a proposal for such vacuum string field theory (VSFT), made in [56], and investigated in [57, 58, 59, 60, 61, 62, 63, 64, 65, 66, 67, 68, 69, 70, 71, 72].

Lacking an exact analytic solution of OSFT that describes the tachyon vacuum, it has not been possible yet to confirm directly, or to derive the VSFT action from first principles. Therefore VSFT has been tested for consistency. The main property of VSFT is that the kinetic operator, which in OSFT is the BRST operator, is chosen to be independent of the matter conformal theory, and is thus built only using the reparametrization ghost conformal field theory. Families of consistent candidates for this kinetic term, many of which are related via field redefinitions, were exhibited in [56]. It was possible to show that in VSFT the ratios of tensions of D-branes are correctly reproduced from the classical solutions purporting to represent such D-branes. This was seen in numerical experiments [57], and analytically using a boundary conformal field theory (BCFT) analysis whose key ingredient was the construction of the sliver state [59] associated with a general BCFT. The sliver is a projector in the star algebra of open strings (see for the next chapter for

more about projectors); its matter part is identified with the matter part of the solution representing a D-brane [57, 12, 73]. These tests did not select a particular kinetic term, in fact, data concerning the kinetic term, as long as it is only ghost dependent, cancel in the computation of ratios of tensions.

The formulation of VSFT cannot be considered complete unless a choice is made for its kinetic term. This choice seems necessary in order to understand confidently issues related to: (a) the normalization of the action giving us the brane tensions, (b) the spectrum of states around classical solutions, and (c) the emergence of closed string amplitudes. It has been suggested by Gross and Taylor [62] and by Schnabl [16] that it may be difficult to obtain solutions of VSFT with non-zero action if we insist on finite normalization of the kinetic term, leading to the conclusion that VSFT could be a workable, but singular limit of a better defined theory. Even if this is the case, it is important to find which particular choice of the kinetic term appears in this limit, and to investigate it thoroughly.

We are led by various pieces of evidence to a specific form of $\mathcal{Q}$ that is quite canonical and interesting. We should say at the outset that this form of $\mathcal{Q}$ leads to vanishing action for classical solutions unless its overall normalization is taken to be infinite. Hence regulation appears to be necessary, and as we shall discuss, possible. $\mathcal{Q}$ is a ghost insertion at the open string midpoint. More precisely it takes the form

$$\mathcal{Q} \propto \frac{1}{2i}(c(i) - c(-i)) = c_0 - (c_2 + c_{-2}) + (c_4 + c_{-4}) - \cdots \tag{3.1.1}$$

The open string is viewed as the arc $|z| = 1,\ \Im(z) > 0$, and thus $z = i$ is the midpoint. The selected $\mathcal{Q}$ arises from a consideration of the equations of motion in the Siegel gauge. Again, there was early evidence, based on level expansion [56], that for a finite kinetic term the Siegel gauge would yield zero action, and perhaps other gauges would be more suitable. But in the spirit of the present chapter, where we are willing to allow infinite normalization of the kinetic term, the Siegel gauge is a good starting point. This strategy was investigated in a stimulating paper by Hata and Kawano [66]. In the Siegel gauge the equation of motion $\Psi + b_0(\Psi * \Psi) = 0$ can be solved analytically not only in the matter sector, where the matter

sliver arises [73, 57], but also in the ghost sector[1] . It is then possible to compute $\Psi * \Psi$ and determine $\mathcal{Q}$ by requiring that that $\Psi * \Psi$ takes the form $-\mathcal{Q}\Psi$. The authors of [66] obtained expressions that could be analyzed numerically to glean the form of $\mathcal{Q}$. We have done this analysis and obtained evidence that the operator in (3.1.1) arises.

We can also do a rather complete analytical study using BCFT techniques to obtain a solution of the equations of motion with kinetic term given in (3.1.1). Here, as a first step we twist the ghost conformal field theory stress tensor to obtain an auxiliary BCFT where the ghost fields (c, b) have spins $(0, 1)$. This is clearly a natural operation in view of (3.1.1) since local insertions of dimension zero fields are simple to deal with. Moreover the resulting Virasoro operators commute with b_0 and the new SL(2,R) vacuum coincides with the zero momentum tachyon. Analytic treatment of the string field equations of motion becomes possible by rewriting the original equations in this twisted BCFT, and one finds that the solution is simply the sliver of the twisted BCFT! This geometrical approach gives a directly calculable expression for the Neumann coefficients characterizing the solution, as opposed to the analytic solution [66] that involves inverses and square roots of infinite matrices. We give numerical evidence that the solutions are one and the same.

Given that the classical solution in OSFT describing the tachyon vacuum is quite regular, one could wonder about the origin of the infinite normalization factor that appears in the choice of our kinetic term. The only way this could arise is if the variables of VSFT are related to those of OSFT by a singular field redefinition. We give examples of singular field redefinitions which could do this. They involve reparametrizations of the open string coordinate which are symmetric about the mid-point and hence preserve the $*$-product. We start with a $\mathcal{Q}$ that is sum of integrals of local operators made of matter and ghost fields, and consider a reparametrization that has an infinite squeezing factor around the mid-point. This transforms the various local operators (if they are primary) according to their scaling dimension, with the coefficient of the lowest dimension operator growing at fastest rate. Thus if the initial $\mathcal{Q}$ contains a piece involving the integral of c, then under

[1]The methodology was introduced in [73], but the correct expressions were given in [66].

this reparametrization the coefficient of this operator at the mid-point grows at the fastest rate. This not only provides a mechanism for explaining how the coefficient of the kinetic term could be infinite, but also explains how a kinetic operator of the form $c(i) - c(-i)$ emerges under such field redefinition even if the initial $\mathcal{Q}$ contains combinations of matter and ghost operators. This scenario supports a viewpoint, stressed in [62, 74], that a purely ghost $\mathcal{Q}$ is a singular representative of an equivalence class of kinetic operators having regular representatives built from matter and ghost operators. This singular limit is useful for some computations, *e.g.* ratios of tensions of D-branes, but working with a regular representative may be necessary for other computations like the overall normalization of the tension.

While the BRST operator Q_B happens to be invariant under the action of the reparametrization generators K_n that are symmetric about the the string midpoint, $\mathcal{Q}$ is not invariant under an arbitrary reparametrization of this type. Nevertheless, being a midpoint insertion, it transforms naturally under reparametrizations $z \to f(z)$ leaving invariant the midpoint. $c(\pm i)$ simply scale with factors proportional to the inverse of the derivatives of f at $\pm i$.

The expression for $\mathcal{Q}$ chosen here is rather special in that it is concentrated at the midpoint, and thus it would seem to be an operator that cannot be treated easily by splitting into left and right pieces. In particular the action of $\mathcal{Q}$ on the identity string field is not well defined. One can define $\mathcal{Q}$, however, as the limit of ghost insertions $\mathcal{Q}_\epsilon$ that approach symmetrically the midpoint as $\epsilon \to 0$, so that $\mathcal{Q}_\epsilon$ annihilates the identity for every non-zero ϵ. Although the action of $\mathcal{Q}_\epsilon$ on a state $|A\rangle$ can be represented as $|S_\epsilon * A\rangle - |A * S_\epsilon\rangle$ for an appropriate state $|S_\epsilon\rangle$, and thus $\mathcal{Q}_\epsilon$ would be seen to be an inner derivation, the state $|S_\epsilon\rangle$, involving insertion of a c on the identity string state just left of the midpoint, diverges as ϵ approaches zero. It thus seems unlikely that $\mathcal{Q}$ can be viewed as an inner derivation.

As mentioned above, $\mathcal{Q}$ defined this way has infinite normalization. Via a field redefinition we could make $\mathcal{Q}$ finite, at the cost of having an infinite overall normalization of the VSFT action. In either description regularization is necessary. We examine this directly at the gauge fixed level. Working in the Siegel gauge we introduce a parameter "a" to define

a deformation $S(a)$ of the gauge fixed action, such that the VSFT action is recovered for $a = \infty$. We introduce a multiplicative factor $\kappa_0(a)$ in front of the action to have a complete action $S_a = \kappa_0(a)S(a)$. In order to have a succesful regularization we require that $S(a)$ for any fixed a gives a finite value for the energy of the classical solution representing a D-brane. We find evidence that this is the case using the level expansion procedure. The prefactor $\kappa_0(a)$ can then be adjusted to give, by construction, the correct tension of the D-brane solution. The Feynman rules in this regulated VSFT generate correlation functions on world-sheet with boundary, with an additional factor involving a boundary perturbation, in close analogy with the effect of switching on constant tachyon background in boundary string field theory (BSFT) [75].

The level expansion analysis of the VSFT equations of motion leads to a surprise. The numerical data indicates that the solution is converging towards a projector that is different from the sliver. Like the sliver the new projector is a surface state. Considering that the sliver represents only one of an infinite set of projectors, this result is not totally unexpected. We provide a list of a whole class of surface states, refered to as the butterfly states, satisfying properties similar to the sliver. There is strong numerical evidence that the solution in level expansion is approaching one particular member of this class, − a state which is a product of the vacuum state of the left half string and the vacuum state of the right half-string. Further properties of the butterfly states are currently under investigation [76].

Another subject we discuss in great detail is that of closed strings.[2] Our analysis begins with the introduction of gauge invariant operators in OSFT. These open string field operators $\mathcal{O}_V(\Psi)$ are parametrized by on-shell closed string vertex operators V, and concretely arise from an open/closed transition vertex that emerged in studies of closed string factorization in OSFT loop diagrams[77]. This open/closed vertex was studied geometrically in [51] where it was shown that supplemented with the cubic open string vertex it would generate a cover of the moduli spaces of surfaces involving open and closed string punctures. In OSFT the correlation functions of such gauge invariant operators gives us the S-matrix

[2]For other attempts at getting closed strings from open string theory around the tachyon vacuum, see refs.[86, 87, 71].

elements of the corresponding closed string vertex opertors computed by integration over the moduli spaces of surfaces with boundaries.

We argue that in VSFT gauge invariant operators take an identical form, and confirm that our choice of $\mathcal{Q}$ is consistent with this. We then sketch how the correlation function of n gauge invariant operators in regulated VSFT could be related to the closed string S-matrix of the n associated vertex operators arising by integration over moduli spaces of surfaces *without boundaries*. This means that conventional pure closed string amplitudes could emerge from correlators of gauge invariant operators in VSFT. In this analysis we begin by noting that at the level of string diagrams $a = 0$ gives us back the usual OSFT Feynman rules, whereas as we take the regularization parameter a to ∞ this corresponds to selecting a region of the moduli space where the length of the boundary is going to zero. By a scaling transformation, and a factorization analysis we find that the amplitude reduces to one involving the n closed string vertex operators and an additional zero momentum closed string vertex operator of dimension ≤ 0. We show in detail how a new minimal area problem guarantees that the string diagrams for these $n+1$ closed string vertex operators do generate a cover of the relevant moduli space of closed Riemann surfaces. This shows how closed string moduli arise from the original open string moduli. If the only contribution to this $(n + 1)$-point amplitude comes from the term where the additional closed string vertex operator is the zero momentum dilaton, then we get back the n-point closed string amplitude of the external vertex operators. In the picture that emerges, closed string states are not introduced by hand – bulk operators of the CFT (necessary to even define the BCFT in question) are used to write open string functionals that represent the closed string states. Those are simply the gauge invariant operators of the theory. Since the analysis, however, is sensitive to the regularization procedure, complete understanding will require a better control of the regularization procedure.

3.2 The Proposal for a Ghost Kinetic Operator

In this section we state our proposal for the purely ghost kinetic operator $\mathcal{Q}$ in VSFT and discuss the novel gauge structure that emerges. The kinetic operator $\mathcal{Q}$ is a local insertion of a ghost field with infinite coefficient. We explain how such kinetic term could arise from less singular choices via reparametrizations that map much of the string to its midpoint. With this choice of kinetic term, the gauge symmetry is enlarged as compared with that of usual open string field theory. Finally we explain the sense in which $\mathcal{Q}$ is not an inner derivation, but can be viewed as the limit element of a set of derivations that are inner.

3.2.1 Ghost kinetic operator and gauge structure

The conjectured action for vacuum string field theory is given by [60]:

$$S = -\kappa_0 \Big[\frac{1}{2} \langle \Psi, \mathcal{Q}\Psi \rangle + \frac{1}{3} \langle \Psi, \Psi * \Psi \rangle \Big] , \tag{3.2.1}$$

where κ_0 is an overall normalization constant, $\mathcal{Q}$ is an operator made purely of the ghost world-sheet fields, $|\Psi\rangle$ is the string field represented by a ghost number one state in the matter-ghost BCFT, and $\langle A, B\rangle \equiv \langle A|B\rangle$ denotes the BPZ inner product of the states $|A\rangle$ and $|B\rangle$. If $\mathcal{Q}$ is nilpotent, is a derivation of the $*$-algebra, and satisfies the hermiticity condition $\langle \mathcal{Q}A|B\rangle = -(-1)^A \langle A|\mathcal{Q}|B\rangle$, then this action is invariant under the gauge transformation:

$$\delta|\Psi\rangle = \mathcal{Q}|\Lambda\rangle + |\Psi * \Lambda\rangle - |\Lambda * \Psi\rangle . \tag{3.2.2}$$

Although the constant κ_0 can be absorbed into a rescaling of Ψ, this changes the normalization of $\mathcal{Q}$. We shall instead choose a convenient normalization of $\mathcal{Q}$ and keep the constant κ_0 in the action as in eq.(3.2.1).

A class of kinetic operators $\mathcal{Q}$ satisfying the required constraints for gauge invariance was constructed in [56]. They have the form:

$$\mathcal{Q} = \sum_{n=0}^{\infty} u_n \mathcal{C}_{2n} , \tag{3.2.3}$$

where the u_n's are constants, and,

$$\begin{aligned} \mathcal{C}_n &= c_n + (-1)^n c_{-n} \quad n \neq 0, \\ \mathcal{C}_0 &= c_0 \,. \end{aligned} \tag{3.2.4}$$

We propose the following form of $\mathcal{Q}$ as a consistent and canonical choice of kinetic operator of VSFT:

$$\begin{aligned} \mathcal{Q} &= \frac{1}{2i}(c(i) - \bar{c}(i)) = \frac{1}{2i}(c(i) - c(-i)) = \sum_{n=0}^{\infty}(-1)^n \mathcal{C}_{2n} \,, \\ &= c_0 - (c_2 + c_{-2}) + (c_4 + c_{-4}) - \cdots \,. \end{aligned} \tag{3.2.5}$$

With this choice of $\mathcal{Q}$, the overall normalization κ_0 will turn out to be infinite, but we shall discuss a specific method for regularizing this infinity. In writing the expression for $\mathcal{Q}$ we are using the standard procedure of using the double cover of the open string world-sheet, with anti-holomorphic fields in the upper half plane being identified to the holomorphic fields in the lower half plane.

It is instructive to discuss in which sense the cohomology of $\mathcal{Q}$ so defined vanishes. In fact, the equation $\mathcal{Q}|\Psi\rangle = 0$ has no solutions if $|\Psi\rangle$ is a Fock space state. This is clear since any state built from finite linear combinations of monomials involving finite number of oscillators must have bounded level, while $\mathcal{Q}$ involves oscillators of all levels, including therefore infinitely many oscillators that do not annihilate the state $|\Psi\rangle$. Therefore, there is no standard Fock-space open string cohomology simply because there are no $\mathcal{Q}$ closed states in the Fock space. Suppose on the other hand that a more general state $|\chi\rangle$ is annihilated by $\mathcal{Q}$. Then, given that $\mathcal{Q}$ contains c_0 with unit coefficient, we have that $|\chi\rangle = \{\mathcal{Q}, b_0\}|\chi\rangle = \mathcal{Q}(b_0|\chi\rangle)$. Two things should be noted: $|\chi\rangle$ also has a local insertion at the string midpoint, and, it appears to be always $\mathcal{Q}$ trivial. The only subtlety here is that $(b_0|\chi\rangle)$ could be infinite in which case the triviality of $|\chi\rangle$ is questionable. In fact, this possibility arises for the case of gauge invariant operators related to closed strings, as will be discussed in section 3.7.

As discussed in earlier papers, field redefinitions relate many of the kinetic terms of the form (3.2.3). Typically these field redefinitions are induced by world-sheet reparametrization

symmetries which are symmetric around the string mid-point, and leaves the mid-point invariant. Such a reparametrization $z \to f(z)$, while acting on the kinetic operator of the form (3.2.5), will transform $\mathcal{Q}$ to $(2i)^{-1}((f'(i))^{-1}c(i) - (f'(-i))^{-1}c(-i))$. This leaves $\mathcal{Q}$ invariant if $f'(i) = 1$. Thus we see that the kinetic operator $\mathcal{Q}$ is actually invariant under a complex codimension 1 subgroup of the group generated by the K_n transformations.

The choice of kinetic term is special enough that the action defined by (3.2.1) and (3.2.5), generally invariant only under the gauge transformations in(3.2.2), is in fact invariant under two separate sets of gauge invariances:

$$\delta|\Psi\rangle = \mathcal{Q}|\Lambda\rangle\,, \tag{3.2.6}$$

and

$$\delta|\Psi\rangle = |\Psi * \Lambda\rangle - |\Lambda * \Psi\rangle\,. \tag{3.2.7}$$

In fact, the quadratic and the cubic terms in the action are separately invariant under each of these gauge transformations. These follow from the usual associativity of the $*$-product, nilpotence of $\mathcal{Q}$, and the additional relation:

$$\langle \mathcal{Q}A, B * C\rangle = 0\,, \tag{3.2.8}$$

which holds generally for arbitrary Fock space states A, B and C (other orderings, such as $\langle A, \mathcal{Q}B * C\rangle$ and $\langle A, B * \mathcal{Q}C\rangle$ also vanish). This relation in turn follows from the fact that $\mathcal{Q}$ involves operators $c, \bar{c}$ of dimension -1 inserted at i. As a result:

$$\langle \mathcal{Q}A, B * C\rangle = \langle f_1 \circ (\mathcal{Q}A(0)) f_2 \circ B(0) f_3 \circ C(0)\rangle \tag{3.2.9}$$

vanishes since the conformal transformation of $\mathcal{Q}$ gives a factor of $(f_1'(i))^{-1}$, and $f_1'(i)$ is infinite.[3] (f_i's are the standard conformal maps appearing in the definition of the $*$-product and have been defined below eq.(3.4.11)). The symmetry of the action under the homogeneous transformation (3.2.7) is in accordance with the conjecture that at the tachyon vacuum many broken symmetries should be restored[88, 87].

[3]For more general states, such as surface states or squeezed states the inner product (3.2.9) might be nonvanishing. For example, note that (3.2.8) *does not* imply that $\langle A, \mathcal{Q}B\rangle = 0$ as might be suggested by the identity $\langle A, \mathcal{Q}B\rangle = \langle \mathcal{I}, A * \mathcal{Q}B\rangle$. This latter expression does not vanish since the identity string field is not a Fock space state. We cannot therefore assume that $A * \mathcal{Q}B$ can be set to zero even for Fock space states A and B.

3.2.2 Possible origin of a singular $\mathcal{Q}$

While the VSFT action described here is singular, the original OSFT action is non-singular. In this subsection we shall attempt to understand how a singular action of the type we have proposed could arise from OSFT.

In order to compare VSFT with OSFT, it is more convenient to make a rescaling $|\Psi\rangle = (g_o^2\kappa_0)^{-1/3}|\widetilde{\Psi}\rangle$ to express the action as:

$$S = -\frac{1}{g_o^2}\Big[\frac{1}{2}\langle\widetilde{\Psi}, \widetilde{\mathcal{Q}}\widetilde{\Psi}\rangle + \frac{1}{3}\langle\widetilde{\Psi}, \widetilde{\Psi} * \widetilde{\Psi}\rangle\Big]\,, \tag{3.2.10}$$

where

$$\widetilde{\mathcal{Q}} = (g_o^2\kappa_0)^{1/3}\mathcal{Q}\,. \tag{3.2.11}$$

Here g_o is the open string coupling constant. OSFT expanded around the tachyon vacuum solution $|\Phi_0\rangle$ has the same form except that $\widetilde{\mathcal{Q}}$ is replaced by the operator $\widehat{\mathcal{Q}}$:

$$\widehat{\mathcal{Q}}|A\rangle = Q_B|A\rangle + |\Phi_0 * A\rangle - (-1)^A|A * \Phi_0\rangle\,. \tag{3.2.12}$$

Since κ_0 is infinite, so is $\widetilde{\mathcal{Q}}$. On the other hand, since the classical solution $|\Phi_0\rangle$ describing the tachyon vacuum in OSFT is perfectly regular, we expect $\widehat{\mathcal{Q}}$ to be regular. Thus one could ask how a singular $\widetilde{\mathcal{Q}}$ of the kind we are proposing could arise. Clearly for this to happen the OSFT and the VSFT variables must be related by a singular field redefinition. We shall now provide an example of such field redefinition which not only explains how the coefficient of the kinetic term could be infinite, but also provides a mechanism by which ghost kinetic operator proportional to $c(i) - c(-i)$ could arise.

Let us begin with a $\widetilde{\mathcal{Q}}$ of the form:

$$\widetilde{\mathcal{Q}} = \sum_r \int d\sigma a_r(\sigma) O_r(\sigma)\,, \tag{3.2.13}$$

where a_r are smooth functions of σ and O_r are local operators of ghost number 1, constructed from products of b, c, and matter stress tensor. The above expression is written on the double cover of the strip so that σ runs from $-\pi$ to π and we only have holomorphic fields. Since a_r are finite such a $\widetilde{\mathcal{Q}}$ might be obtained from OSFT by a non-singular field

redefinition. Given this $\widetilde{\mathcal{Q}}$, we can generate other equivalent $\widetilde{\mathcal{Q}}$ by reparametrization of the open string coordinate σ to $f(\sigma)$ such that $f(\pi-\sigma)=\pi-f(\sigma)$ for $0\leq\sigma\leq\pi$ and $f(-\sigma-\pi)=-\pi-f(\sigma)$ for $-\pi\leq\sigma\leq 0$. Such reparametrizations do not change the structure of the cubic term but changes the kinetic term. If O_r corresponds to a primary field of dimension h_r, then under this reparametrization $\widetilde{\mathcal{Q}}$ transforms to:

$$\sum_r \int d\sigma a_r(\sigma)(f'(\sigma))^{h_r} O_r(f(\sigma))\,. \tag{3.2.14}$$

Consider now a reparametrization such that $f'(\pm\pi/2)$ is small and in particular $\int d\sigma (f'(\sigma))^{-1}$ gets a large contribution from the region around $\sigma=\pm\pi/2$. Let us for example take $f'(\sigma)\simeq(\sigma\mp\frac{\pi}{2})^2+\epsilon^2$ for $\sigma\simeq\pm\pi/2$.[4] In this case the dominant contribution to eq.(3.2.14) will come from the lowest dimensional operator c as long as the corresponding a_r does not vanish at $\pm\pi/2$, and the transformed $\widetilde{\mathcal{Q}}$ will be proportional to

$$\frac{1}{\epsilon}(c(\pi/2)+c(-\pi/2))\,. \tag{3.2.15}$$

The relative coefficient between $c(\pi/2)$ and $c(-\pi/2)$ has been fixed by requiring twist invariance. In the upper half plane coordinates ($z=e^{\tau+i\sigma}$) this is proportional to $\epsilon^{-1}(c(i)-c(-i))$, – precisely the kinetic term of our choice. Thus this analysis not only shows how a divergent coefficient could appear in front of the kinetic term, but also explains how such singular field redefinition could give rise to the pure ghost kinetic term even if the original $\widetilde{\mathcal{Q}}$ contained matter operators.

If O_r is not a primary operator, then its transformation properties under a reparametrization is more complicated. Nevertheless, given any such operator containing a product of matter and ghost pieces, the dominant contribution to its transform under a singular reparametrization of the form described above will come from the lowest dimensional operator, i.e. c or $\bar{c}$, unless the coefficients of these terms cancel between various pieces (which will happen, for example, if the operator is a (total) Virasoro descendant of a primary other than c, *e.g.* the BRST current).

[4] Another special case of this would be a choice of $f(\sigma)$ where a finite region around the mid-point is squeezed to an infinitesimal region.

To summarize, according to the above scenario the singular $\widetilde{\mathcal{Q}}$ of VSFT given in eq.(3.2.11), (3.2.5) is a singular member of an equivalence class of $\widetilde{\mathcal{Q}}$'s whose generic member is non-singular and is made of matter and ghost operators. The singular pure ghost representative is useful for certain computations *e.g.* ratios of tensions of D-branes, construction of multiple D-brane solutions etc., whereas the use of a regular member may be necessary for other computations *e.g.* overall normalization of the D-brane tension, closed string amplitudes etc.

Singular reparametrizations of the kind discussed above could also explain the appearance of a sliver or other projectors as classical solutions of VSFT. As an example we shall illustrate how an appropriate singular reparametrization could take any finite $|m\rangle$ wedge state to the sliver. From refs.[12, 59] we know that the wave-functional of a wedge state $|m\rangle$ can be represented as a result of functional integration on a wedge of angle $\alpha_m = 2\pi(m-1)$ in a complex ($\widehat{w}$) plane, bounded by the radial lines $\widehat{w} = \rho e^{i\frac{\pi}{2}}$ and $\widehat{w} = \rho e^{i(\frac{\pi}{2}+2\pi(m-1))}$. We put open string boundary condition on the arc, and identify the lines $\widehat{w} = \rho e^{i\frac{\pi}{2}}$ and $\widehat{w} = \rho e^{i(\frac{\pi}{2}+2\pi(m-1))}$ as the left and the right halves of the string respectively. In particular if σ denotes the coordinate on the open string with $0 \le \sigma \le \pi$, then the line $\widehat{w} = \rho e^{i\frac{\pi}{2}}$ is parametrized as:

$$\widehat{w} = \frac{1+ie^{i\sigma}}{1-ie^{i\sigma}} = i\tan(\frac{\pi}{4}-\frac{\sigma}{2})\,, \qquad \text{for} \quad 0 \le \sigma \le \frac{\pi}{2}\,. \tag{3.2.16}$$

From the above description it is clear that we can go from an wedge state $|m\rangle$ to an wedge state $|n\rangle$ via a reparametrization:

$$(\widehat{w}'/i) = (\widehat{w}/i)^{\gamma}, \qquad \gamma = \frac{\alpha_n}{\alpha_m} = \frac{n-1}{m-1}\,. \tag{3.2.17}$$

In terms of σ, this corresponds to the transformation:

$$\tan(\frac{\pi}{4}-\frac{\sigma'}{2}) = \tan^{\gamma}(\frac{\pi}{4}-\frac{\sigma}{2})\,. \tag{3.2.18}$$

In order to get the sliver, we need to take the $n \to \infty$ limit. In this limit $\gamma \to \infty$. Since for $0 < \sigma < \pi/2$, $|\tan(\pi/4 - \sigma/2)| < 1$, we see that as $\gamma \to \infty$ any σ in the range $0 < \sigma < \pi/2$ gets mapped to the point $\sigma' = \pi/2$. This corresponds to squeezing the whole string into the

mid-point. This shows that using such singular reparametrization we can transform any wedge state $|m\rangle$ into the sliver, and provides further evidence to the conjecture that the VSFT action with pure ghost kinetic term arises from OSFT expanded around the tachyon vacuum under such singular reparametrization.

3.2.3 Action of $\mathcal{Q}$ on the identity state

Among the constraints for gauge invariance is the derivation property

$$\mathcal{Q}(A * B) = \mathcal{Q}A * B + (-1)^A A * \mathcal{Q}B \tag{3.2.19}$$

which must hold. This property indeed holds for each $\mathcal{C}_n$ and therefore holds for the chosen $\mathcal{Q}$. On the other hand, there was a criterion related to the identity string field $\mathcal{I}$ that distinguished two classes of kinetic operators. There are candidate operators for $\mathcal{Q}$ which viewed as integrals over the string, have vanishing support at the string midpoint. Those operators annihilate the identity and they split into left and right parts, as discussed in [62]. On the other hand there are operators, such as c_0, which do not kill the identity.[5]

As we will discuss below, our choice of $\mathcal{Q}$, using insertions precisely at the midpoint, does not annihilate the identity. In fact, a direct computation shows that $\mathcal{Q}\mathcal{I}$ is divergent. However, we will also show that $\mathcal{Q}$ can be considered as the limit of a sequence such that every member of the sequence annihilates the identity state.

Recall that $|\mathcal{I}\rangle$ is defined through the relation:

$$\langle \mathcal{I}|\phi\rangle = \langle h_1 \circ \phi(0)\rangle_D \tag{3.2.20}$$

for any Fock space state $|\phi\rangle$. Here $h \circ \phi(0)$ denotes the conformal transform of the vertex operator $\phi(0)$ by the conformal map h, $\langle\ \rangle_D$ denotes correlation function on a unit disk, and the conformal map h_N for any N is defined as

$$h_N(z) = \Big(\frac{1+iz}{1-iz}\Big)^{2/N}. \tag{3.2.21}$$

[5]Since they are derivations of the star algebra we believe they should be viewed as outer derivations. Indeed, an inner derivation D_ϵ acts as $D_\epsilon A = \epsilon * A - A * \epsilon$, so it is reasonable to demand that all inner derivations annihilate the identity string field. Not being inner, c_0 would have to be outer.

Thus $\langle \mathcal{I}|c(i)|\phi\rangle = \langle h_1 \circ c(i) h_1 \circ \phi(0)\rangle$ is divergent since $h_1 \circ c(i) = h_1'(i)^{-1} c(0)$ and $h_1'(i)$ vanishes.

We now define a new operator $\mathcal{Q}_\epsilon$ by making the replacements

$$\begin{aligned} c(i) &\rightarrow \frac{1}{2}\Big(e^{-i\epsilon}c(ie^{i\epsilon}) + e^{i\epsilon}c(ie^{-i\epsilon})\Big), \\ c(-i) &\rightarrow \frac{1}{2}\Big(e^{-i\epsilon}c(-ie^{i\epsilon}) + e^{i\epsilon}c(-ie^{-i\epsilon})\Big), \end{aligned} \tag{3.2.22}$$

in (3.2.5). In the local coordinate picture where the open string is represented by the arc $|\xi| = 1$ in the upper ξ half-plane, this corresponds to splitting the midpoint insertion $c(\xi = i)$ into two insertions, one on the left-half and the other on the right-half of the string. The splitting is such that for $\epsilon \to 0$ we recover the midpoint insertion, but this time

$$\langle \mathcal{I}|\Big(e^{-i\epsilon}c(ie^{i\epsilon}) + e^{i\epsilon}c(ie^{-i\epsilon})\Big) = 0\,, \tag{3.2.23}$$

as can be verified using equations (3.2.20), (3.2.21) – the point being that by the geometry of the identity conformal map the two operators land on the same point but with opposite sign factors multiplying them, and thus cancel each other out exactly.

The replacements (3.2.22) in (3.2.5) lead to the operator $\mathcal{Q}_\epsilon$:

$$\begin{aligned} \mathcal{Q}_\epsilon &= \frac{1}{4i}\Big(e^{-i\epsilon}c(ie^{i\epsilon}) + e^{i\epsilon}c(ie^{-i\epsilon}) - e^{-i\epsilon}c(-ie^{i\epsilon}) - e^{i\epsilon}c(-ie^{-i\epsilon})\Big) \\ &= \sum_{n=0}^{\infty}(-1)^n \mathcal{C}_{2n}\cos(2n\epsilon)\,. \end{aligned} \tag{3.2.24}$$

Because of (3.2.23), and an analogous result for the split version of $c(-i)$, the operator $\mathcal{Q}_\epsilon$ defined above annihilates the identity $|\mathcal{I}\rangle$ for every $\epsilon \neq 0$. In addition, being a superposition of the anti-commuting derivations $\mathcal{C}_n$, it squares to zero, and is a derivation. It also has the expected BPZ property

$$\langle \mathcal{Q}_\epsilon A, B\rangle = -(-)^A \langle A, \mathcal{Q}_\epsilon B\rangle\,. \tag{3.2.25}$$

Therefore, $\mathcal{Q}_\epsilon$ satisfies all the conditions for gauge invariance.

Since $\mathcal{Q}_\epsilon$ approaches the $\mathcal{Q}$ defined in (3.2.5) as $\epsilon \to 0$, we could *define*

$$\mathcal{Q} \equiv \lim_{\epsilon \to 0} \mathcal{Q}_\epsilon\,. \tag{3.2.26}$$

Defined in this way, $\mathcal{Q}$ annihilates the identity. Acting on Fock space states, such care is not necessary, and we can simply use (3.2.5), but in general the definition (3.2.26) is useful.

We can express the action of $\mathcal{Q}_\epsilon$ on a state $|A\rangle$ as an inner derivation:

$$\mathcal{Q}_\epsilon|A\rangle = |S_\epsilon * A\rangle - (-1)^A|A * S_\epsilon\rangle\,, \tag{3.2.27}$$

where

$$|S_\epsilon\rangle = \frac{1}{4i}\Big(e^{-i\epsilon}c(ie^{i\epsilon}) - e^{i\epsilon}c(-ie^{-i\epsilon})\Big)|\mathcal{I}\rangle\,. \tag{3.2.28}$$

However note that $|S_\epsilon\rangle$ diverges in the $\epsilon \to 0$ limit since $\langle S_\epsilon|\phi\rangle$ for any Fock space state $|\phi\rangle$ involves $(h_1'(ie^{i\epsilon}))^{-1}$, which diverges as $\epsilon \to 0$. Thus while the $\mathcal{Q}_\epsilon$ operators may be viewed as inner derivations for $\epsilon \neq 0$, it does not follow that $\mathcal{Q}$ can also be viewed as an inner derivation.

3.3 Algebraic Analysis of the Classical Equations

In this section we reconsider the algebraic analysis of the classical equations of motion of VSFT in the Siegel gauge carried out in refs.[66, 73]. The main result of the analysis of [66] is an expression for the coefficients u_n defining $\mathcal{Q}$ (see (3.2.3)) in terms of infinite matrices of Neumann coefficients in the ghost sector of the three string vertex. We shall summarize briefly their results and evaluate numerically the coefficients u_n, finding striking evidence that the $\mathcal{Q}$ that emerges is indeed that in (3.2.5).

As usual we begin by looking for a factorized solution:

$$\Psi = \Psi_g \otimes \Psi_m\,, \tag{3.3.1}$$

with Ψ_g and Ψ_m denoting ghost and matter pieces respectively, and satisfying:

$$|\Psi_m\rangle = |\Psi_m *^m \Psi_m\rangle\,, \tag{3.3.2}$$

and

$$\mathcal{Q}|\Psi_g\rangle + |\Psi_g *^g \Psi_g\rangle = 0\,. \tag{3.3.3}$$

If we start with a general class of kinetic operators of the form (3.2.3) with u_0 normalized to one, and make the Siegel gauge choice

$$b_0|\Psi\rangle = 0\,, \tag{3.3.4}$$

then the equation of motion (3.3.3) takes the form

$$|\Psi_g\rangle + b_0|\Psi_g * \Psi_g\rangle = 0\,. \tag{3.3.5}$$

Note that these contain only part of the equations (3.3.3) which are obtained by varying the action with respect to fields satisfying the Siegel gauge condition. The full set of equations will be used later for determining $\mathcal{Q}$.

The solution for $|\Psi_m\rangle$ can be taken to be any of the solutions discussed in [58, 59, 60, 61]. The solution for $|\Psi_g\rangle$ is given as follows. Denote the ghost part of the 3-string vertex as:[6]

$$|V_g\rangle_{123} = \exp\Big(\sum_{r,s=1}^{3}\sum_{n\geq 1,m\geq 0} c_{-n}^{(r)}\,\widetilde{V}_{nm}^{rs}\,b_{-m}^{(s)}\Big)\prod_{r=1}^{3}(c_0^{(r)}c_1^{(r)})|0\rangle_{(1)}\otimes|0\rangle_{(2)}\otimes|0\rangle_{(3)}\,, \tag{3.3.6}$$

where $c_n^{(r)}$, $b_n^{(r)}$ are the ghost oscillators associated with the r-th string and $|0\rangle_{(r)}$ denotes the SL(2,R) invariant ghost vacuum of the r-th string. The matrices $\widetilde{V}_{mn}^{rs}$ have cyclic symmetry $\widetilde{V}_{mn}^{rs} = \widetilde{V}_{mn}^{r+1,s+1}$ as usual. We now define:

$$\begin{aligned}
&(\widetilde{V}_0)_{mn} = \widetilde{V}_{mn}^{rr}, \qquad (\widetilde{V}_\pm)_{mn} = \widetilde{V}_{mn}^{r,r\pm1}, \qquad \widetilde{C}_{mn} = (-1)^m\delta_{mn},\\
&(\widetilde{v}_0)_m = \widetilde{V}_{m0}^{rr}, \qquad (\widetilde{v}_\pm)_m = \widetilde{V}_{m0}^{r,r\pm1}, \qquad \text{for}\quad 1\leq m,n<\infty\,,
\end{aligned} \tag{3.3.7}$$

$$\widetilde{M}_0 = \widetilde{C}\widetilde{V}_0, \qquad \widetilde{M}_\pm = \widetilde{C}\widetilde{V}_\pm\,, \tag{3.3.8}$$

and,

$$\widetilde{T} = \frac{1}{2\widetilde{M}_0}\Big(1+\widetilde{M}_0 - \sqrt{(1-\widetilde{M}_0)(1+3\widetilde{M}_0)}\Big), \qquad \widetilde{S} = \widetilde{C}\widetilde{T}\,. \tag{3.3.9}$$

The solution to eq.(3.3.5) is then given by:

$$|\Psi_g\rangle = \mathcal{N}_g\exp\Big(\sum_{n,m\geq 1} c_{-n}\widetilde{S}_{nm}b_{-m}\Big)\,c_1|0\rangle\,, \tag{3.3.10}$$

[6]The coefficients $\widetilde{V}_{nm}^{rs}$ are related the ghost Neumann functions $\widetilde{N}_{mn}^{sr}$ introduced in ref.[78] as $\widetilde{V}_{nm}^{rs} = -n\,\widetilde{N}_{mn}^{sr}$.

for some appropriate normalization constant $\mathcal{N}_g$. Given the solution $|\Psi_g\rangle$, one can explicitly construct $|\Psi_g *^g \Psi_g\rangle$. It was shown in ref.[66] that

$$|\Psi_g *^g \Psi_g\rangle = -\Big(c_0 + \sum_{n\geq 1} u_n \mathcal{C}_n\Big)|\Psi_g\rangle, \tag{3.3.11}$$

where the vector $u = \{u_1, u_2, \ldots\}$ is given by:

$$\begin{aligned} u &= (1-\widetilde{T})^{-1}\Big[\ \widetilde{v}_0 \\ &+(\widetilde{M}_+, \widetilde{M}_-)(1-\widetilde{M}_0)^{-1}(1+\widetilde{T})^{-1}\begin{pmatrix} 1-\widetilde{T}\widetilde{M}_0 & \widetilde{T}\widetilde{M}_+ \\ \widetilde{T}\widetilde{M}_- & 1-\widetilde{T}\widetilde{M}_0\end{pmatrix}\widetilde{T}\begin{pmatrix}\widetilde{v}_+ \\ \widetilde{v}_-\end{pmatrix}\ \Big]. \end{aligned} \tag{3.3.12}$$

This expression was simplified in refs.[67, 70], but we use eq.(3.3.12) for our analysis. Using eqs.(3.3.3) and (3.3.11) we see that $\mathcal{Q}$ can be identified as:

$$\mathcal{Q} = c_0 + \sum_{n\geq 1} u_n \mathcal{C}_n\,. \tag{3.3.13}$$

The coefficients $\widetilde{V}^{rs}_{mn}$ and hence the matrices $\widetilde{M}_0$, $\widetilde{M}_\pm$, $\widetilde{T}$ and the vectors $\widetilde{v}_0$, $\widetilde{v}_\pm$ can be calculated using the results of [78]. In turn, this can be used to calculate u_n from eq.(3.3.12). For odd n, u_n vanishes by twist symmetry. The numerical results for u_n's for even n at different levels of approximation, and the values extrapolated to infinite level using a fit, have been shown in table 3.1. The results are clearly consistent with $u_{2n} = (-1)^n$ and hence the choice of $\mathcal{Q}$ given in (3.2.5).

3.4 BCFT Analysis of Classical Equations of Motion

In this section we shall discuss a method of solving the equations of motion (3.3.3) using the techniques of boundary conformal field theory. As a first step we introduce a twisted version of the ghost CFT where the ghost field $c(z)$ is of dimension zero. We also establish a one to one map between the states of the twisted and untwisted theory. We then study the star product in the twisted theory and relate it to that in the untwisted theory. The upshot of this analysis is that with our $\mathcal{Q}$ the ghost part of the standard string field equations is solved by the state representing the sliver of the twisted ghost CFT. We conclude with a

L	f_2	f_4	f_6	f_8	f_{10}
40	-0.87392	0.830099	-0.803468	0.784561	-0.770184
80	-0.881488	0.840223	-0.814839	0.796433	-0.781999
160	-0.888335	0.849592	-0.825743	0.808389	-0.7947
240	-0.892017	0.85465	-0.831672	0.814956	-0.801763
320	-0.894496	0.858053	-0.835666	0.819388	-0.806544
∞	-0.97748	0.96864	-0.961296	0.953502	-0.944372

Table 3.1: Numerical results for f_{2n} at different level approximation. The last row shows the interpolation of the various results to $L = \infty$, obtained via a fitting function of the form $a_0 + a_1/\ln(L) + a_2/(\ln(L))^2 + a_3/(\ln(L))^3$.

direct CFT construction of the Fock space representation of this twisted sliver and find that it compares well with the algebraic construction of the solution [66].

3.4.1 Twisted Ghost Conformal Theory

We introduce a new conformal field theory CFT$'$ by changing the energy momentum tensor on the strip as

$$T'(w) = T(w) - \partial j_g(w), \qquad \bar{T}'(\bar{w}) = \bar{T}(\bar{w}) - \bar{\partial}\bar{j}_g(\bar{w})\,, \tag{3.4.1}$$

where T, $\bar{T}$ denote the energy momentum tensor in the original matter-ghost system, T', $\bar{T}'$ denote the energy momentum tensor of new theory, and $j_g = cb$, $\bar{j}_g = \bar{c}\bar{b}$ are the ghost number currents in the original theory. The ghost operators in the new theory, labeled as b', c', $\bar{b}'$, and $\bar{c}'$, to avoid confusion, have spins (1,0), (0,0), (0,1) and (0,0) respectively, and satisfy the usual boundary condition $b' = \bar{b}'$, $c' = \bar{c}'$ on the real axis. A few important facts about the b', c' system are given below:

- The first order system (b', c') has a central charge of minus two.
- Since c' has dimension zero, the SL(2,R) vacuum $|0'\rangle$ of this system, defined as usual

in the complex plane, satisfies

$$c'_{n\geq 1}|0'\rangle = 0\,. \tag{3.4.2}$$

- The Virasoro operators from T' commute with b_0.

The mode expansions of T, T' and j_g on the cylinder with coordinate $w = \tau + i\sigma$ (obtained from the double cover of the strip, identifying the holomorphic fields at (τ, σ) with anti-holomorphic fields at $(\tau, -\sigma)$ for $-\pi \leq \sigma \leq 0$) are given by:

$$T(w) = \sum_n L_n e^{-nw} - \frac{c}{24}, \quad T'(w) = \sum_n L'_n e^{-nw} - \frac{c'}{24}, \quad j_g(w) = \sum_n j_n e^{-nw}, \tag{3.4.3}$$

where $c = 0$ is the total central charge of the original theory and $c' = 24$ is the total central charge of the auxiliary ghost-matter theory. It follows from (3.4.1) and (3.4.3) that

$$L'_n = L_n + n j_n + \delta_{n,0}\,. \tag{3.4.4}$$

In the path integral description the euclidean world-sheet actions $\mathcal{S}$ and $\mathcal{S}'$ of the two theories are related as:

$$\mathcal{S}' = \mathcal{S} + \frac{i}{2\pi}\int d^2\xi \sqrt{\gamma} R^{(2)}(\varphi + \bar{\varphi})\,, \tag{3.4.5}$$

where ξ denotes the world-sheet coordinates, γ denotes the Euclidean world-sheet metric, $R^{(2)}$ is the scalar curvature computed from the metric γ and φ, $\bar{\varphi}$ are the bosonized ghost fields related to the anti-commuting ghost fields as follows:

$$c \sim e^{i\varphi}, \quad \bar{c} \sim e^{i\bar{\varphi}}, \quad b \sim e^{-i\varphi}, \quad \bar{b} \sim e^{-i\bar{\varphi}}\,, \tag{3.4.6}$$

and

$$c' \sim e^{i\varphi}, \quad \bar{c}' \sim e^{i\bar{\varphi}}, \quad b' \sim e^{-i\varphi}, \quad \bar{b}' \sim e^{-i\bar{\varphi}}\,. \tag{3.4.7}$$

It should be noted that on general world-sheets the φ field has different dynamics in the two theories. On the strip, however, the world-sheet curvature vanishes and we have $\mathcal{S} = \mathcal{S}'$. The φ fields in the two theories can be identified, and hence the above equations allow an identification of states in the two theories by the following map between the oscillators and the vacuum states of the two theories:

$$b_n \leftrightarrow b'_n, \qquad c_n \leftrightarrow c'_n, \qquad c_1|0\rangle \leftrightarrow |0'\rangle \qquad \langle 0|c_{-1} \leftrightarrow \langle 0'|\,, \tag{3.4.8}$$

where $|0\rangle$ and $|0'\rangle$ denote the SL(2,R) invariant vacua in the original theory and the auxiliary theory respectively. The last two relations follows from the oscillator identification and (3.4.2). We thus see that the zero momentum tachyon in the original theory is the SL(2,R) vacuum of CFT$'$. The two vacua are normalized as

$$\langle 0|c_{-1}c_0c_1|0\rangle = \langle 0'|c_0'|0'\rangle = V^{(26)}\,, \tag{3.4.9}$$

where $V^{(26)}$ denotes the volume of the 26-dimensional space-time. We shall denote by $\langle\cdots\rangle$ and $\langle\cdots\rangle'$ the expectation values of a set of operators in $|0\rangle$ and $|0'\rangle$ respectively. Also given a state $|A\rangle$ we shall denote by A and A' the vertex operators of the state in the two theories in the upper half plane coordinates. Thus:

$$|A\rangle = A(0)|0\rangle = A'(0)|0'\rangle\,. \tag{3.4.10}$$

Finally we note that BPZ conjugation in the twisted theory, obtained by the map $|0'\rangle \to \langle 0'|$, $c_n \to (-1)^n c_{-n}$, and $b_n \to (-1)^{n+1}b_{-n}$, can be shown to give a state identical to the one obtained by BPZ conjugation in the original theory, given by $|0\rangle \to \langle 0|$, $c_n \to (-1)^{n+1}c_{-n}$, and $b_n \to (-1)^n b_{-n}$. Thus we do not need to use separate symbols for the BPZ inner product in the two theories.

3.4.2 Relating Star Products and the analytic solution

Next we would like to find the relationship between the star-products in the two theories. We shall denote by $*$ and $*'$ the star products in the original and the auxiliary theory respectively. Thus:

$$\begin{aligned}\langle A|B*C\rangle &= \langle f_1\circ A(0)f_2\circ B(0)f_3\circ C(0)\rangle,\\ \langle A|B*'C\rangle &= \langle f_1\circ A'(0)f_2\circ B'(0)f_3\circ C'(0)\rangle'\,,\end{aligned} \tag{3.4.11}$$

where we have $f_1(z) = h_2^{-1}(h_3(z))$, $f_2(z) = h_2^{-1}(e^{2\pi i/3}h_3(z))$, and $f_3(z) = h_2^{-1}(e^{4\pi i/3}h_3(z))$, with $h_N(z)$ defined as in eq.(3.2.21), are the standard conformal maps used in the definition of the $*$ product. The simplest way to relate these two star products is to use the path integral prescription for $\langle A|B*C\rangle$ and $\langle A|B*'C\rangle$ given in [6]. In this description the star

product is a result of path integral over a two dimensional surface in which three strips, each of of width π and infinitesimal length ϵ, representing the external open strings, are joined together such that the second half of the r-th string coincides with the first half of the $(r+1)$-th string, for $1 \leq r \leq 3$, with the identification $r \equiv r+3$. The result is a flat world-sheet with a single defect at the common mid-point of the three strings where we have a deficit angle of $-\pi$. Thus for this geometry $\int d^2\xi \sqrt{\gamma} R^{(2)}$ gets a contribution of $-\pi$ from the mid-point, and $\mathcal{S}$ and $\mathcal{S}'$ are related as:

$$\mathcal{S}' = \mathcal{S} - \frac{i}{2}(\varphi(M) + \bar{\varphi}(M)) \tag{3.4.12}$$

where M denotes the location of the midpoint. Since the action appears in the path integral through the combination $e^{-\mathcal{S}}$, we have

$$\langle f_1 \circ A(0) f_2 \circ B(0) f_3 \circ C(0) \rangle = K_0 \langle f_1 \circ A'(0) f_2 \circ B'(0) f_3 \circ C'(0) \sigma^{+\prime}(M) \sigma^{-\prime}(M) \rangle' \tag{3.4.13}$$

where K_0 is an overall finite normalization constant,

$$\sigma^{+\prime} = e^{i\varphi/2}, \qquad \sigma^{-\prime} = e^{i\bar{\varphi}/2}, \tag{3.4.14}$$

and $M = f_1(i) = f_2(i) = f_3(i)$. The primes on $\sigma^{\pm\prime}$ denote that these are operators in the auxiliary b', c' system. These operators have conformal weights $(-1/8, 0)$ and $(0, -1/8)$ respectively. We have explicitly verified eq.(3.4.13) using specific choices of the states $|A\rangle$, $|B\rangle$, $|C\rangle$. Since in the local coordinate system the mid-point of the string is at i, we can write

$$f_1 \circ A'(0) \sigma^{+\prime}(M) \sigma^{-\prime}(M) = \lim_{\epsilon \to 0} |f_1'(i+\epsilon)|^{1/4} f_1 \circ (A'(0) \sigma^{+\prime}(i+\epsilon) \sigma^{-\prime}(i+\epsilon)) \,. \tag{3.4.15}$$

This, together with (3.4.11) and (3.4.13), and the relation $I \circ (\sigma^{+\prime}(i+\epsilon)\sigma^{-\prime}(i+\epsilon)) \simeq \sigma^{+\prime}(i-\epsilon)\sigma^{-\prime}(i-\epsilon)$ for $I(z) = -1/z$ gives

$$\begin{aligned} |B * C\rangle &= \lim_{\epsilon \to 0} K_0 |f_1'(i+\epsilon)|^{1/4} \sigma^{+\prime}(i-\epsilon)\sigma^{-\prime}(i-\epsilon) |B *' C\rangle \,, \\ &\propto \sigma^{+\prime}(i-\epsilon)\sigma^{-\prime}(i-\epsilon) |B *' C\rangle \,, \end{aligned} \tag{3.4.16}$$

where the constant of proportionality is infinite since $f_i'(i+\epsilon) \sim \epsilon^{-1/3}$ diverges as $\epsilon \to 0$. However at this stage we are analyzing the solution only up to a (possible infinite) scale factor, and so we shall not worry about this normalization.

The equations of motion

$$\mathcal{Q}|\Psi\rangle + |\Psi * \Psi\rangle = 0\,, \tag{3.4.17}$$

can now be written as:

$$\mathcal{Q}|\Psi\rangle \propto -\sigma^{+\prime}(i-\epsilon)\sigma^{-\prime}(i-\epsilon)|\Psi *' \Psi\rangle\,. \tag{3.4.18}$$

We shall show that for the choice of $\mathcal{Q}$ given in (3.2.5), eq.(3.4.18) is satisfied by a multiple of Ξ' where Ξ' is the sliver of the auxiliary ghost - matter system, satisfying

$$\langle \Xi'|\phi\rangle = \langle f\circ\phi'(0)\rangle'\,, \tag{3.4.19}$$

for any Fock space state $|\phi\rangle$. Here $f(\xi) = \tan^{-1}\xi$. For this we first need to know what form the operator $\mathcal{Q}$ takes in the auxiliary ghost-matter theory. We use

$$\begin{aligned}\mathcal{Q} &= c_0 + \sum_{n\geq 1}(-1)^n(c_{2n}+c_{-2n}) \\ &= c_0' + \sum_{n\geq 1}(-1)^n(c_{2n}'+c_{-2n}') \\ &= c'(i)+c'(-i)\,,\end{aligned} \tag{3.4.20}$$

where the argument of $c'(\pm i)$ in the last two expressions refer to the coordinates on the upper half plane. If we now take the inner product of eq.(3.4.18) with a Fock space state $\langle\phi|$, then for the choice $|\Psi\rangle \propto |\Xi'\rangle$, the left hand side is proportional to:

$$\langle f\circ\Big(\phi'(0)\big(c'(i)+c'(-i)\big)\Big)\rangle' = \langle f\circ\phi'(0)\Big(c'(i\infty)+c'(-i\infty)\Big)\rangle'\,. \tag{3.4.21}$$

Note that since c has dimension zero in the auxiliary BCFT, there is no conformal factor in its transformation. On the other hand, since $\Xi' *' \Xi' = \Xi'$, and $f(i+\epsilon) \simeq -\frac{i}{2}\ln\epsilon \equiv i\eta$, the right hand side is proportional to

$$\begin{aligned}\langle f\circ\Big(\phi'(0)\sigma^{+\prime}(i+\epsilon))\sigma^{-\prime}(i+\epsilon)\Big)\rangle' &\propto \langle f\circ\phi'(0)\sigma^{+\prime}(i\eta)\sigma^{-\prime}(i\eta)\rangle' \\ &\propto \langle f\circ\phi'(0)\sigma^{+\prime}(i\eta)\sigma^{+\prime}(-i\eta)\rangle'\,,\end{aligned} \tag{3.4.22}$$

where in the last expression we have used the Neumann boundary condition on φ to relate $\sigma^{-\prime}(i\eta)$ to $\sigma^{+\prime}(-i\eta)$. Thus we need to show that (3.4.21) and (3.4.22) are equal up to an overall normalization factor independent of $\langle\phi|$. This is seen as follows. Since both correlators are being evaluated on the upper half plane, the points $\pm i\infty$ correspond to the same points.[7] Thus on the right hand side of eq.(3.4.21) we can replace $c'(i\infty)+c'(-i\infty)$ by $2c'(i\infty)$. On the other hand on the right hand side of (3.4.22) we can replace $\sigma^{+\prime}(i\eta)\sigma^{+\prime}(-i\eta)$ by the leading term in the operator product expansion of $\sigma^{+\prime}$ with $\sigma^{+\prime}$, i.e. $c'(i\infty)$. As a result both (3.4.21) and (3.4.22) are proportional to $\langle f\circ\phi'(0)c'(i\infty)\rangle'$.

At this point we would like to note that a different kind of star product has been analyzed in works by Kishimoto [67] and Okuyama [72] which helps in solving the Siegel gauge equations of motion in the oscillator formalism. It will be interesting to examine the relation between the $*'$ product and the product discussed by these authors.

3.4.3 The twisted sliver state from CFT and a comparison

Since in the arguments above we have ignored various infinite normalization factors, the result may seem formal. In this subsection, therefore, we verify explicitly that the solution Ξ' obtained this way agrees with the solution obtained in refs.[73, 66] by algebraic method. This has an added advantage. The geometrical construction of Ξ' given below expresses the Neumann coefficients in terms of simple contour integrals that can be evaluated exactly for arbitrary level. On the other hand the algebraic solution, as usual, involves inverses and square roots of infinite matrices, and therefore can only be evaluated approximately using level expansion.

This is done as follows. Writing $\Xi'=\Xi'_g\otimes\Xi_m$, we have for the ghost part:

$$\langle\Xi'_g|=\widehat{\mathcal{N}}_g\langle 0'|\exp\Big(-\sum_{n,m\geq 1}c_n\bar{S}_{nm}b_m\Big) \tag{3.4.23}$$

[7] This can be made manifest by making an SL(2,R) transformation that brings the point at ∞ to a finite point on the real axis.

where $\widehat{\mathcal{N}}_g$ is a normalization factor. The BPZ dual ket is

$$|\Xi'_g\rangle = \widehat{\mathcal{N}}_g \exp\Big(\sum_{n,m\geq 1} c_{-n}\widehat{S}_{nm}b_{-m}\Big)\,|0'\rangle, \qquad \widehat{S}_{nm} = (-1)^{n+m}\bar{S}_{nm}\,. \tag{3.4.24}$$

The calculation of the matrix elements $\bar{S}$ (or $\widehat{S}$) is done using the a small variant of the CFT methods in [79]. The idea is to evaluate

$$h(z,w) \equiv \langle 0'|\exp\Big(-\sum_{n,m\geq 1} c_n\bar{S}_{nm}b_m\Big)c(w)b(z)\,c_0|0'\rangle \tag{3.4.25}$$

in two different ways. In the first one we expand using $c(w) = \sum_p c_{-p}w^p$ and $b(z) = \sum_q b_{-q}z^{q-1}$ and find

$$h(z,w) = -\sum_{n,m} w^m z^{n-1}\bar{S}_{nm} \;\rightarrow\; \bar{S}_{nm} = -\oint_0 \frac{dz}{2\pi i}\frac{1}{z^n}\oint_0 \frac{dw}{2\pi i}\frac{1}{w^{m+1}}h(z,w)\,. \tag{3.4.26}$$

In the second evaluation of (3.4.25) the right hand side is viewed as a correlator

$$\begin{aligned} h(z,w) &= \langle f\circ c'(w) f\circ b'(z) f\circ c'(0)\rangle' \\ &= \Big\langle c'(f(w))\,b'(f(z))\frac{df(z)}{dz}\,c'(f(0))\Big\rangle' \\ &= \frac{df(z)}{dz}\,\frac{1}{f(w)-f(z)}\,\frac{f(w)-f(0)}{f(z)-f(0)}\,, \end{aligned} \tag{3.4.27}$$

where the function $f(\xi)$ denotes the insertion map associated with the geometry of the surface state, and the derivative $\frac{df}{dz}$ arises because b has conformal dimension one. The general result now follows from comparison of (3.4.26) and (3.4.27) together with (3.4.24)

$$\widehat{S}_{nm} = (-1)^{n+m}\oint_0 \frac{dz}{2\pi i}\frac{1}{z^n}\oint_0 \frac{dw}{2\pi i}\frac{1}{w^{m+1}}\frac{df(z)}{dz}\,\frac{1}{f(z)-f(w)}\,\frac{f(w)-f(0)}{f(z)-f(0)}. \tag{3.4.28}$$

This is the general expression for the Neumann coefficients of a once punctured disk in the twisted ghost CFT. For our particular case, the twisted sliver is defined by $f(z) = \tan^{-1}(z)$ and the Neumann coefficients vanish unless $n+m$ is even. Therefore we find:

$$\widehat{S}_{nm} = \oint_0 \frac{dz}{2\pi i}\frac{1}{z^n}\oint_0 \frac{dw}{2\pi i}\,\frac{1}{w^{m+1}}\frac{1}{1+z^2}\frac{1}{(\tan^{-1}(z)-\tan^{-1}(w))}\frac{\tan^{-1}(w)}{\tan^{-1}(z)}\,. \tag{3.4.29}$$

The first few coefficients are

$$\begin{aligned} &\widehat{S}_{11} = -\frac{1}{3} \cong -0.33333\,, \quad \widehat{S}_{31} = \frac{4}{15} \cong 0.26667\,, \quad \widehat{S}_{22} = \frac{1}{15} \cong 0.06667\,, \\ &\widehat{S}_{51} = -\frac{44}{189} \cong -0.23280\,, \quad \widehat{S}_{33} = -\frac{83}{945} \cong -0.08783\,, \\ &\widehat{S}_{42} = -\frac{64}{945} \cong -0.067724\,. \end{aligned} \tag{3.4.30}$$

L	$\widetilde{S}_{11}$	$\widetilde{S}_{31}$	$\widetilde{S}_{22}$	$\widetilde{S}_{51}$	$\widetilde{S}_{33}$	$\widetilde{S}_{42}$
100	-0.31526	0.248339	0.066288	-0.21432	-0.081680	-0.067263
150	-0.316448	0.249482	0.066269	-0.21543	-0.082030	-0.067220
200	-0.317244	0.250270	0.066271	-0.21621	-0.082281	-0.067215
250	-0.31783	0.250862	0.066279	-0.21680	-0.082473	-0.067220
∞	-0.33068	0.26345	0.067965	-0.22916	-0.08642	-0.06698

Table 3.2: Numerical results for $\widetilde{S}_{nm}$ at different level approximation. The last row shows the interpolation of the various results to $L = \infty$, obtained via a fitting function of the form $a_0 + a_1/\ln(L)$.

Since $|0'\rangle = c_1|0\rangle$, we see that $|\Psi_g\rangle$ defined in eq.(3.3.10) and $|\Xi'_g\rangle$ describe the same state if the matrices $\widetilde{S}_{mn}$ defined in eq.(3.3.9) and $\widehat{S}_{mn}$ defined in eq.(3.4.29) are the same. The numerical results for $\widetilde{S}_{mn}$ are given in table 3.2, and can be seen to be in good agreement with $\widehat{S}_{mn}$ given in eq.(3.4.30).

3.5 Regularizing the VSFT action

As pointed out already in section 3.2, in order to get a D-25-brane solution of finite energy density, we need to take the overall multiplicative factor κ_0 appearing in eq.(3.2.1) to be infinite. We shall now discuss a precise way of regularizing the theory so that for any fixed value of the regulator a, the value of $\kappa_0(a)$, needed to reproduce the D-25-brane tension correctly, is finite. The action (3.2.1) is then recovered by taking the $a \to \infty$ limit. Presumably this regularization captures some of the physics of the correct regularization procedure coming from the the use of nearly singular reparametrization instead of the singular reparametrization discussed in section 3.2.2.

3.5.1 The proposal for regulated gauge fixed VSFT

The regularization is done by first fixing the Siegel gauge $b_0|\Psi\rangle = 0$. In this way, the kinetic operator in (3.2.1), with $\mathcal{Q}$ given in (3.2.5), becomes c_0. We then replace this gauge fixed kinetic operator by $c_0(1 + a^{-1}L_0)$. The result is the regulated action S_a given by:

$$S_a = -\kappa_0(a)\Big[\frac{1}{2}\langle\Psi, c_0(1 + a^{-1}L_0)\Psi\rangle + \frac{1}{3}\langle\Psi, \Psi * \Psi\rangle\Big]\,. \tag{3.5.1}$$

The gauge fixed unregulated VSFT is recovered in the $a \to \infty$ limit.

Although the parameter a has been introduced as a regulator, the Feynman rules derived from the regulated action (3.5.1) have some close resemblence to boundary string field theory (BSFT) rules [75] in the presence of a constant tachyon background. To see this, let us note that the propagator computed from this action is proportional to:

$$\frac{b_0}{L_0 + a} = b_0 \int_0^\infty dl e^{-l(L_0+a)}\,. \tag{3.5.2}$$

This is similar to the propagator in OSFT except for the factor of e^{-la} in the integrand. The three string vertex computed from the action (3.5.1) is also proportional to the three string vertex of OSFT. Thus when we compute the Feynman amplitudes using these Feynman rules, we shall get an expression similar to that in OSFT except for an additional factor of $\exp(-a\sum_i l_i)$, where the sum over i is taken over all the propagators in the Feynman diagrams. Now in OSFT a Feynman diagram can be interpreted as correlation function on a Riemann surface obtained by gluing strips of length l_i using the three string overlap vertices. Since each strip of length l_i contributes $2l_i$ to the total length of the boundary in the Feynman diagram, we see that a factor of $e^{-a\sum_i l_i}$ can also be interpreted as $e^{-aB/2}$, where B is the total length of the boundary of the Riemann surface associated with the Feynman diagram. This is reminiscent of the term $a\int d\theta$ representing constant tachyon perturbation in the boundary string field theory, with θ denoting the coordinate on the boundary. We should, however, keep in mind that the world-sheet metric used in defining constant tachyon background in boundary SFT is different from the world-sheet metric that appears naturally in the Feynman digrams of OSFT, and so we cannot directly relate the

tachyon of boundary SFT to the parameter a appearing here. Presumably the $a \to \infty$ limit corresponds to the same configuration in both descriptions.

3.5.2 Level truncation analysis

To test the consistency of our regulation scheme, we now perform a numerical analysis using the level truncation approximation. We must find that for any fixed value of the regulator a, computations with the regulated action (3.5.1) have a well-defined finite limit as the level of approximation L is sent to infinity. We define in the standard way the level approximation $(L, 2L)$ by truncating the string field up to level L (level is defined as $L \equiv L_0 + 1$) and keeping the terms in the action which have a total level of $2L$. For a fixed value of a, and a given level of approximation $(L, 2L)$, we look for translationally invariant solutions Ψ_a^L in Siegel gauge corresponding to D-25 brane.

The energy density of the D-25-brane solution in the regulated theory at level $(L, 2L)$ approximation can be expressed as:

$$\mathcal{E}_a(L) = \frac{\kappa_0(a)}{6}\langle \Psi_a^L,\, (c_0 + a^{-1}L_0)\Psi_a^L\rangle \equiv \kappa_0(a) f(a, L)\,, \tag{3.5.3}$$

where $f(a, L)$ can be computed numerically. It indeed turns out that for a fixed a, as the level of approximation L becomes larger than a, the function $f(a, L)$ approaches a finite value $F(a)$. This is best seen from Fig.3.1, where we have displayed the plot of $a^3 f(a, L)$ vs. a for different levels of approximation L. Thus for a fixed a, we get the energy density of the D-25-brane solution to be:

$$\mathcal{E}_a = \kappa_0(a) F(a)\,. \tag{3.5.4}$$

We can now take the $a \to \infty$ limit keeping $\kappa_0(a)F(a)$ to be fixed at the D-25-brane tension $\mathcal{T}_{25}$. In other words we choose the overall normalization of the action as

$$\kappa_0(a) \equiv \frac{\mathcal{T}_{25}}{F(a)}\,. \tag{3.5.5}$$

This gives a precise way of defining the vacuum string field theory using level truncation scheme.

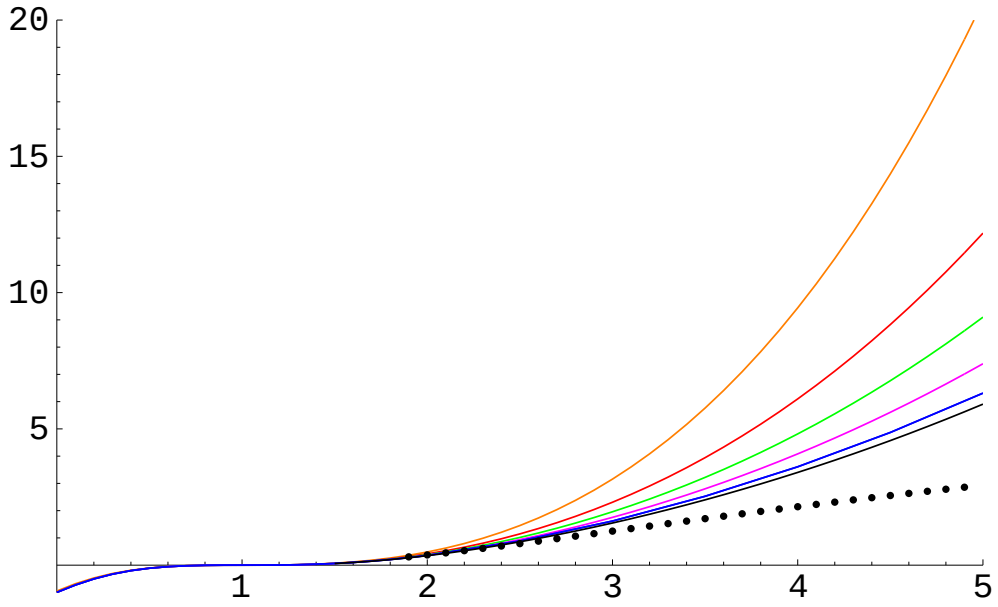

Figure 3.1: This figure shows the plot of the function $a^3 f(a,L)$, computed at level $(L,2L)$ approximation, as a function of a. Starting from the topmost graph, the six continuous curves correspond to $L = 2$, 4, 6, 8, 10 and 12 respectively. The lowermost dotted curve is an $L = \infty$ extrapolation of the data obtained with a fit of the form $a_0+a_1/L+a_2/L^2+a_3/L^3$.

If we go back to the analog of the $\widetilde{\Psi}$ variables by defining

$$\Psi = (\kappa_0(a) g_o^2)^{-1/3} \widetilde{\Psi} \tag{3.5.6}$$

then the action takes the form:

$$S_a = -\frac{1}{g_o^2}\left[\frac{1}{2}\langle\widetilde{\Psi},\, \widetilde{\mathcal{Q}}_a\widetilde{\Psi}\rangle + \frac{1}{3}\langle\widetilde{\Psi},\, \widetilde{\Psi}*\widetilde{\Psi}\rangle\right], \tag{3.5.7}$$

where

$$\widetilde{\mathcal{Q}}_a \;=\; (g_o^2\kappa_0(a))^{1/3}(c_0 + a^{-1}c_0L_0) = \left(\frac{g_o^2\mathcal{T}_{25}}{F(a)}\right)^{1/3} c_0 + \left(\frac{g_o^2\mathcal{T}_{25}}{a^3F(a)}\right)^{1/3} c_0L_0\,. \tag{3.5.8}$$

The data in Fig.3.1 suggests that $a^3F(a)$ grows linearly, *i.e.* $F(a) \sim 1/a^2$ for large a. Hence, in the $a \to \infty$ limit, the coefficient of c_0 diverges, and that of c_0L_0 vanishes.

We now examine the form of the D-25 brane solution. The solutions Ψ_L^a are string fields belonging to the universal ghost number one subspace [8, 12] obtained by acting on the

$U(a,L)$	$L=4$	$L=6$	$L=8$	$L=10$	$L=12$	$L=\infty$
$a=2.0$	-.0812	-.0834	-.0846	-.0855	-.0861	-0.0904
$a=2.5$	-.1121	-.1164	-.1191	-.1210	-.1224	-0.1315
$a=3.0$	-.1372	-.1436	-.1478	-.1508	-.1530	-0.1673
$a=3.5$	-.1576	-.1660	-.1715	-.1754	-.1785	-0.1994
$a=4.0$	-.1744	-.1845	-.1911	-.1959	-.1996	-0.2251
$a=4.5$	-.1884	-.1999	-.2075	-.2130	-.2173	-0.2468
$a=5.0$	-.2002	-.2130	-.2214	-.2275	-.2323	-0.2656

Table 3.3: Sample numerical results for the coefficient $U(a,L)$ at different level approximation $(L,2L)$ for different values of a.

$V(a,L)$	$L=4$	$L=6$	$L=8$	$L=10$	$L=12$	$L=\infty$
$a=2.0$	-.1440	-.1440	-.1438	-.1436	-.1435	-0.1429
$a=2.5$	-.1884	-.1887	-.1886	-.1885	-.1884	-0.1878
$a=3.0$	-.2225	-.2232	-.2234	-.2234	-.2234	-0.2227
$a=3.5$	-.2495	-.2506	-.2510	-.2512	-.2513	-0.2515
$a=4.0$	-.2712	-.2728	-.2735	-.2738	-.2740	-0.2742
$a=4.5$	-.2892	-.2912	-.2920	-.2925	-.2928	-0.2946
$a=5.0$	-.3043	-.3066	-.3076	-.3082	-.3086	-0.3109

Table 3.4: Sample numerical results for the coefficient $V(a,L)$ at different level approximation $(L,2L)$ for different values of a. The last column of tables 3.3 and 3.4 shows a large L extrapolation obtained with a fit $c_0+c_1/L+c_2/L^2+c_3/L^3$. The further large a extrapolation in (3.5.10) is done with a more complete set of data than shown in these tables (all values of a from 2 to 5 with an increment of 0.1).

vacuum with ghost oscillators and matter Virasoro generators. Up to level 4,

$$\begin{aligned}\Psi_a^L = \; T(a,L)\Big[\;& c_1|0\rangle + U(a,L)L_{-2}^m c_1|0\rangle + V(a,L)c_{-1}|0\rangle \\ & + A(a,L)L_{-4}^m c_1|0\rangle + B(a,L)(L_{-2}^m)^2 c_1|0\rangle + C(a,L)L_{-2}^m c_{-1}|0\rangle + \\ & D(a,L)(-3\,c_{-3} + b_{-3}c_{-1}c_1)|0\rangle + E(a,L)b_{-2}c_{-2}c_1|0\rangle + \ldots\Big]\,.\end{aligned} \tag{3.5.9}$$

Our regulation prescription instructs us to first take the large L limit of Ψ_a^L, and then remove the regulator by sending $a \to \infty$. As shown in tables 3.3 and 3.4, up to the overall normalization $T(a,L)$ which has been factored out, the coefficients of the solution for a given regulator a are fairly stable as the level is increased. Considering data for $2 \le a \le 5$, and $L = 2, 4, 6, 8, 10, 12$, we first perform a large L extrapolation with a fitting function of the form $c_0 + c_1/L + c_2/L^2 + c_3/L^3$; then we extrapolate to $a = \infty$ with a fit $\gamma_0 + \gamma_1/a + \gamma_2/a^2 + \gamma_3/a^3$. This procedure gives

$$\begin{aligned}\lim_{a\to\infty}\lim_{L\to\infty}\frac{\Psi_a^L}{T(a,L)} \;\cong\; & c_1|0\rangle - 0.4564\,L_{-2}^m c_1|0\rangle - 0.4901\,c_{-1}|0\rangle \\ & + 0.0041\,L_{-4}^m c_1|0\rangle + 0.0917\,(L_{-2}^m)^2 c_1|0\rangle + 0.2037\,L_{-2}^m c_{-1}|0\rangle \\ & -0.1131(-3c_{-3} + b_{-3}c_{-1})|0\rangle - 0.0024\,b_{-2}c_{-2}c_1|0\rangle + \ldots\end{aligned} \tag{3.5.10}$$

While this double extrapolation procedure is the correct general prescription, we would like to show that for certain purposes it is possible to work in the non-regulated theory, or in other words to commute the limits in (3.5.10) by first removing the regulator sending $a \to \infty$ and then performing level truncation in the theory with $\mathcal{Q} = (c(i) - c(-i))/(2i)$. In fact, we know that the non-regulated theory gives correct results about existence of classical D-p brane solutions and the *ratios* of their tensions [57, 59] so it should be the case that the limits in (3.5.10) can be commuted for this class of physical questions. This will obviously be the case if we can show that *up to an overall normalization*, classical solutions are the same regardless of the order of limits,

$$\lim_{a\to\infty}\lim_{L\to\infty}\frac{\Psi_a^L}{T(a,L)} = \lim_{L\to\infty}\lim_{a\to\infty}\frac{\Psi_a^L}{T(a,L)}\,. \tag{3.5.11}$$

It is easy to perform numerical analysis directly at $a = \infty$ for a given level of approximation. Although the energy, being proportional to $F(a)$, goes to zero in this limit unless we

	$U(L)$	$V(L)$	$A(L)$	$B(L)$	$C(L)$	$D(L)$	$E(L)$
$L=2$	-.2879	-.4576	–	–	–	–	–
$L=4$	-.3015	-.4357	.0094	.0358	.1082	-.0844	-.0103
$L=6$	-.3394	-.4596	.0080	.0523	.1440	-.0995	-.0037
$L=8$	-.3631	-.4708	.0072	.0627	.1640	-.1072	-.0019
$L=10$	-.3798	-.4771	.0066	.0700	.1768	-.1114	-.0011
$L=12$	-.3923	-.4811	.0060	.0755	.1858	-.1141	-.0007
$L=\infty$	-.4603	-.4900	.0029	.1049	.2311	-.1258	.0001

Table 3.5: Coefficients of the $a=\infty$ solution, at different level approximation $(L, 2L)$ (we use $U(\infty, L) \equiv U(L)$, and he same convention for the other coefficients). The last row shows an extrapolation to infinite level with a fitting function of the form $a_0+a_1/L+a_2/L^2+a_3/L^3$.

compensate for it by making $\kappa_0(a)$ large, the solution approaches a finite limit up to the overall normalization. Numerical results are shown in table 3.5.

We find:

$$\begin{aligned}\lim_{a\to\infty}\lim_{L\to\infty}\frac{\Psi_a^L}{T(a,L)} \;\cong\; & c_1|0\rangle - 0.4603\, L_{-2}^m c_1|0\rangle - 0.4900\, c_{-1}|0\rangle \\ & + 0.0029\, L_{-4}^m c_1|0\rangle + 0.1049\, (L_{-2}^m)^2 c_1|0\rangle + 0.2311\, L_{-2}^m c_{-1}|0\rangle \\ & -0.1258(-3c_{-3}+b_{-3}c_{-1})|0\rangle + 0.0001\, b_{-2}c_{-2}c_1|0\rangle + \dots\end{aligned} \tag{3.5.12}$$

This is compatible with (3.5.10) and (3.5.11).

We thus find evidence that classical solutions of VSFT are independent of the order of limits, up to an overall normalization factor that needs to be adjusted so as to keep the tension fixed. This justifies the analytic treatment of the equations of motion based on matter/ghost factorization, which has been an important assumption in all studies of VSFT, and which holds only in the $a\to\infty$ limit. Moreover, we can study numerically the D-25 brane solution in the $a\to\infty$ theory at fixed L, which is much simpler than taking the $L\to\infty$ limit first and then taking the $a\to\infty$ limit.

It is illuminating to write the D-25 brane solution in a basis of Fock states obtained by

	v_2	$\widetilde{v}_2$	v_4	$\widetilde{v}_4$	v_6
$L=2$	-.2879	-.4576	–	–	–
$L=4$	-.3364	-.4736	.0056	-.00193	–
$L=6$	-.3655	-.4816	.0048	-.00216	-.00111
$L=8$	-.3852	-.4861	.0043	-.00197	-.00080
$L=10$	-.3999	-.4891	.0039	-.00176	-.00065
$L=12$	-.4105	-.4912	.0036	-.00157	-.00056
$L=\infty$	-.4778	-.5027	.0012	-.00007	-.0002

Table 3.6: Coefficients of the $a=\infty$ solution written as an exponential of matter and twisted ghost Virasoro operators, at different level approximation $(L,3L)$. The last row shows an extrapolation to infinite level with a fitting function of the form $a_0+a_1/L+a_2/L^2+a_3/L^3$.

acting on the zero-momentum tachyon with the matter Virasoro generators L^m_{-n} and the ghost Virasoro generators $L^{'g}_{-n}$ $(n\geq 2)$ of the twisted bc system introduced in section 3.4.[8]

It turns out that to a very good degree of accuracy the solution can be written as

$$\Psi_{a=\infty}\sim \exp(\sum_{n=1}^{\infty} v_{2n}L^m_{-2n})\exp(\sum_{n=1}^{\infty}\widetilde{v}_{2n}L^{'g}_{-2n})c_1|0\rangle. \tag{3.5.13}$$

This is precisely the form expected for a surface state of the twisted BCFT introduced in section 3.4. The results for the coefficients v_{2n} and $\widetilde{v}_{2n}$ at various level approximations $(L,3L)$ are shown in table 3.6. Extrapolating for $L\to\infty$ with a fit of the form $a_0+a_1/L+a_2/L^2+a_3/L^3$ we find

$$\begin{aligned}\Psi_{a=\infty} \;\sim\; & \exp(-0.5027L^{'g}_{-2}-0.00007L^{'g}_{-4}+\dots)c_1|0\rangle_g \\ & \otimes\exp(-0.4778L^m_{-2}+0.0012L^m_{-4}-0.0002L^m_{-6}+\dots)|0\rangle_m\,.\end{aligned} \tag{3.5.14}$$

We note that although the solution has precisely the form expected for a surface state of the auxiliary matter-ghost system, it does not approach the twisted sliver Ξ', for which the

[8] A simple counting argument along the lines of section 2.2 of [12] shows that all ghost number one Siegel gauge string fields that belong to the $SU(1,1)$ singlet subspace [47] can be written in this form.

coefficient of L'_{-2} is $-1/3$. This should not bother us, however, since we can generate many other surface states (related to the sliver by a singular or non-singular reparametrization of the string coordinate symmetric about the mid-point) which are all projectors. Moreover, at least formally, all rank one projectors are gauge-related in VSFT. The numerical result (3.5.14) strongly suggests that as $L \to \infty$ the solution is in fact approaching the remarkably simple state

$$|B'\rangle \sim \exp(-\frac{1}{2}(L^m_{-2} + L'^g_{-2})c_1|0\rangle, \tag{3.5.15}$$

which we call the (twisted) *butterfly* state. It is possible to show that the state $|B'\rangle$ is indeed a projector of the $*'$ algebra and an exact solution of the VSFT equations. In the next section we shall come back to this point.

Let us finally check numerically that the Siegel gauge D-25 brane solution obtained in level truncation solves the equation of motion of VSFT with our proposed $\mathcal{Q}$. To this end we take the solution $\Psi_{a=\infty}$ compute $\Psi_{a=\infty} * \Psi_{a=\infty}$, and try to determine $\mathcal{Q} = (c_0 + \sum_{n\geq 1} u_{2n}(c_{2n} + c_{-2n}))$ up to a constant of proportionality using the equation:

$$\Psi_{a=\infty} * \Psi_{a=\infty} \propto \mathcal{Q}\Psi_{a=\infty}\,. \tag{3.5.16}$$

The results for the coefficients u_{2n} at various level approximation $(L, 3L)$ are shown in table 3.7 and are indeed consistent with our choice (3.2.5) for $\mathcal{Q}$.

3.6 The Butterfly State

The level truncation results have led to the discovery of a new simple projector, the butterfly state, different from the sliver. There are in fact several surface states that can be written in closed form and shown to be projectors using a variety of analytic approaches. In this section we briefly state without proof some of the relevant results. A thorough discussion will appear in a separate publication [76].

Consider the class of surface states $|B_\alpha\rangle$, defined through:

$$\langle B_\alpha|\phi\rangle \equiv \langle f_\alpha \circ \phi(0)\rangle_D \tag{3.6.1}$$

	u_2	u_4	u_6	u_8	u_{10}
$L=2$	-.8020	–	–	–	–
$L=4$	-.8672	.7249	–	–	–
$L=6$	-.9003	.7918	-.6854	–	–
$L=8$	-.9201	.8333	-.7451	.6615	–
$L=10$	-.9334	.8627	-.7868	.7138	-.6457
$L=\infty$	-.9969	.9983	-.923	–	–

Table 3.7: Coefficients of the BRST operator deduced from the $a=\infty$ solution, at different level approximations $(L, 3L)$.The last row shows an extrapolation to infinite level with fits of the form $a_0 + a_1/L + a_2/L^2 + a_3/L^3$ ($a_3 \equiv 0$ for u_4, $a_3 = a_2 \equiv 0$ for u_6).

with

$$f_\alpha(\xi) = \frac{1}{\alpha}\sin(\alpha \tan^{-1}\xi)\,. \tag{3.6.2}$$

As $\alpha \to 0$, we recover the sliver. For $\alpha = 1$ we have the butterfly state $|B\rangle \equiv |B_{\alpha=1}\rangle$, defined by the map

$$f_1(\xi) = \frac{\xi}{\sqrt{1+\xi^2}}\,. \tag{3.6.3}$$

In operator form the butterfly can be written as

$$|B\rangle = \exp(-\frac{1}{2}L_{-2})|0\rangle\,. \tag{3.6.4}$$

For any α, these states can be shown to be idempotents of the $*$ algebra,

$$|B_\alpha\rangle * |B_\alpha\rangle = |B_\alpha\rangle\,. \tag{3.6.5}$$

Moreover, in analogy with the sliver, the wave-functional of $|B_\alpha\rangle$ factorizes into a product of a functional of the left-half of the string and another functional of the right half of the string. These states are thus naturally thought as rank-one projectors in the half-string formalism [58, 61, 62]. The key property that ensures factorization is the singularity of the conformal maps at the string midpoint,

$$f_\alpha(\pm i) = \pm i\infty\,. \tag{3.6.6}$$

It is possible to give a general argument [76] that all sufficiently well-behaved conformal maps with this property give rise to split wave-functionals.

The case $\alpha = 1$ is special because the wave-functional of the butterfly $|B_{\alpha=1}\rangle$ factors into the product of the *vacuum* wave-functional of the right half-string and the *vacuum* wave-functional of the left half-string. It is thus in a sense the simplest possible projector. It is quite remarkable that the same state emerges in VSFT as the numerical solution preferred by the level truncation scheme.

Finally, in complete analogy with the 'twisted' sliver Ξ', the 'twisted' states $|B'_\alpha\rangle$ solve the VSFT equations of motion with $\mathcal{Q} = (c(i) - c(-i))/(2i)$,

$$\mathcal{Q}|B'_\alpha\rangle \propto |B'_\alpha\rangle * |B'_\alpha\rangle \,. \tag{3.6.7}$$

Indeed the proof of section 3.4 that Ξ' satisfies the VSFT equations of motion $\mathcal{Q}\Xi' \propto \Xi' * \Xi'$ only depends on the fact that the map $f(\xi) = \tan^{-1}\xi$ associated with the sliver takes the points $\pm i$ to $\pm i\infty$. As can be seen from (3.6.6), this property is shared by the map f_α associated with the state $|B_\alpha\rangle$.

3.7 Gauge invariant operators in OSFT and VSFT

Since open string field theory on an unstable D-brane has no physical excitations at the tachyon vacuum, the only possible observables in this theory are correlation functions of gauge invariant operators. A natural set of gauge invariant operators in this theory has been constructed in [51] by using the open/closed string vertex that emerges from the studies of [77]. In this section we will describe in detail these gauge invariant operators in OSFT and show how they give rise to gauge invariant operators in VSFT. It would be interesting to analyze the correlation functions of these operators around the tachyon vacuum by using OSFT in the level truncation scheme.

The same gauge invariant operators discussed here have been considered independently by Hashimoto and Itzhaki, who examined the gauge invariance in an explicit oscillator construction, and motivated their role mostly in the context of OSFT [52].

We shall begin by reviewing the construction of ref.[51] and then we will consider the generalization to VSFT.

3.7.1 Gauge invariant operators in OSFT

The original cubic open string field theory [6] describing the dynamics of the unstable D-brane, is described by the action:

$$S = -\frac{1}{g_o^2}\left[\frac{1}{2}\langle\Phi, Q_B\Phi\rangle + \frac{1}{3}\langle\Phi, \Phi * \Phi\rangle\right], \tag{3.7.1}$$

with gauge invariance:

$$\delta|\Phi\rangle = Q_B|\Lambda\rangle + |\Phi * \Lambda\rangle - |\Lambda * \Phi\rangle\,. \tag{3.7.2}$$

Here Q_B is the BRST charge, g_o is the open string coupling constant, $|\Phi\rangle$ is the string field, and $|\Lambda\rangle$ is the gauge transformation parameter. In this theory there are gauge invariant operators $\mathcal{O}_V(\Phi)$ corresponding to every on-shell closed string state represented by the BRST invariant, dimension $(0,0)$ vertex operator $V = c\bar{c}V_m$, where V_m is a dimension (1,1) primary in the bulk matter CFT. Given any such closed string vertex operator V, we define $\mathcal{O}_V(\Phi)$ as the following linear function of the *open* string field Φ:

$$\mathcal{O}_V(\Phi) \equiv \langle h_1 \circ (V(i)\Phi(0))\rangle_D = \langle V(0)h_1 \circ \Phi(0)\rangle_D\,, \tag{3.7.3}$$

where h_N has been defined in eq.(3.2.21), and $\langle\ \rangle_D$ denotes correlation function on a unit disk. Since V is dimension $(0,0)$ it is not affected by the conformal map h_1 despite being located at the singular point $z = i$.[9] In [51] these operators were added to the OSFT action and it was shown that the resulting Feynman rules would generate a cover of the moduli spaces of closed Riemann surfaces *with boundaries* and closed string punctures thus producing the appropriate closed string amplitudes. The operators $\mathcal{O}_V(\Phi)$ can be interpreted as the open string one point function

$$\mathcal{O}_V(\Phi) = \langle\mathcal{I}|V(i)|\Phi\rangle\,, \tag{3.7.4}$$

[9] In dealing separately with ghost and matter contributions, however, it may be useful to define $\mathcal{O}_V(\Phi)$ as $\lim_{\epsilon\to 0^+}\lim_{\eta\to 0^+}\langle V(-\eta)h_{1+\epsilon}\circ\Phi(0)\rangle$.

where $\langle\mathcal{I}|$ is the identity state of the $*$-product. The world sheet picture is clear, $\mathcal{O}_V(\Phi)$ corresponds to the amputated version of a semi-infinite strip whose edge represents an open string, the two halves of which are glued and a closed string vertex operator is located at the conical singularity. Gauge invariance of $\mathcal{O}_V(\Phi)$ under (3.7.2) follows from the BRST invariance of V and the relations

$$|A\rangle * (V(i)|B\rangle) = V(i)|A * B\rangle, \qquad (V(i)|A\rangle) * |B\rangle = V(i)|A * B\rangle\,. \tag{3.7.5}$$

3.7.2 Gauge invariant operators in VSFT

Since the VSFT field Ψ must be related to the original unstable D-brane OSFT field $|\Phi\rangle$ by a field redefinition, the existence of gauge invariant observables in the OSFT implies that there must exist such quantities in the VSFT as well. Even though the explicit relation between $|\Psi\rangle$ and $|\Phi\rangle$ is not yet known, we now argue that the VSFT gauge invariant observables actually take the same form as in OSFT.

The possible field redefinitions relating VSFT and OSFT were discussed in ref.[56]. If we denote by $|\Phi_0\rangle$ the classical OSFT solution describing the tachyon vacuum, then the shifted string field $|\widetilde{\Phi}\rangle = |\Phi\rangle - |\Phi_0\rangle$ may be related to $|\Psi\rangle$ by homogeneous redefinitions preserving the structure of the cubic vertex, namely

$$(g_o^2\kappa_0)^{1/3}\,|\Psi\rangle = e^{-K}|\widetilde{\Phi}\rangle\,, \tag{3.7.6}$$

where K satisfies:

$$\begin{aligned} K(A*B) &= (KA)*B + A*(KB)\,, \\ \langle KA, B\rangle &= -\langle A, KB\rangle\,. \end{aligned} \tag{3.7.7}$$

The explicit normalization factor $(g_o^2\kappa_0)^{1/3}$ on the left hand side of eq.(3.7.6) has been chosen to ensure the matching of the cubic terms in (3.2.1) and (3.7.1) (see eq.(3.2.10)). Two general class of examples of K satisfying (3.7.7) are:

$$K|A\rangle = \sum_n a_n K_n|A\rangle\,, \tag{3.7.8}$$

where $K_n = L_n - (-1)^n L_{-n}$, and

$$K|A\rangle = |S * A\rangle - |A * S\rangle\,, \tag{3.7.9}$$

for some ghost number zero state $|S\rangle$. Let us now consider the gauge invariant operator

$$\mathcal{O}_V(\widetilde{\Phi}) = \langle V(0) h_1 \circ \widetilde{\Phi}(0))\rangle_D = \langle \mathcal{I}|V(i)|\widetilde{\Phi}\rangle\,, \tag{3.7.10}$$

invariant under the gauge transformation

$$\delta|\widetilde{\Phi}\rangle = Q_B|\Lambda\rangle + |(\widetilde{\Phi} + \Phi_0) * \Lambda\rangle - |\Lambda * (\widetilde{\Phi} + \Phi_0)\rangle\,, \tag{3.7.11}$$

and study what happens to this under an infinitesimal field redefinition generated by a K of the form (3.7.8) or (3.7.9). It is easy to see that both these field redefinitions preserve the form of $\mathcal{O}_V$, replacing $\widetilde{\Phi}$ by $(g_o^2\kappa_0)^{1/3}\Psi$. For transformations of the form (3.7.8) this follows because $V(i)$, being a dimension zero primary, commutes with the K_n's and the identity is annihilated by K_n. For transformations of the form (3.7.9), form invariance follows from eq.(3.7.5). Thus if $\widetilde{\Phi}$ and Ψ are related by a field redefinition of the form (3.7.6), with K being a combination of transformations of the type (3.7.8) or (3.7.9), then we can conclude that $\mathcal{O}_V(\widetilde{\Phi})$ is given by $(g_o^2\kappa_0)^{1/3}\mathcal{O}_V(\Psi)$, with

$$\mathcal{O}_V(\Psi) = \langle V(0) h_1 \circ \Psi(0))\rangle_D = \langle \mathcal{I}|V(i)|\Psi\rangle\,. \tag{3.7.12}$$

This must be a gauge invariant operator in VSFT. Invariance of (3.7.12) under the VSFT gauge transformation (3.2.7) follows directly from (3.7.5), and the relation $\langle \mathcal{I}|A * B\rangle = \langle A|B\rangle$. Invariance under (3.2.6) requires

$$\langle \mathcal{I}|V(i)\mathcal{Q}|\Lambda\rangle \equiv \langle h_1 \circ (V(i)\mathcal{Q}\Lambda(0))\rangle_D = 0\,. \tag{3.7.13}$$

If we choose $\mathcal{Q}$ to be of the form $\sum_n u_n \mathcal{C}_n$, then for any choice of the coefficients u_n, $\mathcal{Q}$ commutes with $V(i)$. Thus if we further restrict the u_n's so that $\mathcal{Q}$ annihilates $|\mathcal{I}\rangle$, then the gauge invariance of $\mathcal{O}_V$ is manifest. Our choice $\mathcal{Q} = (c(i) - c(-i))/2i$, however, does not annihilate $|\mathcal{I}\rangle$ unless we define $\mathcal{Q}$ in a specific manner discussed in (3.2.24). Nevertheless, as we shall now show, $\mathcal{Q}$ annihilates $V(i)|\mathcal{I}\rangle$ independently of the definition (3.2.24) and

simply because of the collision of local ghost insertions. Consider a definition of $\mathcal{Q}$ that does not annihilate $|\mathcal{I}\rangle$, by putting the operators in $\mathcal{Q}$ at $i+\epsilon$ for some finite ϵ and then take the $\epsilon \to 0$ limit. This gives:

$$\begin{aligned} & \langle h_1 \circ (V(i)\mathcal{Q}\Lambda(0))\rangle_D \propto \lim_{\epsilon\to 0} \Big\langle h_1 \circ \Big(V(i)(c(i+\epsilon)-\bar{c}(i+\epsilon))\Lambda(0)\Big)\Big\rangle_D \\ = & \lim_{\epsilon\to 0} \Big\langle V(h_1(i))\Big\{\frac{c(h_1(i+\epsilon))}{h_1'(i+\epsilon)} - \frac{\bar{c}(h_1(i+\epsilon))}{\bar{h}_1'(i+\epsilon))}\Big\} h_1 \circ \Lambda(0)\Big\rangle_D . \end{aligned} \tag{3.7.14}$$

Using the results:

$$h_1(i+\epsilon) \sim \epsilon^2, \quad h_1'(i+\epsilon) \sim \epsilon, \quad V(0)c(\eta) \sim \eta, \qquad V(0)\bar{c}(\eta) \sim \eta\,, \tag{3.7.15}$$

we see that the expression between $\Big\langle \cdots \Big\rangle$ vanishes linearly in ϵ. Thus $\mathcal{O}_V(\Psi)$ defined in (3.7.12) is invariant under each of the transformations (3.2.6) and (3.2.7) for $\mathcal{Q}$ given in (3.2.5).

It is interesting to relate the present discussion to our observations on the cohomology of $\mathcal{Q}$ below equation (3.2.5). It was noted there that $\mathcal{Q}$ closed states had to have ghost insertions at the open string midpoint. The question that emerges is whether or not the gauge invariant operators discussed here are $\mathcal{Q}$ trivial. Presumably they are not. Indeed, thinking of $c\bar{c}V_m$ as c acting on $\bar{c}V_m$ we find that the insertion of $\bar{c}V_m$, which is not of dimension zero but rather of negative dimension, on a point with a defect angle leads to a divergence. Therefore one cannot think of the gauge invariant operators as ordinary trivial states. Alternatively, one may wonder if the condition that the closed string vertex operator V be a dimension-zero primary can be relaxed and still have $\mathcal{O}_V$ be a sensible gauge invariant operator. Again, the answer is expected to be no. Inserting an operator with dimension different from zero at the conical singular point either gives zero or infinity. Moreover, if the operator is not primary there are also difficulties with equation (3.7.5).

3.7.3 Classical expectation value of $\mathcal{O}_V$

Given a classical solution of VSFT representing a D-brane we can ask what is the value of

$$\mathcal{O}_V(\Psi_{cl}) = \langle \mathcal{I}|V(i)|\Psi_{cl}\rangle\,. \tag{3.7.16}$$

For $|\Psi_{cl}\rangle = |\Psi_g\rangle \otimes |\Psi_m\rangle$, and $V = c\bar{c}V_m$, we have:

$$\mathcal{O}_V(\Psi_{cl}) = \langle \mathcal{I}_g | c\bar{c}(i) | \Psi_g \rangle \, \langle \mathcal{I}_m | V_m(i) | \Psi_m \rangle \, . \tag{3.7.17}$$

The ghost factor is universal, – common to all D-brane solutions, and all closed string vertex operators of the form $c\bar{c}V_m$. If we take $|\Psi_m\rangle$ to be a solution of the form discussed in [60], representing a D-brane associated with some boundary CFT $\widetilde{BCFT}$, then it is easy to show following the techniques of [60] that $\langle \mathcal{I}_m | V(i) | \Psi_m \rangle$ has the interpretation of a one point correlation function on the disk, with closed string vertex opertor V_m inserted at the center of the disk, and the boundary condition associated with $\widetilde{BCFT}$ on the boundary of the disk. This, in turn can be interpreted as $\langle \widetilde{B}_m | V_m \rangle$ where $\langle \widetilde{B}_m |$ is the matter part of the boundary state associated with $\widetilde{BCFT}$ and $|V_m\rangle$ is the closed string state created by the vertex operator V_m.

3.8 Closed string amplitudes in VSFT

In this section we give our proposal for the emergence of pure closed string amplitudes in the context of VSFT. The basic idea is that the open string correlation of the gauge invariant observables discussed in the previous section give rise to closed string amplitudes obtained by integration over the moduli spaces of Riemann surfaces *without boundaries*. In order to justify this we will have to make use of the regularized version of VSFT.

3.8.1 Computation of correlation functions of $\mathcal{O}_V$

We shall now study correlation functions of the operators $\mathcal{O}_V$ in VSFT. In particular, we shall analyze the following gauge invariant correlation functions:

$$\langle\langle \mathcal{O}_{V_1}(\Psi) \cdots \mathcal{O}_{V_n}(\Psi) \rangle\rangle \tag{3.8.18}$$

where $\langle\langle \, \rangle\rangle$ stands for correlation functions in string field theory and should not be confused with correlation functions in two dimensional conformal field theory. These correlation functions are calculated by the usual Feynman rules of string field theory, – in particular

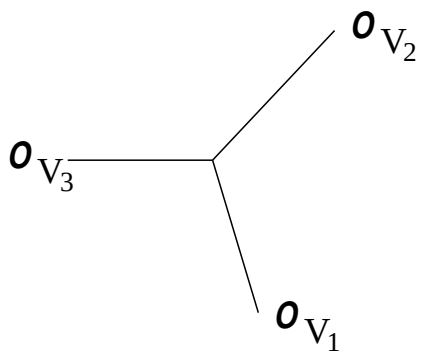

Figure 3.2: The feynman diagram contributing to the correlation function $\langle\langle \mathcal{O}_{V_1}\mathcal{O}_{V_2}\mathcal{O}_{V_3}\rangle\rangle$.

for $n = 3$ the tree level correlation function receives contribution from just one Feynman diagram shown in Fig.3.2. In computing these Feynman diagrams we shall work with the regulated action (3.5.1) and take the $a \to 0$ limit at the end. Including all the normalization factors, the Siegel gauge propagator is given by:

$$a(\kappa_0(a))^{-1}\frac{b_0}{L_0+a} = \frac{a}{\kappa_0(a)}b_0\int_0^\infty dl e^{-l(L_0+a)}\,. \tag{3.8.19}$$

We should, however, keep in mind that this regularization procedure is ad hoc, and so the results obtained from this should be interpreted with caution The correct regularization procedure presumably comes from replacing the singular reparametrization discussed in section 3.2.2 by a nearly singular reparametrization.

Since the propagator (3.8.19) is closely related to the propagator of OSFT, and reduces to it up to an overall normalization in the $a \to 0$ limit, it will be useful to first review the calculation of these correlation function in OSFT around the D-25-brane background. In OSFT, the Feynman diagrams just have closed string vertex operators attached to strips of length ℓ_i and these strips, together with internal open string propagators, are glued with three open string vertices. So a typical diagram will have schematically

$$\prod_i \int_0^\infty d\ell_i e^{-\ell_i L_0} \prod_J \int_0^\infty d\ell_J e^{-\ell_J L_0}$$

where the ℓ_J are intermediate propagator lengths. For an amplitude with n external closed strings there are altogether $(2n-3)$ propagators and $(n-2)$ vertices. Let us denote by l_α

$(1 \le \alpha \le (2n-3))$ the lengths of the strips associated with these $(2n-3)$ propagators. Thus the contribution to the amplitude can be written as (ignoring powers of the open string coupling constant g_o):

$$\int \prod_{\alpha=1}^{2n-3} dl_\alpha F(l_1, \ldots l_{2n-3}) \tag{3.8.20}$$

for some appropriate integrand F which is computed in terms of correlators of closed string vertex operators and ghost factors associated with the propagators on an appropriate Riemann surface.

If we repeat the calculation in VSFT with the regularized propagator (3.8.19), we get an additional factor $e^{-a\sum l_\alpha}$ in the integrand. This, in effect will restrict the integration region to l_α of order a^{-1} or less. Also each propagator carries a multiplicative factor of $a/\kappa_0(a)$ and each vertex carries a multiplicative factor of $\kappa_0(a)$. Thus the amplitude now takes the form:

$$\begin{aligned} A_n &= (a/\kappa_0(a))^{2n-3}(\kappa_0(a))^{n-2} \int \prod_{\alpha=1}^{2n-3} dl_\alpha e^{-a\sum l_\alpha} F(l_1, \ldots l_{2n-3}) \\ &= (a^2/\kappa_0(a))^n a^{-3}\kappa_0(a) \int_0^\infty dv \int \prod_{\alpha=1}^{2n-3} dl_\alpha \delta(v - \sum l_\alpha) e^{-av} F(l_1, \ldots l_{2n-3})\,. \end{aligned} \tag{3.8.21}$$

We can absorb the n factors of $(a^2/\kappa_0(a))$ into a multiplicative renormalization of the operators $\mathcal{O}_V$. Using eq.(3.5.4) with $\mathcal{E}_a = \mathcal{T}_{25}$, the renormalized amplitude may be written as:

$$A_n = \frac{\mathcal{T}_{25}}{a^3 F(a)} \int_0^\infty dv\, e^{-av} \int \prod_{\alpha=1}^{2n-3} dl_\alpha\, \delta(v - \sum l_\alpha) F\Big(l_1, \ldots l_{2n-3}\Big)\,. \tag{3.8.22}$$

$F(l_1, \ldots l_{2n-3})$ is computed by evaluating a correlation function on a Riemann surface of the form shown in Fig.3.3. Since v in the above integral represents the sum of the length parameters l_α, we have $l_\alpha \le v$, and the closed string vertex operators are inserted within a distance of order v of each other. The boundary, shown by the thick line at the bottom, has length $2v$ since each length parameter l_α contributes a length $2l_\alpha$ to the boundary. Finally, the height of the diagram, measured by the distance between the boundary and the closed

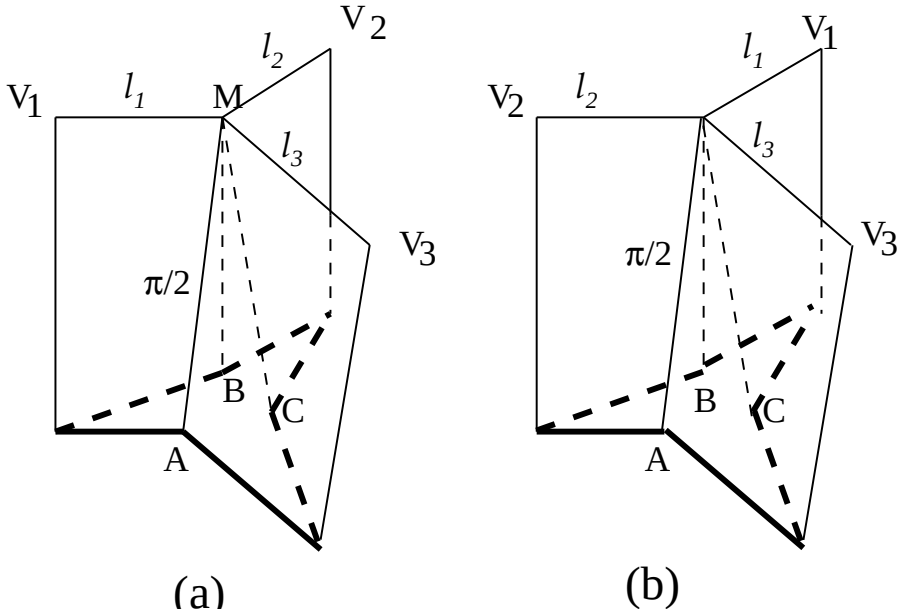

Figure 3.3: The Riemann surface representations of the Feynman diagram contribution to the three closed string amplitude. V_i denote the locations of the closed string vertex operators, l_α denote the lengths of the strips representing open string propagators, and AMB, BMC and CMA denote the three strings interacting via the three string vertex with a common mid-point M. The thick line at the bottom is the boundary of the world-sheet diagram created from the Feynman diagram. The two diagrams originate from two different contributions to the three string vertex, corresponding to $\langle A,\, B{*}C\rangle$ and $\langle A,\, C{*}B\rangle$ respectively.

string vertex operators, is constant and equal to $\pi/2$ – this is because open string strips have width π. In addition to the closed string vertex operators, the correlator also includes an insertion of b_0 on each propagator.

Let us now rescale the metric on this world-sheet by multiplying all lengths by πv^{-1}. In the resulting metric, and with v now small, the Riemann surface looks like a long cigar of circumference 2π and height $l_c = \pi^2/(2v)$. All the closed string vertex operators are inserted within a finite distance of each other at the closed end of the cigar, and their positions are naturally parametrized by quantities u_α defined, for $\alpha = 1, 2\cdots, 2n-3$, as

$$u_\alpha = 2\pi\,\frac{l_\alpha}{v} \quad \rightarrow \quad \sum_\alpha u_\alpha = 2\pi\,. \tag{3.8.23}$$

The other end of the cigar is open and represents the boundary of the surface. The inte-

gration contours for the b-integrals run parallel to the length of the cigar. We will call this surface $\mathcal{C}_v(\vec{u})$, and as defined it is a cylinder of height $\pi^2/(2v)$, circumference 2π, with one end open and the other sealed and having closed string punctures with positions parameterized by the u_α. We can use v and u_α as independent variables of integration. Since the b-contour integrals in the correlation function guarantee that the integrand transforms as a volume form $dv \wedge du_1 \wedge \cdots$ in the moduli space, we can formally denote these insertions as $B_v B_{\vec{u}}$, where B_v denotes a single b insertion associated with the v-integration and $B_{\vec{u}}$ is product of $(2n-4)$ b-insertions associated with the integration over $\vec{u}$. Calling $\mathcal{M}(\vec{u})$ the moduli space of u_α's, the amplitude in (3.8.22) can thus be written as

$$A_n = \frac{\mathcal{T}_{25}}{a^3 F(a)} \int_0^\infty dv\, e^{-av} \int_{\mathcal{M}(\vec{u})} \langle V_1 \cdots V_n B_v B_{\vec{u}} \rangle_{\mathcal{C}_v(\vec{u})} \,. \tag{3.8.24}$$

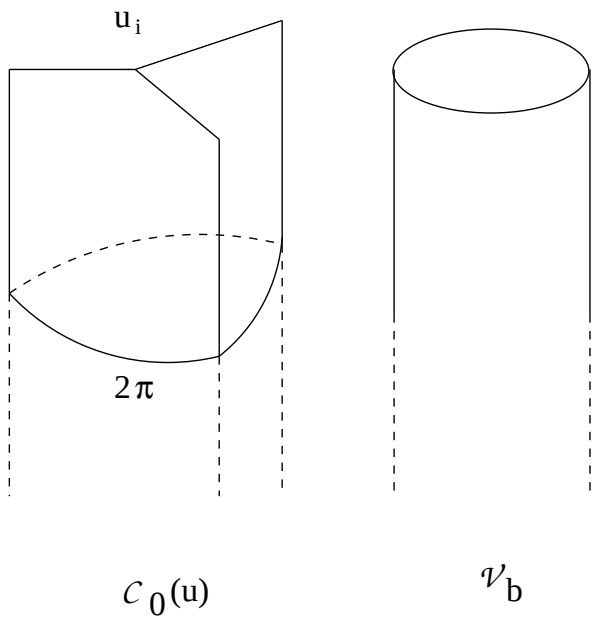

Figure 3.4: Pictorial representation of $\mathcal{C}_0(\vec{u})$ and $\mathcal{V}_b$ which are glued together to produce the surface $\mathcal{C}_v(\vec{u})$.

In order to proceed further we build the surface $\mathcal{C}_v(\vec{u})$ by sewing the semi-infinite cylinder $\mathcal{C}_0(\vec{u})$, obtained when $v = 0$, to the closed/boundary vertex $\mathcal{V}_b$ represented by a semi-infinite cylinder of circumference 2π ending on an open boundary. If we denote by w_1 and w_2 the coordinates used to describe the above two cylinders $\mathcal{C}_v(\vec{u})$ and $\mathcal{V}_b$, with $w_i \equiv w_i + 2\pi$ and

$\Im(w_i) < 0$, and we let $z_i = \exp(-iw_i)$; the sewing relation $z_1 z_2 = t$, with real t produces the surface $\mathcal{C}_v$ with $v = -\pi^2/(2\ln t)$. We therefore have that the amplitude in question can be written as:

$$\begin{aligned} A_n &= \frac{\mathcal{T}_{25}}{a^3 F(a)} \int_0^\infty dv\, e^{-av} \int_{\mathcal{M}(\vec{u})} \sum_k \langle V_1 \cdots V_n B_{\vec{u}} \chi_k \rangle_{\mathcal{C}_0(\vec{u})} \\ &\qquad \cdot \langle \chi_k^c | B_v e^{-\frac{\pi^2}{2v}(L_0 + \bar{L}_0)} | \mathcal{V}_b \rangle \,, \end{aligned} \tag{3.8.25}$$

where the χ_k is a basis element in the space of ghost number two closed string vertex operators, χ_k^c is the conjugate basis of ghost number four vertex operators satisfying $\langle \chi_k^c | \chi_l \rangle = \delta_{kl}$, $|\mathcal{V}_b\rangle$ denotes the boundary state associated with the D-brane under consideration, and $L_0, \bar{L}_0$ refers to the closed string Virasoro generators. In the first correlator, χ_k is inserted on the puncture at infinity, and the second correlator is the one point function on the semi-infinite cylinder.

We now need to determine B_v. This is done by going to the $l_c = \pi^2/2v$ coordinate system, and using the transformation property of the b-insertions under a change of coordinates. In particular, we have

$$B_v dv = B_{l_c} dl_c \,. \tag{3.8.26}$$

Furthermore the form of B_{l_c} is well known, – it simply corresponds to an insertion of a contour integral of $(b + \bar{b})$ along the circumference of the cigar. We shall denote this by $(b_0 + \bar{b}_0)$. This gives:

$$dv B_v = \frac{\pi^2}{2v^2} dv (b_0 + \bar{b}_0) \,. \tag{3.8.27}$$

Substituting this into eq.(3.8.25) we get,

$$\begin{aligned} A_n &= \frac{\mathcal{T}_{25}}{a^3 F(a)} \frac{\pi^2}{2} \int_0^\infty \frac{dv}{v^2}\, e^{-av} \int_{\mathcal{M}(\vec{u})} \sum_k \langle V_1 \cdots V_n B_{\vec{u}} \chi_k \rangle_{\mathcal{C}_0(\vec{u})} \\ &\qquad \cdot \langle \chi_k^c | (b_0 + \bar{b}_0) e^{-\frac{\pi^2}{2v}(L_0 + \bar{L}_0)} | \mathcal{V}_b \rangle \,, \end{aligned} \tag{3.8.28}$$

The key geometrical insight now is that the moduli space $\mathcal{M}(\vec{u})$ defines a space of surfaces $\mathcal{C}_0(\vec{u})$ which is precisely the moduli space $\mathcal{M}_{n+1}$ of $n+1$-punctured spheres. This is a rigorous result and follows from a new minimal area problem that will be discussed in

the next subsection. Therefore the integral above can be written as

$$\begin{aligned} & \frac{\mathcal{T}_{25}}{a^3F(a)}\,\frac{\pi^2}{2}\,\sum_k \int \frac{dv}{v^2} e^{-av} e^{-\frac{\pi^2}{2v}(h_k+\bar{h}_k)} \langle \chi_k^c|(b_0+\bar{b}_0)|\mathcal{V}_b\rangle \\ & \qquad\qquad \cdot \int_{\mathcal{M}_{n+1}} \langle V_1 \cdots V_n B_{\vec{u}} \chi_k\rangle_{\mathcal{C}_0(\vec{u})} \\ = & \sum_k C_k A_c(V_1, \ldots V_n, \chi_k)\,, \end{aligned} \tag{3.8.29}$$

where $(h_k, \bar{h}_k)$ is the conformal weight of χ_k, and $A_c(V_1, \ldots V_n, \chi_k)$ is the $(n+1)$-point closed string amplitude of states $V_1, \ldots V_n$ and χ_k. C_k are constants defined as:

$$C_k = \frac{\mathcal{T}_{25}}{a^3F(a)}\,\frac{\pi^2}{2}\,\int \frac{dv}{v^2} e^{-av} e^{-\frac{\pi^2}{2v}(h_k+\bar{h}_k)} \langle \chi_k^c|(b_0+\bar{b}_0)|\mathcal{V}_b\rangle\,. \tag{3.8.30}$$

The multiplicative factor C_k is non-zero in the $a \to 0$ limit only for $h_k + \bar{h}_k \leq 0$. For this range of values of $(h_k, \bar{h}_k)$ C_k's are actually infinite due to the divergence in the v-integral from $v \simeq 0$ region. However, note that the multiplicative factor $\mathcal{T}_{25}/(a^3F(a))$ vanishes as $a \to \infty$ as is seen from Fig.3.1. Thus this competes against the divergent v-integral. It will be interesting to see if in the correct regularization procedure inherited from OSFT, the divergences in the v integral are also regulated (as will happen, for example, if the kinetic operator is multiplied by an additional factor of $e^{\epsilon L_0}$ for some small ϵ), and the final answer for the closed string amplitude is actually finite.

We also note that among the contributions to (3.8.29) is the contribution due to the zero momentum dilaton intermediate state. By the soft dilaton theorem, this is proportional to the on-shell n-point closed string amplitude on the sphere. One could again speculate that in the correct regularization procedure this is the only contribution that survives, and so the correlation function (3.8.18) in the correctly regularized VSFT actually gives us back the on-shell n-point amplitude at genus zero. A similar argument has been given in [87] in the context of boundary string field theory.

Since the regularization procedure we have been using is ad hoc, one can ask what aspect of our results can be trusted in a regularization independent manner. To this end, note that if the kinetic operator is simply c_0, then the corresponding propagator is represented by a strip of zero length. Thus whatever be the correct regularization procedure, the regulated

propagator will be associated with strips of small lengths if the regularization parameter (analog of a^{-1}) is small. As our analysis shows, in this case the corresponding Feynman diagram contribution to (3.8.18) will be associated with a world-sheet diagram with small hole, and this, in turn, is related to genus zero correlation functions of closed string vertex operators with one additional closed string insertion. Thus we can expect that whatever be the correct regularization procedure, the correlation function (3.8.18) will always be expressed in terms of a genus zero correlation function of closed string vertex operators.

In the absence of a proper understanding of the correct regularization procedure of the VSFT propagator, a more direct approach to the problem of computing closed string amplitude in the tachyon vacuum will be to try to do this computation directly in OSFT around the tachyon vacuum. There are two competing effects. On the one hand we have divergence due to the dilaton and other tadpoles. On the other hand, the coefficient of the divergence vanishes since the tachyon vacuum has zero energy. Both of these are regulated in level truncation. Thus it is conceivable that if we compute the correlation functions of the operators $\mathcal{O}_V$ in OSFT around the tachyon vacuum by first truncating the theory at a given level L, and then take the limit $L \to \infty$, then we shall get a finite result for these correlation functions.

3.8.2 Closed string moduli from open string moduli

We have seen in the previous subsection that the calculation of a correlator of gauge invariant observables in regulated VSFT can be related to the amplitude involving closed string states parametrizing these observables if a certain kind of string diagrams produces a full cover of the moduli space of closed Riemann surfaces with punctures. The diagrams in question are obtained by drawing all the diagrams of OSFT supplemented by the open/closed vertex with the constraint that the total boundary length is $2v$. Here $v = \sum l_\alpha$ where the l_α's are the lengths of the open string propagators. The diagrams are then conventionally scaled to have cylinder with a total boundary length of 2π and height of $\pi^2/(2v)$. The patterns of gluing are described by the parameters $u_\alpha \geq 0$ defined in (3.8.23) and satisfying $\sum_\alpha u_\alpha = 2\pi$. At

this stage one lets $v \to 0$ and thus the cylinder becomes semi-infinite, with the boundary turning into the $(n+1)$-th puncture. The claim is that the set of surfaces obtained by letting the u_α parameters vary generate precisely the moduli space of $(n+1)$ punctured spheres.

In order to prove this we will show that the above diagrams arise as the solution of a minimal area problem. As is well-known, minimal area problems guarantee that OSFT, closed SFT, and open/closed SFT generate full covers of the relevant moduli spaces.[10] The basic idea is quite simple; given a specific surface, the metric of minimal area under a set of length conditions exists and is unique. Thus if we can establish a one to one correspondence between the string diagrams labelled by $\{u_\alpha\}$ and such metrics, we would establish that the u_α integration region covers the moduli space in a one to one fashion. The minimal area problem for our present purposes is the following

Consider a genus zero Riemann surface with $(n+1)$ punctures. Pick one special pucture P_0, and find the minimal area metric under the condition that all curves homotopic to P_0 have length larger or equal to 2π.

As usual homotopy equivalence does not include moving curves across punctures, thus a curve surrounding P_0 and P_1 is not said to be homotopic to a curve surrounding P_0. This problem is a modification of the minimal area problem defining the polyhedra of classical closed string field theory [80] – in this case one demands that the curves homotopic to all the punctures be longer than or equal to 2π [85].

We use the principle of saturating geodesics to elucidate the character of the minimal area metric solving our stated problem. This principle [81] states that through every point in the string diagram there must exist a curve saturating the length condition. Therefore the solution must take the form of a semi-infinite cylinder of circumference 2π. The infinite end represents the puncture P_0. The other side must be sealed somehow, and the other n punctures must be located somewhere in this cylinder. Since there are no length conditions

[10] In the case of OSFT, the first proof of cover of moduli space was given in [83] who focused on the case of surfaces without open string punctures, and argued that by factorization the result extends to the case with punctures. In [84] a direct proof based on minimal area metrics is seen to apply for all situations.

for the other punctures, they do not generate their own cylinders.

Assume now that the other punctures are met successively as we move up the cylinder towards the sealed edge. This is actually impossible, as we now show. Let P_1 be the first puncture we meet as we move up from P_0. Consider a saturating circle just below the first such puncture. That circle has to be of length 2π since it is still homotopic to P_0. If the cylinder continues to exist beyond P_1 a geodesic circle of length 2π just above P_1 is not homotopic any more to P_0, and there is no length constraint on it anymore. This cannot be a solution of the minimal area problem since the metric could be shrunk along that circle without violating any length condition. This shows that all the punctures must be met at once. Thus the picture is that of a semiinfinite cylinder, where on the last circle the n closed string punctures are located, and the various segments of the circle are glued to each other to seal the cylinder, so that any nontrivial curve not homotopic to P_0 can be shrunk to zero length.

This is exactly the pattern of the string diagrams that we obtained. It is clear that the u_α parameters associated to a fixed Feynman graph are in fact gluing parameters. Thus the string diagrams solve the minimal area problem and due to the uniqueness of the minimal area metric they do not double count. Can they miss any surface ? There are two alternative ways to see that the answer is no. First, the space of u_α parameters has no codimension one boundaries, and includes all the requisite degenerations of the $(n+1)$ punctured sphere associated with the collision of two or more punctures. Since these are the standard properties of moduli spaces, no surfaces can be missing. Second, for any surface there is a string diagram – this is guaranteed because this minimal area problem is known to have a solution defined by a Jenkins-Strebel quadratic differential. Such quadratic differential builds a string diagram consistent with our Feynman rules, and thus must have been included.

We illustrate the above result with an example, the case of four-punctured spheres generated by considering the correlation of three gauge invariant observables. We shall explain that the only boundaries of the u_α integration region are the known boundaries of

the moduli space corresponding to degeneration of the four-punctured sphere. In this case three strips of lengths ℓ_1, ℓ_2, ℓ_3 representing the three external propagators are joined by a 3 open string vertex – no internal propagator is possible here. The amplitude contains sum over two different world-sheet digrams, coming from two different cyclic arrangements of the open strings at the vertex, as shown in Fig.3.3(a) and (b). If we denote by l_1, l_2, l_3 the lengths of the strips associated with the open string propagators, and $v = l_1 + l_2 + l_3$, then the region of integration, with $u_i = 2\pi l_i/v$, is

$$u_i \geq 0\,, \quad \sum u_i = 2\pi\,. \tag{3.8.31}$$

There are apparently three codimension one boundaries of the u_i integration region, associated with each $u_i = 0$. These correspond to $l_i = 0$. It is easy, however, to see from Fig.3.3 that the configuration $l_i = 0$ for any i are actually identical configurations in the two diagrams, and hence in the sum of two diagrams the $l_i = 0$ configuration simply marks the transition from the component of the moduli space covered by the first diagram to another component of the moduli space covered by the second diagram. On the other hand the codimension two boundaries corresponding to the three cases of $u_i = 2\pi$, represent the configurations where two length parameters vanish and produce the expected degenerations of the 4-punctured sphere. In particular the $l_i = l_j = 0$ configuration represents the degeneration where the i-th and the j-th vertex operators come close to each other, and the other vertex operator approaches, in the conformal sense, the boundary of the surface.

Indeed even if the height of the cylinders is finite we are producing a boundaryless subspace of the moduli space of a sphere with three punctures and one hole. As the height of the cylinder goes to infinity we really have four punctures and again we are producing a boundaryless moduli space involving four punctures on a sphere and all the requisite degenerations. This must be the moduli space of four punctured spheres.

The generalization to the case of n-point amplitude is straightforward. Any codimension one boundary corresponding to a single l_i vanishing marks a transition to another component of the moduli space represented by another diagram, whereas if a group of l_i associated with a connected part of the diagram, and containing at least two external propagator vanishes,

it corresponds to a degeneration of the Riemann surface. A detailed argument along the lines of [84] should be possible to construct, but as we do not expect complications, we shall not attempt to give the complete argument here.

The discussion above clearly holds for surfaces of arbitrary genus, and the minimal area problem is just the same one. More interestingly, however, the discussion also generalizes for the case of multiple boundary components. Given our Feynman rules of regularized VSFT, the analysis of the previous subsection would lead to surfaces in which each boundary component would give rise to a semi-infinite cylinder of circumference 2π. The various cylinders would join simultaneously with a generalized set of u_α parameters describing their gluing. If the Feynman graph represents a surface of genus g with n gauge invariant operators and b boundaries, the space of u_α parameters will generate the moduli space $\mathcal{M}_{g,n+b}$ of genus g boundariless Riemann surfaces with $n+b$ punctures. The associated minimal area problem justifying this result would consider the metric of minimal area on a genus g surface with $n+b$ punctures under the condition that all curves homotopic to the b punctures be longer than or equal to 2π. Thus the correlation function would reduce to the pure closed string amplitude of n closed string vertex operators and b zero momentum massless states.

3.9 Discussion

In this chapter we have presented a specific form of the kinetic term $\mathcal{Q}$ of VSFT that can give a precise definition of the theory and make it possible to study in detail various questions. While the selected $\mathcal{Q}$ is special in several ways, VSFT thus defined needs regulation for some but not all computations. Our regulation of VSFT is admittedly somewhat tentative. If VSFT can be shown explicitly to arise as a singular reparametrization of the OSFT action expanded around the tachyon vacuum, a more natural regulator may be obtained by viewing the reparametrization as a flow and using the representatives near the singular endpoint.

We believe other results presented in this chapter may have uses beyond the ones investigated presently.

- Our explicit level expansion calculations have uncovered the existence of surface states different from the sliver and still satisfying the projector condition. These new projectors may have important applications and we further analyze them in the next chapter.

- The twisted CFT used to obtain exact analytic solutions may be a useful tool to obtain exact solution of string field theory even for the original OSFT representing the vacuum around unstable D-branes.

- We have uncovered local gauge invariant operators in open string field theory. Their natural relation to closed string vertex operators is reminiscent of AdS/CFT, and of gauge invariant operators in non-commutative gauge theory. There could be interesting uses for these operators in studying observables of VSFT.

- We have seen how closed string moduli arise from the open string moduli of regulated VSFT, by noting how a minimal area problem involving open string curves naturally dovetails into a minimal area problem involving closed string curves. This, we believe may capture the essence of the mechanism by which closed strings emerge in vacuum string field theory.

Chapter 4

Projectors for the Star Product

4.1 Introduction and Summary

The star-algebra of open string fields, the associative multiplication introduced in [6], is the key algebraic structure in string field theory theory. We saw in the previous chapter that D-brane solutions for Vacuum SFT correspond to open string fields were projectors of the star algebra, *i.e.* elements which square to themselves.

As the complicated algebraic structure of the star product is one big obstacle to the effort of finding exact solutions to OSFT equations of motion, and as the set of projectors of an algebra contains rich information about the algebra itself, it is interesting to learn more about projectors of the star algebra.

For many years, the only string field known to multiply to itself was the identity string field. In fact, there were heuristic reasons to believe that projectors should be scarce in the star algebra.[1] One can understand the difficulty in constructing projectors within the large class of field configurations that arise from path integration over fixed Riemann surfaces whose boundary consists of a parametrized open string and a piece with open string boundary conditions. Such string fields, called surface states, are easily star multiplied.[2]

[1] We learned of such ideas from E. Witten.

[2] We shall be using the standard correspondence between quantum states of the first quantized theory and classical field configurations in the second quantized theory to refer to string field configurations as "states". In the same spirit we use the term "wave-functional" to refer to the functional of the string coordinates that

One glues the right-half of the open string in the first surface to the left-half of the open string in the second surface, and the surface state corresponding to the glued surface is the desired product. It is clear from this description that multiplication of a surface state to itself leads to a surface state that looks different from the initial state. This is the reason why it seemed difficult, in general, to find projectors.

Leaving aside the identity string field, the first projector of the star algebra to be found was the sliver state [12, 73, 57]. It circumvents the above mentioned difficulty in an interesting way. Consider wedge states, surface states where the Riemann surface is an angular sector of the unit disk, with the left-half and the right-half of the open string being the two radial segments, and the unit radius arc having the open string boundary conditions. A wedge state is thus defined by the angle at the open string midpoint, and this angle simply adds under star multiplication, as is readily verified using the gluing prescription. The identity string field is the wedge state of zero angle, and the sliver is the wedge state of infinite angle! The addition of infinity to infinity is still infinity, and the sliver does star multiply to itself.[3]

The sliver state was later recognized to be a string wave-functional that is split: it is the product of a functional of the left-half of the string times the same functional of the right-half of the open string. From this viewpoint, however, it seemed surprising that projectors would be hard to find: any symmetric split string wave-functional could serve as a projector. At least algebraically other projectors could easily be constructed by transforming the sliver by the action of star conjugation. Geometrically, however, it was not clear if there are other projectors which could be simply interpreted as other surface states.

In this chapter we find large classes of projectors that indeed arise as surface states, and we explain the general mechanism by which they all evade the heuristic argument sketched earlier. All the projectors we find correspond to surface states where in the Riemann surface, the open string midpoint reaches the boundary where the open string boundary conditions

represents the classical string field configuration.

[3]The only question here is whether the sliver defined as the infinite angle limit of a sector state exists. It does, as seen in [12], explained in detail in [59] and confirmed numerically.

are imposed (this is also the case for the sliver). The general situation is illustrated in figure 4.1. The vertical boundary is the open string, and its midpoint is indicated by a heavy dot. The rest of the boundary has open string boundary condition. More precisely, one can regulate the surface state by letting the open string midpoint reach the boundary when the regulator is removed. We explain that in the limit as the regulator is removed, the string wave-functional splits into a product of functionals. In considering the projector property, we examine the gluing of two regulated projector surface states. The gluing of the two regulated surfaces does not give a surface that looks like the original one, but rather, a surface that looks like the original one plus a short neck connecting it to an additional disk. We will explain that, conformally speaking, the short neck and the extra disk are in fact negligible perturbations in the sense that the resulting surface is accurately conformally equivalent to the original one without the extra disk. The agreement becomes exact as the regulator is removed. We consider this a key insight in the present chapter. It shows how conformal equivalence is subtle enough to circumvent the heuristic arguments against the existence of projectors.

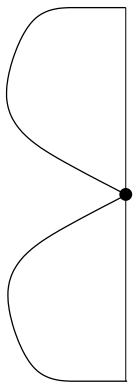

Figure 4.1: The generic kind of surface state providing a projector of the star algebra. The open string is the vertical boundary, and the open string midpoint is shown with a heavy dot. The rest of the boundary has open string boundary condition. Note that this part of the boundary touches the open string midpoint.

All the above are rank one projectors, and are expected to be related by star conjugation. Nevertheless there are special projectors that deserve special attention, for they satisfy a

number of unusual conditions that may be of some relevance. In addition to the sliver, our studies have uncovered two special projectors – the butterfly and the 'nothing' state. We now summarize the special properties of these three projectors.

For the sliver $|\Xi\rangle$ we have:

- It is the projector that arises by repeated star multiplication of the SL(2,R) vacuum, namely $|\Xi\rangle = \lim_{n\to\infty}(|0\rangle)^n$.
- It is a projector whose Neumann matrix in the oscillator representation commutes with those defining the star product.
- It is the limit element of a sequence of surface states, the wedge states, defining an abelian subalgebra of the star algebra. The sliver state is annihilated by the star algebra derivation $K_1 = L_1 + L_{-1}$.

The properties of the "butterfly" state were announced in [24]:

- It has an extremely simple presentation in the Virasoro basis. It is just $\exp(-\frac{1}{2}L_{-2})|0\rangle$. It is annihilated by the star derivation $K_2 = L_2 - L_{-2}$.
- Its wave-functional is the product of *vacuum* wave-functionals for the left-half and the right-half of the string. Thus, it is the simplest projector from the viewpoint of half-strings.
- This is the state that appears to arise when considering the projector equations in the level expansion.

We constructed a family of projectors, all of them generalized butterflies, that interpolate from the sliver to the above canonical butterfly. The family can be continued beyond this canonical butterfly state up to a projector that we call the "nothing state". The nothing state has the following properties:

- As we reach this state the Riemann surface becomes vanishingly small.

- It is annihilated by all the derivations $K_{2n} = L_{2n} - L_{-2n}$.
- It has a constant wave-functional.

Our general discussion shows that the condition that the open string midpoint touches the boundary ensures that projectors have split wave-functionals, that is, wave-functionals that factorize into a product of functionals each involving a half-string. We also show that the half-string states associated to surface state projectors are themselves surface states defined with the same boundary condition as the original projector, and give an explicit algorithm for the construction of such half-string states (see (4.4.14) and (4.4.15)). For example, our construction explains why the butterfly is the state corresponding to the tensor product of half string vacua with Neumann boundary condition at both ends if the original butterfly is defined with Neumann boundary condition. We believe this is an interesting insight into half-string formalisms, where boundary conditions at the string midpoint are subject to debate, and little geometrical understanding is available. We also point out a subtletly. When we say that a surface state is *defined* using a boundary condition, this means that the functional integral defining the state is done imposing the boundary condition in question along the boundary of the surface. A surface state $|\Sigma\rangle$ *defined* using a given boundary condition, say of Neumann type, may not necessarily satisfy this condition, namely, expectation values of the operator $\partial_\sigma X(\sigma)$ on the state $|\Sigma\rangle$ may not necessarily vanish at $\sigma = 0, \pi$. This may happen when the boundary of the surface Σ has a corner type singularity at the string endpoints. While such corner type singularities are not common in familiar surface states, they are generic for half-string states. Thus, for example, we find that unlike the canonical butterfly half-string state, the nothing half-string state satisfies a Dirichlet boundary condition at the point corresponding to the full string midpoint.

We also show that, just as for the sliver [71], all projectors defined with Neumann boundary condition have wave-functionals invariant under constant and opposite translations of the half-strings. This implies that the Neumann matrices associated to projectors all have a common eigenvector, the $\kappa = 0$ eigenvector of K_1. This simply follows, as we explain in the text, because the associated half-string surface states carry no momentum.

This chapter is organized as follows. We begin in section 4.2 by reviewing various geometrical presentations of surface states, and various concrete algebraic representations of the states. Section 4.3 is devoted to a discussion of some properties of conformal maps and conformal field theories which we use in later analysis. In particular we discuss factorization properties of conformal field theory correlators on a pinched disk that is about to split into two disconnected disks. Although we do not attempt to state precisely the way in which the surface must be pinched to achieve the desired factorization property, we state a conjecture that we expect to hold, and would guarantee the key properties. We also illustrate the conjecture with an example.

In section 4.4 we explain in general terms our understanding of the construction of split wave-functionals. In particular we argue, based on the results of sections 4.2, 4.3 that the surface state associated with a conformal map that sends the string midpoint to a point on the boundary of the disk will give a state whose wave-functional factorizes into a functional of the left half of the string and a functional of the right half of the string. The analysis in this section is done in the context of a general boundary conformal field theory. We show how to construct the half-string *surface* states corresponding to split wave-functionals.

In section 4.5 we explain in general terms that the same condition that gives rise to split wave-functionals also guarantees that the corresponding states are projectors. We show that the projectors are of rank one. In addition, we prove that all surface state projectors have Neumann matrices that share a common eigenvector.

In section 4.6 we describe in detail the butterfly state. We show how to regulate it and prove explicitly that the state satisfies the projector equation by constructing the requisite conformal maps. We also use the method of section 4.4 to show the factorization property of the butterfly wave-functional, and explicitly determine the functional of the left and the right-half of the string to which the butterfly wave-functional factorizes. Both of these turn out to be the wave-functional of the vacuum state. Section 4.7 is devoted to a similar study of the nothing state.

In section 4.8 we introduce the family of generalized butterflies parametrized by a pa-

rameter α, interpolating from the sliver at $\alpha = 0$ up to the 'nothing' state at $\alpha = 2$, passing through the butterfly at $\alpha = 1$. We show explicitly that for every α the associated surface state is a projector. The nothing state at $\alpha = 2$ is particularly interesting, since after removing the local coordinate patch the corresponding surface has vanishing area. We also show explicitly that the wave-functionals of these generalized butterfly states factorize into functionals of the left- and the right-half string coordinates, and determine these functionals.

In section 4.9 we discuss additional simple projectors, which just as the butterfly, can be represented by the exponentiation of a single Virasoro operator. We discuss some properties of these projectors, and sketch the construction of certain star-subalgebras. In section 4.10 we discuss butterfly states associated to general boundary conformal field theories (BCFT's), represented as a state in the state space of some fixed reference BCFT. This generalizes previous arguments that were known to hold for the sliver state. Finally we offer some concluding remarks in section 4.11. We include an appendix where we give the explicit numerical computation of the $*$-product of the butterfly state with itself to show that it indeed behaves as a projector of the $*$-algebra. We also test sucessfully the expected rank one property of the projector.

Related but independent research on the matter of projectors and butterfly states has been published recently by M. Schnabl [102].

4.2 Surface States – Presentations and Representations

In this section we shall discuss general properties of surface states. After reviewing the geometric description of surface states in various coordinates, we discuss the computation of star products and inner products of surface states in the geometric language. We then discuss the explicit operator, oscillator and functional representations of general surface states.

4.2.1 Reviewing various presentations

For the purposes of the arguments in this chapter we will review the various coordinate systems used to describe surface states. A surface state $\langle\Sigma|$ for the present purposes arises from a Riemann surface Σ with the topology of a disk, with a marked point P, the puncture, lying on the boundary of the disk, and a local coordinate around it.

The ξ coordinate. This is the local coordinate. The local coordinate, technically speaking is a map from the canonical half-disk $|\xi| \leq 1, \Im(\xi) \geq 0$ into the Riemann surface Σ, where the boundary $\Im(\xi) = 0, |\xi| < 1$ is mapped to the boundary of Σ and $\xi = 0$ is mapped to the puncture P. The open string is the $|\xi| = 1$ arc in the half-disk. The point $\xi = i$ is the string midpoint. The surface Σ minus the image of the canonical ξ half-disk will be called $\mathcal{R}$. Using any *global coordinate* u on the disk representing Σ, and writing

$$u = s(\xi)\,, \quad \text{with} \quad s(0) = u(P)\,, \tag{4.2.1}$$

the surface state $\langle\Sigma|$ is then defined through the relation:

$$\langle\Sigma|\phi\rangle = \langle s \circ \phi(0)\rangle_\Sigma\,, \tag{4.2.2}$$

for any state $|\phi\rangle$. Here $\phi(x)$ is the vertex operator corresponding to the state $|\phi\rangle$ and $\langle\ \rangle_\Sigma$ denotes the correlation function on the disk Σ. There is nothing special about a specific choice of global coordinate u, and the state $\langle\Sigma|$ built with the above prescription does not change under a conformal map taking u to some other coordinate and Σ into a different looking (but conformally equivalent) disk. Nevertheless there are particularly convenient choices which we now discuss in detail.

The z- presentation. In this presentation the Riemann surface Σ is mapped to the *full* upper half z-plane, with the puncture lying at $z = 0$. The image of the canonical ξ half-disk is some region around $z = 0$. Thus if $z = f(\xi)$, we have

$$\langle\Sigma|\phi\rangle = \langle f \circ \phi(0)\rangle_{UHP}\,. \tag{4.2.3}$$

The $\widehat{z}$-presentation. In this presentation the Riemann surface Σ is mapped such that the image of the canonical ξ half-disk is the full strip $|\Re(\widehat{z})| \leq \pi/4, \Im(\widehat{z}) \geq 0$, with $\xi = i$

mapping to $\widehat{z} = i\infty$, and the open string mapping to the vertical half lines at $\Re(\widehat{z}) = \pm\frac{\pi}{4}$. This is implemented by the map

$$\widehat{z} = \tan^{-1}\xi\,. \tag{4.2.4}$$

The rest $\mathcal{R}$ of Σ will take some definite shape that will typically fail to coincide with the full upper-half $\widehat{z}$ plane. This shape actually carries the information about the surface Σ.

The $\widehat{w}$- presentation. In this presentation the Riemann surface Σ is mapped such that the image of the canonical ξ half-disk is the canonical half disk $|\widehat{w}| \leq 1, \Re(\widehat{w}) \geq 0$, with $\xi = 0$ mapping to $\widehat{w} = 1$. This is implemented by the map

$$\widehat{w} = \frac{1 + i\xi}{1 - i\xi} \equiv h(\xi)\,. \tag{4.2.5}$$

The rest $\mathcal{R}$ of the surface will take some definite shape $\widehat{\mathcal{R}}$ in this presentation. This shape actually carries the information about the surface Σ. We also note that the $\widehat{w}$-presentation and the $\widehat{z}$ presentation are related as

$$\widehat{w} = \exp(2i\widehat{z})\,. \tag{4.2.6}$$

The ξ- presentation. In this presentation the Riemann surface Σ is mapped into the ξ-plane by extending to the whole surface Σ the map that takes the neighborhood of the puncture $P \in \Sigma$ into the ξ-half-disk. This extended map, of course, may require branch cuts. In this presentation the surface is the canonical ξ half-disk plus some region in the ξ-plane whose shape carries the information of the state. We call Σ_ξ the surface in this presentation. In this case the equation defining the state takes a particularly simple form since no conformal map is necessary

$$\langle\Sigma|\phi\rangle = \langle\phi(0)\rangle_{\Sigma_\xi}\,. \tag{4.2.7}$$

The ξ presentation can be obtained from the $\widehat{w}$ presentation by the action of h^{-1}.

4.2.2 Inner products and star-products of surface states

In this subsection we will address the computation of correlation functions of the form $\langle\Sigma|\prod_{i=1}^{n}\mathcal{O}_i(\xi_i)|\Sigma\rangle$ with ξ_i's lying on the unit circle. These are inner products of surface

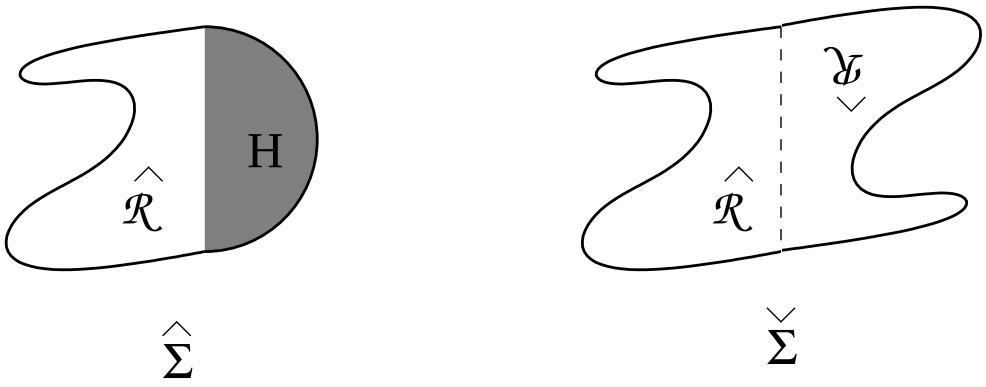

Figure 4.2: The geometry involved in computing the inner product of a surface state $|\Sigma\rangle$ with itself.

states with operator insertions. Such computations will play a role in our later analysis of split wave-functionals and half-string states. We will also discuss star products of surface states.

These computations are particularly simple in the representation of the surface Σ in the $\widehat{w}$ coordinate system. Let $\widehat{\mathcal{R}}$ and $\widehat{\Sigma}$ denote the images of $\mathcal{R}$ and Σ in the $\widehat{w}$ plane. Then we can rewrite eq.(4.2.2) as

$$\langle\Sigma|\phi\rangle = \langle h\circ\phi(0)\rangle_{\widehat{\Sigma}}\,, \tag{4.2.8}$$

where h has been defined in eq.(4.2.5). To compute $\langle\Sigma|\prod_{i=1}^{n}\mathcal{O}_i(\xi_i)|\Sigma\rangle$ we begin with two copies of $\widehat{\Sigma}$, remove the local coordinate patches from each so that we are left with two copies of $\widehat{\mathcal{R}}$, and then simply construct a new disk by gluing the left-half string of the first disk to the right half-string of the second string and vice versa, as shown in Fig.4.2. If we denote the new disk by $\check{\Sigma}$ then we have

$$\langle\Sigma|\prod_{i=1}^{n}\mathcal{O}_i(\xi_i)|\Sigma\rangle = \langle\prod_{i=1}^{n}h\circ\mathcal{O}(\xi_i)\rangle_{\check{\Sigma}}\,. \tag{4.2.9}$$

The $h\circ\mathcal{O}_i(\xi_i)$ factors are inserted at the images of the points $\xi_i = e^{i\sigma_i}$ in the $\widehat{w}$ plane, *i.e.* on the imaginary axis.

We shall also need to compute the star product of a surface state with itself. This is again simple in the $\widehat{w}$ coordinate system. We begin with two copies of the disk $\widehat{\Sigma}$, remove

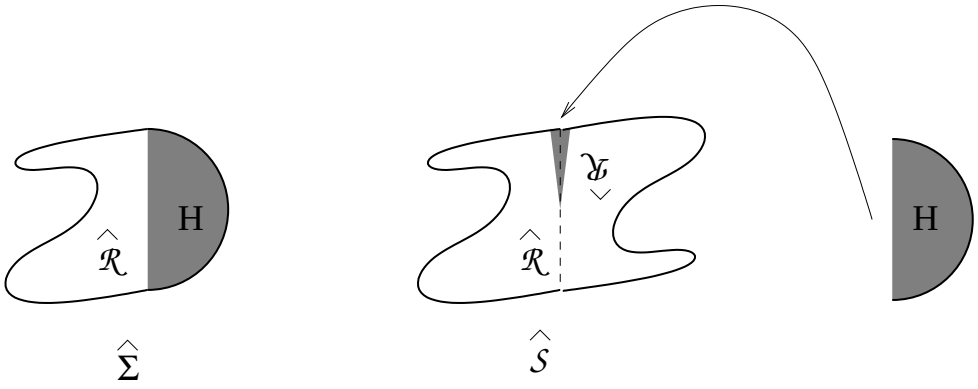

Figure 4.3: The geometry involved in computing the star product of a surface state with itself. The local coordinate patch, shown as the shaded half-disk to the right, is to be glued to the shaded region of the diagram representing $\widehat{\mathcal{S}}$.

the local coordinate patch from the second $\widehat{\Sigma}$, and then glue the right half-string of the first $\widehat{\Sigma}$ with the left half-string of the second $\widehat{\Sigma}$. The result is a new disk $\widehat{\mathcal{S}}$, as shown in Fig.4.3. As indicated in the figure, the local coordinate patch is glued in and thought as part of $\widehat{\mathcal{S}}$. The surface state $|\mathcal{S}\rangle$ associated with the new surface $\widehat{\mathcal{S}}$ gives $|\Sigma * \Sigma\rangle$. Thus we have:

$$\langle \Sigma * \Sigma | \phi \rangle = \langle h \circ \phi(0) \rangle_{\widehat{\mathcal{S}}} \,. \tag{4.2.10}$$

4.2.3 Operator representation of surface states

We shall now review the explicit representation of surface states in terms of Virasoro operators acting on the SL(2,R) invariant vacuum, rather than the implicit representation through correlators given eq.(4.2.3). Using the SL(2,R) invariance of the upper half plane, we can make the map f appearing in eq.(4.2.3) satisfy $f(0) = f''(0) = 0$, $f'(0) = 1$. We can write the corresponding surface state $\langle \Sigma |$ as

$$\langle \Sigma | = \langle 0 | U_f \equiv \langle 0 | \exp \left(\sum_{n=2}^{\infty} v_n^{(f)} L_n \right) , \tag{4.2.11}$$

where the coefficients $v_n^{(f)}$ are determined by the condition that the vector field

$$v(\xi) = \sum_{n=2}^{\infty} v_n^{(f)} \xi^{n+1} \,, \tag{4.2.12}$$

exponentiates to f,

$$\exp\left(v(\xi)\partial_\xi\right)\xi = f(\xi)\,. \tag{4.2.13}$$

We now consider the one-parameter family of maps

$$f_\beta(\xi) = \exp\Big(\beta\, v(\xi)\frac{\partial}{\partial\xi}\Big)\,\xi\,. \tag{4.2.14}$$

This definition immediately gives

$$\frac{d}{d\beta}f_\beta(\xi) = v(f_\beta(\xi))\,. \tag{4.2.15}$$

Solution to this equation, subject to the boundary condition $f_{\beta=0}(\xi) = \xi$, gives:

$$f_\beta(\xi) = g^{-1}(\beta + g(\xi))\,, \tag{4.2.16}$$

where

$$g'(\xi) = \frac{1}{v(\xi)}\,. \tag{4.2.17}$$

Thus

$$f(\xi) = g^{-1}(1 + g(\xi))\,. \tag{4.2.18}$$

Equations (4.2.17) and (4.2.18) readily give $f(\xi)$ if $v(\xi)$ is known. Alternatively, they also determine $v(\xi)$ in terms of $f(\xi)$, although not explicitly, since eqn. (4.2.18) is in general hard to solve for g. When a solution for $v(\xi)$ is available, eqn.(4.2.11) gives the operator expression for $|\Sigma\rangle$.

4.2.4 Oscillator representation of surface states

If the BCFT under consideration is that of free scalar fields with Neumann boundary condition describing D-25-branes in flat space-time, we can also represent the state in terms of the oscillators associated with the scalar fields. For simplicity let us restrict our attention to the matter part of the state only. If a_m, $a_m^\dagger$ denote the annihilation and creation operators associated with the scalar fields, then we have:

$$|\Sigma\rangle = \exp\left(-\frac{1}{2}\sum_{m,n=1}^{\infty} a_m^\dagger V_{mn}^f a_n^\dagger\right)|0\rangle\,. \tag{4.2.19}$$

where we have suppressed spacetime indices and [79]

$$V^f_{mn} = \frac{(-1)^{m+n+1}}{\sqrt{mn}} \oint_0 \frac{dw}{2\pi i} \oint_0 \frac{dz}{2\pi i} \frac{1}{z^m w^n} \frac{f'(z)f'(w)}{(f(z)-f(w))^2} \,. \tag{4.2.20}$$

Both w and z integration contours are circles around the origin, with the w contour lying outside the z contour, and both contours lying inside the unit circle. In eq.(4.2.19) we have also omitted an overall normalization factor.

We now show that when the vector field $v(\xi)$ generating the conformal map $f(\xi)$ is known (see the discussion in the previous subsection) the above integral expression for the matrix V^f of Neumann coefficients can be given an alternate form which is sometimes easier to evaluate. For this purpose, we now consider the matrix $V(\beta)$ associated to the family of maps (4.2.14), and rewrite (4.2.20) as

$$V_{mn}(\beta) \equiv V^{f_\beta}_{mn} = \frac{(-1)^{m+n+1}}{\sqrt{mn}} \oint_0 \frac{dw}{2\pi i} \oint_0 \frac{dz}{2\pi i} \frac{1}{z^m w^n} \frac{\partial}{\partial z} \frac{\partial}{\partial w} \log(f_\beta(z) - f_\beta(w)) \,. \tag{4.2.21}$$

Taking a derivative with respect to the parameter β,

$$\begin{aligned} \frac{d}{d\beta} V_{mn}(\beta) &= \frac{(-1)^{m+n+1}}{\sqrt{mn}} \oint_0 \frac{dw}{2\pi i} \oint_0 \frac{dz}{2\pi i} \frac{1}{z^m w^n} \frac{\partial}{\partial z} \frac{\partial}{\partial w} \frac{\partial}{\partial \beta} \log(f_\beta(z) - f_\beta(w)) \qquad (4.2.22) \\ &= \frac{(-1)^{m+n+1}}{\sqrt{mn}} \oint_0 \frac{dw}{2\pi i} \oint_0 \frac{dz}{2\pi i} \frac{1}{z^m w^n} \frac{\partial}{\partial z} \frac{\partial}{\partial w} \left(\frac{v(f_\beta(z)) - v(f_\beta(w))}{f_\beta(z) - f_\beta(w)} \right) , \end{aligned}$$

where we have exchanged the order of derivatives and used (4.2.15). Integration by parts in z and w then gives

$$\frac{d}{d\beta} V_{mn}(\beta) = (-1)^{m+n+1} \sqrt{mn} \oint_0 \frac{dw}{2\pi i} \oint_0 \frac{dz}{2\pi i} \frac{1}{z^{m+1} w^{n+1}} \frac{v(f_\beta(z)) - v(f_\beta(w))}{f_\beta(z) - f_\beta(w)} \,. \tag{4.2.23}$$

This is a general formula that we have found useful in concrete computations. If the above matrix is calculable, the desired Neumann coefficients $V_{mn}(\beta = 1)$ are then readily obtained by integration over β.

4.2.5 Wave-functionals for surface states

In this subsection we wish to establish a dictionary between the geometric interpretation of surface states as one-punctured disks and their representation as wave-functionals of open

string configurations. For this we consider open strings on a D-25-brane in flat space-time so that we have Neumann boundary condition on all the fields, and write, for a surface state associated to the map $z = f(\xi)$

$$\langle\Sigma|X(\sigma)\rangle = \mathcal{N}_f \exp\left(-\frac{1}{2}\int_0^\pi \int_0^\pi d\sigma d\sigma' X(\sigma) A_f(\sigma,\sigma') X(\sigma')\right) . \tag{4.2.24}$$

Here we have suppressed the Lorentz indices and used the fact that the wave-functional is in fact gaussian. This follows since the vacuum $|0\rangle$ is represented by a gaussian wave-functional, and the action of U_f preserves this property. The normalization constant $\mathcal{N}_f$ is chosen so that $\langle\Sigma|\Sigma\rangle = 1$. The wave-functional can also be represented in terms of modes:

$$\langle\Sigma|X\rangle = \mathcal{N}_f \exp(-\frac{1}{2}\sum_{n,m=1}^{\infty} X_n A^{(f)}_{nm} X_m) , \tag{4.2.25}$$

where we have adopted the convention of ref.[103] to define the modes X_n:

$$X(\sigma) = X_0 + \sqrt{2}\sum_{n=1}^{\infty} X_n \cos(n\sigma) . \tag{4.2.26}$$

For simplicity we are considering the case where the coordinate X has Neumann boundary condition. Using eqs.(4.2.24), (4.2.25), (4.2.26) we see that $A_f(\sigma,\sigma')$ is related to $A^{(f)}_{nm}$ through the relation:

$$A_f(\sigma,\sigma') = \frac{2}{\pi^2}\sum_{m,n\geq 1} A^{(f)}_{nm}\cos(n\sigma)\cos(m\sigma') . \tag{4.2.27}$$

Note that X_0 does not appear in the expression for the wave-functional in (4.2.25), since all surface states are translationally invariant. We shall from now on restrict to twist-even surface states, which is equivalent to the condition that f is an odd function.

The relation between the oscillator representation (4.2.19) and the wave-functional representation (4.2.25) is given by the following relation between the matrices V^f and $A^{(f)}$[58, 61]:

$$A^{(f)} = 2E^{-1}\frac{1-V^f}{1+V^f}E^{-1} , \qquad E_{nm} = \delta_{mn}\sqrt{\frac{2}{n}} . \tag{4.2.28}$$

We want to determine $A_f(\sigma,\sigma')$ from f. To this end, we evaluate the normalized correlator

$$B_f(\sigma_1,\sigma_2) \equiv \langle\Sigma|\partial_{\sigma_1}\hat{X}(\sigma_1)\partial_{\sigma_2}\hat{X}(\sigma_2)|\Sigma\rangle \tag{4.2.29}$$

in two different ways. First, we use the wave-functional representation and obtain

$$\begin{aligned} B_f(\sigma_1,\sigma_2) &= \mathcal{N}_f^2 \int \mathcal{D}X \exp\left(-\int_0^\pi d\sigma d\sigma' X(\sigma) A_f(\sigma,\sigma') X(\sigma')\right) \partial_{\sigma_1} X(\sigma_1) \partial_{\sigma_2} X(\sigma_2) \\ &= \frac{1}{2}\partial_{\sigma_1}\partial_{\sigma_2}(A_f^{-1}(\sigma_1,\sigma_2))\,. \end{aligned} \tag{4.2.30}$$

Here the inverse kernel $A_f^{-1}(\sigma_1,\sigma_2)$ is defined by

$$\int_0^\pi d\sigma A_f(\sigma_1,\sigma) A_f^{-1}(\sigma,\sigma_2) = \delta(\sigma_1-\sigma_2) - \frac{1}{\pi}\,. \tag{4.2.31}$$

The constant $1/\pi$ in the above equation represents the contribution from the zero mode part. Since A_f does not depend on the zero modes, it has an inverse only in the subspace spanned by the functions $\cos(n\sigma)$ for $n \neq 0$. Thus $(A_f^{-1})_{mn}$ is nonzero only for $m,n \geq 1$.

In the second computation, we interpret (4.2.29) as a CFT correlator on an appropriate Riemann surface following the procedure of section 4.2.2. This is nicely done using the $\widehat{z}$ presentation (see section 4.2.1) where the surface will occupy a region $\mathcal{C}_f$ in the $\widehat{z}$ plane, and the local coordinate patch is the strip $\Im(\widehat{z}) \geq 0$, $-\pi/4 \leq \Re(\widehat{z}) \leq \pi/4$. As usual the vertical line corresponding to $\Re(\widehat{z}) = \pi/4$ is the image of the left-half of the string, and the vertical line corresponding to $\Re(\widehat{z}) = -\pi/4$ is the image of the right-half of the string. In order to compute a correlation function of the form $\langle\Sigma|\cdots|\Sigma\rangle$, we simple start with two copies of $\mathcal{C}_f$, strip off the local coordinate patch from each of them, and compute the correlation function on the surface obtained by gluing the left half-string on the first $\mathcal{C}_f$ with the right half-string on the second $\mathcal{C}_f$ and vice versa. Thus the right hand side of (4.2.29) can be computed by this method. If we denote the new surface by $\check{C}_f$, then B_f is given by

$$B_f(\sigma_1,\sigma_2) = \partial_{\sigma_1}\partial_{\sigma_2}\langle X(\widehat{z}_1) X(\widehat{z}_2)\rangle_{\check{C}_f}\,, \tag{4.2.32}$$

where $\widehat{z}_i$ are the images of the points $\xi = e^{i\sigma_i}$. Comparing (4.2.30) with (4.2.32) we can determine $A_f^{-1}(\sigma_1,\sigma_2)$ and hence the wave-functional of the surface state.

Let us illustrate this for the vacuum state $|0\rangle$. In this case the CFT computation is immediate, since we can directly compute the correlator (4.2.29) using the OPE's of X's on

the UHP,

$$\begin{aligned} B_{|0\rangle}(\sigma_1,\sigma_2) &= \partial_{\sigma_1}\partial_{\sigma_2}\Big(-\frac{1}{2}\log(|e^{i\sigma_1}-e^{i\sigma_2}|^2|e^{i\sigma_1}-e^{-i\sigma_2}|^2)\Big) \\ &= -\partial_{\sigma_1}\partial_{\sigma_2}\log(2\cos(\sigma_1)-2\cos(\sigma_2)) \\ &= \partial_{\sigma_1}\partial_{\sigma_2}\sum_{n=1}^{\infty}\frac{2}{n}\cos(n\sigma_1)\cos(n\sigma_2)\,. \end{aligned} \tag{4.2.33}$$

Using (4.2.30) and inverting the kernel, we get

$$A_{|0\rangle}(\sigma_1,\sigma_2) = \frac{2}{\pi^2}\sum_{n=1}^{\infty} n\cos(n\sigma_1)\cos(n\sigma_2)\,. \tag{4.2.34}$$

This gives

$$A^{|0\rangle}_{nm} = n\delta_{nm}\,. \tag{4.2.35}$$

This is the expected result, as can be seen by using eq.(4.2.28) with $V^f = 0$.

4.3 Conformal Field Theories on Degenerate Disks

In this section we shall consider some properties of degenerate disks involving singular conformal maps, and of conformal field theories on such degenerate disks.

4.3.1 A conformal mapping claim

Consider a set of surfaces parametrized by $t \in [0,1]$. For each t different from one, the surface $R(t)$ is a finite region of the complex plane with the topology of a disk (see figure 4.4). As t goes to one the region varies smoothly throughout but develops a thin neck and at $t = 1$ it pinches, breaking into two pieces R_1 and R_2, both of which are finite disks. Let P denote the pinching point, common to R_1 and R_2, and assume there are no other pinching points. Because disks can always be mapped to disks, any $R(t)$ with $t < 1$ can be mapped to R_1. The map in fact is not unique due to SL(2,R) invariance of the disk. We now claim that:

Claim: There exists a family of conformal maps $m(t) : R(t) \to R_1$, for $t \in [0,1]$, continuous in t, where $m(1)$ is the identity map over R_1 and maps all of R_2 to P.

The intuition here is that as far as one of the sides of the pinching surface is concerned, call it side one, all that is going on on the other side, side two, can be viewed as happening near the pinching point. The complete side two, lying on the other side of the neck, can be mapped to a vanishingly small region while the conformal map is accurately close to the identity on side one. An explicit example of this will be given next.

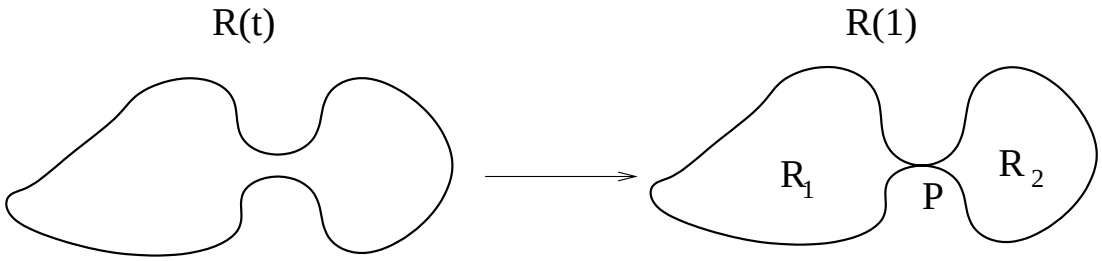

Figure 4.4: The surface $R(t)$ is pinching for $t = 1$. The pinching point P separates the regions R_1 and R_2 of the surface $R(1)$.

4.3.2 A prototype example

To illustrate the claim in the above subsection we consider the following situation. Let a surface Σ with the topology of a disk be the region in the $\hat{u}$-plane defined by $\Im(\hat{u}) \geq -\pi$ with two cuts, both along the real axis, the first for real $\hat{u} \in (-\infty, -\Delta]$ and the second for real $\hat{u} \in [\Delta, +\infty)$ where Δ is a small positive real number. As illustrated as a shaded region in figure 4.5(a), this region is the upper half plane, joined through the small interval $\hat{u} \in [-\Delta, \Delta]$ to an infinite horizontal strip of width π. We have also marked some special points $P_1, \cdots P_n$ at some real coordinates $\hat{u}(P_i)$ with $|\hat{u}(P_i)| \gg \Delta$, for all i.

This surface, in the limit $\Delta \to 0$, is pinching, and in the terminology of the claim, the region R_1 is the upper half $\hat{u}$-plane, and the region R_2 is the horizontal infinite strip of width π in the lower half plane. We will now show that the surface can be mapped completely to the upper-half u plane (figure 4.5(b)) such that the conditions in the claim are satisfied. Indeed, in the limit $\Delta \to 0$, the map will become the identity over the upper half plane (R_1) and will map all of the lower strip (R_2) into a point. We will also see that this is the limit

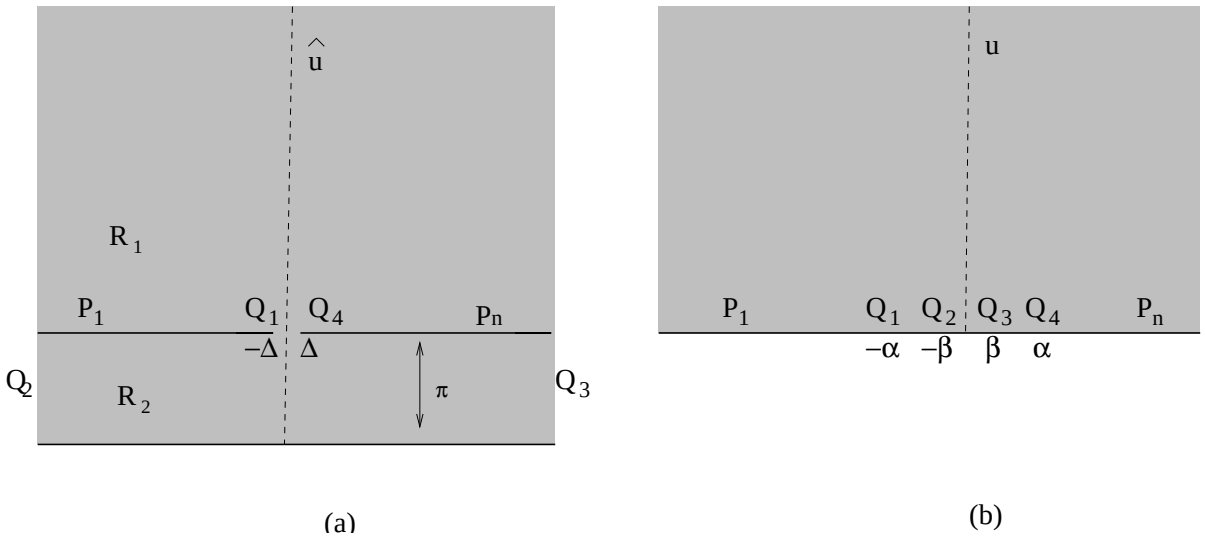

Figure 4.5: Illustration of a conformal map from the upper-half plane plus a strip of width π connected by a narrow neck (part (a)) to the upper-half plane (part (b)).

of a family of maps that near degeneration leave R_1 mostly unchanged (in a quantifiable way).

The conformal map differential equation is readily written, as it is of Schwarz-Christoffel type. Noting that the turning points Q_1 and Q_4 are points of turning angle $(-\pi)$, while Q_2 and Q_3 are turning points of turning angle $(+\pi)$ we write:

$$d\hat{u} = \frac{u^2 - \alpha^2}{u^2 - \beta^2}\, du\,. \tag{4.3.1}$$

The turning points Q_1, Q_2, Q_3, Q_4 are mapped to the points $\{-\alpha, -\beta, \beta, \alpha\}$ on the u-plane real axis, as shown in 4.5(b). We have two parameters $\{\alpha, \beta\}$ and two conditions, one defining the width of the strip, and the other specifying the separation 2Δ between Q_1 and Q_4 in the $\hat{u}$ plane. The normalization above was fixed so that for large $u \gg \{\alpha, \beta\}$, we have $d\hat{u} \sim du$, – a necessary condition for the map to become the identity when u and $\hat{u}$ are large. The condition that the strip corresponding to R_2 has width π demands that the residues of the above right hand side at $u = \pm\beta$ be equal to (∓ 1). This gives

$$\frac{\alpha^2 - \beta^2}{2\beta} = 1\,. \tag{4.3.2}$$

With this condition, the differential relation in (4.3.1) becomes:

$$d\hat{u} = \Big(1 - \frac{1}{u-\beta} + \frac{1}{u+\beta}\Big)\, du\,. \tag{4.3.3}$$

By symmetry, we require that $u = 0$ correspond to $\hat{u} = -i\pi$ and thus we have that

$$\Delta = P\int_0^{\alpha} \Big(1 - \frac{1}{u-\beta} + \frac{1}{u+\beta}\Big)\, du\,, \tag{4.3.4}$$

where P denotes principal value, which must be taken at $u = \beta$. Evaluation gives

$$\Delta = \alpha + \ln\Big(\frac{\alpha+\beta}{\alpha-\beta}\Big)\,. \tag{4.3.5}$$

It is clear from this equation that to have Δ small we need α small and $\beta \ll \alpha$. This, and the constraint in (4.3.2) can be satisfied with

$$\alpha = \sqrt{2\beta+\beta^2}, \qquad \alpha,\beta \ll 1 \quad \rightarrow \quad \beta \simeq \frac{1}{2}\alpha^2\,. \tag{4.3.6}$$

Note that given these relations, (4.3.5) gives us

$$\Delta = 2\alpha + \mathcal{O}(\alpha^2)\,, \quad \rightarrow \quad \Delta \simeq 2\alpha\,. \tag{4.3.7}$$

This shows that the whole boundary of the strip R_2, which is mapped to $u \in [-\alpha, \alpha]$, is indeed mapped to a vanishingly small segment as $\Delta \to 0$.

Finally, we confirm that the map goes to the identity map for $\{u, \hat{u}\} \gg \Delta$ when $\Delta \to 0$. For this purpose integrating from α to $u > \alpha$ we have

$$\hat{u} = \Delta + \int_{\alpha}^{u} \Big(1 - \frac{1}{u-\beta} + \frac{1}{u+\beta}\Big)\, du\,, \tag{4.3.8}$$

which using (4.3.5) gives

$$\hat{u} = u + \ln\Big(\frac{u+\beta}{u-\beta}\Big)\,, \quad u > \alpha\,. \tag{4.3.9}$$

Since $u > \alpha \gg \beta$ we have

$$\hat{u} \simeq u + \frac{2\beta}{u} \simeq u + \frac{\Delta^2}{4u} \quad \rightarrow \quad u \simeq \hat{u} - \frac{\Delta^2}{4\hat{u}}\,. \tag{4.3.10}$$

This confirms that away from the pinching area the map goes to the identity map as $\Delta \to 0$.

4.3.3 Conformal field theory and factorization

Let us now consider a unitary s boundary conformal field theory on a surface $R(t)$ of the type described in section 4.3.1 and consider a correlation function of the form:

$$\langle \prod_{i=1}^{n} \mathcal{O}_i(z_i) \rangle_{R(t)} \,. \tag{4.3.11}$$

$\mathcal{O}_i$ could be bulk or boundary operators of the theory. We shall assume that all operators in the theory have dimension > 0 except the identity operator which has dimension zero. Let us now consider the case where in the $t \to 1$ limit the points $z_1, \ldots z_m$ lie inside the disk R_1 and the points $z_{m+1}, \ldots z_n$ lie inside the disk R_2. In this limit, using the results of the previous subsection we can map the disk R to the disk R_1 in such a way that the map is the identity inside R_1 and maps the whole of R_2 to a point P. Thus the insertion points $z_{m+1}, \ldots z_n$ approach the point P. The correlation function on such a disk can be evaluated by picking up the leading terms in the operator product expansion of the appropriate conformal transforms of the operators $\mathcal{O}_{m+1}, \ldots \mathcal{O}_n$. Since the lowest dimension operator in the theory is the identity operator, we get:

$$\langle \prod_{i=1}^{n} \mathcal{O}_i(z_i) \rangle_{R(t=1)} = \langle \prod_{i=1}^{m} \mathcal{O}_i(z_i) \rangle_{R_1} g(z_{m+1}, \ldots z_n) \,, \tag{4.3.12}$$

where $g(z_{m+1}, \ldots z_n)$ is the function that appears in evaluating the coefficient of the identity operator in the operator product expansion of the appropriate conformal transforms of $\mathcal{O}_{m+1}, \ldots \mathcal{O}_n$.

On the other hand, we could also carry out the analysis using a different conformal transformation that maps the disk $R(1)$ to R_2 and maps the disk R_1 to the point P. In this case we have

$$\langle \prod_{i=1}^{n} \mathcal{O}_i(z_i) \rangle_{R(t=1)} = \langle \prod_{i=m+1}^{n} \mathcal{O}_i(z_i) \rangle_{R_2} f(z_1, \ldots z_m) \,. \tag{4.3.13}$$

Combining eqs.(4.3.12) and (4.3.13), and normalizing the correlator so that the $\langle \mathbf{1} \rangle_\Sigma = 1$ on any disk Σ, we get

$$\langle \prod_{i=1}^{n} \mathcal{O}_i(z_i) \rangle_{R(t=1)} = \langle \prod_{i=1}^{m} \mathcal{O}_i(z_i) \rangle_{R_1} \, \langle \prod_{i=m+1}^{n} \mathcal{O}_i(z_i) \rangle_{R_2} \,. \tag{4.3.14}$$

Thus the correlation function on the splitting surface factors into the product of correlation functions of the separate surfaces.

4.4 Split wave-functionals and Half-string States

In this section we will show that the split wave-functional property of surface states holds when the boundary of the surface reaches the open string midpoint. This is a very general statement, and our purpose here will be to explain it just based on the conformal mapping properties of pinching surfaces, and the factorization properties of CFT correlators, both of which were discussed in the previous sections. In the process we shall find an explicit surface state construction of half-string states that emerge from the split wave-functional. Throughout this section we shall focus on the matter part of the surface state only.

4.4.1 Factorization of the string wave-functional

We shall examine the condition under which a string state $|\Psi\rangle$ gives rise to a wave-functional $\Psi[X(\sigma)]$ that factorizes into a functional of the left half of the string and a functional of the right half of the string. As is clear from the discussion of section 4.2.5, all information about the wave-functional associated to a state $|\Psi\rangle$ is contained in correlation functions of the form

$$\langle\Psi|\prod_{i=1}^{n}\mathcal{O}_i(\xi_i)|\Psi\rangle = \int[\mathcal{D}X(\sigma)]\prod_{i=1}^{n}\widetilde{\mathcal{O}}_i(X(\sigma_i))\Psi[X(\pi-\sigma)]\Psi[X(\sigma)]\,, \tag{4.4.1}$$

where $\xi_i = e^{i\sigma_i}$, $\mathcal{O}_i$ denote an arbitrary set of local vertex operators, and $\widetilde{\mathcal{O}}_i$ are these vertex operators viewed as classical functionals of $X(\sigma)$. Let us consider the case where σ_i for $1 \le i \le m$ lie in the range $[0, \pi/2)$, and σ_i for $(m+1) \le i \le n$ lie in the range $(\pi/2, \pi]$. If the wave-functional is factorized into a functional Φ_L of the coordinates of the left-half of the string ($X(\sigma)$ for $0 \le \sigma < \pi/2$) and a functional Φ_R of the coordinates of the right-half of the string ($X(\sigma)$ for $\pi/2 < \sigma \le \pi$):

$$\Psi[X(\sigma)] = \Phi_L[X(2\sigma)]\Phi_R[X(2(\pi-\sigma))]\,. \tag{4.4.2}$$

Note that the parametrization of the right half-string has reversed direction; as σ increases we move towards the full string midpoint, just as for the left half-string. It now follows that the correlation function (4.4.1) has the factorized form:

$$\langle\Psi|\prod_{i=1}^{n}\mathcal{O}_i(\xi_i)|\Psi\rangle = f(\sigma_1,\ldots\sigma_m)\,g(\sigma_{m+1},\ldots\sigma_n)\,. \tag{4.4.3}$$

Alternatively, if eq.(4.4.3) is satisfied by all such correlation functions, we can conclude that Ψ has a factorized wave-functional. This will be our test of factorization.

Furthermore, if $|\Phi_L\rangle$ and $|\Phi_R\rangle$ denote the states associated with the left and the right half of the string respectively, then we have:

$$f(\sigma_1,\ldots\sigma_m) = \langle\Phi_R^c|\prod_{i=1}^{m}s\circ\mathcal{O}_i(\xi_i)\,|\Phi_L\rangle\,, \tag{4.4.4}$$

where s denotes the conformal transformation $s:\xi\to\xi^2$ and the superscript c denotes twist transformation: $\sigma\to(\pi-\sigma)$, needed for the right half-string. Here the conformal transformation s rescales the coordinate σ so that the coordinate labeling the left half-string runs from 0 to π. Similarly we have

$$g(\sigma_{m+1},\ldots\sigma_n) = \langle\Phi_R^c|\prod_{i=m+1}^{n}\tilde{s}\circ\mathcal{O}_i(\xi_i)\,|\Phi_L\rangle\,, \tag{4.4.5}$$

where $\tilde{s}$ denotes the conformal transformation $\xi\to\xi^{-2}$.

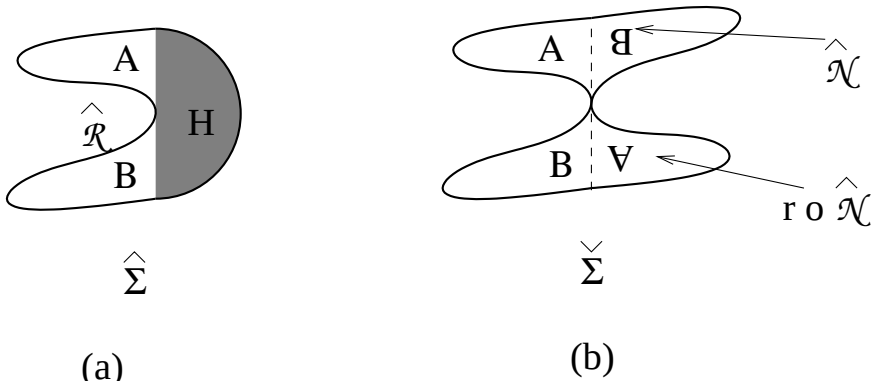

Figure 4.6: The geometry of the disks $\widehat{\Sigma}$ and $\check{\Sigma}$ when the boundary of $\widehat{\Sigma}$ touches the string midpoint.

We shall now show that (4.4.3) is satisfied for $|\Psi\rangle = |\Sigma\rangle$ if any part of the boundary of $\mathcal{R}$, – the part of the disk Σ outside the local coordinate patch – touches the point $\xi = i$, or equivalently, if in the $\widehat{w}$ plane any part of the boundary of $\widehat{\mathcal{R}}$ touches the point $\widehat{w} = 0$. Such a situation has been shown in Fig.4.6(a). According to the general result discussed in section 4.2.2, the left hand side of (4.4.3) for $|\Psi\rangle = |\Sigma\rangle$ is expressed as a correlation function on a surface $\widehat{\mathcal{S}}$, obtained by gluing together two copies of $\widehat{\mathcal{R}}$ along the procedure illustrated in Fig.4.2. In the present context, the gluing of two such disks produces a disk $\check{\Sigma}$ which is pinched at the origin of the $\widehat{w}$ plane, as shown in Fig.4.6(b). In the diagram the images of the points $\sigma_1, \ldots \sigma_m$, lying on the left half-string, are on the positive imaginary axis, whereas those of the points $\sigma_{m+1}, \ldots \sigma_n$, lying on the right half-string, are on the negative imaginary axis. $\check{\Sigma}$ can be viewed as the union of two disks $\widehat{\mathcal{N}}$ and $r \circ \widehat{\mathcal{N}}$, joined at the origin, where r denotes the conformal map $\widehat{w} \to -\widehat{w}$. Since the total surface is pinched, the conformal field theory results of section 4.3.3 hold, and working with normalized correlation functions so that the partition function on a disk equals one, the correlation function (4.2.9) factorizes as

$$\langle \prod_{i=1}^{n} h \circ \mathcal{O}(\xi_i) \rangle_{\check{\Sigma}} = \langle \prod_{i=1}^{m} h \circ \mathcal{O}(\xi_i) \rangle_{\widehat{\mathcal{N}}} \, \langle \prod_{i=m+1}^{n} h \circ \mathcal{O}(\xi_i) \rangle_{r \circ \widehat{\mathcal{N}}} \, . \tag{4.4.6}$$

This establishes eq.(4.4.3). Furthermore this gives:

$$f(\sigma_1, \ldots \sigma_m) = \langle \prod_{i=1}^{m} h \circ \mathcal{O}(\xi_i) \rangle_{\widehat{\mathcal{N}}} \, . \tag{4.4.7}$$

Comparing with eq.(4.4.4) we have:

$$\langle \Phi_R^c | \prod_{i=1}^{m} s \circ \mathcal{O}_i(\xi_i) \, | \Phi_L \rangle = \langle \prod_{i=1}^{m} h \circ \mathcal{O}_i(\xi_i) \rangle_{\widehat{\mathcal{N}}} = \langle \prod_{i=1}^{m} s \circ \mathcal{O}_i(\xi_i) \rangle_{s \circ h^{-1} \circ \widehat{\mathcal{N}}} \, . \tag{4.4.8}$$

where in the last step we used the conformal invariance of the correlator to act on the region $\widehat{\mathcal{N}}$ first by the h^{-1} conformal map, and then by s. If the region $s \circ h^{-1} \circ \widehat{\mathcal{N}}$ is simple enough the explicit identification of the half string state is possible.

4.4.2 Half-string surface states

The above results lead to a representation of the state of the half-string as a surface state. For convenience, let us restrict ourselves to the case where the original projector was twist

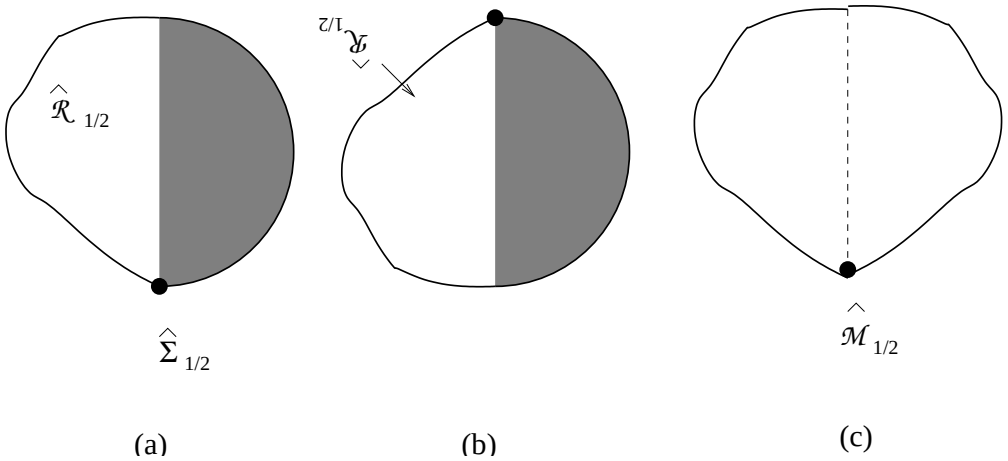

Figure 4.7: Fig. (a) shows the the disk associated with a a surface state, describing the state of the half-string, in the $\widehat{w}$ plane. Fig.(b) shows the twist conjugate of the surface state of Fig.(a). Fig.(c) shows the result of computing inner product between these two stares. $\widehat{\mathcal{M}}_{1/2}$ in this figure is the union of $\widehat{R}_{1/2}$ with its image under a reflection about the imaginary axis. The dots signal the half-string endpoint corresponding to the full-string midpoint. The other half- string endpoint coincides with one of the end-points of the original string.

invariant, which in this context means that $\widehat{\Sigma}$ (and hence $\widehat{\mathcal{R}}$) are symmetric under reflection about the real axis. Thus for these states $|\Phi_L\rangle = |\Phi_R\rangle \equiv |\Phi\rangle$. In that case we can rewrite eq.(4.4.8) as

$$\langle \Phi^c | \prod_{i=1}^{m} s \circ \mathcal{O}_i(\xi_i) \, |\Phi\rangle = \langle \prod_{i=1}^{m} s \circ \mathcal{O}_i(\xi_i) \rangle_{s \circ h^{-1} \circ \widehat{\mathcal{N}}} \, . \tag{4.4.9}$$

Let us take as a trial solution for $\langle \Phi^c |$ a surface state, represented by a disk $\widehat{\Sigma}_{1/2}$ in the $\widehat{w}$ coordinate system, so that

$$\langle \Phi^c | \phi \rangle = \langle h \circ \phi(0) \rangle_{\widehat{\Sigma}_{1/2}} \, . \tag{4.4.10}$$

As usual we denote by $\widehat{\mathcal{R}}_{1/2}$ the part of $\widehat{\Sigma}_{1/2}$ with local coordinate patch removed. This has been shown in Fig.4.7(a). The surface state associated with $\langle \Phi |$ will have an associated $\widehat{\mathcal{R}}$ which is the reflection of $\widehat{\mathcal{R}}_{1/2}$ about the real axis. This has been shown in Fig.4.7(b). In this case, we can represent the left hand side of (4.4.9) as

$$\langle \Phi^c | \prod_{i=1}^{m} s \circ \mathcal{O}_i(\xi_i) \, |\Phi\rangle = \langle \prod_{i=1}^{m} h \circ s \circ \mathcal{O}_i(\xi_i) \rangle_{\widehat{\mathcal{M}}_{1/2}} \, , \tag{4.4.11}$$

where $\widehat{\mathcal{M}}_{1/2}$ represents the disk obtained by the union of $\widehat{\mathcal{R}}_{1/2}$ with its image under a reflection about the imaginary axis. This has been shown in Fig.4.7(c). The operators $h \circ s \circ \mathcal{O}_i(\xi_i)$ are inserted on the dotted line in this figure. We can rewrite this equation as

$$\langle \Phi^c | \prod_{i=1}^{m} s \circ \mathcal{O}_i(\xi_i) \, |\Phi\rangle = \langle \prod_{i=1}^{m} s \circ \mathcal{O}_i(\xi_i) \rangle_{h^{-1} \circ \widehat{\mathcal{M}}_{1/2}} \, . \tag{4.4.12}$$

Comparing (4.4.9) and (4.4.12) we get

$$\widehat{\mathcal{M}}_{1/2} = h \circ s \circ h^{-1} \circ \widehat{\mathcal{N}} \, . \tag{4.4.13}$$

Let $\widehat{\mathcal{R}}_{top}$ denote the top wing of $\widehat{\mathcal{R}}$ associated with the original projector describing a state of the full string. This is what has been labeled as the region A in Fig.4.6(a). Given that for twist invariant state the region B in Fig.4.6(a) is related to the region A by a reflection about the real axis, we see from Fig.4.6(b) that the region $\widehat{\mathcal{N}}$ is the union of $\widehat{\mathcal{R}}_{top}$ with its reflection about the imaginary axis. On the other hand we have already seen that $\widehat{\mathcal{M}}_{1/2}$ is the result of the union of $\widehat{\mathcal{R}}_{1/2}$ with its reflection I about the imaginary axis. Finally, it can be easily seen that conjugation by $h \circ s \circ h^{-1}$ leaves invariant the reflection I. Thus (4.4.13) implies that:

$$\widehat{\mathcal{R}}_{1/2} = h \circ s \circ h^{-1} \circ \widehat{\mathcal{R}}_{top} \, . \tag{4.4.14}$$

Conversely

$$\widehat{\mathcal{R}}_{top} = h \circ s^{-1} \circ h^{-1} \circ \widehat{\mathcal{R}}_{1/2} \, . \tag{4.4.15}$$

These equations show how to pass back and forth from the split full-string surface state to the associated half-string surface state. We will use this strategy to identify the half-string state associated to the butterfly.

Before concluding this section we would like to explain an issue concerning boundary conditions. From Fig.4.6(a) we see that other than the part of the boundary representing the string, the boundary of the region A (called $\widehat{\mathcal{R}}_{top}$ in the current discussion) has boundary condition identical to that of the original disk $\widehat{\Sigma}$, since this part of the boundary of A comes from part of the boundary of $\widehat{\Sigma}$. Eq.(4.4.14) then implies that the disk $\widehat{\mathcal{R}}_{1/2}$ also has the

same boundary condition. Thus the half-string state is given by the surface state associated with the disk $\widehat{\Sigma}_{1/2}$ in the $\widehat{w}$-coordinate system, with the same boundary condition as that in the original full string surface state.

This, however, does not imply that both the half-string end-points satisfy the same boundary conditions as the end-points of the original string, since, as we now explain, the surface states *defined* with certain boundary conditions may actually fail to *satisfy* the boundary condition. In a surface state "the open string" is a specific line with endpoints at the boundary – in the $\widehat{w}$ presentation it is the vertical boundary of the shaded region called H. Consider a boundary condition of Neumann type. This is the statement that the normal derivative of fields at the boundary vanishes. We may thus expect on a surface state to find that the expectation values of the operator $\partial_\sigma X(\sigma)$ vanish at $\sigma = 0, \pi$. But this vanishing will only happen if the tangent to the open string at the boundary coincides with the normal derivative to the boundary. This need not be the case when the boundary has corners at the open string endpoints. Corners at the open string endpoints happen when the map $z = f(\xi)$ has singularities at the points $\xi = \pm 1$. While this is not the case for slivers nor butterflies, we will see examples of this phenomenon in section 4.9.1.

In the case of half-string states associated to projectors, the above subtleties are in fact quite generic. If the original projector is such that the tangent to the open string coincides with the normal to the boundary, the corresponding half-string endpoint will carry the boundary condition (this is the case illustrated in figure 4.7). On the other hand the nature of the boundary near the full string midpoint, which is controlled by the behavior of $f(\xi)$ near $\xi = i$, will tell whether or not the boundary condition is satisfied at the other half-string endpoint. Getting a little ahead of ourselves we can have a look at the butterfly state, in particular at figure 4.9(d). Note that the tangent to the half-string AQ at Q is indeed along the normal to the boundary DQ at Q. Thus we may expect the half-string state for the butterfly to satisfy Neumann boundary conditions at both endpoints. It does, because as it will be checked, the half string state is simply the vacuum state. On the other hand, for a generalized butterfly, such as that shown in figure 4.19 the two directions do not

coincide and we do not expect the half-string state to satisfy a simple boundary condition. For the nothing state, shown in figure 4.17, the normal to the boundary at the midpoint is orthogonal to the open string tangent. Thus the interpretation here is that $\partial_\tau \widehat{X}$ vanishes at this point. This is a Dirichlet boundary condition.

The above considerations may be relevant for understanding the applicability of the two different half-string formalisms [104], – one where the mid-point satisfies Dirichlet boundary condition [105] and the other where the midpoint satisfies Neumann boundary condition [106]. We now see that for half-string states arising from projectors, neither formalism is natural in all cases. Since the set of functions are (at least formally) complete, we can use either formalism, but the results will take simplest forms when the boundary conditions match those that arise geometrically at the string midpoint.

4.5 Star Algebra Projectors

In this section we will show that the projection property of surface states also holds when the boundary of the surface reaches the open string midpoint. We will explain why the projectors that arise are of rank one. Finally we will prove that the Neumann matrix of any projector has a common eigenvector, the $-1/3$ eigenvector of the star algebra Neumann matrices. An intuitive explanation for this fact is given.

4.5.1 Projection properties

A surface state $|\Sigma\rangle$ defined as in (4.2.8) will be called a projector if it satisfies:

$$|\Sigma * \Sigma\rangle = |\Sigma\rangle\,. \tag{4.5.1}$$

We shall show that a surface states $|\Sigma\rangle$ is a projector if the corresponding surface Σ has the property that the boundary of Σ touches the string mid-point $\xi = i$, – the same condition under which its wave-functional factorizes. However, unlike in the previous section, in this subsection we shall work with the full surface state in the matter-ghost conformal field theory so that the total central charge vanishes, and the gluing relations required for

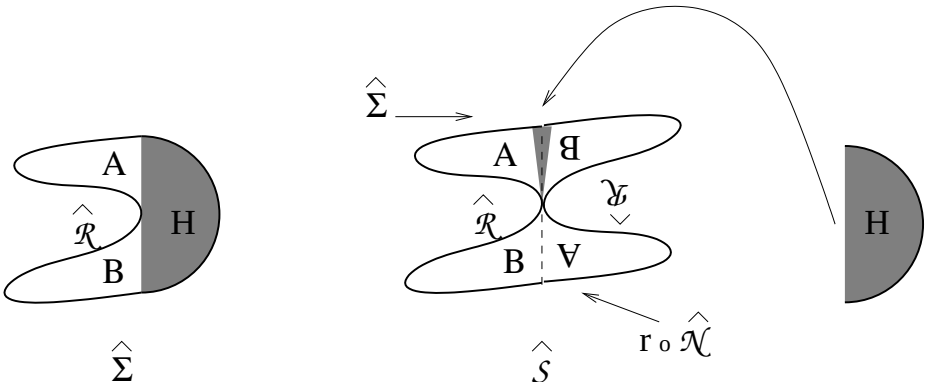

Figure 4.8: The geometry of $\widehat{\mathcal{S}}$ when the boundary of $\widehat{\Sigma}$ touches the string midpoint. The local coordinate patch, shown to the right by the shaded half disk, is to be glued to the shaded region of the diagram representing $\widehat{\mathcal{S}}$.

the computation of $*$-product are valid without any additional multiplicative factors. For computing $|\Sigma * \Sigma\rangle$ we follow the procedure described in section 4.2.2. In this case the surface $\widehat{\mathcal{S}}$ that appears in eq.(4.2.10), constructed following Fig.4.3, is the pinched union of $\widehat{\Sigma}$ and an extra disk $r \circ \widehat{\mathcal{N}}$ as shown in Fig.4.8. We have, as in eq.(4.2.10),

$$\langle \Sigma * \Sigma | \phi \rangle = \langle h \circ \phi(0) \rangle_{\widehat{\mathcal{S}}} \,. \tag{4.5.2}$$

The operator $h \circ \phi(0)$ is being inserted on the $\widehat{\Sigma}$ component of $\widehat{\mathcal{S}}$, on the boundary of H, as usual. Hence there is no operator insertion on $r \circ \widehat{\mathcal{N}}$. Our factorization result of section 4.3.3 implies that the correlator factorizes and the contribution of $r \circ \widehat{\mathcal{N}}$ is simply a multiplicative factor of one. Thus eq.(4.5.2) can be rewritten as:

$$\langle \Sigma * \Sigma | \phi \rangle = \langle h \circ \phi(0) \rangle_{\widehat{\Sigma}} \,. \tag{4.5.3}$$

But the above right hand side is precisely $\langle \Sigma | \phi \rangle$ and therefore this establishes (4.5.1).

There is also a nice geometrical understanding that projectors that arise as surface states of the type discussed above are of rank one, – at least in a limited sense. For operators on separable Hilbert spaces, a projector P is of rank one if and only if $PAP = \mathrm{Tr}(AP)\, P$ for all A. Let now Σ be a surface state projector $\Sigma * \Sigma = \Sigma$, and let Υ denote an arbitrary state of the star algebra (a Fock space state, or a surface state, for example). We then claim that

the condition characterizing Σ as a rank one projector holds:

$$\Sigma * \Upsilon * \Sigma = \langle \Sigma | \Upsilon \rangle \, \Sigma \, . \tag{4.5.4}$$

This equation is understandable in terms of pictures. Back to Fig.4.8, the above left hand side would be represented by a modified $\widehat{\mathcal{S}}$ where the $r \circ \widehat{\mathcal{N}}$ disk would be changed by cutting open the dashed line separating the sides B and A, and gluing in the state Υ. The new $r \circ \widehat{\mathcal{N}}$ disk, still pinched with respect to the remaining surface $\widehat{\Sigma}$ would be producing the $\langle \Sigma | \Upsilon \rangle$ inner product. The factorization implied by the pinching of the surfaces then yields (4.5.4).

There is, however, a subtlety involved in the derivation of (4.5.4) which we now discuss. In order to apply the factorization results of section 4.3.3 we need a unitary BCFT – otherwise the contribution from operators of negative dimension to the operator product expansion will invalidate (4.3.14). Thus (4.5.4) is not valid in general for the combined matter-ghost system, but could be valid for example for the matter part of the surface state. On the other hand since the matter part of the BCFT has a non-zero central charge, gluing of surface states typically involve (possibly infinite) multiplicative factors. Thus we expect (4.5.4) to be valid for the matter part of the state up to an overall multiplicative factor that depends only on the central charge of the matter BCFT and does not depend on the state $|\Upsilon\rangle$ or the particular BCFT under consideration. Alternatively, (4.5.4) is valid without any additional multiplicative factor in the combined matter-ghost BCFT *if we restrict* $|\Upsilon\rangle$ *to be a state of ghost number 0*, so that the leading contribution to the factorization relation comes from the identity operator as has been assumed in the derivation of (4.3.14).

4.5.2 A universal eigenvector of V^f for all projectors

Give a projector of the type described above, we can use the procedure of section 4.2.3 to represent it as the exponentials of matter (and ghost) oscillators acting on the vacuum as in (4.2.19). We shall now show that the matrix V^f_{mn} associated with any projector has the property that it has an eigenvector of eigenvalue one, the eigenvector being the same as

the $\kappa = 0$ eigenvector of K_1[91]. This generalizes the same property obeyed by the sliver Neumann matrix.

We start with (4.2.20) and integrate by parts with respect to w,

$$V^f_{mn} = \frac{(-1)^m}{\sqrt{m}} \oint \frac{dw}{2\pi i} \oint \frac{dz}{2\pi i} \frac{1}{z^m} \frac{f'(z)}{f(z)-f(w)} \sqrt{n} \Big(-\frac{1}{w}\Big)^{n+1} . \tag{4.5.5}$$

For definiteness we shall take the w contour to be outside the z contour. Acting on an eigenvector with components v_n we find

$$\sum_{n=1}^{\infty} V^f_{mn}\, v_n = \frac{(-1)^m}{\sqrt{m}} \oint \frac{dw}{2\pi i} \oint \frac{dz}{2\pi i} \frac{1}{z^m} \frac{f'(z)}{f(z)-f(w)} \; \frac{1}{w^2} \sum_{n=1}^{\infty} \sqrt{n}\, v_n \Big(-\frac{1}{w}\Big)^{n-1} . \tag{4.5.6}$$

We have argued that for all sufficently well-behaved maps $f(\xi)$ such that $f(\pm i) = \infty$, Ψ_f is a projector. We now show that $f(\pm i) = \infty$ suffices to show that the C-odd $\kappa = 0$ eigenvector v^- of the Neumann matrices is in fact an eigenvector of eigenvalue one for the matrix V^f. The eigenvector in question is defined by the generating function

$$\sum_{n=1}^{\infty} \frac{v^-_n}{\sqrt{n}}\, u^n = \tan^{-1} u \quad \rightarrow \quad \sum_{n=1}^{\infty} \sqrt{n} v^-_n\, u^{n-1} = \frac{1}{1+u^2} \qquad |u| < 1. \tag{4.5.7}$$

For regulation purposes we pick a number a slightly bigger than one and write

$$\sum_{n=1}^{\infty} \sqrt{n} v^-_n\, u^{n-1} = \frac{1}{1+(u/a)^2} \,, \qquad |u| < a \,, \tag{4.5.8}$$

with the understanding that the limit $a \to 1^+$ is to be taken. Therefore back in (4.5.6) we get

$$\sum_{n=1}^{\infty} V_{mn}\, v^-_n = \frac{(-1)^m}{\sqrt{m}} \oint \frac{dw}{2\pi i} \oint \frac{dz}{2\pi i} \frac{1}{z^m} \frac{f'(z)}{f(z)-f(w)} \; \frac{a^2}{1+a^2w^2} \,, \quad |w| > \frac{1}{a}. \tag{4.5.9}$$

The w integral must run over a contour of radius bigger than $1/a$ because of the use of (4.5.7) with $w = -1/u$. At the same time the radius of the contour must be less than 1 so that the contour does not enclose the singularities at $w = \pm i$. Therefore we pick up contributions from the poles at $w = \pm i/a$ and $w = z$. After this we can take the $a \to 1$ limit. Since $f(\pm i) = \infty$, only the $w = z$ pole contributes and we get

$$\sum_n V_{mn} v^-_n = \frac{(-1)^{m+1}}{\sqrt{m}} \oint \frac{dz}{2\pi i} \frac{1}{z^m} \frac{1}{1+z^2} = v^-_m \,. \tag{4.5.10}$$

This establishes the claim.

An intuitive explanation for this property can be given using the half-string interpretation. The eigenvector in question implies that the projector wave-functional is invariant under constant and opposite translation of the half-strings [71]. If we denote by P_L and P_R respectively the momentum carried by the left and right half-strings we have that the eigenvector condition is interpreted as the condition that

$$(P_L - P_R)|\Sigma\rangle = 0\,, \tag{4.5.11}$$

where $|\Sigma\rangle$ is the projector surface state. Being a surface state defined with Neumann boundary condition (in the sense described in section 4.4.2), the total momentum $P_L + P_R$ carried by the state vanishes. Thus the condition above is simply the statement that P_L *and* P_R annihilate $|\Sigma\rangle$. But this must be so, since $|\Sigma\rangle = |\Sigma_L\rangle \otimes |\Sigma_R\rangle$, where $|\Sigma_L\rangle$ and $|\Sigma_R\rangle$ are themselves surface states defined with Neumann boundary condition.

4.6 The Butterfly State

In this section we shall introduce and investigate in detail the butterfly surface state. After giving the details of its definition and viewing it in various possible ways we shall verify that it is a projector of the star algebra. Throughout this section except in section 4.6.4 we shall work in the combined matter-ghost system with zero central charge so that we can apply the gluing theorem without any additional factors coming from conformal anomaly.

4.6.1 A picture of the butterfly

The butterfly state, just as any surface state, is completely defined by a map from ξ to the upper half z plane (z-presentation, as reviewed in section 2.1). We thus write

$$z = \frac{\xi}{\sqrt{1+\xi^2}} \equiv f_{\mathcal{B}}(\xi)\,, \tag{4.6.1}$$

and define the butterfly state $|\mathcal{B}\rangle$ through the relation:

$$\langle \mathcal{B}|\phi\rangle = \langle f_{\mathcal{B}} \circ \phi(0)\rangle_{UHP}\,. \tag{4.6.2}$$

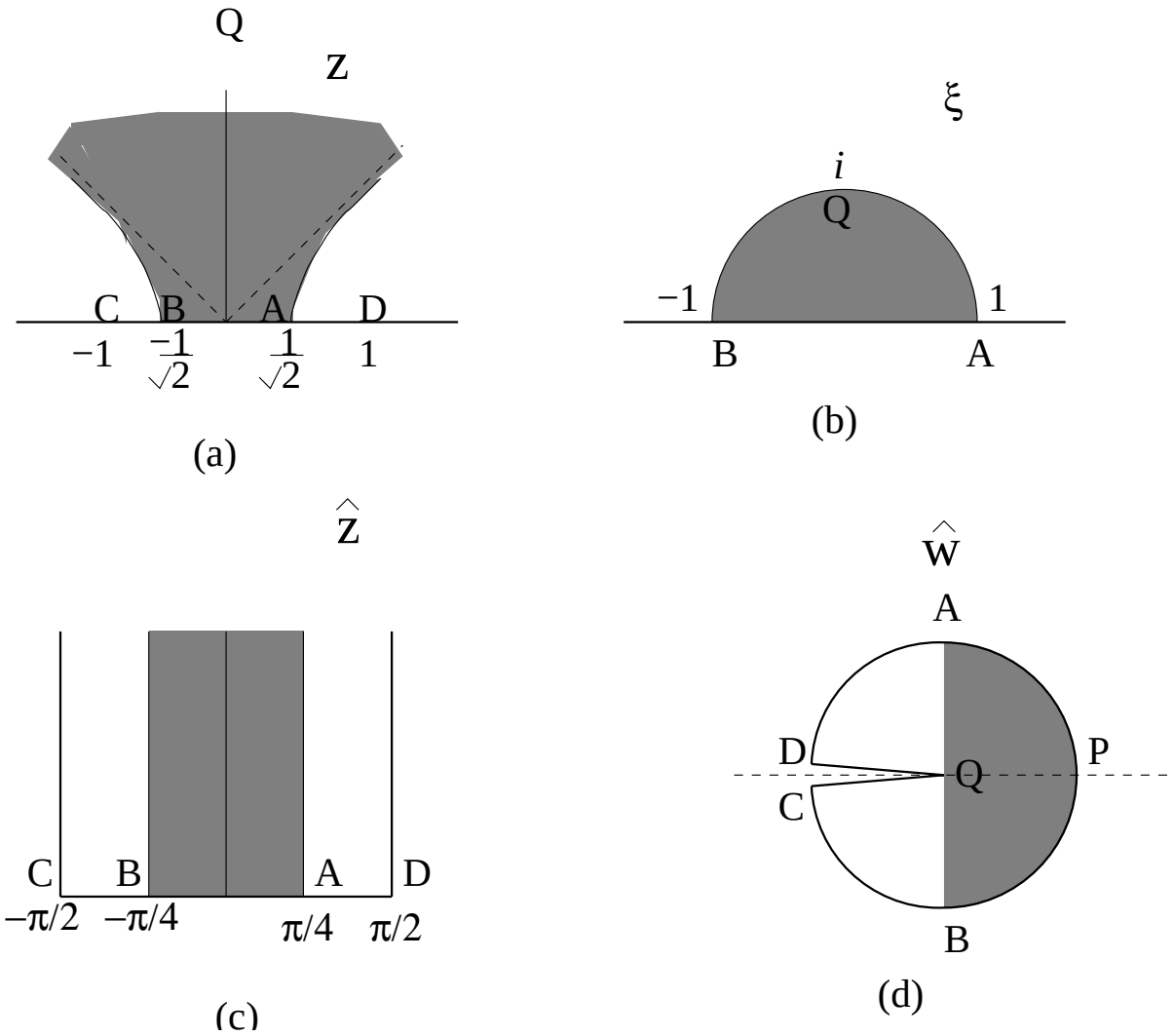

Figure 4.9: Representation of the disk associated with the butterfly state in various coordinate systems. The shaded region denotes the local coordinate patch.

In the z-presentation the surface is the full upper half plane, and therefore in order to gain intuition about the type of state this is, we plot the image of the canonical ξ half-disk in the z-plane (see Fig. 4.9 (a) and (b)). The open string $|\xi| = 1, \Im(\xi) \geq 0$ is seen to map to the hyperbola $x^2 - y^2 = \frac{1}{2}$ (in the upper half plane, with $z = x + iy$). We note that $z(\xi = i) = \infty$ and thus, as expected for a projector, the open string midpoint coincides with the boundary of the disk.

Further insight into the nature of the state is obtained by examination of the disk in the $\widehat{z}$-presentation. To this end we use (4.2.4) to recognize that (4.6.1) can be rewritten as

$$z = \sin(\tan^{-1}(\xi)) = \sin \widehat{z} \tag{4.6.3}$$

This maps the image of the local coordinate in the $\widehat{z}$-presentation to the image of the local coordinate in the z-presentation. As explained before, the surface need not fill the upper-half $\widehat{z}$-plane. To figure out the extension of the surface in the $\widehat{z}$ presentation we simply invert the previous equation to write

$$\widehat{z} = \sin^{-1} z \, . \tag{4.6.4}$$

As shown in the figure (4.9 (c)), this transformation maps the full upper half z-plane into the region $|\Re(\widehat{z})| \leq \pi/2 \, , \Im(\widehat{z}) \geq 0$. Note that the vertical lines $\Re(\widehat{z}) = \pm\pi/2$ are images of the boundary and not identification lines. Even though the surface occupies a portion of the $\widehat{z}$-plane the boundary reaches the point at infinity, and so does the midpoint (as expected). The above conformal map is perhaps most easily thought about in differential form, where it belongs to the class of Schwarz-Christoffel transformations. We have

$$d\widehat{z} = \frac{dz}{\sqrt{(1-z)(1+z)}} \tag{4.6.5}$$

The real line in the z-plane is mapped into a polygon in the $\widehat{z}$ presentation, where the turning points are $z = \pm 1$ and the turning angles are both $\pi/2$. This, of course is the result shown in the figure.

Finally, we give the $\widehat{w}$ presentation (fig. 4.9(d)). Using (4.2.6) the region $|\Re(\widehat{z})| \leq \pi/2 \, , \Im(\widehat{z}) \geq 0$ of the $\widehat{z}$ presentation turns into the full disk with a pair of cuts zooming into the $\widehat{w}$ origin from $\widehat{w} = -1$. Indeed the boundary of the surface is the arc $e^{i\theta}$ with $0 < \theta < \pi$ together with the line going from $\widehat{w} = -1$ to $\widehat{w} = 0$, plus the backwards line from $\widehat{w} = 0$ to $\widehat{w} = -1$ plus the arc $e^{i\theta}$ with $-\pi < \theta < 0$. It is perhaps in this presentation that it is clearest that the string midpoint $\widehat{w} = 0$ touches the boundary of the disk.

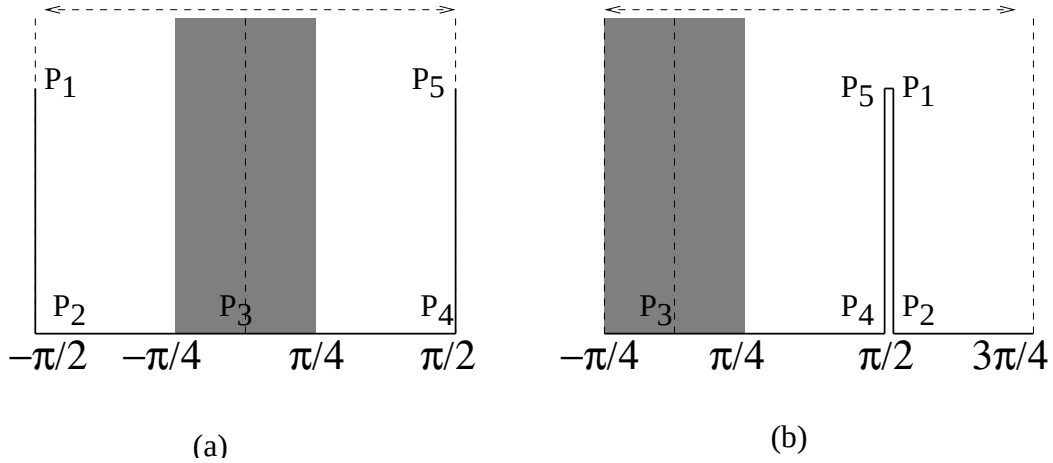

Figure 4.10: The geometry of the disk associated with the regularized butterfly in the complex $\widehat{z}$ plane. The shaded region denotes the local coordinate patch. The lines $\Re(\widehat{z}) = -\pi/4$, $\Re(\widehat{z}) = 3\pi/4$ are identified in the second figure.

4.6.2 The regulated butterfly

In order to regulate the butterfly it is simplest to do it in the $\widehat{w}$ coordinates. Here we simply stop the cut at some point $\widehat{w}_0$ with $-1 < \widehat{w}_0 < 0$ a real negative number. In the $\widehat{z}$- presentation this turns into a picture shown in fig 4.10 (a). Note that the vertical lines $\Re(\widehat{z}) = \pm\pi/2$ are not all boundary. Indeed the segments $\overline{P_1P_2}$ and $\overline{P_4P_5}$ are part of the boundary, but the remaining parts of the vertical lines, shown dashed in the figure, are identification lines. For more clarity and also later convenience we have shown in fig. 4.10(b) the same regulated butterfly where the region to the left of the right-half string has been moved, and the two extreme vertical lines are identified.

In order to find the relation between z and $\widehat{z}$ in the regulated butterfly we must construct the map, which is a variation on (4.6.5). In order to produce the identification shown by dashed lines, while preserving the property that the real line is mapped to a polygon a pair of complex conjugate poles are necessary. We write

$$d\widehat{z} = \frac{dz}{(1+\beta^2 z^2)\sqrt{1-z^2t^2}} \tag{4.6.6}$$

where we have fixed the normalization from the condition $\frac{d\widehat{z}}{dz} = 1$ at $z = 0$. The images of

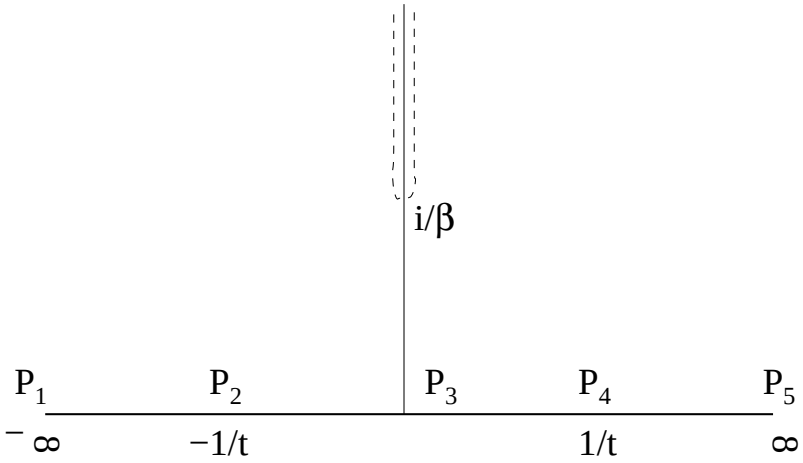

Figure 4.11: The singular points of the map $z \to \widehat{z}$ for the regulated butterfly in the z-plane.

the marked points $P_1, \ldots P_5$ in Fig.4.10(a) in the z-plane is indicated in figure 4.11. The identification lines emerge from the pole at $z = i/\beta$. Since the identification lines differ by $\Delta\widehat{z} = \pi$ the residue at the pole $z = i/\beta$ in (4.6.6) must equal $\frac{1}{2i}$. This requires $\beta^2 = 1 - t^2$ and thus we have

$$d\widehat{z} = \frac{dz}{(1 + (1-t^2)z^2)\sqrt{1 - z^2t^2}}\,. \tag{4.6.7}$$

This equation is readily integrated to give

$$\widehat{z} = \tan^{-1}\Big(\frac{z}{\sqrt{1 - z^2t^2}}\Big)\,, \tag{4.6.8}$$

and inverting the relation one finds

$$z = \frac{\tan\widehat{z}}{\sqrt{1 + t^2\tan^2\widehat{z}}} = \frac{\xi}{\sqrt{1 + t^2\xi^2}}\,. \tag{4.6.9}$$

This is a rather simple result. The regulator parameter t can be related to the height h of the points P_1 or P_5. Say, for P_5, $\widehat{z}(P_5) = \frac{\pi}{2} + ih$ must map to $z = \infty$. This requires $1 + t^2\tan^2(\frac{\pi}{2} + ih) = 0$. A short calculation gives

$$h = \tanh^{-1} t\,, \qquad \text{thus} \quad h \to \infty \quad \text{when} \quad t \to 1^-\,. \tag{4.6.10}$$

The regulator parameter t must therefore satisfy $t < 1$. Clearly when $t = 1$ in (4.6.9) we recover the butterfly as defined in (4.6.1).

4.6.3 Star multiplying two regulated butterflies

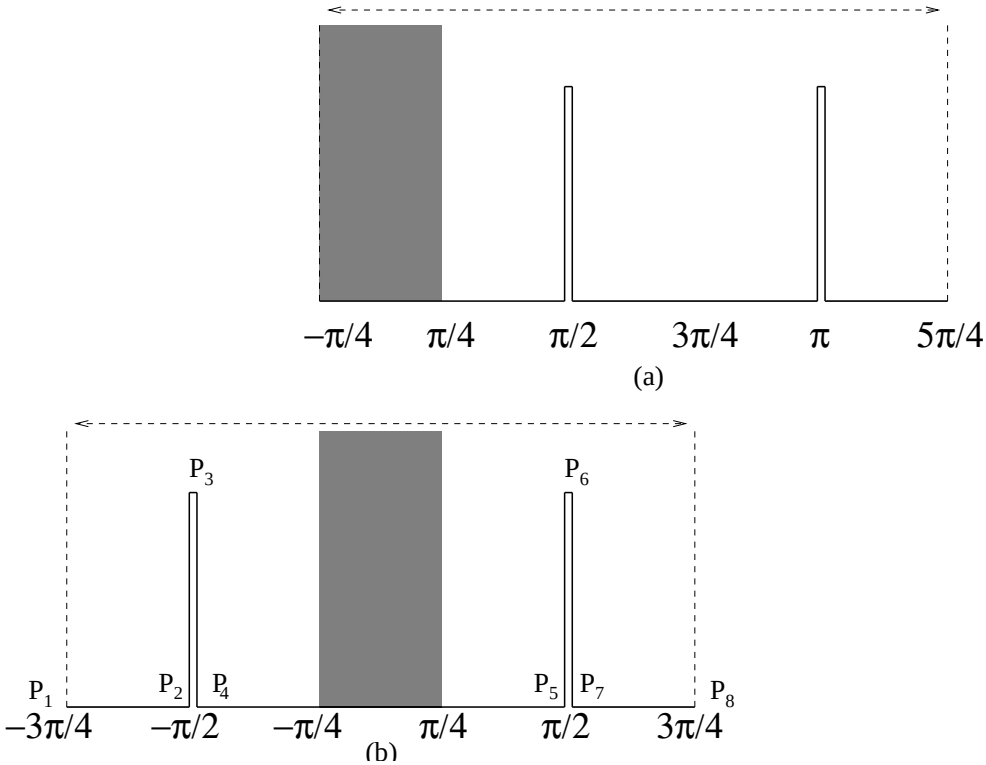

Figure 4.12: Representation of the $*$-product of a regulated butterfly with itself in the $\widehat{z}$ plane.

To star multiply two regulated butterflies we take the first one, and glue to the right-half of its open string the left-half of the open string of the second butterfly, whose local coordinate patch has been removed. In order to perform these operations it is easier to view the butterfly as the cylinder $-\frac{\pi}{4} \leq \Re(\widehat{z}) \leq \frac{3\pi}{4}$, $\Im(\widehat{z}) \geq 0$ with the vertical lines, corresponding to the right half of the open string, identified (see fig. 4.10(b)). The second (amputated) butterfly can be glued to the right of this one giving the result in fig 4.12(a). Finally we choose a symmetric arrangement of this figure as shown in figure 4.12(b). Special points $P_1, \cdots P_8$ have been marked, and the complete picture is a cylinder with circumference $3\pi/2$ and with the dashed lines identified. The image of this disk in the $\widehat{w}$ coordinate system is shown in Fig.4.13. In the $t \to 1$ limit, the vertices P_3 and P_6 of the two wedges approach

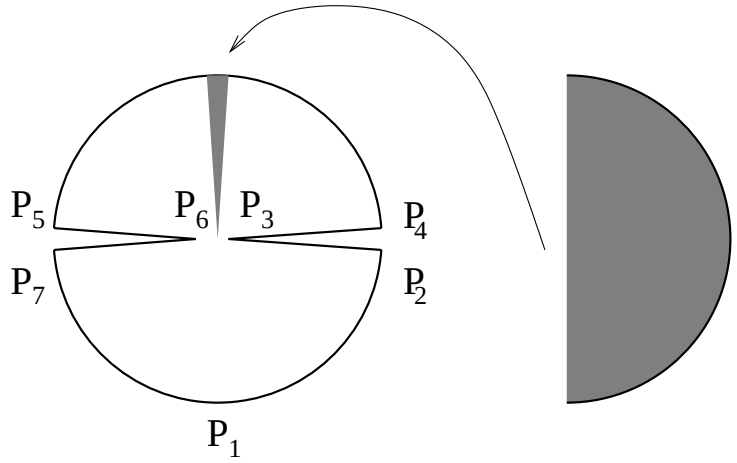

Figure 4.13: Representation of the $*$-product of a regulated butterfly with itself in the $\widehat{w}$ plane. The local coordinate patch, which is to be glued to the rest of the digram, is shown separately on the right.

the origin of the $\widehat{w}$ plane, and in this limit the surface clearly has the stucture of a split disk of the form discussed in section 4.3.1.

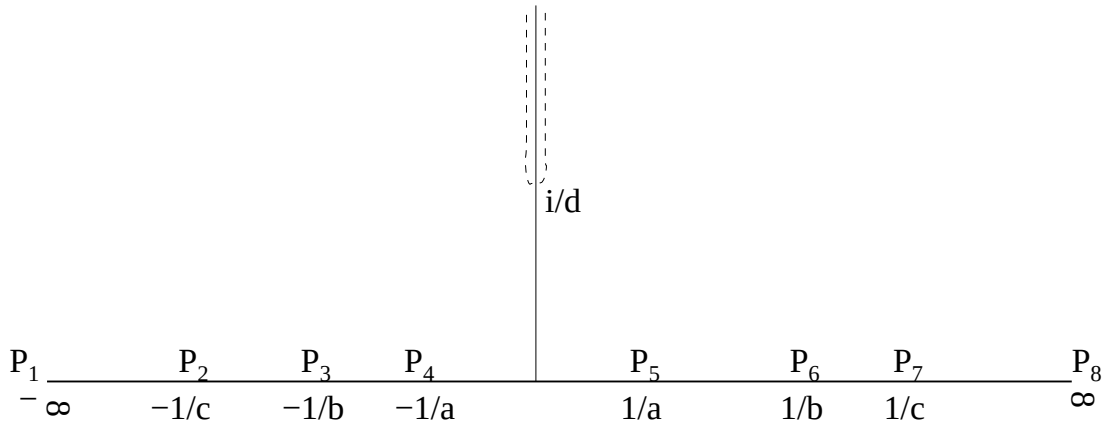

Figure 4.14: The singular points of the map $z \to \widehat{z}$ for the $*$-product of two regulated butterflies in the z-plane.

The map of this nontrivial polygon in the $\widehat{z}$ plane into the upper half z-plane is defined by a map whose singularity structure is symmetrically arranged as shown in figure 4.14.

Taking into account the various turning points, the map is of the form

$$d\widehat{z} = \frac{1}{(1+d^2\,z^2)}\,\frac{(1-b^2z^2)}{\sqrt{(1-a^2z^2)(1-c^2z^2)}}\,dz \equiv H(z)dz\,. \tag{4.6.11}$$

The complex poles at $z = \pm\frac{i}{d}$ play no role in the turning points but are needed for the implementation of the identification of the dashed lines in the $\widehat{z}$-plane (figure 4.12(b)). The length conditions are

$$\int_0^{1/a} H(z)dz = \frac{\pi}{2}\,, \tag{4.6.12}$$

$$\int_{1/a}^{1/b} H(z)dz = ih\,, \tag{4.6.13}$$

$$\int_{1/b}^{1/c} H(z)dz = -ih\,, \tag{4.6.14}$$

$$\int_{\frac{1}{c}}^{\infty} H(z)dz = \frac{\pi}{4}\,, \tag{4.6.15}$$

where

$$h = \tanh^{-1} t\,. \tag{4.6.16}$$

These are four equations, for our four unknowns a, b, c and d. These four equations, with the analogous ones integrating over the negative z axis, added together imply that

$$\int_{-\infty}^{\infty} H(z)dz = \frac{3\pi}{2}\,. \tag{4.6.17}$$

This means that that the residue around $z = \frac{i}{d}$ in (4.6.11) must equal $\frac{3}{4i}$. A short calculation shows that this residue condition requires

$$\frac{9}{4}\,d^2\,(d^2+a^2)(d^2+c^2) = (d^2+b^2)^2\,. \tag{4.6.18}$$

It should be noted that this residue condition is not independent from conditions listed in (4.6.12) to (4.6.15).

The issue to be examined here is how to achieve very large h by adjusting the parameters a, b, c and d. The analysis that follows is a special case of the discussion in section 2.2. As the slits become higher and higher by growing h the surface is pinching. In the representation of Fig.4.12(a), the role of R_2 is played by the region $\frac{\pi}{2} \le \Re(\widehat{z}) \le \pi$, $\Im(\widehat{z}) \ge 0$, which

in Fig.4.12(b) corresponds to the region $\frac{\pi}{2} \leq |\Re(\widehat{z})| \leq \frac{3\pi}{4}\,, \Im(\widehat{z}) \geq 0$. Our expectation is therefore that as the slits go up to infinity, this region vanishes away in a map that preserves the inner region, and we recover a single butterfly. We will now show that the large h limit can be achieved by taking b, c and d much smaller than a, and c to be much smaller than b, d:

$$\{b, c, d\} \ll a\,, \qquad c \ll \{b, d\}\,. \tag{4.6.19}$$

Since such small parameters imply that the turning points $1/b, 1/c$ and $1/d$ are going to infinity, it is convenient to bring them near zero to understand how they are collapsing into each other. We therefore let $z = -1/z'$ and find that (4.6.11) gives

$$d\widehat{z} = \frac{1}{(z'^2 + d^2)} \frac{(z'^2 - b^2)}{\sqrt{(z'^2 - a^2)(z'^2 - c^2)}}\, dz' \equiv G(z')dz'\,. \tag{4.6.20}$$

Our first condition will be to achieve (4.6.12). This gives

$$\int_a^\infty G(z')dz' \simeq \int_a^\infty \frac{dz'}{z'} \frac{1}{\sqrt{z'^2 - a^2}} = \frac{\pi}{2}\,, \tag{4.6.21}$$

where we have noted in (4.6.20) that for $a < z' < \infty$ and the inequalities in (4.6.19), $z' \gg b, c, d$, and the expression for $G(z')$ simplifies considerably. This equation requires

$$a \simeq 1\,. \tag{4.6.22}$$

With $a \simeq 1$ and much bigger than b, c and d, and c much smaller than b, d, equation (4.6.18) now gives

$$\frac{1}{2}\, d^2 \simeq b^2\,. \tag{4.6.23}$$

With d comparable to b, and $c \ll \{d, b\}$ we now claim that all the conditions listed in (4.6.12) to (4.6.15), and the demand that h be large, can be satisfied. Since (4.6.18) and thus (4.6.23) is a consequence of (4.6.12) and (4.6.15), and we have already satisfied (4.6.12), we should be able to see that (4.6.15) is satisfied. Indeed, we must have

$$\int_0^c G(z')dz' \simeq \int_0^c \frac{b^2}{d^2\sqrt{c^2 - z'^2}} dz' \simeq \frac{\pi}{4}\,. \tag{4.6.24}$$

A short calculation shows that this equation holds on accound of (4.6.23).

It only remains now to verify that conditions (4.6.13) and (4.6.14) can be satisfied with ever increasing h. Condition(4.6.13) requires that the integral

$$\int_b^1 \frac{1}{z'^2+2b^2}\,\frac{z'^2-b^2}{\sqrt{1-z'^2}}\,\frac{dz'}{z'} \tag{4.6.25}$$

obtained using (4.6.19) grow without bounds as b is made progressively small. This is clearly the case, since the integral diverges at the bottom limit when b is set to zero. This means that for any h we can satisfy (4.6.13) for sufficiently small b, with $c \ll b$. Condition (4.6.14) requires that the integral

$$\int_c^b \frac{dz'}{z'^2+2b^2}\,\frac{z'^2-b^2}{\sqrt{z'^2-c^2}} \tag{4.6.26}$$

obtained using (4.6.19), grow without bounds as c is made progressively small. This is clearly the case, since the integral diverges at the bottom limit when c is set to zero. This means that having satisfied (4.6.13) for a fixed and very large h by choosing a sufficiently small b while keeping $c \ll b$, we can now satisfy (4.6.14) by making c sufficiently small.

We have thus shown that as we multiply two regulated butterflies and let the regulator go away, the map defining the composite surface is that of (4.6.11), with the limit $a \to 1$, and $\{b, c, d\} \to 0$ taken. This gives us

$$d\widehat{z} = \frac{1}{\sqrt{1-z^2}}\,dz\,, \tag{4.6.27}$$

which, by comparison to (4.6.5), it is immediately recognized to be the definition of the butterfly. This concludes our proof that the butterfly emerges from the star product of two regulated butterflies in the limit as the regulator is removed.

It is natural to wonder if the multiplication of two regulated butterflies also gives a regulated butterfly for $t \simeq 1$. We find that this product is a butterfly regulated in a slightly different way. To see this note that using (4.6.23), we can go back to (4.6.18) to find a more accurate evaluation of a, which previously was just set to one. We find

$$d^2 \simeq 1 - a^2\,. \tag{4.6.28}$$

With such relation, the map (4.6.11) becomes

$$d\widehat{z} = \frac{1}{(1+(1-a^2)\,z^2)}\,\frac{(1-\frac{1}{2}(1-a^2)z^2)}{\sqrt{1-a^2z^2}}\,dz\,, \tag{4.6.29}$$

where we used $c \ll \{b, d\}$. The correspondence with the regulated butterfly map given in (4.6.7) is very close, but not exact. The reason for this is intuitively clear. Our conformal map statement in section 4.3.1 states that the map that shrinks away the extra surface at the other side of a thin neck only affects the region around this neck. In addition, regulators control the approach of the boundary to the open string midpoint. Since the neck arising from star multiplication occurs around the open string midpoint of the product string (see, for example fig. 4.8), the regulator arising after star product is affected by the way in which the map shrinks away the extra surface.

4.6.4 Half-string wave-functional for the butterfly state

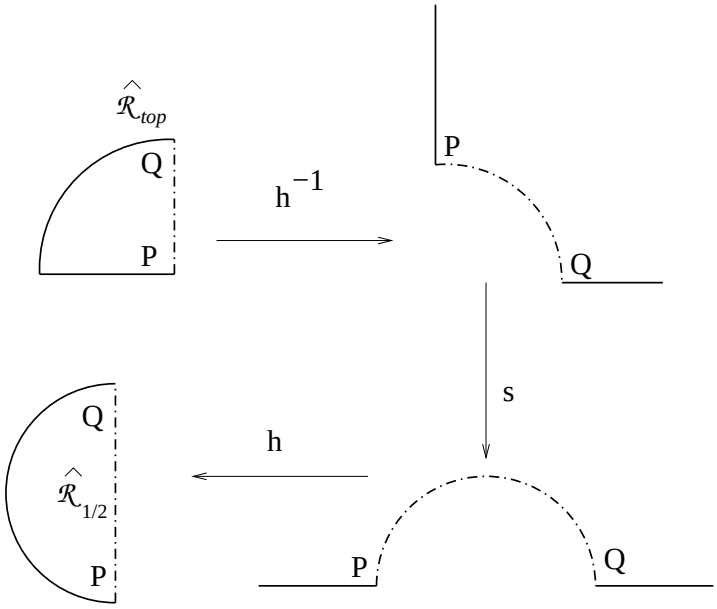

Figure 4.15: The $\widehat{\mathcal{R}}_{1/2}$ associated with the butterfly state, and its images under the maps h^{-1}, $s \circ h^{-1}$ and $h \circ s \circ h^{-1}$. P and Q are two marked points on the boundary of the disk, and the labels P and Q are always located in the inside of the disk.

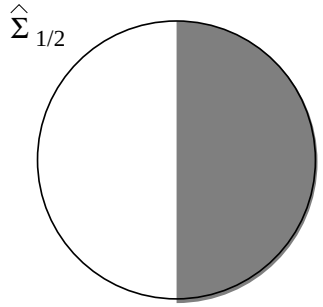

Figure 4.16: The $\widehat{\Sigma}_{1/2}$ associated with the butterfly.

According to the general arguments given in section 4.4.1, the wave-functional of the butterfly state splits into a product of a functional of the left half of the string and a functional of the right half of the string. We can now ask: what particular half-string wave-functional does the butterfly state have? To answer this question we go back to eq.(4.4.14). In the case of the butterfly, $\widehat{\mathcal{R}}_{top}$ is the unit quarter disk in the second quadrant as shown in the top left hand diagram of Fig.4.15. As shown in the rest of the figure, under the map $h \circ s \circ h^{-1}$ this gets mapped to the unit half-disk to the left of the vertical axis. This then is the $\widehat{\mathcal{R}}_{1/2}$ for the butterfly. Thus the disk $\widehat{\Sigma}_{1/2}$, obtained by joining with $\widehat{\mathcal{R}}_{1/2}$ the copy of the local coordinate patch, is the full unit disk as shown in Fig.4.16. This gives the half string state associated with the butterfly to be:

$$|\Phi\rangle = |0\rangle\,, \tag{4.6.30}$$

thereby establishing that the half-string wave-functional associated with the butterfly state is the vacuum state.

4.6.5 Operator representation of the butterfly state

We can represent the regulated butterfly $|\mathcal{B}_t\rangle$ in the operator formalism following the general procedure outlined in section 4.2.3. In this case we have

$$z = f_t(\xi) = \frac{\xi}{\sqrt{1+t^2\xi^2}} = \exp\Big(v_t(\xi)\frac{\partial}{\partial\xi}\Big)\,\xi\,. \tag{4.6.31}$$

Eqs.(4.2.18), (4.2.17) give

$$v_t(\xi) = -t^2\,\xi^3/2\,. \tag{4.6.32}$$

Eq.(4.2.11), (4.2.13) now gives:

$$|\mathcal{B}_t\rangle = \exp\left(-\frac{t^2}{2}\,L_{-2}\right)|0\rangle\,. \tag{4.6.33}$$

This is a remarkably simple expression involving a single Virasoro operator in the exponent.

The formalism of Virasoro conservation laws [12] allows us to derive an interesting property of the butterfly state,

$$K_2|\mathcal{B}\rangle = 0\,, \tag{4.6.34}$$

where $K_2 = L_2 - L_{-2}$. Indeed, consider in the global UHP the vector field

$$\tilde{v}_2(z) = 2z - \frac{1}{z}\,, \tag{4.6.35}$$

which is holomorphic everywhere, including infinity, except for the pole at the puncture $z = 0$. It follows that

$$\Big\langle \oint dz\,\tilde{T}(z)\,\tilde{v}_2(z) f_{\mathcal{B}}\circ\phi(0)\Big\rangle_{UHP} = 0\,, \tag{4.6.36}$$

for any state $|\phi\rangle$, where the contour circles the origin. Changing variables to the local coordinate ξ, we find

$$\Big\langle f_{\mathcal{B}}\circ\Big(\oint d\xi\;T(\xi)(\xi^3-\xi^{-1})\phi(0)\Big)\Big\rangle_{UHP} = 0\,. \tag{4.6.37}$$

This gives

$$\langle\mathcal{B}|K_2|\phi\rangle = 0 \tag{4.6.38}$$

since $\langle\mathcal{B}|\chi\rangle = \langle f_{\mathcal{B}}\circ\chi(0)\rangle$ for any state $|\chi\rangle$. This, in turn, is equivalent to (4.6.34).

4.6.6 Oscillator representation of the butterfly state

We can also represent the matter part of the regulated butterfly state in the oscillator representation using eq.(4.2.19), (4.2.23). In this case, with $\beta \equiv t^2$,

$$v(\xi) = -\frac{\xi^3}{2}\,, \qquad f_\beta(\xi) = \frac{\xi}{\sqrt{1+\beta\xi^2}}\,. \tag{4.6.39}$$

Equ. (4.2.23) gives

$$\begin{aligned}\frac{d}{d\beta}V_{mn}(\beta) &= (-1)^{m+n}\frac{\sqrt{mn}}{2}\oint_0\frac{dw}{2\pi i}\oint_0\frac{dz}{2\pi i}\,\frac{1}{z^{m+1}w^{n+1}}\,\frac{f_\beta(z)^3-f_\beta(w)^3}{f_\beta(z)-f_\beta(w)} \\ &= (-1)^{m+n}\frac{\sqrt{mn}}{2}\oint_0\frac{dw}{2\pi i}\,\frac{f_\beta(w)}{w^{m+1}}\oint_0\frac{dz}{2\pi i}\,\frac{f_\beta(z)}{z^{m+1}} = (-1)^{m+n}\frac{\sqrt{mn}}{2}\,x_m x_n\,,\end{aligned} \tag{4.6.40}$$

where

$$\begin{aligned}x_m = \oint_0\frac{dw}{2\pi i}\,\frac{f_\beta(w)}{w^{m+1}} &= (-\beta)^{\frac{m-1}{2}}\,\frac{\Gamma[\frac{m}{2}]}{\sqrt{\pi}\Gamma[\frac{m+1}{2}]} \quad \text{for } m \text{ odd}\,, \\ &= 0 \qquad\qquad\qquad\qquad\quad \text{for } m \text{ even}\,.\end{aligned} \tag{4.6.41}$$

Integrating (4.6.40) with the initial condition $V(\beta=0)=0$, we find the Neumann coefficients of the regulated butterfly ($\beta \to t^2$):

$$\begin{aligned}V_{mn}(t) &= -(-1)^{\frac{m+n}{2}}\,\frac{\sqrt{mn}}{m+n}\,\frac{\Gamma[\frac{m}{2}]\Gamma[\frac{n}{2}]}{\pi\Gamma[\frac{m+1}{2}]\Gamma[\frac{n+1}{2}]}\,t^{m+n}\,, \quad \text{for } m \text{ and } n \text{ odd}\,, \\ &= 0\,, \qquad\qquad\qquad\qquad\qquad\qquad\qquad\qquad\quad \text{for } m \text{ or } n \text{ even}\,.\end{aligned} \tag{4.6.42}$$

4.7 The Nothing State

The nothing state is defined by the relation:

$$\langle \mathcal{N}|\phi\rangle = \langle f_{\mathcal{N}}\circ\phi(0)\rangle_{UHP}\,, \tag{4.7.1}$$

with

$$f_{\mathcal{N}}(\xi) = \frac{\xi}{\xi^2+1}\,. \tag{4.7.2}$$

Under the map $\widehat{w}(\xi) = h(\xi)$ with $h(\xi)$ defined as in eq.(4.2.5), the upper half $z = f_{\mathcal{N}}(\xi)$ plane gets mapped to the vertical half-disk $\widehat{\Sigma}$ as shown in Fig.4.17. Clearly the boundary along the vertical line passes through the string mid-point which is at the origin of the $\widehat{w}$-plane, and hence this state satisfies the usual criterion of being a projector of the $*$-algebra.

Various properties of the nothing state can be derived along the same lines as those of the butterfly. Here we summarize the main results:

- The nothing state factorizes into a product of the nothing state for the left half-string and the nothing state for the right half-string. This follows from the results of section

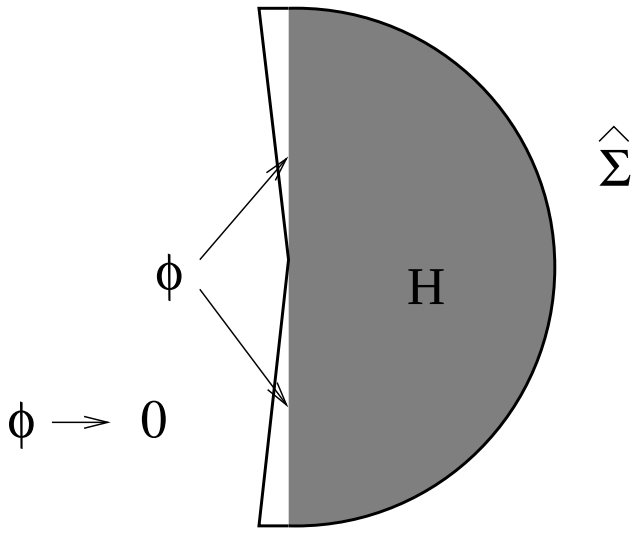

Figure 4.17: The geometry of the disk $\widehat{\Sigma}$ for the nothing state. Since the local coordinate patch fills the whole disk, the region $\widehat{\mathcal{R}}$, which represents the full disk $\widehat{\Sigma}$ minus the local coordinate patch, collapses to nothing.

4.4.2, – since in this case $\widehat{\mathcal{R}}$ associated with the original projector collapses, $\widehat{\mathcal{R}}_{top}$ also collapses and hence from (4.4.14) it follows that $\widehat{\mathcal{R}}_{1/2}$ also collapses. Thus $\widehat{\Sigma}_{1/2}$ is identical to $\widehat{\Sigma}$. This proves that the half-string state is the same as the original state.

- The map $f_{\mathcal{N}}(\xi)$ defining the nothing state is related to the map $f_{\mathcal{I}}(\xi)$ defining the identity string field by

$$f_{\mathcal{N}}(\xi) = -if_{\mathcal{I}}(i\xi)\,. \tag{4.7.3}$$

It follows from (4.2.11)–(4.2.13) that the operator expressions of the identity and of the nothing state are related by the formal replacement $L_{-2n} \leftrightarrow (-)^n L_{-2n}$. The identity admits an elegant operator expression [43] as an infinite product of exponentials of Virasoro generators. Changing the sign of L_{-2} in (3.3) of [43], we immediately have

$$\begin{aligned} |\mathcal{N}\rangle &= \left(\prod_{n=2}^{\infty} \exp\left\{-\frac{2}{2^n} L_{-2^n}\right\}\right) e^{-L_{-2}}|0\rangle \\ &= \ldots \exp(-\frac{2}{2^3} L_{-2^3}) \exp(-\frac{2}{2^2} L_{-2^2}) \exp(-L_{-2})|0\rangle\,. \end{aligned} \tag{4.7.4}$$

- V^f_{mn} computed using (4.2.20), (4.7.2) turns out to be equal to δ_{mn}. Thus the oscillator

representation of the matter part of the nothing state is given by:

$$|\mathcal{N}\rangle_m = \exp\left(-\frac{1}{2}\sum_{m,n=1}^{\infty} a_n^\dagger a_n^\dagger\right)|0\rangle\,. \tag{4.7.5}$$

- Computation of A_f following eq.(4.2.28) gives $A_f = 0$. Using eq.(4.2.25) we then see that the wave-functional of the nothing state, expressed as a functional of the coordinates X_n, is a constant independent of X_n.

- The nothing state is annihilated by all *even* reparametrizations of the cubic vertex,

$$K_{2n}|\mathcal{N}\rangle = 0 \qquad \forall n\,, \tag{4.7.6}$$

where $K_{2n} = L_{2n} - L_{-2n}$. This is shown with an argument similar to the one used for the butterfly state, eqs.(4.6.34)-(4.6.38). Taking in this case the globally-defined vector fields

$$\tilde{v}_2(z) = -\frac{1}{z} + 4z\,, \quad \tilde{v}_4(z) = -\frac{1}{z^3} + \frac{6}{z} - 8z\,, \tag{4.7.7}$$

we find that

$$K_2|\mathcal{N}\rangle = 0\,, \quad K_4|\mathcal{N}\rangle = 0\,. \tag{4.7.8}$$

The commutation relations

$$[K_m\,, K_n] = (m-n)K_{m+n} - (-1)^n(m+n)K_{m-n} \tag{4.7.9}$$

then imply (4.7.6) for all n. Let us recall that the identity string field is annihilated by *all*, even and odd, vertex reparametrizations [12], so from this point of view the nothing state is the most symmetric surface state apart from the identity.

4.8 The Generalized Butterfly States

In this section we shall introduce a new class of surface states, − called generalized butterflies, − each of which is a projector of the star algebra. We shall first define these states, and then show that each of these states satisfies the projector equation. We shall also determine the half-string wave-functionals that the wave-functional of the generalized butterfly state factorizes into.

4.8.1 Definition of general butterflies

Let us begin by defining the generalized butterfly state $|\mathcal{B}_\alpha\rangle$. We generalize eq.(4.6.1) to

$$z = \frac{1}{\alpha}\sin(\alpha \tan^{-1}\xi) \equiv f_\alpha(\xi)\,. \tag{4.8.1}$$

As a result eq.(4.6.3) is generalized to

$$z = \frac{1}{\alpha}\sin(\alpha\widehat{z})\,. \tag{4.8.2}$$

Comparing eqs.(4.6.3) and (4.8.2) we see that the generalized butterfly differs from the original butterfly by a rescaling of the $\widehat{z}$ coordinate by a factor α. Having a look at figure 4.9(c), we see that the generalized butterfly occupies the region $-\frac{\pi}{2\alpha} < \Re(\widehat{z}) \leq \frac{\pi}{2\alpha}$ in the upper half $\widehat{z}$ plane. We denote by $\mathcal{C}_\alpha$ this region in the $\widehat{z}$ coordinate system, or more precisely, a convenient translate of it.

As can be easily seen from eq.(4.8.1), the map $f_\alpha(\xi)$ is singular at the string mid-point $\xi = i$. In particular the mid-point is sent to $i\infty$ and hence touches the boundary of the upper half z-plane. Thus from the general analysis of section 4.4 we expect these states to be projectors of the $*$-algebra and have factorized wave-functionals. Also note that we have:

$$f_{\alpha=1} = \frac{\xi}{\sqrt{1+\xi^2}}\,. \tag{4.8.3}$$

Comparison with eq.(4.6.1) shows that the state $|\mathcal{B}_{\alpha=1}\rangle$ is identical to the butterfly state defined in the previous section. On the other hand, we have:

$$f_{\alpha=0} = \tan^{-1}\xi\,. \tag{4.8.4}$$

This shows that the state $|\mathcal{B}_{\alpha=0}\rangle$ is identical to the sliver. The family of surface states $|\mathcal{B}_\alpha\rangle$ gives a family of projectors, interpolating between the butterfly and the sliver. Finally, note that for $\alpha = 2$ we have the map

$$f_{\alpha=2} = \frac{\xi}{1+\xi^2}\,. \tag{4.8.5}$$

For reasons to be explained shortly, we call this the 'nothing' state.

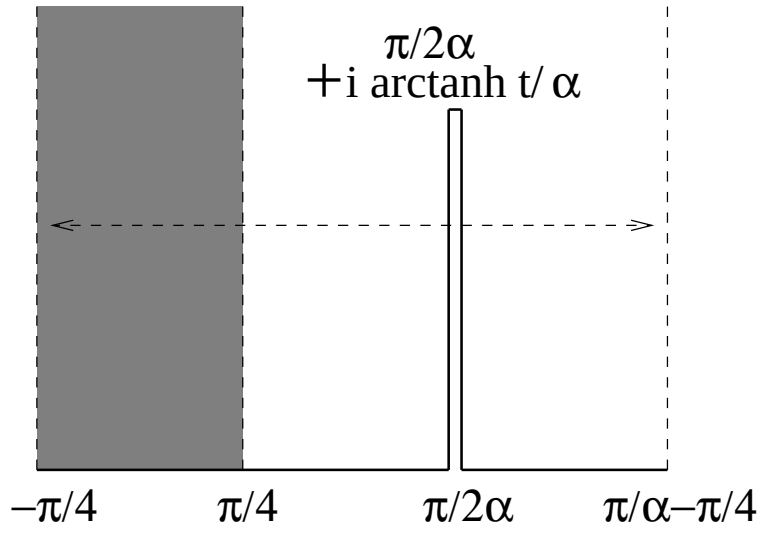

Figure 4.18: The geometry of $\mathcal{C}_{\alpha,t}$ in the complex $\widehat{z}$ plane. The shaded region denotes the local coordinate patch, and the lines $\Re(\widehat{z}) = -\pi/4$, $\Re(\widehat{z}) = \pi/\alpha - \pi/4$ are identified.

We can regularize the singularity at the midpoint and define the regularized butterfly by generalizing (4.6.9) to

$$z = f_{\alpha,t}(\xi) = \frac{1}{\alpha}\frac{\tan(\alpha\tan^{-1}\xi)}{\sqrt{1+t^2\tan^2(\alpha\tan^{-1}\xi)}} = \frac{1}{\alpha}\frac{\tan(\alpha\widehat{z})}{\sqrt{1+t^2\tan^2(\alpha\widehat{z})}}\,. \tag{4.8.6}$$

In the $\widehat{z}$ plane we get

$$\langle \mathcal{B}_{\alpha,t}|\phi\rangle = \langle f^{(0)}\circ\phi(0)\rangle_{\mathcal{C}_{\alpha,t}}\,, \tag{4.8.7}$$

where $\mathcal{C}_{\alpha,t}$ is the image of the upper half z plane in the $\widehat{z}$ coordinate system and $f^{(0)}(\xi) = \tan^{-1}\xi$. Comparison between (4.6.9) and (4.8.6) shows that the regularized butterfly and the regularized generalized butterfly are related by a rescaling of the $\widehat{z}$ coordinate by $1/\alpha$. Thus $\mathcal{C}_{\alpha,t}$ can be obtained by a rescaling of Fig.4.10(a) by $1/\alpha$, and moving the region to the left of the coordinate patch all the way to the right, as shown in Fig.4.18. Note that the local coordinate patch always occupies the same region $|\Re(\widehat{z})| \le \frac{\pi}{4}$, $\Im(\widehat{z}) \ge 0$, since $\widehat{z} = \tan^{-1}\xi$.

As shown, $\mathcal{C}_{\alpha,t}$ is a semi-infinite cylinder with circumference π/α, obtained by the restriction $\Im(\widehat{z}) \ge 0$, $-\pi/4 \le \Re(\widehat{z}) \le \pi/\alpha - \pi/4$, and the identification $\Re(\widehat{z}) = \Re(\widehat{z}) + \pi/\alpha$

in the $\widehat{z}$ plane, with a cut along the line $\Re(\widehat{z}) = \pi/2\alpha$, extending all the way from the base $\widehat{z} = \pi/2\alpha$ to $\widehat{z} = \pi/2\alpha + i(\tanh^{-1} t)/\alpha$. As we move along the real z axis, in the $\widehat{z}$ plane we go from $\widehat{z} = -\pi/4$ to $\pi/2\alpha$ along the real axis, then along the cut to $\pi/2\alpha + i(\tanh^{-1} t)/\alpha$ and back to $\pi/2\alpha$, and finally along the real axis to $-\pi/4+\pi/\alpha$. The local coordinate patch, corresponding to the unit half-disk in the upper half ξ plane, is mapped to the semi-infinite strip $\Im(\widehat{z}) \geq 0$, $-\pi/4 \leq \Re(\widehat{z}) \leq \pi/4$. The lines $\Re(\widehat{z}) = \pi/4$ and $\Re(\widehat{z}) = \pi/\alpha - \pi/4 \equiv -\pi/4$ correspond to the images of the left and the right half of the string respectively. As $t \to 1$ the cut goes all the way to $\pi/2\alpha + i\infty$. The image of $\mathcal{C}_{\alpha,t}$ in the complex $\widehat{w} = e^{2i\widehat{z}}$ plane in the $t \to 1$ limit has been shown in Fig.4.19.

The tip of the cut at $\widehat{z} = \pi/2\alpha + i(\tanh^{-1} t)/\alpha$ corresponds to the branch point coming from the square root in the denominator of (4.8.6). According to our convention we choose the positive sign of the square root to the left of this cut, – this forces us to choose the negative sign to the right of the cut. Thus in the $t \to 1$ limit, the map from the z-plane to the $\widehat{z}$ plane takes the form:

$$\begin{aligned} z = f_{\alpha,t=1}(\xi) &= \frac{1}{\alpha}\sin(\alpha\widehat{z}) \qquad \text{for} \quad \Re(\widehat{z}) < \pi/2\alpha\,, \\ &= -\frac{1}{\alpha}\sin(\alpha\widehat{z}) \qquad \text{for} \quad \Re(\widehat{z}) > \pi/2\alpha\,. \end{aligned} \tag{4.8.8}$$

The difference from (4.8.2) for $\Re(\widehat{z}) > \pi/2\alpha$ arises because we redefined asymmetrically the fundamental domain in the $\widehat{z}$ plane. Note that for $\alpha = 2$ the region of $\mathcal{C}_{\alpha,t}$ outside the local coordinate patch collapses to nothing. For this reason we call the associated surface state the 'nothing' state.

4.8.2 Squaring the generalized butterfly

We now want to show that $|\mathcal{B}_\alpha\rangle$ squares to itself under $*$ product. For this we shall first compute $|\mathcal{B}_{\alpha,t} * \mathcal{B}_{\alpha,t}\rangle$, and then take the $t \to 1$ limit. Throughout this section we shall work in the combined matter-ghost system with zero central charge so that we can apply the gluing theorem without any additional factors coming from conformal anomaly. Since the discussion proceeds in a manner closely parallel to that in section 4.6.3, we shall omit the details and only point out the essential differences.

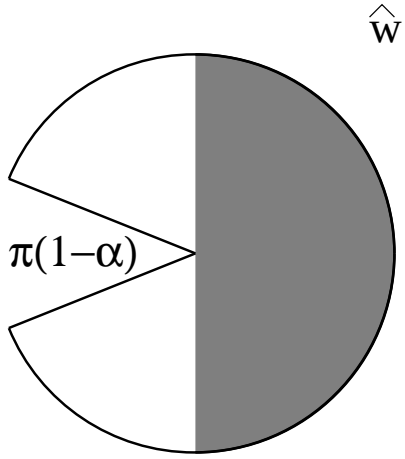

Figure 4.19: The image of $\mathcal{C}_\alpha$ in the complex $\widehat{w} = e^{2i\widehat{z}}$ plane. The shaded region denotes the local coordinate patch.

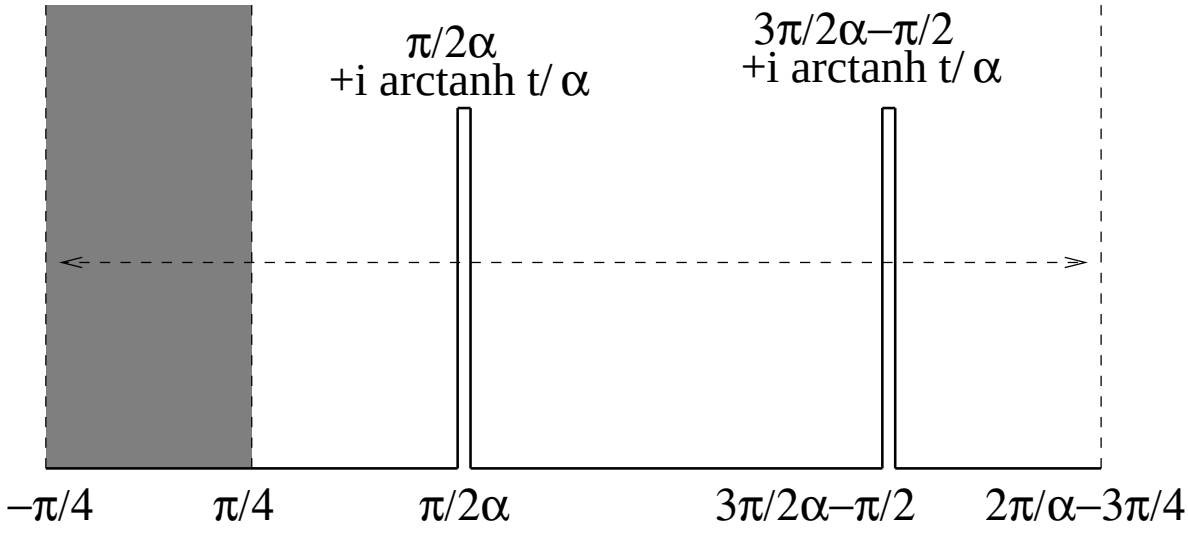

Figure 4.20: The geometry of $\mathcal{C}'_{\alpha,t}$ in the complex $\widehat{z}$ plane. The shaded region denotes the local coordinate patch, and the lines $\Re(\widehat{z}) = -\pi/4$, $\Re(\widehat{z}) = 2\pi/\alpha - 3\pi/4$ are identified.

As in section 4.6.3, we work in the $\widehat{z}$ coordinates. We begin with two copies of $\mathcal{C}_{\alpha,t}$ (one for each $\mathcal{B}_{\alpha,t}$), simply remove the local coordinate patch from the second $\mathcal{C}_{\alpha,t}$ and glue the image of the right half string on the first $\mathcal{C}_{\alpha,t}$ with the image of the left half string on the

second $\mathcal{C}_{\alpha,t}$. The result is a cylinder $\mathcal{C}'_{\alpha,t}$ of circumference

$$\frac{2\pi}{\alpha} - \frac{\pi}{2}\,, \tag{4.8.9}$$

defined as the region $\Im(\widehat{z}) \geq 0$, $-\pi/4 \leq \Re(\widehat{z}) \leq 2\pi/\alpha - 3\pi/4$. It also has two cuts, one along the line $\Re(\widehat{z}) = \pi/2\alpha$, extending from $\widehat{z} = \pi/2\alpha$ to $\widehat{z} = \pi/2\alpha + i(\tanh^{-1} t)/\alpha$, and the other along the line $\Re(\widehat{z}) = 3\pi/2\alpha - \pi/2$, extending from $\widehat{z} = 3\pi/2\alpha - \pi/2$ to $\widehat{z} = 3\pi/2\alpha - \pi/2 + i(\tanh^{-1} t)/\alpha$. The local coordinate patch on $\mathcal{C}'_{\alpha,t}$ is the vertical strip bounded by the lines $\Re(\widehat{z}) = \pm\pi/4$. This has been shown in Fig.4.20.

Let $z = F_{\alpha,t}(\widehat{z})$ describes the map of $\mathcal{C}'_{\alpha,t}$ to UHP. In order to show that $\mathcal{B}_\alpha$ squares to itself, we need to show that as $t \to 1$, the map $F_{\alpha,t}(\widehat{z})$ approaches the map given in (4.8.2) in the vicinity of the origin. Thus the task is now to determine the map $F_{\alpha,t}$ that maps the $\widehat{z}$ plane to the upper half plane labeled by the coordinate z. It is defined implicitly through the differential equation analogous to (4.6.11):

$$d\widehat{z} = \frac{1}{(1+d^2\,z^2)}\,\frac{(1-b^2z^2)}{\sqrt{(1-a^2z^2)(1-c^2z^2)}}\,dz \equiv H(z)dz\,. \tag{4.8.10}$$

The analog of eqs.(4.6.12)-(4.6.15) are:

$$\begin{aligned}
\int_0^{1/a} H(z)dz &= \frac{\pi}{2\alpha}\,, && (4.8.11)\\
\int_{1/a}^{1/b} H(z)dz &= ih/\alpha\,, && (4.8.12)\\
\int_{1/b}^{1/c} H(z)dz &= -ih/\alpha\,, && (4.8.13)\\
\int_{\frac{1}{c}}^{\infty} H(z)dz &= \frac{\pi}{2\alpha} - \frac{\pi}{4}\,, && (4.8.14)
\end{aligned}$$

with h as defined in eq.(4.6.16).

In the $t \to 1$ limit the height h of the cylinder goes to ∞. We shall now show that this can be achieved by taking

$$\{b, c, d\} \ll a, \qquad c \ll \{b, d\}\,. \tag{4.8.15}$$

As in section 4.6.3 we define $z \to -1/z'$ and rewrite (4.8.10) as

$$d\widehat{z} = \frac{1}{(z'^2+d^2)}\,\frac{(z'^2-b^2)}{\sqrt{(z'^2-a^2)(z'^2-c^2)}}\,dz' = G(z')dz'\,. \tag{4.8.16}$$

In the limit $\{b, c, d\} \ll a$, (4.8.11) gives:

$$\int_a^\infty G(z')dz' \simeq \int_a^\infty \frac{dz'}{z'} \frac{1}{\sqrt{z'^2 - a^2}} = \frac{\pi}{2\alpha}\,. \tag{4.8.17}$$

This requires

$$a \simeq \alpha\,. \tag{4.8.18}$$

Proceeding as in the case of section 4.6.3, we can now show that all the other conditions (4.8.12)-(4.8.14), and the requirement of large h can be satisfied by taking:

$$c \ll b, d, \qquad d \sim b\,. \tag{4.8.19}$$

Using eqs.(4.8.15) and (4.8.18), we see that eq.(4.8.10) now takes the form:

$$d\widehat{z} = \frac{1}{\sqrt{1 - \alpha^2 z^2}}\, dz\,, \tag{4.8.20}$$

which gives:

$$z = \frac{1}{\alpha} \sin(\alpha \widehat{z})\,. \tag{4.8.21}$$

This is precisely the map for the generalized butterfly. This establishes that the generalized butterfly squares to itself under $*$-product.

4.8.3 Wave-functionals for generalized butterfly states

In this subsection we shall apply the general method described in section 4.2.5 to compute the wave-functional of the generalized butterfly state. In this process, we shall show explicitly that the wave-functional factorizes into a product of a functional of the left-half of the string and a functional of the right-half of the string. The wave-functional of the butterfly state is expressed as

$$\langle \mathcal{B}_\alpha | X \rangle = \mathcal{N}_{\mathcal{B}_\alpha} \exp\left(-\frac{1}{2} \int_0^\pi \int_0^\pi d\sigma d\sigma' X(\sigma) A_{\mathcal{B}_\alpha}(\sigma, \sigma') X(\sigma') \right)\,. \tag{4.8.22}$$

As seen from eqs.(4.2.29) and (4.2.30), computation of $A_{\mathcal{B}_\alpha}(\sigma_1, \sigma_2)$ defined in eq.(4.8.22) requires computing correlation functions of the form $\langle \mathcal{B}_{\alpha,t}| \cdots |\mathcal{B}_{\alpha,t}\rangle$, and then taking the limit $t \to 1$. To do this computation one simply removes the local coordinate patch from

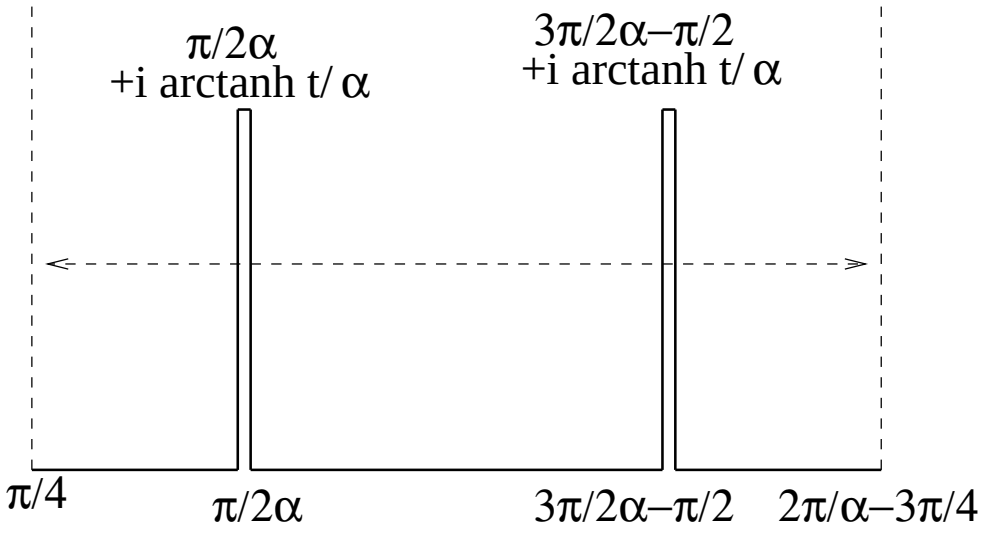

Figure 4.21: The geometry involved in the computation of the inner product of two generalized butterflies in the $\widehat{z}$-plane.

each $\mathcal{C}_{\alpha,t}$ and glues the left half of one with the right half of the other and vice versa. The result is a semiinfinite cylinder $\mathcal{C}''_{\alpha,t}$ of circumference $(2\pi/\alpha-\pi)$, corresponding to the region $\Im(\widehat{z}) \geq 0$, $\pi/4 \leq \Re(\widehat{z}) \leq \pi/4 + 2\pi/\alpha - \pi$, with the identification $\widehat{z} \equiv \widehat{z} + (2\pi/\alpha - \pi)$, and with two vertical cuts, one going from $\widehat{z} = \pi/2\alpha$ to $\widehat{z} = \pi/2\alpha + i(\tanh^{-1} t)/\alpha$, and the other going from $\widehat{z} = 3\pi/2\alpha - \pi/2$ to $\widehat{z} = 3\pi/2\alpha - \pi/2 + i(\tanh^{-1} t)/\alpha$ respectively. The two halves of the string along which we have glued the two copies of $\mathcal{C}_{\alpha,t}$ to produce the cylinder $\mathcal{C}''_{\alpha,t}$ lie along the lines $\Re(\widehat{z}) = \pi/4$ and $\pi/\alpha - \pi/4$ respectively. This has been shown in Fig.4.21. Thus we have, using (4.2.29) and (4.2.30):

$$\frac{1}{2}\partial_{\sigma_1}\partial_{\sigma_2} A^{-1}_{\mathcal{B}_\alpha}(\sigma_1,\sigma_2) = \partial_{\sigma_1}\partial_{\sigma_2}\langle X(\widehat{z}_1)X(\widehat{z}_2)\rangle_{\mathcal{C}''_{\alpha,t}}\,. \tag{4.8.23}$$

This correlation function can be calculated by finding the conformal transformation that maps the cylinder $\mathcal{C}''_{\alpha,t}$ to the upper half plane, and re-expressing (4.8.23) as a correlation function on the upper half plane. This gives

$$\begin{aligned}\frac{1}{2}\partial_{\sigma_1}\partial_{\sigma_2} A^{-1}_{\mathcal{B}_\alpha}(\sigma_1,\sigma_2) &= \partial_{\sigma_1}\partial_{\sigma_2}\langle X(z_1)X(z_2)\rangle_{UHP} \\ &= -\frac{1}{2}\partial_{\sigma_1}\partial_{\sigma_2}\{\ln|z_1-z_2|^2 + \ln|z_1-\bar{z}_2|^2\}\,,\end{aligned} \tag{4.8.24}$$

with z_i's computed in terms of σ_i's with the help of the map that relates $\widehat{z} = \tan^{-1}\xi = \tan^{-1}(e^{i\sigma})$ to the upper half plane coordinate z. We could proceed as in section 4.8.2 to construct the map from the $\widehat{z}$ plane to the z-plane, but in this case we can write down a closed form expression for this map. The function that maps $\mathcal{C}''_{\alpha,t}$ in the $\widehat{z}$ coordinate to the upper half plane labeled by z is given by:

$$z = g_{\alpha,t}(\xi) = g_{\alpha,t}(\tan\widehat{z}) \tag{4.8.25}$$

with

$$g_{\alpha,t}(\xi) = \sqrt{\frac{\tan^2(\beta\tan^{-1}\xi+\gamma)+u^2}{1+u^2\tan^2(\beta\tan^{-1}\xi+\gamma)}} = \sqrt{\frac{\tan^2(\beta\widehat{z}+\gamma)+u^2}{1+u^2\tan^2(\beta\widehat{z}+\gamma)}} \tag{4.8.26}$$

where

$$\frac{1}{\beta} = \frac{2}{\alpha} - 1, \qquad \gamma = \frac{\pi}{2}(1-\frac{\beta}{\alpha}), \qquad \frac{1}{\beta}\tanh^{-1}u = \frac{1}{\alpha}\tanh^{-1}t\,. \tag{4.8.27}$$

To see that this maps $\mathcal{C}''_{\alpha,t}$ to the upper half plane, we can start from $\widehat{z} = \pi/4$ and follow the boundary of $\mathcal{C}''_{\alpha,t}$ to see that it maps to the real line in the z plane. As we start from $\widehat{z} = \pi/4$ and travel along the real axis to $\widehat{z} = \pi/2\alpha$, z travels along the real line from 1 to $1/u$ As $\widehat{z}$ goes from the point $\widehat{z} = \pi/2\alpha$ towards $\pi/2\alpha + i(\tanh^{-1}t)/\alpha$, z goes from $1/u$ to ∞. Then as $\widehat{z}$ returns back to $\pi/2\alpha$ along the same line, z goes from $-\infty$ to $-1/u$, and as $\widehat{z}$ travels along the real axis to $\widehat{z} = (3\pi/2\alpha - \pi/2)$, z goes from $-1/u$ to $-u$, passing through -1 at $\widehat{z} = (\pi/\alpha - \pi/4)$. As $\widehat{z}$ travels along the vertical line from $\widehat{z} = (3\pi/2\alpha - \pi/2)$ to $\widehat{z} = (3\pi/2\alpha - \pi/2) + i(\tanh^{-1}t)/\alpha$, z goes from $-u$ to 0, and as we return back to the point $\widehat{z} = 3\pi/2\alpha - \pi/2$ along the same line, z goes from 0 to u. Finally, as we move from $\widehat{z} = (3\pi/2\alpha - \pi/2)$ to $\widehat{z} = (\pi/4 + 2\pi/\alpha - \pi)$, z goes from u to 1. Since in the $\widehat{z}$ plane we identify the lines $\Re(\widehat{z}) = (\pi/4 + 2\pi/\alpha - \pi)$ with $\Re(\widehat{z}) = \pi/4$, the contour closes.

From the map of the boundary to the real z axis described above we see that the ends of the half strings, $\widehat{z} = \pi/4$ and $\widehat{z} = (\pi/\alpha - \pi/4)$ maps to 1 and -1 respectively. From eqs.(4.8.25), (4.8.26), (4.8.27) we see that the half string $\Re(\widehat{z}) = \pi/4$ gets mapped to

$$z = \sqrt{\frac{(1+iS)^2+u^2(1-iS)^2}{(1-iS)^2+u^2(1+iS)^2}}\,, \tag{4.8.28}$$

where

$$S = \tanh(\beta\Im(\widehat{z}))\,. \tag{4.8.29}$$

On the other hand the half-string $\Re(\widehat{z}) = (\pi/\alpha - \pi/4)$ gets mapped to

$$z = -\sqrt{\frac{(1-iS)^2 + u^2(1+iS)^2}{(1+iS)^2 + u^2(1-iS)^2}}\,. \tag{4.8.30}$$

From eq.(4.8.27) we see that as $t \to 1$ we have $u \to 1$. Eqs.(4.8.28) and (4.8.30) then show that as $u \to 1$, the left and right half-strings are mapped in such a way that all points of the left one, and all points on the right one, except for the one associated to the full string midpoint, approach the points 1 and -1 respectively. The half strings remain infinite in the z plane but are being reparametrized so that all of their inner points are approaching either 1 or -1. Eq.(4.8.24) now gives

$$\frac{1}{2}\partial_{\sigma_1}\partial_{\sigma_2} A^{-1}_{\mathcal{B}_\alpha}(\sigma_1,\sigma_2) = 0 \qquad \text{if} \quad 0 \le \sigma_1 < \pi/2, \quad \pi/2 < \sigma_2 \le \pi\,. \tag{4.8.31}$$

Indeed, since the half-string points σ_1 and σ_2 are mapped to fixed points in the limit $t \to 1$, the derivatives $dz_i/d\sigma_i$ go to zero, and with $|z_1 - z_2|$ finite, the evaluation of the right hand side of Eq.(4.8.24) gives zero. This is consistent with the wave-functional factorizing into a product of a functional of the left half-string and a functional of the right half-string. Indeed, since the interior of the right half-string is going into a point and the interior of the left half-string is going into another point in the z-plane, we have an explicit verification of the factorization relation (4.4.3).

In order to determine which particular state of the half-string appears in the product, we need to evaluate the right hand side of (4.8.24) when σ_1 and σ_2 lie on the same half of the string. For definiteness we shall take $0 \le \sigma_1, \sigma_2 < \pi/2$. The coordinate σ of the half-string is related to $\widehat{z}$ through $\widehat{z} = \tan^{-1}(e^{i\sigma})$. On the left half string, we can rewrite this as:

$$\widehat{z} = \pi/4 + \frac{i}{2}\ln\left(\frac{1+\sin\sigma}{\cos\sigma}\right). \tag{4.8.32}$$

Using eqs.(4.8.29), (4.8.32) we get:

$$S(\sigma) = \frac{(1+\sin\sigma)^\beta - \cos^\beta\sigma}{(1+\sin\sigma)^\beta + \cos^\beta\sigma}\,. \tag{4.8.33}$$

We can now use eqs.(4.8.24), (4.8.30) and (4.8.33) to compute $\partial_{\sigma_1}\partial_{\sigma_2} A^{-1}_{\mathcal{B}_\alpha}(\sigma_1,\sigma_2)$. Note from eqs.(4.8.30), (4.8.33) that as $t \to 1$, the points z_1 and z_2 come close together and $dz_i/d\sigma_i$

also vanishes. Thus we need to do this computation by keeping t slightly away from 1 and then take the limit $t \to 1$. To first order in $(1-t)$,

$$z = 1 + i(1-u^2)\frac{S}{1-S^2}\,. \tag{4.8.34}$$

Substituting this into (4.8.24) we get

$$\partial_{\sigma_1}\partial_{\sigma_2} A^{-1}_{\mathcal{B}_\alpha}(\sigma_1,\sigma_2) = \partial_{\sigma_1}\partial_{\sigma_2}\left[-\ln\left|\frac{S(\sigma_1)}{1-S(\sigma_1)^2} - \frac{S(\sigma_2)}{1-S(\sigma_2)^2}\right|^2 - \ln\left|\frac{S(\sigma_1)}{1-S(\sigma_1)^2} + \frac{S(\sigma_2)}{1-S(\sigma_2)^2}\right|^2\right]. \tag{4.8.35}$$

This, in turn, gives us the wave-functional of the generalized butterfly state through eq.(4.8.22).

As a special example we can consider the case of the butterfly state $\alpha = 1$. In this case we have $\beta = 1$ and hence

$$S(\sigma) = \frac{(1+\sin\sigma) - \cos\sigma}{(1+\sin\sigma) + \cos\sigma}\,. \tag{4.8.36}$$

Substituting this into eq.(4.8.35) we get

$$\partial_{\sigma_1}\partial_{\sigma_2} A^{-1}_{\mathcal{B}_{\alpha=1}}(\sigma_1,\sigma_2) = -\partial_{\sigma_1}\partial_{\sigma_2}\Big[\ln|2\cos(2\sigma_1) - 2\cos(2\sigma_2)|\Big]\,, \qquad \text{for} \quad 0 \le \sigma_1, \sigma_2 < \pi/2\,. \tag{4.8.37}$$

Comparing this with (4.2.33) we see that after a rescaling $\sigma \to 2\sigma$ the half string wave-functional coincides with the ground state wave-functional of the string. This is in accordance with the analysis of section 4.6.4.

We could also try to derive the wave-functional of the nothing state by taking the $\alpha \to 2$ limit. From (4.8.27) we see that in this limit $\beta \to \infty$. Eq.(4.8.29) then gives,

$$S \simeq 1 - 2e^{-2\beta\Im(\widehat{z})}\,. \tag{4.8.38}$$

Eqs.(4.2.29), (4.2.30), (4.8.35) then gives:

$$\begin{aligned}
\langle\mathcal{N}|\partial_{\sigma_1}X(\sigma_1)\partial_{\sigma_2}X(\sigma_2)|\mathcal{N}\rangle &= \partial_{\sigma_1}\partial_{\sigma_2}A^{-1}_{\mathcal{B}_{\alpha=2}}(\sigma_1,\sigma_2) \\
&\simeq -\partial_{\sigma_1}\partial_{\sigma_2}\Big[\ln\left|e^{2\beta\Im(\widehat{z}_1)} - e^{2\beta\Im(\widehat{z}_2)}\right|^2 + \ln\left|e^{2\beta\Im(\widehat{z}_1)} + e^{2\beta\Im(\widehat{z}_2)}\right|^2\Big] \\
&\simeq -\partial_{\sigma_1}\partial_{\sigma_2}\ln\left|1 - e^{-4\beta|\Im(\widehat{z}_1) - \Im(\widehat{z}_2)|}\right|^2.
\end{aligned} \tag{4.8.39}$$

This clearly vanishes in the $\beta \to \infty$ limit for $\sigma_1 \neq \sigma_2$. This is consistent with the fact that the wave-functional of the nothing state is a constant independent of $X(\sigma)$, since as we see

from eq.(4.2.30), if A_f vanishes, then the path integration over X makes the expectation value of $\partial_{\sigma_1} X(\sigma_1)\partial_{\sigma_2} X(\sigma_2)$ vanish for $\sigma_1 \neq \sigma_2$ due to the $X(\sigma) \to -X(\sigma)$ symmetry at each point σ.

4.9 Other Projectors and Star Subalgebras

So far in this chapter we have developed general properties of split wave-functionals and projectors, and also discussed in detail certain projectors, such as the butterfly and its generalizations, and the nothing state. Of these, the butterfly has the simplest representation as the exponential of a single Virasoro generator acting on the vacuum. In this section we exhibit other projectors whose Virasoro representation is as simple as that of the butterfly. We also discuss subalgebras of surface states that generalize the commutative wedge state subalgebra.

4.9.1 A class of projectors with simple Virasoro representation

The butterfly state, which is simply given as $\exp(-\frac{1}{2}L_{-2})|0\rangle$ (see Eq.(4.6.33)), suggests the question whether there are other projectors which can be written as an exponential involving a single Virasoro operator. To this end, we consider the vector fields

$$v_{(n)}(\xi) = -\frac{\beta}{n}\,\xi^{n+1}\,, \tag{4.9.1}$$

which generate the diffeomorphisms [79]

$$z = f_{(n)}(\xi) = \exp\Big(v_{(n)}(\xi)\frac{\partial}{\partial\xi}\Big)\,\xi = \frac{\xi}{(1+\beta\,\xi^n)^{1/n}}\,. \tag{4.9.2}$$

The associated surface states are

$$|B_n(\beta)\rangle = \exp\Big(-\frac{\beta}{n}(-1)^n L_{-n}\Big)|0\rangle\,. \tag{4.9.3}$$

For even n one can readily implement the projector condition $f(\xi = \pm i) = \infty$ by a choice of the parameter β. Indeed, this condition fixes

$$\beta = -(-)^{n/2}\,, \qquad n \text{ even}\,. \tag{4.9.4}$$

We therefore obtain candidate projectors

$$|P_{2m}\rangle = \exp\Big((-1)^m \frac{1}{2m} L_{-2m}\Big)\,|0\rangle\,. \tag{4.9.5}$$

The case $m = 1$ is the canonical butterfly, and the next projectors are

$$\exp\Big(\frac{1}{4}L_{-4}\Big)|0\rangle\,, \quad \exp\Big(-\frac{1}{6}L_{-6}\Big)|0\rangle\,, \quad \exp\Big(\frac{1}{8}L_{-8}\Big)|0\rangle \ \cdots \tag{4.9.6}$$

and so on. These projectors obey the conservation law

$$K_{2m}|P_{2m}\rangle = 0\,, \tag{4.9.7}$$

which is the obvious generalization of (4.6.34) and can be proven in the same way considering the global vector fields

$$\tilde{v}_{2m}(z) = 2(-1)^{m+1} z - z^{-2m+1}\,. \tag{4.9.8}$$

It is interesting to note that $|P_4\rangle$ for example, is a state where the open string boundary condition chosen to define the state does not hold at the string endpoint. This is because the map $f_4(\xi) = \xi/(1-\xi^4)^{1/4}$ is singular at $\xi = \pm 1$. The boundary of Σ is discontinuous at the open string endpoints, and the phenomenon discussed at the end of section 4.4.2 occurs.

4.9.2 Subalgebras of surface states annihilated by K_n

The family of wedge states $|\mathcal{W}_r\rangle$ [12, 107], defined in the z representation by the maps

$$z = \frac{r}{2}\tan\Big(\frac{2}{r}\arctan(\xi)\Big)\,, \tag{4.9.9}$$

obeys $K_1|\mathcal{W}_r\rangle = 0$, for all values of the parameter r, $1 \le r \le \infty$. The wedge states interpolate between the identity $|\mathcal{W}_1\rangle \equiv |\mathcal{I}\rangle$ and the sliver, $|\mathcal{W}_\infty\rangle \equiv |\Xi\rangle$. By analogy, it is natural to ask if there is a family of states all annihilated by K_2, interpolating between the identity and the butterfly, and also containing the nothing state, see (4.7.6). Indeed, we have found such a family, defined by the maps

$$z = g^{(2)}_\mu(\xi) = \frac{1}{\sqrt{4\mu}}\left[1 - \left(\frac{1-\xi^2}{1+\xi^2}\right)^{2\mu}\right]^{\frac{1}{2}}\,. \tag{4.9.10}$$

For $\mu = -1$ we recover the identity, for $\mu = 1/2$ the canonical butterfly and for $\mu = 1$ the nothing state. The condition $g_\mu^{(2)}(\pm i) = \infty$ is satisfied for $\mu \geq 0$, so according to our general arguments all the states with $\mu \geq 0$ are candidate projectors.

More generally, for any given integer n, we can look for the family of all surface states in the kernel of K_n. Since K_n is a derivation, each family will be closed under star-multiplication. Let $z = g^{(n)}(\xi)$ be a map that defines a surface state annihilated by K_n. We require as usual that $g^{(n)}(\xi)$ has a regular Taylor expansion in $\xi = 0$ with $g^{(n)}(0) = 0$, $\frac{dg^{(n)}(0)}{d\xi} = 1$. We can find the general form of $g^{(n)}(\xi)$ by demanding that the vector field

$$\tilde{v}_n(z) = \frac{dz}{d\xi}(\xi^{n+1} - (-1)^n \xi^{-n+1})\,, \tag{4.9.11}$$

be globally defined in the UHP – this is precisely the condition that the state is annihilated by K_n. Clearly $\tilde{v}_n(z)$ must have a pole of order $(n-1)$ at $z = 0$. The most general form for such a globally defined vector field is

$$\tilde{v}_n(z) = \frac{P_{n+1}(z)}{z^{n-1}}\,, \tag{4.9.12}$$

where $P_{n+1}(z)$ is a polynomial of order $(n+1)$ with non-vanishing constant term. The order of P_{n+1} is fixed by the requirement that the vector field is regular at infinity, $\lim_{z\to\infty} z^{-2}\tilde{v}_n(z) =$ const. Distinguishing between the cases of n even or odd we find that the two previous equations lead to the differential equations

$$\begin{aligned} \frac{1}{2n}\, d\ln\left(\frac{1-\xi^n}{1+\xi^n}\right) &= \frac{z^{n-1}}{P_{n+1}(z)}\, dz \qquad \text{for } n \text{ even}\,, \\ \frac{1}{n}\, d\arctan(\xi^n) &= \frac{z^{n-1}}{P_{n+1}(z)}\, dz \qquad \text{for } n \text{ odd}\,. \end{aligned} \tag{4.9.13}$$

Demanding that the surface state is twist even requires that z be an odd function of ξ, and this restricts the polynomial P_{n+1} to contain only even powers of z. For $n = 1$, the most general twist even solution is the family of maps (4.9.9) defining the wedge states; for $n = 2$, imposing again the twist even condition, we find the one-parameter family (4.9.10). Higher values of n give multi-parameter solutions.

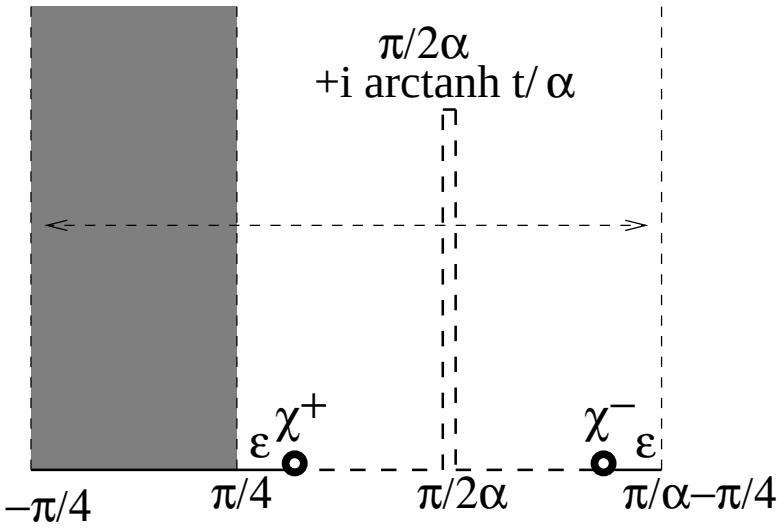

Figure 4.22: The geometry involved in the computation of (4.10.2). The two dots on the real line denote the insertion of $\chi^{\pm}$ at distance ϵ away from the two edges. The thick dashed line on the boundary represents $BCFT'$ boundary condition, whereas the thick continuous line represents $BCFT$ boundary condition.

4.10 Butterfly States Associated with General BCFT

In Ref.[59] we described the construction of sliver states associated with a general boundary conformal field theory (BCFT). A very similar construction can be carried out for generalized butterfly states associated with a general BCFT. For this we denote by $BCFT$ the reference BCFT in whose Hilbert space we wish to represent all the butterfly states, and by $BCFT'$ some other BCFT. Let $\chi^{\pm}$ denote a pair of boundary condition changing operators of dimension h, such that an insertion of χ^+ (χ^-) on the real axis separates $BCFT$ ($BCFT'$) boundary condition to the left of the insertion from $BCFT'$ ($BCFT$) boundary condition to the right of the insertion. Furthermore, $\chi^{\pm}$ are required to satisfy the operator product expansion:

$$\chi^-(x)\chi^+(y) = (y-x)^{-2h} + \text{non-leading terms}\,. \tag{4.10.1}$$

Let us now define the state $|\mathcal{B}'_{\alpha,t}\rangle$ associated to a regulated butterfly through the relation:

$$\langle \mathcal{B}'_{\alpha,t}|\phi\rangle = (2\epsilon)^{2h}\Big\langle f^{(0)}\circ\phi(0)\chi^+(\frac{\pi}{4}+\epsilon)\chi^-(\frac{\pi}{\alpha}-\frac{\pi}{4}-\epsilon)\Big\rangle_{\mathcal{C}_{\alpha,t}}\,, \tag{4.10.2}$$

where ϵ is any finite positive number, $f^{(0)}(\xi) = \tan^{-1}\xi$, and $\mathcal{C}_{\alpha,t}$ denotes the semi-infinite cylinder with circumference π/α with a cut parametrized by t, as shown in Fig. 4.22. Let us define $|\mathcal{B}'_\alpha\rangle$ to be the state $|\mathcal{B}'_{\alpha,t=1}\rangle$ and $\mathcal{C}_\alpha$ to be the cylinder $\mathcal{C}_{\alpha,1}$. Using the conformal transformation

$$z = \frac{1}{\alpha}\sin(\alpha\widehat{z}) \equiv g_\alpha(\widehat{z})\,, \tag{4.10.3}$$

that maps $\mathcal{C}_\alpha$ to the upper-half z-plane, we can reexpress $\langle\mathcal{B}'_\alpha|\phi\rangle$ as

$$\langle\mathcal{B}'_\alpha|\phi\rangle = (2\epsilon)^{2h}\Big\langle g_\alpha\circ f^{(0)}\circ\phi(0)\;\; g_\alpha\circ\chi^+(\frac{\pi}{4}+\epsilon)\;\; g_\alpha\circ\chi^-(-\frac{\pi}{4}-\epsilon)\Big\rangle_{UHP}\,. \tag{4.10.4}$$

In the last step we have used the periodicity in the $\widehat{z}$ plane to replace $\chi^-(\pi/\alpha-\pi/4-\epsilon)$ by $\chi^-(-\pi/4-\epsilon)$.

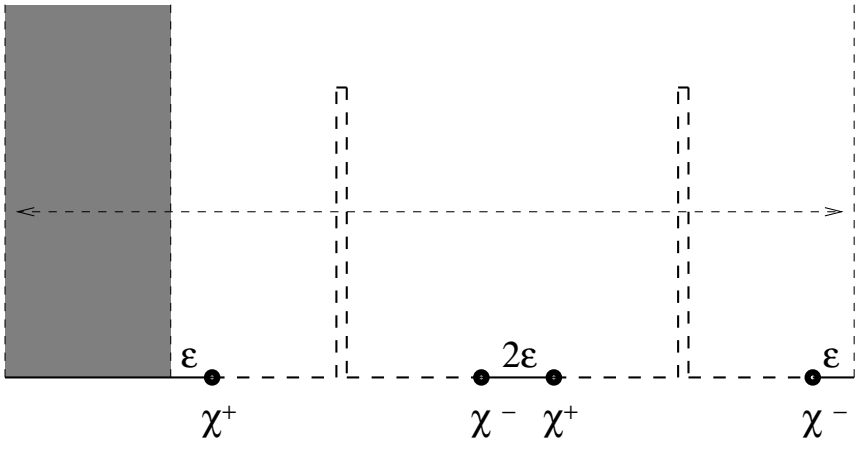

Figure 4.23: The geometry involved in the computation of $|\mathcal{B}'_{\alpha,t} * \mathcal{B}'_{\alpha,t}\rangle$. The boundary components labeled by thick continuous line represent $BCFT$ boundary conditions and the boundary components labeled by thick broken lines label $BCFT'$ boundary conditions. The coordinate labels of various points are identical to those in Fig.4.20.

The computation of $|\mathcal{B}'_{\alpha,t} * \mathcal{B}'_{\alpha,t}\rangle$ is straightforward using the gluing rules in the $\widehat{z}$ coordinate system. The result is:

$$\langle\mathcal{B}'_{\alpha,t}*\mathcal{B}'_{\alpha,t}|\phi\rangle = (2\epsilon)^{4h}\Big\langle f\circ\phi(0)\chi^+(\frac{\pi}{4}+\epsilon)\chi^-(\frac{\pi}{\alpha}-\frac{\pi}{4}-\epsilon)\chi^+(\frac{\pi}{\alpha}-\frac{\pi}{4}+\epsilon)\chi^-(\frac{2\pi}{\alpha}-\frac{3\pi}{4}-\epsilon)\Big\rangle_{\mathcal{C}'_{\alpha,t}}\,. \tag{4.10.5}$$

The geometry of $\mathcal{C}'_{\alpha,t}$ has been shown in Fig.4.23. This correlation function can be evaluated by mapping it to the UHP via the map given in eq.(4.8.10). As shown in section 4.8.2, as $t\to$

1 this approaches eq.(4.8.21), with part of the $\mathcal{C}'_{\alpha,t}$ plane in the middle collapsing to a point in the $\widehat{z}$ plane. In this case this part includes the insertion $\chi^-(\pi/\alpha-\pi/4-\epsilon)\chi^+(\pi/\alpha-\pi/4+\epsilon)$, and hence this can be replaced by the leading term in the operator product expansion which is $(2\epsilon)^{-2h}$. Thus in the $t\to 1$ limit, we can rewrite (4.10.5) as,

$$\langle \mathcal{B}'_\alpha * \mathcal{B}'_\alpha|\phi\rangle = (2\epsilon)^{2h}\Big\langle f\circ\phi(0)\chi^+(\frac{\pi}{4}+\epsilon)\chi^-(-\frac{\pi}{4}-\epsilon)\Big\rangle_{\mathcal{C}'_{\alpha,1}}\,, \tag{4.10.6}$$

where we have used the periodicity in the $\widehat{z}$ plane to replace $\chi^-(2\pi/\alpha-3\pi/4-\epsilon)$ by $\chi^-(-\pi/4-\epsilon)$. Using the result of section 4.8.2 that the map $g_\alpha(\widehat{z})$ defined in eq.(4.10.3), that maps $\mathcal{C}_\alpha$ to the upper half plane, also maps $\mathcal{C}'_{\alpha,t}$ to the upper half plane for $t=1$, we have:

$$\langle \mathcal{B}'_\alpha * \mathcal{B}'_\alpha|\phi\rangle = (2\epsilon)^{2h}\Big\langle g_\alpha\circ f\circ\phi(0)g_\alpha\circ\chi^+(\frac{\pi}{4}+\epsilon)g_\alpha\circ\chi^-(-\frac{\pi}{4}-\epsilon)\Big\rangle_{UHP}\,. \tag{4.10.7}$$

Comparing eqs.(4.10.4) and (4.10.7) we see that

$$\langle \mathcal{B}'_\alpha| = \langle \mathcal{B}'_\alpha * \mathcal{B}'_\alpha|\,, \tag{4.10.8}$$

as we wanted to show. We end this section by noting that this construction can be easily generalized to construct any of the projectors discussed in section 4.5 associated with a general BCFT.

4.11 Concluding Remarks

In this chapter we have given a rather general discussion of projectors of the open string $*$-algebra and split wave-functionals. It was found that in addition to the sliver, infinitely many projectors exist which have pure geometrical interpretation as surface states. We have also seen that such surface states, in general, can be viewed as tensor products of half-string surface states. This viewpoint makes it clear that the half-string surface states are naturally defined with the same open string boundary conditions as the full string states. Moreover, all projectors are clearly recognized as being invariant under opposite constant translations of the half strings. We have illustrated in detail our general considerations, by discussing explicitly several interesting projectors.

While we have indicated that the projectors considered here are expected to be equivalent in that they define physically equivalent solutions of vacuum string field theory, our focus on specific projectors and their properties may have applications in other contexts. For example, it seems clear that OSFT solutions are not projectors. It follows, that if OSFT solutions are eventually built in terms of deformations of projectors, particular projectors could be of special use. As noted, level expansion does seem to single out the butterfly as a special projector. There may still be other surface state projectors deserving particular attention which we have not uncovered.

One question we have not attempted to investigate is how the approach of the midpoint to the boundary controls the behavior of the projector. While $f(\xi = i) = \infty$ seems necessary to have a projector, it may be of interest to understand the full significance the behavior of f near $\xi = i$. We have already seen that this behavior controls the boundary conditions satisfied by the half string states.

In this chapter we have only considered string fields which have a purely geometric interpretation as surface states associated to Riemann surfaces. All such string fields belong to the Virasoro module on the vacuum. We have uncovered the general geometric mechanism that gives rise to rank-one surface state projectors. It should be kept in mind that there are many projectors that lie outside the Virasoro module of the vacuum and do not have a purely geometric interpretation. For example there are squeezed states built with flat space oscillators that star-multiply to themselves but are not surface states.

It has been recently recognized [106, 21] that the open string star product can be interpreted as a continuous tensor product of mutually commuting two-dimensional Moyal products. This algebraic approach is likely to shed new light on projectors, and it will be interesting to understand in detail the connection with the geometric methods of the present chapter. A complete understanding of projectors could well help eventually give a concrete description of the star-algebra. In fact, given the central role of projectors in the study of non-commutative field theory, it is natural to expect that star-algebra projectors will have an important role in our future understanding of string field theory.

4.12 Numerical Computations Involving the Butterfly

In this appendix we shall present numerical results for computations involving the butterfly at various levels of approximation. We approximate the butterfly by truncating it to a given level L, and calculate various star products keeping only terms up to level L. The results are given in Tables 1, 2 and 3. The last column gives the expected answers, and the last but one column gives the extrapolation of the numerical answers to infinite level using a fit of the form $a + b/L + c/L^2$.

Table 1 contains numerical results for the square of the butterfly. As we see from this table, as we include more and more terms in the expression for the butterfly, the closer is its square to the expected answer.

We can also test the property (4.5.4) that the butterfly is a rank-one projector. We need to work in a unitary BCFT, so we choose to consider butterfly states $|\mathcal{B}^{c=1}\rangle$ built with Virasoro generators of central charge one. Star multiplication of surface states in this theory works as in the $c = 0$ case but with extra (infinite) overall factors arising from the conformal anomaly. These infinite factors are regulated by the level truncation procedure and we ignore them, considering the results up to their overall normalization. In Table 2 and Table 3 we present the numerical results for the normalized products $|\mathcal{B}^{c=1}\rangle * |0\rangle * |\mathcal{B}^{c=1}\rangle$ and $|\mathcal{B}^{c=1}\rangle * L_{-2}|0\rangle * |\mathcal{B}^{c=1}\rangle$. From (4.5.4) we expect these products to be proportional to the butterfly, and indeed this is seen to hold more and more accurately as the level is increased.

These numerical results confirm the formal arguments of this chapter that the butterfly is a rank-one projector of the $*$-algebra.

	$L=2$	$L=4$	$L=6$	$L=8$	$L=10$	$L=12$	$L=\infty$	Exp
$\|0\rangle$	1.00000	1.00000	1.00000	1.00000	1.00000	1.00000	1.00000	1.00000
$L_{-2}\|0\rangle$	-0.43230	-0.46035	-0.47214	-0.47858	-0.48263	-0.48540	-0.49981	-0.50000
$L_{-4}\|0\rangle$	0	-0.00351	-0.00213	-0.00146	-0.00108	-0.00084	0.00021	0.00000
$L_{-2}L_{-2}\|0\rangle$	0	0.10845	0.11309	0.11567	0.11732	0.11847	0.12307	0.12500
$L_{-6}\|0\rangle$	0	0	0.00168	0.00117	0.00087	0.00068	0.00005	0.00000
$L_{-4}L_{-2}\|0\rangle$	0	0	0.00040	0.00027	0.00021	0.00017	0.00003	0.00000
$L_{-3}L_{-3}\|0\rangle$	0	0	-0.00034	-0.00023	-0.00016	-0.00012	0.00001	0.00000
$(L_{-2})^3\|0\rangle$	0	0	-0.01771	-0.01843	-0.01887	-0.01918	-0.02017	-0.02083

Table 4.1: Numerical results for the coefficients of $|\mathcal{B}\rangle * |\mathcal{B}\rangle$.

	$L=2$	$L=4$	$L=6$	$L=8$	$L=10$	$L=12$	$L=\infty$	Exp
$\|0\rangle$	1.00000	1.00000	1.00000	1.00000	1.00000	1.00000	1.00000	1.00000
$L_{-2}\|0\rangle$	-0.39892	-0.44581	-0.46296	-0.47192	-0.47743	-0.48115	-0.50002	-0.50000
$L_{-4}\|0\rangle$	0	-0.00617	-0.00231	-0.00136	-0.00093	-0.00069	0.00009	0.00000
$L_{-2}L_{-2}\|0\rangle$	0	0.09982	0.10808	0.11217	0.11465	0.11633	0.12312	0.12500
$L_{-6}\|0\rangle$	0	0	0.00349	0.00143	0.00088	0.00063	-0.00002	0.00000
$L_{-4}L{-}2\|0\rangle$	0	0	0.00117	0.00054	0.00033	0.00024	-0.00005	0.00000
$L_{-3}L_{-3}\|0\rangle$	0	0	-0.00005	-0.00011	-0.00009	-0.00007	0.00000	0.00000
$L_{-2}L_{-2}L_{-2}\|0\rangle$	0	0	-0.01652	-0.01761	-0.01825	-0.01867	-0.02007	-0.02083

Table 4.2: Numerical results for the coefficients of $|\mathcal{B}^{c=1}\rangle * |0\rangle * |\mathcal{B}^{c=1}\rangle$. The coefficient of $|0\rangle$ in the result has been normalized to one.

	$L=2$	$L=4$	$L=6$	$L=8$	$L=10$	$L=12$	$L=\infty$	Exp
$\|0\rangle$	1.00000	1.00000	1.00000	1.00000	1.00000	1.00000	1.00000	1.00000
$L_{-2}\|0\rangle$	-0.48377	-0.49010	-0.48462	-0.48562	-0.48720	-0.48862	-0.48519	-0.50000
$L_{-4}\|0\rangle$	0	-0.05238	-0.00861	-0.00461	-0.00312	-0.00233	-0.00689	0.00000
$L_{-2}L_{-2}\|0\rangle$	0	0.11387	0.11410	0.11565	0.11712	0.11823	0.12254	0.12500
$L_{-6}\|0\rangle$	0	0	0.02146	0.00456	0.00247	0.00166	0.00258	0.00000
$L_{-4}L{-}2\|0\rangle$	0	0	0.00288	0.00054	0.00043	0.00035	0.00086	0.00000
$L_{-3}L_{-3}\|0\rangle$	0	0	-0.00083	-0.00093	-0.00055	-0.00038	0.00059	0.00000
$L_{-2}L_{-2}L_{-2}\|0\rangle$	0	0	-0.01738	-0.01795	-0.01848	-0.01886	-0.02016	-0.02083

Table 4.3: Numerical results for the coefficients of $|\mathcal{B}^{c=1}\rangle * L_{-2}|0\rangle * |\mathcal{B}^{c=1}\rangle$. The coefficient of $|0\rangle$ in the result has been normalized to one.

Chapter 5

Closed string emission and D-brane decay

5.1 Introduction

Our starting point for the work in this chapter is the real-time process of D-brane creation and annihilation. In [109] Sen introduced a simple class of models in bosonic string theory obtained by perturbing the flat-space $c = 26$ CFT with the exactly marginal deformation

$$\lambda \int dt \, \cosh(X^0(t)) \,, \tag{5.1.1}$$

where t is a coordinate on the worldsheet boundary, and λ is a free parameter in the range $0 \leq \lambda \leq \frac{1}{2}$. This is a family of exact solutions of classical open string theory whose space-time picture is that of an unstable brane being created at a time $X^0 \sim -\tau$ and decaying at a time $X^0 \sim +\tau$, with $\tau = -\log(\sin(\pi\lambda))$. For $\lambda = \frac{1}{2}$ the lifetime of the brane is zero, that is, there is no brane to be found anywhere. Moreover, the corresponding boundary state appears to vanish identically [109]. This is fascinating as it seems to suggest that for $\lambda = \frac{1}{2}$ the BCFT (5.1.1) describes the stable closed string vacuum, where open string degrees of freedom are absent. Somehow the boundary perturbation (5.1.1) with $\lambda = \frac{1}{2}$ must get rid of the worldsheet boundary!

In the framework of (5.1.1), we have the opportunity to precisely test a scenario [53, 24] for how purely closed string amplitudes may be obtained at the tachyon vacuum. The basic idea is that as the tachyon condenses, worldsheets with large holes are suppressed, and the integration over moduli space should localize to the region where the holes shrink to points. This heuristic picture was made somewhat more concrete in chapter two, where it was argued that amplitudes for m external closed strings on the disk reduce at the tachyon vacuum to *sphere* amplitudes with the same m closed string punctures *plus* an additional insertion of a zero-momentum state (possibly a soft dilaton), a remnant of the shrunk boundary. This analysis [24] was performed in the framework of a regulated version of vacuum string field theory [129]. However, due to subtleties in the regulation procedure, it was difficult to make this conclusion completely precise.

Since we wish to focus on the case $\lambda = \frac{1}{2}$, it is very useful to realize that at this critical value the BCFT admits a simple description. By Wick rotation $X^0 \to iX$, one obtains the well-known exactly marginal deformation $\lambda \cos(X)$ [130] (infact this is how Sen arrived at (5.1.1) in the first place), which for $\lambda = \frac{1}{2}$ is equivalent to an infinite array of D-branes located at $X = 2\pi(n + \frac{1}{2})$ [130, 131]. We could thus say that at the critical value $\lambda = \frac{1}{2}$, the time-dependent boundary deformation (5.1.1) becomes an array of D-branes located at *imaginary* times

$$X^0 = i\, 2\pi(n + \frac{1}{2}) \,, \quad n \in \mathbf{Z} \,. \tag{5.1.2}$$

This is an empty statement if we do not define the meaning of D-branes in imaginary time. Our approach to that issue is very simple: Any quantity that one wishes to compute for a configuration of D-branes in imaginary time should be obtained by Wick rotation of the configuration in real space. This prescription gives consistent answers with an interesting physical meaning.

A natural class of observables is given by scattering amplitudes of closed strings on the disk in the background of the brane configuration (5.1.2). We find that these reduce to sphere amplitudes with $m+1$ punctures. The extra puncture is, however, *not* a soft dilaton as in [24], but a non-trivial closed string state that involves the whole tower of massive

modes. Thus the BCFT (5.1.1) with $\lambda = \frac{1}{2}$ describes a purely closed string background with no physical open string degrees of freedom. This background, however, is not the closed string *vacuum*, but a specific time-dependent state with non-zero energy. The detailed features of this background are very reminiscent of 'tachyon matter' [110, 111].

While these results were first obtained in the special case (5.1.2), the basic conclusion is much more general. A generic configuration of imaginary D-branes defines a closed string background. The details of the background depend on the details of the configuration of imaginary D-branes. Exactly marginal open string deformations, for example deformations that move the positions of the imaginary branes, are naturally reinterpreted as deformations of the closed string background. The case (5.1.2) is seen to be very special as the closed string state has divergent norm [119], and the background admits an additional exactly marginal deformation which is associated with the creation of an actual brane in real time.

An outline of the chapter is as follows. In section 2 we spell out the basic prescription for how to deal with the array of D-branes in imaginary time. We consider a more general case in which $X^0 = ia(n+\frac{1}{2})$, where a is an arbitrary parameter, and find a general formula for disk amplitudes associated with such an array. In section 3 we analyze in detail disk amplitudes for scattering of m external closed strings from the array of D-branes in imaginary time. By an exact computation, we show that they are *equivalent* to *sphere* amplitudes with the same m closed strings insertions plus the insertion of an extra closed string state $|W\rangle$. The details of this closed string state, in particular its space-time interpretation, are studied in section 4. The energy of the state is finite and of order $O(g_s^0) = O(1)$ for any $a > 2\pi$. The case $a = 2\pi$, corresponding to $\lambda = \frac{1}{2}$ in the BCFT (5.1.1), is seen to be special as the normalization and energy of the state diverge [119]. We suggest a heuristic mechanism to cutoff this divergence, namely we point out that the gravitational back-reaction makes the effective distance $a_{eff} = 2\pi + \gamma\, g_s$, with $\gamma > 0$, leading to a total energy of order $1/g_s$.

In section 5 it is shown that although the imaginary array of branes does not have propagating open string degrees of freedom, open strings still play an important role. There still exists a discrete set of on-shell open string vertex operators corresponding to exactly

marginal deformations, for example deformations that move the branes around in imaginary time. These open string moduli are re-interpreted as closed string deformations, according to a precise dictionary. In section 6 we show that, subject to certain reality conditions, one can distribute D-branes quite freely in the complex X^0 plane. The reduction of disk amplitudes to sphere amplitudes still holds in this general case. We briefly comment on extensions to the superstring. In section 7 we briefly discuss some ideas about the open string field theory associated with D-branes in imaginary time and speculate that a version of vacuum string field theory may be obtained in the limit $a \to \infty$.

Section 8 is devoted to the case $a = 2\pi$. In this case there is an additional exactly marginal open string deformation (which we may label as '$\cosh(X^0)$') which is *not* dual to a purely closed deformation, as it introduces instead an actual D-brane in real time. We give a treatment of (5.1.1) for all $\lambda \leq \frac{1}{2}$ by representing the boundary state as an infinite array of some specific *smeared* sources, and then performing the Wick rotation. We find that for $\lambda < \frac{1}{2}$ a time-delay of order τ is introduced between the incoming and the outgoing parts of the closed string wave, while for $|X^0| < \tau$ there is an actual source for the closed string fields.

Finally in section 9 we describe a curious application of our set-up. We consider an array of branes in imaginary time, and tune various parameters in such a way that the closed string state $|W\rangle$ becomes simply a *classical*, spherically symmetric dilaton wave with barely enough energy to form a black hole. Fascinating critical behavior was discovered by Choptuik [132] in such a system. We observe that in the corresponding Euclidean theory this critical point corresponds to a phase transition reminiscent of the Gregory-Laflamme [133] phase transition. We speculate on a possible realization of this phase transition in large N open string field theory.

5.2 Preliminaries

We wish to give a meaning to the notion of an array of D-branes located at imaginary times $X^0 = i(n + \frac{1}{2})a$. The distance $a = 2\pi$ (in units $\alpha' = 1$) corresponds to the $\lambda = \frac{1}{2}$ case

of the BCFT (5.1.1), but it is interesting and not more difficult to keep a arbitrary. In this section we define our basic prescription to compute disk amplitudes of external closed strings in the background of this 'imaginary array'. We first give a naive argument why all such scattering amplitudes vanish. Then we illustrate, via a simple example, a natural analytic continuation prescription that actually yields non-zero answers. Finally we derive a simple general formula that expresses the scattering amplitude S in the background of the imaginary array in terms of the scattering amplitude $\widetilde{A}$ for a single D-brane in real time.

5.2.1 Naive argument

Let us denote the scattering amplitude of some closed strings off a single D-brane located at $X = 0$ by $\widetilde{A}$. Here X is a spatial coordinate. To find the scattering amplitude S for an array of D-branes located at imaginary time we could proceed in two steps:

(i) Find the scattering amplitude $\widetilde{S}$ for an array of D-branes located at the real positions $X = (n + \frac{1}{2})a$, $n \in \mathbf{Z}$. This is given by

$$\widetilde{S}(P, \dots) = \sum_{n=-\infty}^{\infty} \widetilde{A}(P, \dots) e^{i\left(n+\frac{1}{2}\right)aP} = \widetilde{A}(P, \dots) \sum_{n=-\infty}^{\infty} (-1)^n \, 2\pi\delta(Pa - 2\pi n), \qquad (5.2.1)$$

where P is the total momentum in the X direction and the dots denote other variables that the amplitude may depend on. This is a precise equality in the sense of distributions. Simply put, the momentum has to be quantized due to the periodicity in X.

(ii) Apply (inverse) Wick rotation

$$X \to -iX^0, \quad P \to iE, \qquad (5.2.2)$$

where now X^0 and E are real. This has the effect of turning the spatial coordinate X into a temporal coordinate X^0 and of rotating the array of D-branes from the real axis to the imaginary axis, $X^0 = i(n + \frac{1}{2})a$. So it takes us exactly to the set-up that we wish to study. Wick rotating (5.2.1) we get the formal expression

$$S(E, \dots) \equiv \widetilde{S}(iE, \dots) = \widetilde{A}(iE, \dots) \sum_{n=-\infty}^{\infty} (-1)^n \, 2\pi\delta(iEa - n). \qquad (5.2.3)$$

Naively this implies that $S(E,\dots)$ is identically zero since for any real E the delta functions vanish. However one has to be more careful, as $\widetilde{A}(iE,\dots)$ may blow up for some real values of E yielding a non-zero $S(E)$. Clearly the discussion so far has been quite formal, for example the summation (5.2.1) does not commute with the Wick rotation (5.2.2) in the sense that if we first Wick rotate and then sum over the array, the sum does not converge for any real E. We need to specify an unambiguous prescription for the analytic continuation (5.2.2). Let us illustrate how a natural prescription comes about in a simple example.

5.2.2 Example

The example we wish to study is

$$\widetilde{A}(P,\dots) = \frac{1}{P^2+c^2}, \tag{5.2.4}$$

where c is a real number (we take for definiteness $c>0$) that can depend on the other variables but not on P. This is the one-dimensional Euclidean propagator. In position space,

$$\widetilde{G}(X) = \int dP\, \widetilde{A}(P)\, e^{iPX} = \frac{\pi}{c} e^{-c|X|}\,, \tag{5.2.5}$$

which obeys $\left(\frac{d^2}{dX^2} - c^2\right)\widetilde{G}(X) = -\delta(X)$. All the amplitudes we study in this chapter can be expanded in terms of (5.2.4). Hence this example is of special importance.

The advantage of working in position space is that now we can simply sum over all the contributions of the array of D-branes explicitly:

$$\widetilde{G}_{array}(X) = \frac{\pi}{c}\sum_{n=-\infty}^{\infty} e^{-c|a(n+\frac{1}{2})+X|}\ . \tag{5.2.6}$$

This is a periodic function with period a (see Fig.1), given in a neighborhood of $X=0$ by

$$\widetilde{G}_{array}(X) = \frac{\pi\cosh(cX)}{c\sinh(\frac{ca}{2})}\,, \quad |X| \le \frac{a}{2}\,. \tag{5.2.7}$$

Now we wish to Wick rotate. Of course, $\widetilde{G}_{array}(X)$ is *not* an analytic function, precisely because of the δ-function sources located at $X=(n+\frac{1}{2})a$. So we need to specify what we

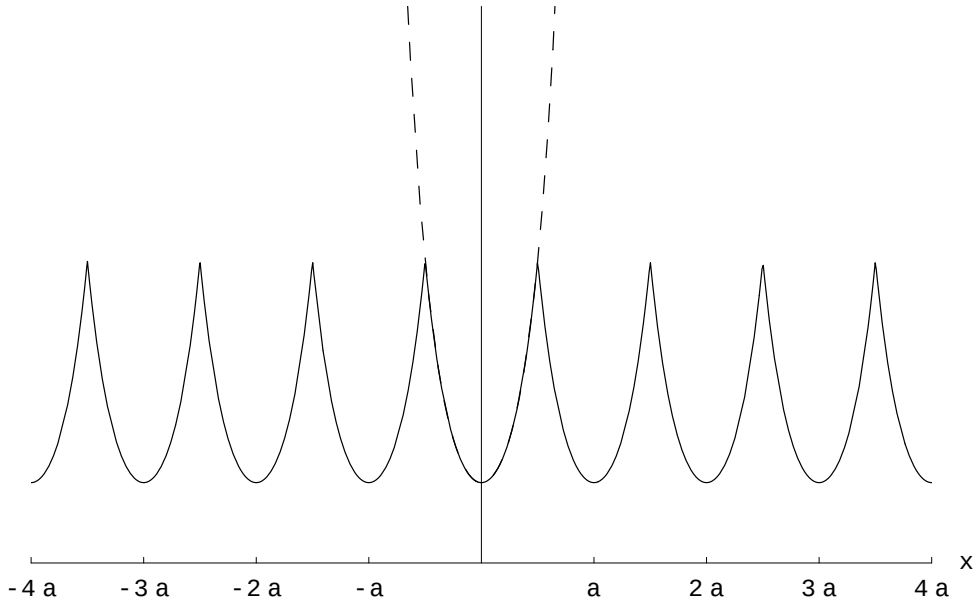

Figure 5.1: A graph of $\widetilde{G}_{array}(X)$, which has the interpretation of the field produced by an infinite array of δ-function sources ('D-branes') located at $X = a(n + \frac{1}{2})$. The dashed line represents the analytic continuation to $|X| > \frac{a}{2}$ of the branch around the origin.

exactly mean by the analytic continuation $X \to -iX^0$. A natural prescription is to focus on the branch around the origin to find

$$G_{array}(X^0) = \frac{\pi \cos(cX^0)}{c \sinh(\frac{ca}{2})} \,. \tag{5.2.8}$$

Fourier transforming (5.2.8) back to momentum space we find

$$S(E, \dots) = \frac{\pi}{2c \, \sinh(\frac{ca}{2})} \, (\delta(E - c) + \delta(E + c)). \tag{5.2.9}$$

As anticipated by the heuristic discussion in the previous subsection, while $\tilde{A}(P, \dots)$ is non-zero for any real P, we find that $S(E, \dots)$ has support only for those values of E corresponding to singularities of $\tilde{A}(P, \dots)$, namely $E = -iP = \pm c$. As we shall see in the context of string theory this will have the interpretation of a change in the dimension of the moduli space.

5.2.3 General prescription

In principle, all amplitudes considered in the chapter could be expanded in terms of the example studied above. It would be nice however to have a general formula that gives $S(E,...)$ in terms of $\widetilde{A}(P,\dots)$. To this end consider, for generic $\widetilde{A}(P,\dots)$,

$$\widetilde{G}_{array}(X) = \int_{-\infty}^{\infty} dP\, e^{iP\,X} \sum_{n=-\infty}^{\infty} (-1)^n\, 2\pi\delta(aP - 2\pi n)\widetilde{A}(P,\dots). \tag{5.2.10}$$

In all cases that we study in the present chapter $\widetilde{A}(P,\dots)$ is an analytic function with poles or cuts only along the *imaginary* P axis. Moreover $\widetilde{A}(P,\dots)$ goes to zero for $|P| \to 0$ sufficiently fast to validate to following argument.

With the help of the residues theorem we can write

$$\widetilde{G}_{array}(X) = \frac{1}{2i} \oint_{\mathcal{C}} dP\, e^{iP\,X} \frac{\widetilde{A}(P,\dots)}{\sin(\frac{aP}{2})}\,, \tag{5.2.11}$$

where the contour $\mathcal{C}$ is depicted in Fig.2. By our analyticity assumptions on $\widetilde{A}(P,\dots)$, the curve $\mathcal{C}$ can be deformed to $\tilde{\mathcal{C}}$ without crossing any singularities (see Fig.2) and without picking up any contributions from the two semi-circles at infinity (that are not shown in the figure). So we conclude, after Fourier transforming back to momentum space, that

$$S(E) = F(E)\,\mathrm{Disc}_E[\widetilde{A}(iE)] \tag{5.2.12}$$

where

$$F(E) = \frac{1}{2\sinh\left(\frac{aE}{2}\right)}\,. \tag{5.2.13}$$

Here by Disc_E we mean the discontinuity with respect to E, namely

$$\mathrm{Disc}_E[f(E)] = \frac{f(E+i\epsilon) - f(E-i\epsilon)}{i}\,, \tag{5.2.14}$$

so for example $\mathrm{Disc}_E(1/E) = -2\pi\delta(E)$. Let us check our master formula (5.2.12, 5.2.13) in the example studied in the previous subsection. From (5.2.4), $\widetilde{A}(iE) = 1/(-E^2 + c^2)$; applying (5.2.12, 5.2.13) we immediately reproduce the result (5.2.9).

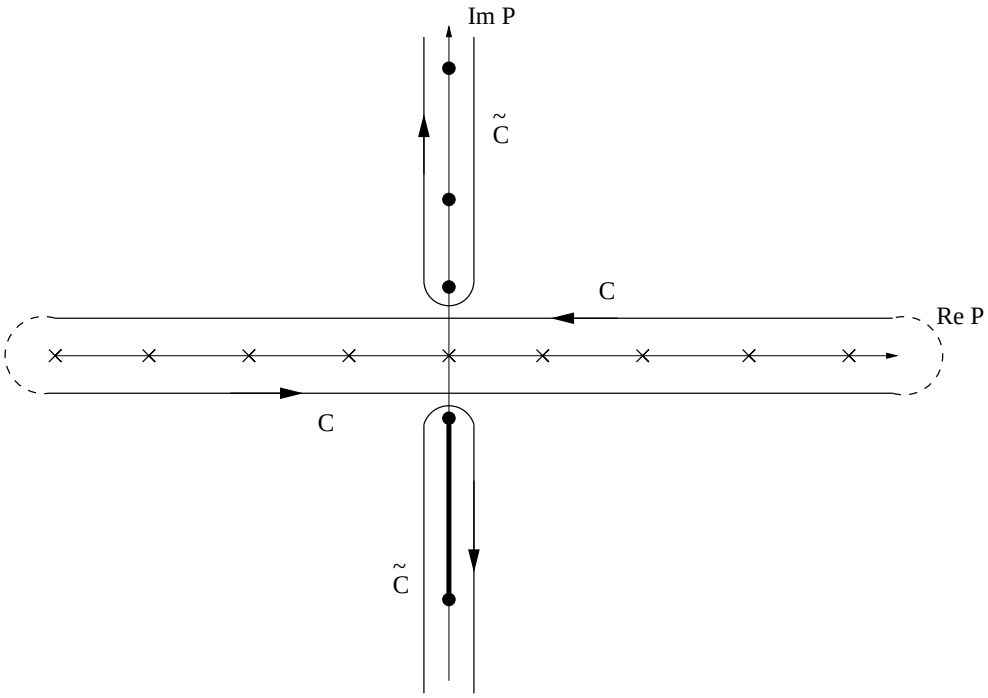

Figure 5.2: Integration contours in the complex P plane. The zeros of $\sin(aP/2)$ are denoted by the symbols 'x' along the real P axis. The black dots represent possible poles of $\widetilde{A}$ and the thick line represents a possible cut. We assume that the only singularities of $\widetilde{A}$ are on the imaginary P axis.

5.3 Disk amplitudes

To gain some insight into the meaning of the D-brane array at imaginary times (5.1.2), we now turn to a detailed analysis of disk scattering amplitudes of external closed strings. We start by considering the simplest possible case, namely the amplitude of two closed string tachyons. We first study this concrete example using standard methods, and then describe a more abstract point of view, that can be generalized easily to m-point functions involving arbitrary on-shell closed strings. A clear physical interpretation will emerge.

5.3.1 Tachyon two-point amplitude

The simplest non-trivial case that we consider is the disk amplitude with the insertion of two closed string tachyons. This example, which we are going to work out in full detail, contains already much of the essential physics.

To apply the prescription derived in the previous section, we need to evaluate the disk two-point function $\widetilde{A}(p_1, p_2)$ for a standard D-brane. We consider a D(p-1) brane with Dirichlet boundary conditions for $\widetilde{X}^M$, $M = 0, \cdots, 25-p$ and Neumann boundary conditions for $\widetilde{X}^m$, $m = 26-p, \cdots, 25$. We are using a notation that will be natural for the theory *after* the Wick rotation: $\widetilde{X}^0$ is a spatial coordinate that will become timelike after Wick rotation. In order to have a standard D-brane with Neumann conditions in time, we take one of the $\widetilde{X}^m$ to be timelike. So the Wick rotation is actually a double Wick rotation: It transforms $\widetilde{X}^0$ from spacelike to timelike and one of the parallel directions $\widetilde{X}^m$ from timelike to spacelike[1] . In practice, the amplitude $\widetilde{A}(p_1, p_2)$ will be written in terms of kinematic invariants, so these distinctions are of no much consequence.

It is convenient to break up the momenta into parallel and perpendicular directions,

$$p^\mu = (p_\perp^M, p_\parallel^m)\,, \tag{5.3.1}$$

and define the kinematic invariants

$$\begin{aligned} s &= p_{1\parallel}^2 = p_{2\parallel}^2 \\ t &= (p_1 + p_2)^2 = (p_{1\perp} + p_{2\perp})^2\,. \end{aligned} \tag{5.3.2}$$

In our conventions[2] $\alpha' = 1$, so that the on-shell condition for closed string tachyons is $p^2 = 4$.

The two-point disk amplitude has one modulus (four real coordinates minus three conformal Killing vectors). We work with a slightly unconventional parametrization of this moduli space that will be easy to generalize later when we turn to higher-point functions. Namely we shall fix the positions of the two vertex operators and integrate over the radius of the disk. We represent the disk as the complex domain $\mathcal{H}_\rho = \{z \in \mathbf{C}, |z| \geq \rho\}$, that is we cut out a hole of radius ρ from the complex plane. The measure for the modulus ρ is

$$(b_0 + \bar{b}_0)\frac{d\rho}{\rho}\,. \tag{5.3.3}$$

[1]The case $p = 0$ is special, as we must choose one of the transverse directions $\widetilde{X}^M$ to be timelike.

[2]Moreover in writing a string amplitude $\widetilde{A}(p_1, \ldots p_m)$, we treat all momenta as incoming. Finally our convention for the Minkowski metric is 'mostly plus'.

Using the standard doubling trick, a closed string vertex operator $V(p,z,\bar{z})$ is replaced by the two chiral insertions $V_L(p,z)$ and $V_L(p',\rho^2/\bar{z})$, where $p'=(-p_\perp,p_\parallel)$. For closed string tachyons, $V(p,z,\bar{z})=c(z)\bar{c}(\bar{z})\exp(ipX(z,\bar{z}))$ and $V_L(p,z)=c(z)\exp(ipX_L(z))$. Fixing the tachyon vertex operators at $z=1$ and $z=\infty$, we have

$$\widetilde{A}(p_1,p_2)=\frac{1}{2\pi i}\int_0^1\frac{d\rho}{\rho}\oint_{|z|=\rho}dz\,\langle\, V_L(p_1;\infty)V_L(p_2;1)\,b(z)\,V_L(p_2';\rho^2)V_L(p_1';0)\,\rangle\,, \qquad (5.3.4)$$

where the symbol $\langle\,,\rangle$ denotes a CFT correlator on the plane. A short calculation gives

$$\widetilde{A}(p_1,p_2)=\int_0^1 d\rho\,\rho^{t/2-3}(1-\rho^2)^{s-2}\;=\frac{\Gamma(t/4-1)\Gamma(s-1)}{2\,\Gamma(t/4+s-2)}\,. \qquad (5.3.5)$$

This is of course a standard result, with a familiar interpretation [134, 135]. The scattering amplitude of a closed string off a D-brane shows the usual 'dual' structure with poles both in the open and in the closed string channel. In the open string channel, the poles are located at $s=1,0,-1,\ldots$ and arise from expanding around $\rho=1$ where the vertex operators approach the boundary. In the closed string channel, we see poles at $t=4,0,-4,\ldots,$ arising from expanding around $\rho=0$ where the boundary shrinks to zero size.

We are now in a position to apply the prescription (5.2.12)[3] . The discontinuity with respect to $E=E_1+E_2=-i(p_1^0+p_2^0)$ comes from the poles in the variable t, and so we find that

$$S(p_1,p_2)=\frac{1}{2\sinh\left(\frac{a|E|}{2}\right)}\;\sum_{k=0}^{\infty}f_k(s)\,\delta(t/4-1+k)\,, \qquad (5.3.6)$$

where

$$f_k(s)=\frac{(-1)^k\Gamma(s-1)}{2\,k!\Gamma(s-k-1)}=\frac{(2-s)(3-s)\cdots(1+k-s)}{2\,k!}\,. \qquad (5.3.7)$$

Several remarks are in order. First, all the contributions to S come from the $\rho\to 0$ region of the moduli space. The sharpest way to see this is to introduce a cut-off $\epsilon\le\rho\le 1$. Then the amplitude $\widetilde{A}$ becomes analytic in t since the poles in the closed string channel disappear. Applying (5.2.12) yields $S=0$ for any ϵ. This vindicates the original intuition that the boundary state for the array of imaginary D-branes should correspond to a 'hole

[3]Notice that $\widetilde{A}(p_1,p_2)$ obeys our analyticity assumptions, indeed it is an analytic function of the total momentum P^0 with singularities (poles) only for imaginary P^0, and behaves as $1/|P^0|^{2s}$ for large $|P^0|$.

of zero size' (an extra puncture) in the worldsheet. This intuition will be made very precise below. Second, S has no poles in s, the open string channel! The external closed strings do not couple to any on-shell open string degrees of freedom. Since there are no D-brane sources in real time, this is as expected. We are describing a *purely closed* string background.

More precisely, (5.3.6) describes a *sphere* amplitude with the two tachyons insertions and an additional on-shell closed string state that involves excitation at all levels of the tower of massive modes. Indeed, the prefactor $f_k(s)$ is a polynomial of degree $2k$ in $p_\parallel$, consistently with the fact that a closed string mode at level k has up to $2k$ Lorentz indices.

5.3.2 Boundary state computation

In order to secure this result, and to prepare for the generalization to higher-point amplitudes, we now repeat the computation in a more abstract language. We still write the amplitude in the domain $\mathcal{H}_\rho$, but instead of using the doubling trick, we represent the effect of the boundary at $|z| = \rho$ by the insertion of a boundary state $|\widetilde{\mathcal{B}}^{p-1}\rangle_{|z|=\rho}$. This is the full boundary state defining the D(p-1) brane located at $\widetilde{X}^M = 0$.

A boundary state is a ghost number three state in the closed string Hilbert space, obeying among other things the conditions

$$(Q_B + \bar{Q}_B)|\widetilde{\mathcal{B}}^{p-1}\rangle = 0\,, \quad (b_0 - \bar{b}_0)|\widetilde{\mathcal{B}}^{p-1}\rangle = 0\,. \tag{5.3.8}$$

In radial quantization, a state at radius ρ can be obtained from a state at radius $\rho = 1$ by propagation in the closed string channel,

$$|\widetilde{\mathcal{B}}^{p-1}\rangle_{|z|=\rho} = \rho^{L_0+\bar{L}_0}\,|\widetilde{\mathcal{B}}^{p-1}\rangle_{|z|=1}\,. \tag{5.3.9}$$

We can then write

$$\widetilde{A}(p_1,p_2) = \int_0^1 \frac{d\rho}{\rho}\,\langle|\, V(p_1;\infty,\infty)V(p_2;1,1)\,(b_0+\bar{b}_0)\,\rho^{L_0+\bar{L}_0}\,|\widetilde{\mathcal{B}}^{p-1}\rangle_{|z|=1}\,. \tag{5.3.10}$$

To proceed, we insert a complete set of states $\{|k,i\rangle\}$,

$$\widetilde{A}(p_1,p_2) = \int dk\,\sum_i \int_0^1 \frac{d\rho}{\rho}\,\langle|\, V(p_1;\infty,\infty)V(p_2;1,1)\,|k,i\rangle\,\rho^{(\frac{k^2}{2}+2l_i)}\,\langle k,i|(b_0+\bar{b}_0)|\widetilde{\mathcal{B}}^{p-1}\rangle_{|z|=1}\,, \tag{5.3.11}$$

where l_i is the level of the state $|k,i\rangle$, and we integrate over the modulus ρ to get

$$\widetilde{A}(p_1,p_2) = \int dk \sum_i \langle |\, V(p_1;\infty,\infty) V(p_2;1,1)\,|k,i\rangle\, \frac{1}{\frac{k^2}{2}+2l_i}\, \langle k,i|(b_0+\bar{b}_0)|\widetilde{\mathcal{B}}^{p-1}\rangle_{|z|=1}\,. \tag{5.3.12}$$

This expression exhibits the decomposition of the amplitude into a source term from the boundary state, a closed string propagator, and the 3-point interaction vertex. If we now apply the master formula (5.2.12) we find

$$S(p_1,p_2) = \langle |\, V(p_1;\infty,\infty)\, V(p_2;1,1)\,|W\rangle\,, \tag{5.3.13}$$

where[4]

$$\begin{aligned} |W\rangle &\equiv \int dk \sum_i |k,i\rangle\, \frac{\delta(k^2/2+2l(i))}{2\sinh\left(\frac{a|E|}{2}\right)}\, \langle k,i|\,(b_0+\bar{b}_0)|\mathcal{B}^{p-1}\rangle_{|z|=1} \\ &= \frac{\delta(L_0+\bar{L}_0)}{2\sinh\left(\frac{a|E|}{2}\right)}\,(b_0+\bar{b}_0)|\mathcal{B}^{p-1}\rangle_{|z|=1}\,. \end{aligned} \tag{5.3.14}$$

We see that the interaction of the two tachyons with the imaginary array is captured by a ghost number two closed string state $|W\rangle$. Using (5.3.8) and $\{b_0, Q_B\} = L_0$, we have

$$(Q_B+\bar{Q}_B)|W\rangle = 0\,, \quad (b_0-\bar{b}_0)|W\rangle\,. \tag{5.3.15}$$

These are precisely the physical-state conditions for closed strings. Moreover, we have the freedom to add to $|W\rangle$ BRST trivial states, that would decouple in the computation of the correlator (5.3.13). We recognize $|W\rangle$ as an element of the closed string cohomology. A more detailed discussion of this state and of its space-time interpretation will be carried out in section 4.

Finally we can trade the state $|W\rangle$ with a vertex operator insertion at the origin, and re-write the amplitude (5.3.13) as a CFT correlator in the plane,

$$S(p_1,p_2) = \langle\, V(p_1;\infty,\infty)\, V(p_2;1,1)\, \mathcal{W}(0,0)\,\rangle\,. \tag{5.3.16}$$

[4]Notice that in the formula below we drop the 'tilde' on the symbol for the boundary state: $|\mathcal{B}^{p-1}\rangle$ denotes the boundary state *after* double Wick rotation.

This is manifestly the scattering amplitude for three closed strings on the *sphere*! Having explicitly performed the integral over ρ there are no remaining moduli, as it should be for a *sphere* three-point function.

Clearly this conclusion does not depend on the vertex operators $V(p_i, z, \bar{z})$ being closed string tachyons. The analysis immediately generalizes to arbitrary physical closed string vertex operators: in the background of the imaginary array, a two-point function on the disk is *equal* to a three-point function on the sphere, with the on-shell vertex operator $\mathcal{W}$ as the extra insertion.

5.3.3 Higher-point disk amplitudes

The computation of higher-point amplitudes is now a straightforward generalization. We still represent the disk as the complex domain $\mathcal{H}_\rho$ and describe the moduli space of m closed strings on the disk by fixing the positions of two vertex operators, say V_1 at $z = \infty$ and V_2 at $z = 1$, and varying the positions of the other $m - 2$ insertions and the radius ρ of the hole. More precisely, we vary the $m - 2$ coordinates over the full complex plane, $\{z_i \in \mathbf{C}, i = 3, \dots m\}$, and for a given choice of the $\{z_i\}$ we vary the radius ρ between 0 and the distance of the closest insertion, $0 \le \rho \le \rho_0 = \min[|z_i|, i = 1, \dots m]$ (see Fig.3). This way we cover moduli space exactly once, as can be easily checked for example by mapping the above configuration to the the interior of the unit disk. We then have

$$\widetilde{A}(p_1, \dots, p_n) = \int d^2 z_3 \dots d^2 z_m \int_0^{\rho_0} \frac{d\rho}{\rho} \tag{5.3.17}$$
$$\langle | \, \mathcal{R}\{ \, V_1(p_1; \infty, \infty) V_2(p_2; 1, 1) \dots V_m(p_m; z_m, \bar{z}_m) \} \, (b_0 + \bar{b}_0) \, \rho^{L_0 + \bar{L}_0} \, |\widetilde{\mathcal{B}}^{p-1}\rangle_{|z|=1} \, ,$$

where $\mathcal{R}\{ \, . \}$ denotes radial ordering. Inserting as before an intermediate complete set of states, and performing the ρ integral, we find

$$\widetilde{A}(p_1, \dots, p_n) = \int dk \sum_i \int d^2 z_3 \dots d^2 z_m \tag{5.3.18}$$
$$\langle | \, \mathcal{R}\{V_1(p_1; \infty, \infty) V_2(p_2; 1, 1) \dots V_m(p_m; z_m, \bar{z}_m)\} |k, i\rangle \frac{\rho_0^{\frac{k^2}{2} + 2l_i}}{\frac{k^2}{2} + 2l_i} \langle k, i | \, (b_0 + \bar{b}_0) \, |\widetilde{\mathcal{B}}^{p-1}\rangle_{|z|=1} \, .$$

Now we extract the discontinuity with respect to the energy E. Clearly we get contributions from the poles in the propagators $\sim \frac{1}{k^2/2+2l_i}$. A priori, the integrals over the coordinates z_i may generate additional singularities. However it is not difficult to show that extra singularities can only arise when a (proper) subset of the vertex operators have an on-shell total momentum. We can define the amplitude by analytic continuation away from these singular points, and then disregard these singularities. This is reminiscent of the celebrated canceled propagator argument [5]. We can then write[5] (see Fig.3)

$$S(p_1, \cdots, p_m) = \int d^2z_3 \dots d^2z_m \, \langle \, V_1(p_1; \infty, \infty) V_2(p_2; 1, 1) \dots V_m(p_m; z_m, \bar{z}_m) \} \mathcal{W}(0, 0) \, \rangle \ . \tag{5.3.19}$$

The coordinates z_i, $i = 3, \dots m$, are integrated over the full complex plane, so this is the string theory amplitude for $m+1$ insertions on the sphere. We can check that the counting of moduli is consistent with this result. We started with $2m-3$ moduli for a disk with m closed punctures and performed an explicit integration over ρ. This gives $2m - 4 = 2(m + 1) - 6$, which is the number of moduli for a sphere with $m + 1$ punctures.

5.3.4 Interpretation

Let us summarize what we have learned. *Disk amplitudes for* m *external closed strings off the D-brane array at the imaginary times* $X^0 = i(n + 1/2)a$ *are completely equivalent to* m+1*-point amplitudes on the* sphere*, with the extra closed string insertion*

$$g_s \int d^2z \, \mathcal{W}(z, \bar{z}) \, ,$$

where $\mathcal{W}$ *is given by* (5.3.14). The explicit factor of g_s, which was omitted in the previous formulae, comes from the relative normalization of disk amplitudes to standard sphere amplitudes. Unlike the case of an ordinary brane, we are finding that for the imaginary array disk amplitudes give a *purely closed* correction (of order g_s) to the background. There are no D-brane sources in real time, only closed strings satisfying the *homogeneous* wave equation.

[5]Notice that the dependence on ρ_0 drops because of the delta function $\delta(L_0 + \bar{L}_0)$. In other terms, the ρ integral localizes to $\rho \to 0$ and the upper limit of integration ρ_0 is immaterial.

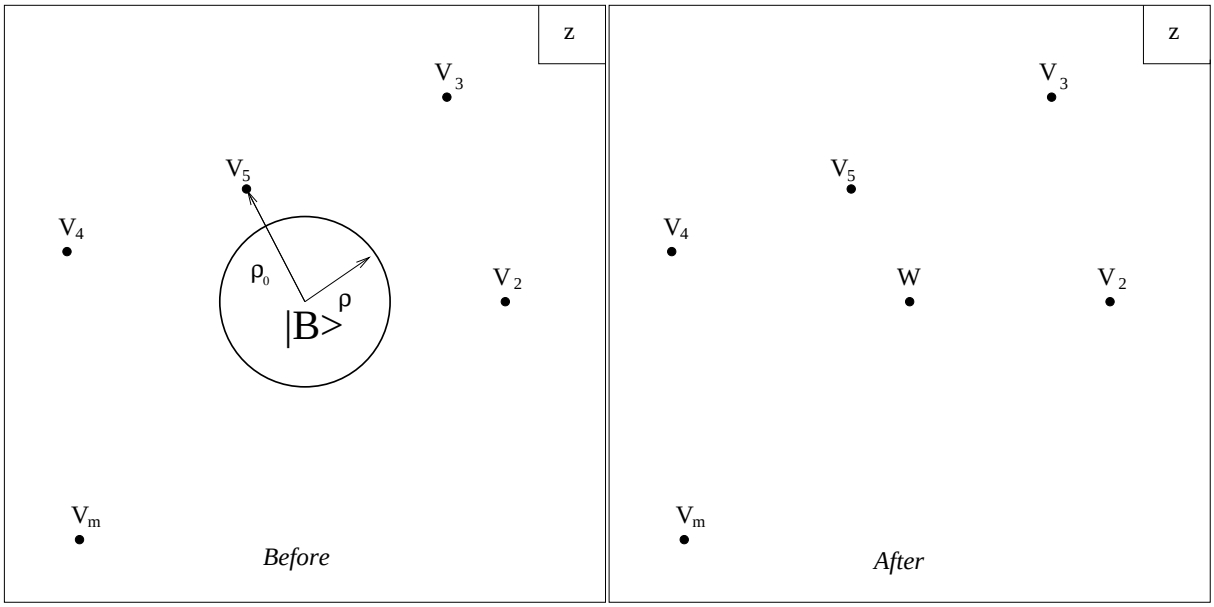

Figure 5.3: Before the double Wick rotation we have a standard disk amplitude. The disk can be viewed as the region $\mathcal{H}_\rho$, which is the complex plane with a hole of radius ρ. There are contributions to the scattering amplitude from all values of $\rho \leq \rho_0$, where ρ_0 is the distance of the closest puncture. After the double Wick rotation the only contribution is coming from $\rho = 0$. The hole shrinks to a point leaving behind an extra puncture $\mathcal{W}$ inserted at the origin.

The absence of sources in real time can also be deduced from the fact that all *one*-point functions on the disk are trivially zero in our prescription. This is consistent with the computations in [110], where the stress tensor (related to the graviton one-point function) was found to vanish in the BCFT (5.1.1) for $\lambda = \frac{1}{2}$. There are two equivalent ways to see this in our language. The one-point function on the disk is a smooth function of the total energy E, so there is no discontinuity in E. Alternatively, the discussion above implies that a disk one-point function is equal to a sphere *two*-point function with the extra insertion of $\mathcal{W}$; but sphere two-point functions are zero because of the infinite volume of the unfixed moduli.

Since disk amplitudes provide the first order correction to the background, it is very natural to expect that amplitudes with multiple boundaries give the necessary higher-order corrections. A genus zero amplitude with m external closed strings and b boundaries, is expected to become after Wick rotation a sphere amplitude with $m + b$ punctures, with b insertions of $g_s \int d^2z \mathcal{W}$. Notice that since the boundaries are indistinguishable, the sum over boundaries *exponentiates* to the insertion of $\exp(\int d^2z\, g_s \mathcal{W})$, which has the interpretation of a coherent state of closed strings. One may investigate this issue rigorously by representing the effect of the boundaries using boundary states, and decomposing the moduli space of a surface with b boundaries and m closed string punctures in terms of closed string vertices and propagators [80]. The moduli space integration should localize to the region where each boundary shrinks to an extra puncture. A priori, one may also expect that regions of moduli space where zero-size boundaries collide could provide additional contributions. For example one may expect that an annulus amplitude would reduce to a sphere amplitude with two insertions of $g_s\mathcal{W}$, *plus* a sphere amplitude with a single insertion of a new operator $g_s^2\mathcal{W}_1$ coming from the shrinking of both boundaries to the same point. This issue should be investigated further.

5.4 The closed string state

In this section we study the physical properties of $|W\rangle$ in more detail and make contact with [118] and [119]. Our starting point is the boundary state $|\mathcal{B}^{p-1}\rangle$, which is obtained from double Wick rotation of $|\widetilde{\mathcal{B}}^{p-1}\rangle$. So $|\mathcal{B}^{p-1}\rangle$ is associated with a D(p-1) brane located at $X^M = 0$, in a space with metric (η_{MN}, δ_{mn}). One has

$$|\mathcal{B}^{p-1}\rangle = \mathcal{N}\delta(X^M)\exp\left(-\sum_{n=1}^{\infty} a_n^{\mu\dagger} S_{\mu\nu} \tilde{a}_n^{\nu\dagger}\right)|0; k=0\rangle\,. \tag{5.4.1}$$

$\mathcal{N}$ is a normalization constant that can be found for example in [136], and

$$S_{MN} = -\eta_{MN}, \;\; S_{mn} = \delta_{mn}. \tag{5.4.2}$$

With the help of (5.3.14) we can expand $|W\rangle$ in terms of closed string physical states,

$$|W\rangle = \mathcal{N}\, c_1\bar{c}_1|0\rangle_{gh} \otimes \int \frac{dk_\perp^{25-p}}{(2\pi)^{25-p}} \frac{1}{2|E|} \frac{1}{2\sinh\left(\frac{a|E|}{2}\right)} \left(|k^2=4\rangle - S_{\mu\nu}\,\partial X^\mu \bar{\partial} X^\nu |k^2=0\rangle + \cdots\right),$$

where the dots indicate higher massive modes. The first term is the closed string tachyon, which is an artifact of the bosonic string and is standard practice to ignore. Below we first discuss the massless modes and then consider the massive modes.

5.4.1 Massless sector

In order to read off the dilaton and gravity wave profile from the second term we have to undo their mixing. The unmixed dilaton and graviton (in the Einstein frame) take the form (see *e.g.* [136])

$$h_{\mu\nu} = S_{\mu\nu} - \frac{S\cdot\epsilon^{(\phi)}}{\eta\cdot\epsilon^{(\phi)}}\,\eta_{\mu\nu}, \quad \phi = S\cdot\epsilon^{(\phi)}, \tag{5.4.3}$$

where

$$\epsilon^{(\phi)} = \frac{1}{2}(\eta_{\mu\nu} - k_\mu l_\nu - k_\nu l_\mu)\,, \quad k\cdot l = 1, \quad l^2 = 0. \tag{5.4.4}$$

Let us first look at the case $p = 0$ (an array of imaginary D(-1) branes). One finds that the Einstein metric is completely flat as all the expectation values of $h_{\mu\nu}$ vanish. This means that the part of the leading term in the ADM mass, which scales like $1/g_s$, vanishes (see

also [119])[6] . The dilaton, on the other hand, does not vanish. So for $p = 0$, the massless fields in $|W\rangle$ consist of a spherically symmetric dilaton wave $\phi(r, X^0)$ in 25+1 dimensions, whose energy is of order $O(g_s^0) = O(1)$.

For $p > 0$ the 26-dimensional metric in the Einstein frame is non-trivial. However the fields profiles are translationally invariant in the p longitudinal directions X^m, and to read off the ADM mass we are instructed to dimensionally reduce to the $26 - p$ transverse dimensions. One finds that in the $26 - p$-dimensional Einstein frame the metric *is* zero, and we have again only a spherically-symmetric dilaton wave. We conclude that to order $1/g_s$ the mass vanishes for general p.

The space-time profile of this dilaton wave is quite interesting [118].[7] For fixed radius $r = \sqrt{X^M X^M}$, the field decays exponentially fast as $X^0 \to \pm\infty$. For fixed X^0, the field decays as $1/r^{23-p}$ as $r \to \infty$, just like the fields produced by an ordinary Dp-brane, but with a different numerical coefficient. (These two asymptotic behaviors match in a region of thickness of the order of a around the light-cone $X^0 = \pm r$). To be precise, up to an overall numerical constant that will not be relevant for the discussion below, the leading asymptotic behavior as $r \to \infty$ of the various fields is, in the 26-dimensional Einstein frame,

$$\begin{aligned} h_{00} &\to \frac{(1+K)(d-3)-2p}{d-2}\,\frac{1}{r^{23-p}}, \\ h_{mn} &\to \frac{\delta_{mn}}{2}\left(\frac{2d-2p-5-K}{d-2}\right)\frac{1}{r^{23-p}}, \\ h_{MN} &\to \frac{\delta_{MN}}{2}\left(\frac{2p+1+K}{d-2}\right)\frac{1}{r^{23-p}}, \\ \phi &\to \frac{d-2p-3-K}{4}\,\frac{1}{r^{23-p}}\,. \end{aligned} \tag{5.4.5}$$

Here $d = 26$ and the parameter K is set to 1 for the standard Dp-brane and is set to -1 for the background $|W\rangle$.

An exercise one can now do is to compute the force acting on a probe D0-brane in this dilaton wave background [118]. One has to be a bit careful here with the exact meaning

[6] This is consistent with Sen's observation [110] that the stress tensor vanishes for the $\lambda = \frac{1}{2}$ BCFT (5.1.1).

[7] From the discussion in section 6 of [118] it is not obvious that eq.(6.27) in that section describes just a dilaton wave. However, this can be verified with the help of eq. (5.4.3) above.

of the 'force' between the brane and the wave since this is not a static set-up. The 'force' that can be computed using (5.4.5) for $K = -1$ is acting during a finite time interval $-T \leq X^0 \leq T$ at a distance r in the limit $\frac{T}{r} \to 0$. In the Einstein frame in 26 dimensions the DBI action for the D0 brane takes the form

$$\int dX^0 \, e^{-\frac{11}{12}\phi} \sqrt{g_{00}} \, . \tag{5.4.6}$$

From this and (5.4.5) with $p = 0$ we can deduce that the ratio between the force acted upon the D0 by a standard brane and the 'force' acted on it by the dilatonic wave in $|W\rangle$ is

$$\frac{F_{standard}}{F_W} = \frac{\frac{11}{12}\phi(K=1) + \frac{1}{2}h_{00}(K=1)}{\frac{11}{12}\phi(K=-1) + \frac{1}{2}h_{00}(K=-1)} = \frac{12}{11}. \tag{5.4.7}$$

This is in agreement with [118] where this ratio was calculated in a different way.

5.4.2 Massive modes

The massive closed string states in $|W\rangle$ obey the dispersion relation $E^2 = k_\perp^2 + m^2$, with $m^2 = 4(n-1)$. For $n > 1$, their field profile (proportional to $1/\sinh(a|E|/2)$) is strongly peaked at energies $|E| - m \leq 1/a$. This means that for any $a \geq 2\pi$, the states are with good approximation *non-relativistic* already at level $n = 2$, with the approximation improving at higher levels. Their fields at $X^0 = 0$ are Gaussians of the form

$$\delta(k_\parallel) \, \exp(-\frac{ma}{2}) \exp(-\frac{ak_\perp^2}{4m}) \, , \tag{5.4.8}$$

that is, the closed string modes occupy the directions X^m and are localized at $X^M = 0$ ($M \neq 0$) with a width of order $\sqrt{a/m}$ in the transverse directions. The time evolution of these field profiles follows non-relativistic Schrödinger equation, so their width scales as $|X^0|/\sqrt{am}$ for large times. Interestingly, the massive modes behave as non-relativistic matter located at the would-be position of the brane. This conclusion was also reached in [119].

Let us now compute the normalization of $|W\rangle$ and its the space-time energy, following [119][8] . The normalization has the interpretation of (the expectation value of) the total

[8] Equs. (5.4.9) and (5.4.11) below were *not* obtained independently of [119].

number of particles $\bar{n}$ in the background. One has

$$\begin{aligned} \bar{n} = \langle \mathcal{W}|c_0\bar{c}_0|\mathcal{W}\rangle &= \mathcal{N}^2 \sum_{n=0}^{\infty} d_n \int \frac{dk_\perp^{25-p}}{(2\pi)^{25-p}} \frac{1}{2|E|} \frac{1}{4\sinh^2\left(\frac{aE}{2}\right)}\,, \\ \bar{E} &= \mathcal{N}^2 \sum_{n=0}^{\infty} d_n \int \frac{dk_\perp^{25-p}}{(2\pi)^{25-p}} \frac{1}{2|E|} \frac{|E|}{4\sinh^2\left(\frac{aE}{2}\right)}\,, \end{aligned} \tag{5.4.9}$$

where d_n can be computed from the generating function

$$\sum_{n=0}^{\infty} d_n w^n = f(w)^{-24}, \quad f(w) = \prod_{m=1}^{\infty}(1-w^n). \tag{5.4.10}$$

The asymptotic behavior of d_n for large n is [4] $d_n \sim n^{-27/4} e^{4\pi\sqrt{n}}$. It is easy to see that for $a > 2\pi$ the exponential suppression from $1/\sinh^2(\frac{a|E|}{2})$ wins over the exponential growth of states, and both $\bar{n}$ and $\bar{E}$ are perfectly *finite*. On the other hand, in the limit $a \to 2\pi$ we get

$$\bar{E} \sim \sum_{n=0}^{\infty} \frac{e^{-2(a-2\pi)\sqrt{n}}}{n^{p/4}} \sim (a-2\pi)^{p/2-1}\,. \tag{5.4.11}$$

For $a = 2\pi$ the expectation value of the energy diverges for $p = 0, 1, 2$. Naively, for $p > 2$ the energy is finite. However, for any p the expectation values of powers $\langle E^k \rangle$ will eventually diverge for sufficiently high k [119], and hence for $a = 2\pi$ the uncertainty in the energy[9] is infinite for any p.

This divergence has a very natural physical interpretation. As reviewed in the introduction and further discussed in section 8 below, for $a = 2\pi$ the background of imaginary branes admits an *infinitesimal* deformation that introduces a D-brane source in real time, and we should then expect that this background also has an energy of order $1/g_s$. Since we are computing this energy in the limit $g_s \to 0$ in a perturbative expansion $\bar{E} = \sum_{n=0} (g_s)^n E^{(n)}$, it is natural to find that leading term $E^{(0)} = \infty$. At finite g_s this divergence should be regulated in such a way that $\bar{E} \sim 1/g_s$.

Before discussing a heuristic mechanism that supports this expectation, we would like to point out that for $a = 2\pi$ the state $|W\rangle$ has all the features to be *identified* with 'tachyon matter' [110, 111]. Indeed for $a = 2\pi$ the energy is stored in very massive closed strings

[9] A similar behavior is found for $\bar{n}$, which is logarithmically divergent for $p = 0$ and finite for $p > 0$, but with higher moments diverging for any p.

modes that behave like non-relativistic matter strongly localized along the directions X^m. This is the closed string dual of Sen's discussion on 'tachyon matter' in the context of *open* string field theory; for large times $|X^0| \to \infty$ the classical open string solution corresponding to the BCFT (5.1.1) approaches, for all λ, an open string configuration with zero pressure and with all the energy localized along the X^m directions[10] .

It is very tempting to suspect that at finite g_s the distance a is renormalized to an effective value

$$a_{eff} = 2\pi + \varepsilon \quad \text{where} \quad \varepsilon = \gamma\, g_s^b\,, \tag{5.4.12}$$

where both b and γ are positive numbers of order one. This would make the energy finite. Restricting in the following to $p = 0$[11] , we find from (5.4.11)

$$\bar{E} \sim \frac{1}{\varepsilon}. \tag{5.4.13}$$

So to obtain the expected scaling $\sim 1/g_s$ the parameter b has to be equal to one. An argument why this is plausible was given in [119] from the point of view of *open* string field theory. Here we provide an alternative heuristic argument from the *closed* string channel, that justifies why $b = 1$ and also why $\gamma > 0$.

Let us think about this issue from the point of view of the array before Wick rotation. When $g_s = 0$ the distance between the branes is 2π. When g_s is turned on the branes will slightly curve space-time due to their mass so that the distance between them is no longer 2π. Actually since their mass is $\sim 1/g_s$ and the Newton constant scales like g_s^2 the back-reaction is of order g_s and so the proper distance between the branes is indeed as in (5.4.12). γ is positive simply because the metric components in the transverse direction to the brane scale like

$$g_\perp \sim 1 + g_s\, \frac{\tilde{\gamma}}{r^{23-p}}, \tag{5.4.14}$$

with $\tilde{\gamma} > 0$.

[10] More precisely, as shown in [119] and further elaborated in section 8 of this chapter, the limit $X^0 \to \infty$ of (5.1.1) corresponds for all λ (up to a trivial time translation) to the *outgoing* ($X^0 > 0$) part of our state $|W\rangle$, and symmetrically $X^0 \to -\infty$ of (5.1.1) corresponds to the *incoming* ($X^0 < 0$) part of $|W\rangle$.

[11] For $p > 0$ (5.4.11) cannot be trusted as the higher moments of the energy $(\langle E^k\rangle - \langle E\rangle^k)^{1/k}$ have a worse degree of divergence than the mean value $\bar{E} = \langle E\rangle$.

It is interesting to check if this argument generalizes when we put N rather than just one brane at each site. First, the back-reaction of the metric scales like $g_s N$ which means that now $\varepsilon \sim g_s N$. Combining this with (5.4.13) and with the fact that $|W\rangle$ gets multiplied by a factor of N we find for the total energy

$$\bar{E}_N \sim \frac{N^2}{\varepsilon} \sim \frac{N}{g_s}, \tag{5.4.15}$$

which is the correct scaling for the tension of N D-branes.

Clearly this heuristic reasoning is not powerful enough to fix γ in (5.4.12). One obvious reason is that the distance between the branes is of the order of the string scale and hence the gravity approximation should not be trusted. A closely related point is the following. Suppose that we could somehow fix γ and that we found the correct D-brane mass. If γ was just a fixed number then it is easy to see that the *uncertainty* in the D-brane mass would be of the same order as the mass itself, which is of course not the case for D-branes at weak coupling. This seems to suggest that γ should not be viewed as a constant but rather as a fluctuating field.

5.5 On open and closed string moduli

In section 3 we showed that scattering amplitudes off the imaginary array do not have any open string poles. This means that there are no propagating open strings degrees of freedom, consistently with the fact that there are no branes in real time. However there still is a discrete set of on-shell open string vertex operators, which demand an interpretation. In this section we argue that they are dual to deformations of the closed string state $|W\rangle$.

For simplicity let us start by considering the case $p = 0$, the array of D(-1) branes at imaginary times $X^0 = i(n + \frac{1}{2})a$. The open string spectrum should be read off from the theory before double Wick rotation, where we have an array of D(-1) branes at the spatial locations $\widetilde{X}^0 = (n + \frac{1}{2})a$. For generic[12] distance a, the only matter primaries of dimension one are $\widetilde{V}_\mu^{(n)} = \partial \widetilde{X}_\mu^{(n)}$, where μ are space-time indices and $n \in \mathbf{Z}$ labels the position of the

[12]The case $a = 2\pi$ is of course special and will be discussed in section 8.

D(-1) brane. In the double-Wick rotated theory the physical open string states are just the same, up to trivial relabeling. So the most general state in the open string cohomology of the theory of D(-1) branes at imaginary times can be written as

$$|f\rangle = \sum_{\mu=0}^{25} \sum_{n=-\infty}^{\infty} f^{\mu}_{(n)}\, \partial X^{(n)}_{\mu}(0)\, c_1|0\rangle\,. \tag{5.5.1}$$

Clearly these are the exactly marginal open string deformations that correspond to moving the positions of the D(-1) branes.

Next we can consider disk amplitudes $S(p_1 \dots p_m; f)$ for m closed strings scattering off the imaginary array, with one additional insertion of (5.5.1) on the boundary of the disk. Without any open strings puncture, $S(p_1, \dots p_m)$ was shown in section 3 to be a *sphere* amplitude with an extra insertion of the closed string state $|W\rangle$. How does the addition of $|f\rangle$ change this conclusion?

To get some insight, consider first the case $f^{\mu}_{(n)} = f^{\mu}$ for all n. This deformation is simply a Goldstone mode associated with a rigid translation $X_\mu \to X_\mu + f_\mu$ of the whole array. It is clear that in this simple case $S(p_1 \dots p_m; f)$ is obtained from $S(p_1 \dots p_m; f)$ by replacing $|W\rangle$ with its infinitesimal translation, $|W\rangle \to f^{\mu}\partial_{\mu}|W\rangle$. In this special example the open string insertion $|f\rangle$ corresponds to a symmetry of the vacuum broken by the closed string background $|W\rangle$.

In the more general case (5.5.1), it is not difficult to show[13] that $S(p_1 \dots p_m; f)$ will still be a sphere amplitude with $m+1$ punctures, where the extra closed puncture is now $\delta_f \mathcal{W}$, the infinitesimal deformation of $\mathcal{W}$ obtained by displacing the branes according to $|f\rangle$. Generically this deformation will change the total energy of the closed string state. The intuitive picture is that the branes act as sources for the closed string fields. Since these sources are not in real time, the resulting closed string fields are *homogeneous* solutions of the wave equation, and we have a purely closed background. Changing the positions of the branes changes the details of the closed string field profiles. Thus the open string

[13] We cannot directly apply the prescription of section 2. However, the relevant disk amplitude is simple enough that can be evaluated directly in the theory of the spatial array $\widetilde{X}^0 = a(n + \frac{1}{2})$, and then Wick rotated.

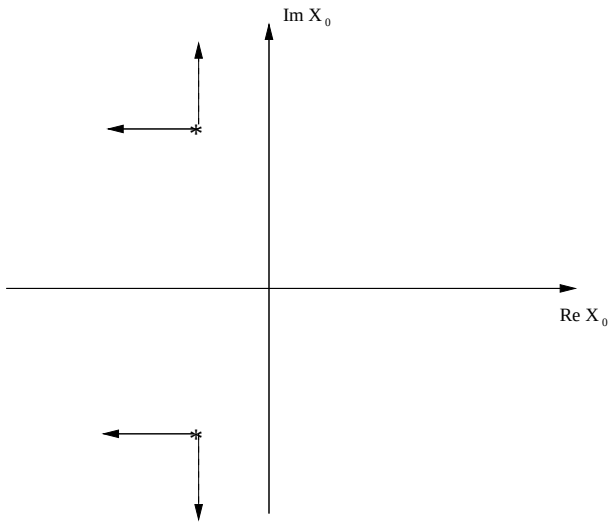

Figure 5.4: The two possible motion modes of a pair of D-branes in the complex X^0 plane.

moduli (5.5.1) are re-interpreted as deformations of the closed string background. In the next section this picture is made precise.

There is one important restriction on the allowed motions of the branes: The resulting closed string fields must be *real*. This imposes certain constraints on the moduli $f^\mu_{(n)}$. Starting from the array at $X^0 = in(a + \frac{1}{2})$, reality of the closed string fields demands that the D(-1) branes be moved in *pairs*, that is, the k-th D(-1) brane at $X^0 = ia(k + \frac{1}{2})$, $k > 0$, together with its mirror partner at $X^0 = ia(-k + \frac{1}{2})$. The reality condition is

$$f^\mu_{(k)} = (f^\mu_{(-k)})^* \quad \forall k \in \mathbf{N}\,, \tag{5.5.2}$$

where $*$ denotes complex conjugation. As long as we refrain from considering branes with complex *spatial* coordinates X^i, $i = 1, \ldots 25$, we should keep the spatial moduli $f^i_{(k)}$ real, and then (6.4.4) implies $f^i_{(k)} = f^i_{(-k)}$. For the time coordinate X^0 on the other hand, there are two possible motions for a given pair of branes, as illustrated in Fig.4[14] .

The reality condition can be simply rephrased by saying that the D-brane configuration must be symmetric under reflection with respect to real time axis. A simple way to see this constraint is to focus for example on the massless closed string fields. The field produced by

[14]Interestingly, for a pair of branes before the double Wick rotation there are also *two* allowed exactly marginal motions along $X = -iX^0$, but of course they are the independent translations of each brane along the real X axis.

some δ-function sources located at the origin in space and at times $X^0 = Y^0_k$ is schematically [118]

$$\phi(X^\mu) \sim \sum_k \frac{1}{[-(X^0 - Y^0_k)^2 + (X^i)^2]^\sigma} \tag{5.5.3}$$

where the power σ depends on the number of transverse directions. We are interested in measuring the field $\phi(X^\mu)$ for *real* values of its arguments X^μ. It follows that for $\phi(X^\mu)$ to be real, the locations of the sources $\{Y^0_k\}$ must either be real or come in complex conjugate pairs. In the next section we write down the prescription to obtain the closed string background associated with an arbitrary configuration of imaginary branes, and it will be apparent that the same reality condition is valid in full generality.

For $p > 0$ there are additional on-shell open strings since the open string tachyon can be put on-shell provided $p^m p^m = 1$, where p^m is the momentum along the Neumann directions. These are precisely the exactly marginal deformations studied in the original work by Callan et al. [130]. For example the deformation $\lambda' \cos(X^m)$, where X^m is one of the directions along the brane, continuously interpolates between Neumann and Dirichlet boundary conditions for the coordinate X^m. At the critical value $\lambda' = \frac{1}{2}$, we get an array of D(p-2) branes localized at $X^m = 2\pi(n + \frac{1}{2})i$. The deformed boundary state is known for all values of λ' [130] and we can easily apply our prescription (5.3.14) to compute $|W(\lambda')\rangle$. As λ' varies, these states are a family of purely closed string backgrounds. An open string deformation, in this case $\cos(X^m)$, is then again re-interpreted as a closed string deformation.

5.6 A more general set-up

One important conclusion from the discussion in the previous section is that there is nothing *fundamentally* special about the array of D-branes at $X^0 = i(n + \frac{1}{2})a$. Exactly marginal open string deformations allow to move the positions of the branes in the complex X^0 plane, with the only constraints coming from the reality condition. By sending off most of the branes to large imaginary time, we can also consider configurations with a finite number of

branes.

The simplest configuration consists of only one pair of branes at $X^0 = \pm i\beta$ (with β real, $\beta > 0$). As in section 2.2, we start with the pair in Euclidean space at $X = \pm\beta$. The analog of (5.2.7) is

$$\widetilde{G}_{pair}(X) = \frac{2\pi}{c} e^{-\beta c} \cosh(cX)\,, \quad |X| \leq \beta\,. \tag{5.6.1}$$

Notice that the only change relative to (5.2.7) is in the prefactor. This was foreordained since in a finite neighborhood of $X = 0$ both $\widetilde{G}_{pair}(X)$ and $\widetilde{G}_{array}(X)$ obey *homogeneous* wave equation $\left(\frac{d}{dX^2} - c^2\right)\widetilde{G} = 0$ and are even under $X \to -X$. Wick rotation then gives the usual *sourceless* solution $\sim \cos(cX^0)$. In Fourier transform

$$S_{pair}(E, \dots) = \frac{\pi}{2c}\, e^{-\beta c}\, (\delta(E - c) + \delta(E + c))\,, \tag{5.6.2}$$

which we can write

$$S_{pair}(E, \dots) = F_{pair}(E)\, \mathrm{Disc}_E[\widetilde{A}(iE)]\,, \tag{5.6.3}$$

where

$$F_{pair}(E) = \mathrm{sign}(E)\, e^{-\beta|E|}\,. \tag{5.6.4}$$

This result should be compared with (5.2.9), (5.2.12), (5.2.13).

This formula can be generalized further by displacing the D-brane pair along real time, that is at $X^0 = \alpha \pm i\beta$. In this case $F_{pair}(E) \to \mathrm{sign}(E) e^{-\beta|E| + i\alpha E}$. By linear superposition, an arbitrary configuration of M D-brane pairs at positions $X^0 = \alpha_k \pm i\beta_k$, $k = 1, \dots M$, leads again to an amplitude of the form (5.2.12), where now the prefactor takes the general form

$$F(E) = \sum_{k=1}^{M} \mathrm{sign}(E)\, e^{-\beta_k|E| + i\alpha_k E}\,. \tag{5.6.5}$$

The usual array is a special case of this formula: With $= \infty$, $\alpha_k = 0$, $\beta_k = a(k - \frac{1}{2})$ we immediately recover (5.2.13).

All the conclusions of section 3 are valid in this more general case. The basic step is the extraction of the discontinuity in E, which localizes the moduli space integration to $\rho \to 0$. A general configuration of imaginary D-branes leads to a sphere amplitude with an extra

closed string insertion $\mathcal{W}$, only the details of this insertion change. All we have to do is to replace $1/\sinh(\frac{|E|a}{2})$ in (5.3.14) with the general $F(E)$ given in (5.6.5). The state $|\mathcal{W}\rangle$ is normalizable and has finite energy as long as all D-branes are at distances $\beta_k > \pi$ from the real axis, generalizing the condition $a > 2\pi$ that we had for the array.

For a generic configuration of a finite number of imaginary D-branes, the space-time dependence of $\mathcal{W}$ is, however, quite different than the case of the infinite array. This difference is sharpest for the massless fields outside the lightcone, $r \gg |X^0|$. For the array, they have the same dependence $\sim 1/r^{23-p}$ as for a static Dp-brane, whereas for a finite configuration they decay one power faster $\sim 1/r^{24-p}$. This nicely dovetails with the fact that the infinite array with $a = 2\pi$ admits the exactly marginal deformation that creates an actual Dp- brane in real time. The incoming and outgoing radiation that makes up $\mathcal{W}_{array}$ are precisely tuned to admit the deformation that reconstructs the brane, whereas for a generic finite configuration, brane creation would require an abrupt change of the field asymptotics.

It is worth pointing out that our prescription to compute the closed string fields associated with imaginary D-branes is equivalent to the second-quantized point of view taken in section 3 of [119]. They propose to obtain the wavefunction for the closed string fields at $X^0 = 0$ by cutting open the Euclidean path integral in the presence of D-brane sources located at Euclidean time $\widetilde{X}^0 < 0$. To evaluate the expectation value of the closed string fields in such a wave function, one needs to construct the full configuration of sources symmetric under $\widetilde{X}^0 \to -\widetilde{X}^0$ (obtained by simply reflecting the sources located at $\widetilde{X}^0 < 0$ to $\widetilde{X}^0 > 0$), and read off the solution at $\widetilde{X}^0 = 0$. This is the second-quantized version of what we do here.

An interesting open question is whether as we vary the configuration of imaginary D-branes, the state $|W\rangle$ spans the full closed string cohomology. It is clear that to have any chance of success we must introduce more general boundary states than the ones considered in this chapter (for example, D-branes with magnetic and electric fields on their worldvolume), and allow for an infinite number of imaginary branes. If the answer to this question

is in the affirmative then the open/closed string duality takes a new form since at the fundamental level closed strings and D-branes are unified. Each closed string puncture in a string theory amplitude could be effectively represented by a hole in the worldsheet with appropriate boundary conditions.

5.6.1 Superstring

This general set-up can be generalized to the superstring in a straightforward way. There is now more variety of D-brane sources, since we can consider both stable BPS Dp-branes and unstable non-BPS Dp-branes. For non-BPS branes the discussion is completely analogous to the bosonic case. One can distribute non-BPS brane *pairs* freely in the complex X^0 plane, subject to exactly the same reality condition as we discussed in section 5.

BPS Dp branes introduce on the other hand an important novelty: They are sources of Ramond-Ramond fields. The reality condition for the RR fields forces us to consider pairs composed of a BPS brane at $X^0 = \alpha + i\beta$ and of its *anti*-brane partner at $X^0 = \alpha - i\beta$. It can be checked that the RR fields produced by a generic configuration of such pairs are non-vanishing only *inside* the lightcone, $r \ll |X^0|$ (see also [118]); this is consistent with the fact that the configuration has zero total RR charge, so we do not see long range RR fields.

Like in the bosonic string, infinite 'critical' arrays of branes at $X^0 = i\, a_{crit}\, (n + \frac{1}{2})$ correspond to special limits of BCFTs related to real time processes of brane creation and annihilation. Here $a_{crit} = \sqrt{2}\,\pi$ (this is the familiar $\sqrt{2}$ in translating between the bosonic string and the superstring). There are two interesting classes of examples. One can consider a critical array of non-BPS D(p-1) branes in imaginary time, which is dual to the closed string background related to the decay of a Dp-$\bar{\text{D}}p$ pair; or a critical array of alternating BPS D(p-1)/$\bar{\text{D}}$(p-1) in imaginary time, related to the decay of non-BPS Dp. (Needless to say, given p, any of these examples makes sense in either Type IIA or IIB, but not in both). The subject is potentially quite rich.

5.7 Open string field theory

We have found an intriguing relation between D-branes in imaginary time and purely closed backgrounds. Since D-branes admit an open string description, this suggests that one may be able to obtain a dual description of closed string theories in terms of open strings. We have already seen in section 5 that the exactly marginal open string deformations have a natural re-interpretation as deformations of the closed string background. However since there are no propagating on-shell open string degrees of freedom on imaginary D-branes, it is clear that if such a complete open/closed duality exists, it must involve the off-shell open strings. In this section we offer some very brief and incomplete speculations in this direction.

We would like to propose that the open string *field* theory (OSFT) on a configuration of imaginary D-branes is dual to the corresponding closed string theory. To make sense of this speculation we must define what is the OSFT for imaginary branes. Applying our usual strategy, we start with OSFT on standard D-branes, and double Wick rotate. While from a first quantized point of view it may be subtle to define the Wick-rotated open string theory, in the second quantized approach we have the luxury of a space-time action, which seems straightforward to analytically continue.

Let us sketch how this may come about in the example of the array of D(-1) branes. We start with an array of D(-1) branes at $\widetilde{X}^0 = (n + \frac{1}{2})a$. The open string field Ψ_{jk} has Chan-Paton labels $j, k \in \mathbf{Z}$ running over the positions of the D(-1) branes, and the cubic OSFT action [137] takes the form

$$S[\Psi] = -\frac{1}{g_0^2}\left(\frac{1}{2}\sum_{jk}\langle\,\Psi_{jk}, Q_B\Psi_{kj}\rangle + \frac{1}{3}\sum_{jkl}\langle\Psi_{jk},\Psi_{kl},\Psi_{lj}\rangle + \sum_{j}\langle\Psi_{jj},\mathcal{C}\rangle\right). \qquad (5.7.1)$$

Here we have also included the gauge-invariant open/closed vertex [138, 139, 51, 52, 24] $\langle\Psi,\mathcal{C}\rangle$ that couples external on-shell closed strings $\mathcal{C}$ to the open string field. Notice that the string fields Ψ_{ij} do not depend at all on the zero modes of the space-time coordinates. Double Wick rotation is then immediate. There is little to do in all the purely open terms

of the action.[15] Only the open/closed vertex is affected. We conjecture that the resulting action describes the non-trivial closed string state $|W\rangle$.

In principle it should be possible to recover the results of section 3 from the point of view of the second quantized Feynman rules for the action (6.4.1). In OSFT, amplitudes of external closed string on the disk are obtained by computing expectation values of the gauge-invariant operators discussed in [138, 139, 51, 52, 24], or in other terms by the use of the open/closed vertex. We expect that for (6.4.1) such amplitudes collapse to the region of moduli space where the open string propagators have zero length, reducing to sphere amplitudes with an extra insertion of $|W\rangle$. The mechanism for such a collapse must be of a somewhat different nature than in [24] or in [140], since here we are using the conventional BRST operator but a highly unconventional state-space.

Finally, the OSFT (6.4.1) may provide us with new clues about the string field theory around the tachyon vacuum. As $a \to \infty$, the energy of $|W\rangle$ goes to zero, and we approach the tachyon vacuum. Interestingly, in the same limit $|W\rangle$ does not vanish completely, but it becomes purely a zero-momentum dilaton. Thus we recover precisely the scenario of [24]. Since for any a such an open string field theory should make sense this may provide us with a consistent regularization of vacuum string field theory, which should be related to the one considered in [24] by some non-trivial field redefinition.

5.8 $\mathbf{a = 2\pi}$ and reconstruction of the brane

As discussed in section 4, for $a = 2\pi$ the normalization and the energy associated with the closed string state $|\mathcal{W}\rangle$ diverge [119]. This singularity signals the appearance of new open string degrees of freedom. Open strings stretched between neighboring branes in imaginary time have conformal dimension $L_0 = (a/2\pi)^2$, which equals one for $a = 2\pi$. The infinite periodic array has the special property that a specific linear combination of these marginal operators (the one which is invariant under $X_0 \to X_0 + 2\pi i$ and is even under $X_0 \to -X_0$)

[15] Note however that one has to be careful here with the reality conditions discussed in the previous sections [76].

is in fact *exactly* marginal[16] . A new branch of moduli space opens up for $a = 2\pi$. Indeed, the theory for $a = 2\pi$ is equivalent to the $\lambda = \frac{1}{2}$ critical point of the BCFT (5.1.1). Turning on the exactly marginal open string deformation ('$\cosh(X^0)$') we can reduce the value of λ, from $\lambda = \frac{1}{2}$ (the purely closed string background $|W\rangle$) to $\lambda = 0$ (the usual brane with Neumann boundary condition in time). This is the sense in which the array for $a = 2\pi$ is very special: it admits an exactly marginal deformation that *cannot* be interpreted purely as a deformation of the closed background.

5.8.1 Smearing and brane creation

One can obtain many insights into the physics for $\lambda < 1/2$ by a simple extension of the methods in section 2. The basic idea is that in the Euclidean BCFT with $X = -iX^0$, taking $\lambda < \frac{1}{2}$ amounts to regulating the delta-function sources located at $X = 2\pi(n + 1/2)$ with smooth lumps. The precise way to make this regulation can be gleaned from the boundary state [130] for general λ. Focusing on the oscillator free part of the boundary state,

$$|\mathcal{B}_0\rangle \sim \left[1 + 2\sum_{n=1}^{\infty}(-1)^n e^{-n\tau}\cos(nX(0))\right]|0\rangle\,, \quad \tau \equiv -\log(\sin(\pi\lambda))\,. \tag{5.8.1}$$

By Poisson resummation, one finds

$$|\mathcal{B}_0\rangle \sim \sum_{-\infty}^{\infty}\tilde{j}_\tau(X + 2\pi(n + \frac{1}{2}))|0\rangle\,, \quad \tilde{j}_\tau(X) = \frac{\tau}{\pi(X^2 + \tau^2)}\,. \tag{5.8.2}$$

The interpretation of this formula is clear: for $\lambda < \frac{1}{2}$, the boundary state corresponds to an infinite array of smeared sources $\tilde{j}_\tau$; indeed $\tilde{j}_\tau$ is a well-known representation for $\delta(X)$ in the limit $\tau \to 0$.

If we sum the source $\tilde{j}_\tau(X)$ over the infinite array and then Wick rotate $X \to -iX^0$ we find

$$J_\tau(X^0) = \frac{\tanh((X^0 + \tau)/2) - \tanh((X^0 - \tau)/2)}{4\pi}\,. \tag{5.8.3}$$

Already at this stage we see the crucial difference compared to $\lambda = \frac{1}{2}$ ($\tau = 0$). Now there is a non-zero source localized at *real* time for $|X^0| < \tau$, which is to say that an unstable

[16] In principle also the *odd* operator, '$\sinh(X^0)$', is exactly marginal. However in the bosonic string this deformation would bring us to the 'wrong' side of the tachyon potential for $X^0 < 0$.

D-brane appears at $X^0 = -\tau$ and disappears at $X^0 = \tau$. For later use let us record the Fourier transform of this function,

$$\rho_\tau(E) = \frac{\sin(\tau E)}{\sinh(\pi E)} \,. \tag{5.8.4}$$

The next step is to repeat the exercise for the *fields* generated by this smeared array. The Fourier transform of the Euclidean source $\tilde{j}_\tau(X)$ is $e^{-\tau|P|}$. Therefore, in the notations of section 2.2, eq.(5.2.4) should be replaced by

$$\tilde{A}(P,...) = \frac{e^{-\tau|P|}}{P^2 + c^2} \,. \tag{5.8.5}$$

As in section 2.3, we sum over the array and use the residue theorem to write the total field as a contour integral,

$$\widetilde{G}_\tau(X) = \frac{1}{2i} \oint_{\mathcal{C}} dP e^{iPX} \frac{e^{-\tau|P|}}{(P^2 + c^2)\sin(\pi P)} \,. \tag{5.8.6}$$

If we now move the contour over the imaginary P axis as in Fig.2, and Wick rotate, we find

$$S_\tau(E) = \frac{1}{2\sinh(\pi E)} \left(\frac{e^{i\tau E}}{(E + i\epsilon)^2 - c^2} - \frac{e^{-i\tau E}}{(E - i\epsilon)^2 - c^2} \right) , \tag{5.8.7}$$

which we recognize as

$$S_\tau(E) = \frac{1}{2\sinh(\pi E)} \left(G_{ret}(E) e^{i\tau E} - G_{adv}(E) e^{-i\tau E} \right) . \tag{5.8.8}$$

This way of writing the answer makes the space-time interpretation manifest (see also [119]). For $X^0 < -(\tau + r)$, we have purely *incoming* radiation. For $X^0 > \tau + r$, we have purely *outgoing* radiation. Outside of these two cones (for $(X^0)^2 - r^2 < \tau^2$), the fields are the same as the ones produces by a *static* source. The thickness of the transition regions is of the order of the string length. Notice that the outgoing radiation is produced by the rapid change of the source for $X^0 \sim \tau$, and similarly the incoming radiation is correlated with the change at $X^0 \sim -\tau$. This process can be described as some finely tuned incoming closed strings that create an unstable D-brane at $X^0 = -\tau$, which then decays at $X^0 = \tau$ into outgoing closed strings.

We can also write

$$S_\tau(E,...) = G_F(E)\,\rho_\tau(E) + \cos(\tau E)\,\frac{\pi}{2c\sinh(\frac{ca}{2})}(\delta(E-c)+\delta(E+c))\,, \tag{5.8.9}$$

where $G_F(E)$ is the Feynman propagator and $\rho(E)$ the Fourier transform of the source in real time $J_\tau(X^0)$, see (5.8.4). The two terms in (5.8.9) have very different interpretations. While the first term contains a propagator, and is non-zero for any finite E, the second term has support only for $E = \pm c$. The second term in (5.8.9) is proportional to (5.2.9); in section 3 it was seen to correspond to the extra insertion $|W\rangle$ in a sphere amplitude. The first term is instead a real D-brane source, associated to an earnest disk amplitude.

In the limit $\lambda \to \frac{1}{2}$ ($\tau \to 0$) only the second term in (5.8.9) contributes, since the source $\rho_\tau(E) \to 0$. It is a bit less obvious to see why only the first term contributes as $\lambda \to 0$. In this limit, $\tau \to \infty$ and since the oscillations of both terms are controlled by the dimensionless parameter τE, to have a non-zero contribution E must go to zero, hence for any fixed finite c the second term vanishes. The fact the $E \to 0$ is consistent with the fact that the for $\lambda = 0$ the unstable D-brane exists for an infinite amount of time; X^0 becomes an ordinary Neumann direction and the total energy (with all insertions as incoming) must vanish.

We see that as we vary λ, not only does the D-brane source vary, but the closed string background (captured by the second term in (5.8.9)) also changes in a very non-trivial way. This phenomenon requires some comments. Although the BCFT (5.1.1) may be naively thought of as a deformation of the open string background only, infact we need to simultaneously change the closed string background to cancel tadpoles. Indeed, while the operator $\cosh(X^0)$ is exactly marginal in the open string sense, one point functions of *generic* on-shell closed strings have a non-trivial dependence on λ. Of course, tadpoles for closed string operators are also generated in the familiar case of time-independent boundary deformations. However in the time-independent case only one-point functions of *zero-energy* on-shell bulk operators can change, whereas for a time-dependent perturbation like (5.1.1) there are tadpoles with a non-trivial space-time dependence. As we turn on the cosh deformation, the closed string background needs to be corrected introducing closed string

matter. Happily, as (5.8.9) shows, this seems to be automatically taken care of by the analytic continuation procedure.

The discussion in this section has been at the level of the discussion of section 2. It would be very interesting to repeat the analysis of section 3 and compute scattering amplitudes of closed strings for general λ. It would also be of interest to find the behavior of the open string spectrum for $0 < \lambda < \frac{1}{2}$.

5.9 From Choptuik to Gregory-Laflamme

As was explained in section 5.4 the massless sector of $|W\rangle$ is a spherically symmetric dilaton wave in $26 - p$ dimensions. In the limit that the Newton constant G_N goes to zero the linearized solution is an exact solution to the gravity-dilaton equations of motion. As the coupling constant is turned on the non-linearity of the equation of motion becomes more and more important. With spherical symmetry much is known about the non-linear aspects of the system. In particular, Choptuik showed [132], via numerical analysis, that a universal behavior occurs at the critical point where black hole formation first occurs. A crude summary of his results is the following. Consider a spherically symmetric wave of a massless scalar field

$$\eta\, \phi(r, X^0). \tag{5.9.1}$$

The strength of the non-linear effects of the gravitational back-reaction of the wave grows with the overall coefficient η. When $\eta \to 0$ the linearized approximation is exact while for $\eta \to \infty$ a large black hole will be formed, with an exponentially small amount of energy escaping the black hole formation as an outgoing radiation.[17] Therefore, for a given field profile $\phi(r, X^0)$ there is a special value η^* where the black hole formation first takes place. While η^* certainly depends on the details of ϕ, the time evolution of the system for $\eta \to \eta^*$ admits scaling behavior that is fixed by a certain constant, Δ. This constant is universal in the sense that it does not depend on ϕ, but it can depend for example on the

[17] The system is classical so this radiation is classical and should not be confused with Hawking radiation.

number of spatial directions. Another critical exponent δ is related to the scaling of the mass of the black hole near the transition. These fascinating results have been explored quite extensively in the last decade.

In this section we take advantage of the fact that a spherically symmetric dilaton wave can be viewed as a configuration of D-branes located in imaginary time to relate Choptuik's findings to a phase transition somewhat reminiscent of the Gregory-Laflamme instability [133]. For simplicity we will mostly phrase the discussion in the context of the bosonic string, ignoring as usual the closed string tachyon. The extension to the superstring of the scaling arguments given below is straightforward.

The first step is to understand how to get from our $|W\rangle$ a background containing only a classical dilaton wave. It is clear that to suppress massive closed string modes we need to take $\frac{a}{l_s} \to \infty$. (Here we have restored the string length l_s, that was set to one in the rest of the chapter). However the total energy of the wave will then go to zero as $1/a^{25-p}$ in this limit (see (5.4.9)), and a black hole will not be formed this way. A simple way to obtain a configuration with enough energy without exciting the massive modes is to increase the number of branes at each point $X^0 = ia(n+\frac{1}{2})$, as in the discussion at the end of section 5.4. With N D-brane at each point the particles density, $\bar{n}/V$, and the energy density $\epsilon = \bar{E}/V$ (V is the volume along the wave) of the wave for large a are (from (5.4.9))

$$\frac{\bar{n}}{V} \sim \frac{N^2 l_s^{24-2p}}{a^{24-p}}, \qquad \epsilon \sim \frac{N^2 l_s^{24-2p}}{a^{25-p}}\,. \tag{5.9.2}$$

Let us now state the exact conditions that must be satisfied in the limit we want to take:

1. The string coupling g_s should go to zero to suppress quantum effects, and the total number of particles $\bar{n}$ should go to infinity so that $|W\rangle$ is well described by a classical wave.

2. $\frac{l_s}{a} \to 0$ to ensure that the massive closed strings decouple.

3. The gravitational radius associated with the total energy of the wave,

$$r_G = (G_N \epsilon)^{\frac{1}{23-p}}, \tag{5.9.3}$$

(here G_N is the Newton constant in 26 dimensions) should be comparable to the wavelength a. If we define the dimensionless parameter

$$\zeta = \frac{r_G}{a} = \frac{(\, g_s^2 N^2 l_s^{48-2p}/a^{25-p}\,)^{\frac{1}{23-p}}}{a}, \tag{5.9.4}$$

then in our set-up ζ plays the role of η in (5.9.1) That is, for small ζ the linearized approximation is valid and a black hole will not be formed while for large ζ non-linear effects are important and lead to black hole formation. So the critical value ζ^* is a number of order one.

It is easy to verify that these conditions are satisfied in the following limit

$$a \text{ fixed}, \qquad l_s \to 0, \qquad g_s \propto l_s^{\beta}, \qquad N \propto 1/l_s^{24+\beta-p}, \qquad \beta > 0. \tag{5.9.5}$$

-So far what we have done is to take a certain 'decoupling' limit that leaves us with the classical picture of black-hole formation. The obvious question to ask is what does this mean from the D-brane point of view. In particular, does anything special happen at $\zeta = \zeta^*$ in the array of D(p-1) branes located at $\widetilde{X}^0 = (n + \frac{1}{2})a$, *i.e.* in the spatial array before the double Wick rotation?

The gravitational radius associated with N D-branes located at each site is

$$l_G \sim (g_s N)^{\frac{1}{24-p}}\, l_s. \tag{5.9.6}$$

When l_G is much smaller than the distance between the D-branes, a, the gravitational interactions between them is small and they can be considered as separated points. However, when l_G is larger than a the gravitational interaction between them is so strong that effectively they form a black hole along $\widetilde{X}^0$. It is easy to see from (5.9.6,5.9.4) that this transition occurs at the same point as the wave to black hole transition. Since the two processes are related by Wick rotation it is very tempting to suspect that there is a precise numerical relation between the exponents of [132] and the exponents, yet to be found, in the phase transition just described.

It should be stressed that although the transition considered here is somewhat reminiscent of the Gregory-Laflamme instability, there are also obvious differences. In the

Gregory-Laflamme case one starts with a black p-brane and finds, at the level of linearized equations of motion, an instable mode; condensation of this tachyon is then conjectured to lead to an array of black (p-1)-branes. (This expectation however may even be false, see *e.g.* [141, 142, 143] for recent discussions). In our case we start from the array and we turn on the coupling constant to eventually form a (possibly non-uniform) black p brane, so we are going in the opposite direction. More crucially, we do not start with an array of *black* p-branes. The D-branes are extremal to begin with, in the sense that they have no finite area horizon. In the process of turning on the coupling constant the radius of their zero area horizon grows until they meet. At that point a combined finite area horizon will be formed.

Let us illustrate this in the context of the superstring. In this case there are no closed string tachyons so the whole discussion makes more sense. We can consider either an array of BPS D(p-1)-branes, which must then be alternating as D/$\bar{\text{D}}$, or an array of non-BPS D(p-1) branes. Consider for example an array of D3/$\bar{\text{D}}$3 in Type IIB. For small ζ the D3 branes interact weakly and so they can be treated as separated stable objects. As we turn on ζ their gravitational radius start to touch. At that stage the fact that we have alternating branes anti-branes is crucial since the charges can annihilated to form a black 4-brane. This black 4-brane does not carry any 6-form charge (we are in type IIB).

It would be extremely interesting to understand Choptuik's critical behavior from the point of view of the dual open string field theory discussed very briefly in section 7. Very schematically, the way this could work is as follows. From the open string field theory point of view the classical non-linear gravity dynamics is obtained in the loop expansion. We expect that the lightest open string mode stretched between the branes, which at the classical level has large positive m^2, becomes *tachyonic* for $\zeta > \zeta^*$ due to quantum open string effects. It may be possible to see this effect in a one-loop computation, in the spirit of [144]. If this scenario is correct, the universal physics at the transition point would be completely captured by a massless field, and we would have an explanation of gravitational critical behavior in terms of a second order phase transition in the dual OSFT.

Chapter 6

D-branes and the Kontsevich model

6.1 Introduction and Summary

As we saw in the introduction to the thesis it is of interest to develop exactly solvable models of open/closed duality. An important class of such models is offered by topological string theories, the paradigmatic example being the duality between Chern-Simons and the closed topological A-model [145].

Non-critical strings in low dimensions are an ideal context to sharpen our understanding of open/closed duality. Theories with $c \leq 1$ are fully solvable through the double-scaling limit of matrix models.[1] Indeed, the double-scaled matrix model for $c = 1$ strings has recently been re-interpreted [150] as the "open string field theory" for an infinite number of D0-branes. This provides another beautiful incarnation of exact open/closed duality. The doubled-scaled matrix model arises [151] as the worldvolume theory of the localized Liouville branes. These are the so-called "ZZ branes" [152], the unstable Liouville branes localized in the strong coupling region of the Liouville direction.[2]

[1] For reviews, see [146, 147, 148, 149].

[2] A similar understanding is available for the double-scaled matrix models of $c < 1$ and $\hat{c} \leq 1$ theories [153, 154, 155]. See [156] for recent related work.

Liouville theory admits also stable branes, the "FZZT" branes [158, 159], which are extended in the Liouville direction. What is the worldvolume theory on such extended branes?

Besides the well-known double-scaled matrix models, another, more mysterious, class of matrix models makes its appearance in low-dimensional string theories. The prototype of these models, which we shall collectively refer to as topological matrix models, is the Kontsevich cubic matrix integral [160], which computes the exact generating function of minimal $(2, 2k+1)$ matter coupled to gravity. Several other examples exist [161], covering a large class of $c \leq 1$ string theories.[3] These models deserve to be called topological because they compute certain topological invariants associated with the moduli space of Riemann surfaces [166, 160, 167, 168, 169, 165]. However, it must be noted that they actually contain all the information of the physical theories which are reached from the "topological point" by turning on deformations. As a result, any known bosonic string theory with $c < 1$ admits a polynomial matrix model *à la* Kontsevich which completely encodes its exact solution. Topological matrix models are treated in the usual 't Hooft expansion, with no double-scaling limit.

The reader will have guessed our punchline. Our basic contention is that topological matrix models generically arises in topological non-critical string theories as the open string field theory on N extended (FZZT) Liouville branes (tensored with an appropriate matter boundary state depending on the string theory under consideration). In this chapter we work out in detail the prototype of the Kontsevich model. It is easy to envision that several generalizations should exist. We are going to argue that topological matrix models are examples of exact open/closed duality in very much the same spirit as the AdS/CFT correspondence.

Perhaps the most interesting general lesson is that in this exactly solvable context we will able to precisely describe the mechanism by which a Riemann surface with boundaries is turned into a closed Riemann surface. Open string field theory [6] on an infinite number

[3] The Penner model [162], the W_∞ model [163] and the normal matrix model [164] are particularly intriguing examples, related to $c = 1$ at the self-dual radius (see [165] for a recent review).

of D-branes is seen to play a crucial role. Essentially the same mechanism is at work in the large N transition for the topological A-model [170, 145, 171]. The Kontsevich integral offers an even more tractable case-study.

In an interesting [172], building on previous work (*e.g.*[173]), the authors interpret topological matrix models as describing the dynamics of non-compact branes in the topological B-model for non-compact Calabi-Yau spaces. Although the language of [172] is very different from ours, there are clearly deep correspondences as well. Understanding in detail the relation between their point of view and ours should be an illuminating enterprise.

Since the subject of topological matrix model may not be very widely known, and our explicit analysis will involve a few technicalities, in the rest of this introduction we review some background material and summarize our main conceptual points.

6.1.1 From open to closed worldsheets

It may be useful to begin by recalling the classic analysis [7] of the large N limit of a gauge theory. In 't Hooft's double line notation, each gluon propagator becomes a strip, and gauge theory Feynman diagrams take the aspect of "fatgraphs", or open string Riemann surfaces, classified by the genus g and the number h of holes (boundaries). The generating functional for connected vacuum diagrams has then the familiar expansion (assuming all fields are in the adjoint),

$$\log \mathcal{Z}^{open}(g_{YM}, t) = \sum_{g=0}^{\infty} \sum_{h=2}^{\infty} (g_{YM}^2)^{2g-2}\, t^h\, F_{g,h}\ , \quad t \equiv g_{YM}^2 N\, . \tag{6.1.1}$$

Nowadays we interpret this quite literally as the perturbative expansion of an open string theory, either because the full open string theory is just equal to the gauge theory (as *e.g.* for Chern-Simons theory [170]), or because we take an appropriate low-energy limit (as *e.g.* for $\mathcal{N} = 4$ SYM [1]).

The general speculation [7] is that upon summing over the number of holes, (6.1.1) can be recast as the genus expansion for some *closed* string theory of coupling $g_s = g_{YM}^2$. This speculation is sometimes justified by appealing to the intuition that diagrams with a

larger and larger number of holes look more and more like smooth closed Riemann surfaces. This intuition is perfectly appropriate for the double-scaled matrix models, where the finite N theory is interpreted as a discretization of the closed Riemann surface; to recover the continuum limit, one must send $N \to \infty$ and tune t to the critical point t_c where diagrams with a diverging number of holes dominate.

However, in AdS/CFT, or in the Gopakumar-Vafa duality [145], t is a free parameter, corresponding on the closed string theory side to a geometric modulus. The intuition described above clearly goes wrong here. A much more fitting way in which the open/closed duality may come about in these cases is for *each* fatgraph of genus g and with h *holes* to be replaced by a closed Riemann surface of the same genus g and with h *punctures*: each hole is filled and replaced by a single closed string insertion. Very schematically, we may write

$$t \int d\rho \;\; \rho^{L_0} \, |\mathcal{B}\rangle_P \leftrightarrow t \, \mathcal{W}(P) \, . \tag{6.1.2}$$

Here the symbol $|B\rangle_P$ denotes the boundary state creating a hole of unit radius centered around the point P on the Riemann surface. Upon integration over the length of the boundary (indicated here by the modulus ρ), we can replace the boundary state with a closed string insertion $\mathcal{W}$ located at P. This idea is based on a correspondence between the moduli space of open surfaces and the moduli space of closed punctured surfaces which can be made quite precise (see section 8.2 of [24]).

Clearly the position P in (6.1.2) is a modulus to be integrated over. Moreover, summing over the number of holes is equivalent to exponentiating the closed string insertion. As a result, we obtain the operator $\sim \exp(t \int d^2z \, \mathcal{W}(z))$, which implements a finite deformation of the closed string background. This is precisely what is required for the interpretation of t as a geometric parameter.

We were led to this viewpoint about open/closed duality, which probably has a long history (see *e.g.* [174, 175, 145, 171, 176, 24, 177, 178, 179]), by thinking about D-branes in imaginary time [177], where the mechanism (6.1.2) of boundaries shrinking to punctures

can be described exactly.[4] In this chapter we argue that topological matrix models are another very precise realization of this idea.

6.1.2 Review of $(2, 2k+1)$ strings and the Kontsevich model

Minimal bosonic string theories are specified by a pair (p, q) of relatively prime integers.[5]

In the continuum, they are formulated in the usual way by taking the total CFT = $\mathrm{CFT}_{(p,q)} \oplus \mathrm{CFT}_{Liouville} \oplus \mathrm{CFT}_{ghost}$. Here $\mathrm{CFT}_{(p,q)}$ is a minimal (p, q) model [183], of central charge

$$c_{p,q} = 1 - 6\,\frac{(p-q)^2}{pq}\,. \tag{6.1.3}$$

The central charge of the Liouville CFT is of course chosen to be $26 - c_{p,q}$ to cancel the anomaly.

The $(2, 2k+1)$ theories will be the focus of this chapter. Perhaps the most familiar among these models is $(2, 3)$, which is pure two-dimensional quantum gravity ($c = 0$), or string theory embedded in one dimension. One way to find their complete solution is by the double-scaling limit of the one-matrix model, with the potential tuned to the multicritical point of order $k + 2$ [184]. Each of these theories has an infinite discrete set of physical closed string states, conventionally labeled as $\{\mathcal{O}_{2m+1}\}$, $m = 0, 1, 2, \cdots$. Observables are correlators of these operators, which is convenient to assemble in the following partition function, summed over all genera g,

$$\log \mathcal{Z}^{closed}(g_s, t_n) = \sum_{g=0}^{\infty} g_s^{2g-2} \langle \exp(\sum_{n\,\mathrm{odd}} t_n \mathcal{O}_n) \rangle_g\,. \tag{6.1.4}$$

The partition functions for the different $(2, 2k+1)$ theories are connected to each other by flows of the KdV hierarchy. This means that we simply need to expand $\mathcal{Z}^{closed}(g_s, t_n)$ around different background values of the sources t_n in order to obtain the correlators of the different $(2, 2k+1)$ models. We choose our conventions so that $\{t_n = 0\,, \forall n\}$ corresponds to the $(2, 1)$ theory. Then correlators for $(2, 2k+1)$ are found by perturbing around $t_n = \delta_{n,3} - \delta_{n,2k+3}$.

[4] A closely related viewpoint has been explained very clearly by Ooguri and Vafa [171], using a linear sigma-model perspective.

[5] See [146, 181, 180] for reviews and [182] for very recent progress in this subject.

As first conjectured by Witten [166], the $(2,1)$ model is equivalent to two-dimensional *topological* gravity [185, 186, 187], superficially a completely different theory. Topological gravity is a topological quantum field theory of cohomological type. In that context, the operators $\mathcal{O}_{2n+1}$ are interpreted as Morita-Mumford-Miller classes, certain closed forms of degree $2n$ on the moduli space of closed punctured Riemann surfaces; correlators $\langle \mathcal{O}_{k_1} \cdots \mathcal{O}_{k_n} \rangle_g$ are intersection numbers, topological invariants of this moduli space. An index theorem gives the selection rule

$$k_1 + \cdots + k_n = 6g - 6 + 3n \tag{6.1.5}$$

in order for the correlator to receive a non-zero contribution at genus g.

The remarkable equivalence of the $(2,1)$ string theory with topological gravity was proved by Kontsevich [160], who found a combinatorial procedure to compute these intersection numbers. Kontsevich further recognized that his result for the partition function (6.1.4) could be efficiently summarized by the following matrix integral,[6]

$$\begin{aligned} \mathcal{Z}^{closed}(g_s,t) &= \rho(Z)^{-1} \int [dX] \, \exp\left(-\frac{1}{g_s} \mathrm{Tr} \left[\frac{1}{2} Z X^2 + \frac{1}{3} X^3 \right] \right) , \\ \rho(Z) &\equiv \int [dX] \, \exp\left(-\frac{1}{2 g_s} \mathrm{Tr} Z X^2 \right) . \end{aligned} \tag{6.1.6}$$

The integration is over the $N \times N$ *hermitian* matrix X. The matrix Z appearing in the quadratic term is another $N \times N$ hermitian matrix which encodes the dependence on the sources t_k through the dictionary

$$t_k = \frac{g_s}{k} \, \mathrm{Tr} Z^{-k} = \frac{g_s}{k} \sum_{n=1}^{N} \frac{1}{z_n^k} \quad (k \text{ odd}) , \tag{6.1.7}$$

where $\{z_n\}$ are the N eigenvalues of Z.

The Kontsevich integral works in a way which is truly miraculous - but which may also strike a familiar chord. The basic idea is an n-point closed string correlator

$$\langle \mathcal{O}_{k_1} \cdots \mathcal{O}_{k_n} \rangle_g \tag{6.1.8}$$

[6] Of course, as written, the integral diverges. Analytic continuation $X \to iX$ makes the integral convergent for Z negative definite.

is extracted from the genus g vacuum amplitude *with n holes*. One can proceed perturbatively, using the obvious Feynman rules that follow from (6.1.6) (Figure 6.1).

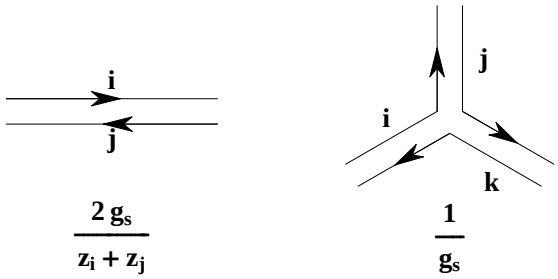

Figure 6.1: Feynman rules for the Kontsevich model.

Let us define $\Gamma_{g,n,N}$ to be the set of all connected fatgraphs of genus g, n holes, and a choice of a Chan-Paton index ranging from 1 to N for each hole (see examples in Figure 6.2). The connected vacuum amplitude at genus g and with n holes is then

$$\mathcal{F}_{g,n,N} = g_s^{2g-2+n} \sum_{\gamma\in\Gamma_{g,n,N}} \frac{1}{\#\,\mathrm{Aut}(\gamma)} \prod_{(i,j)\in\gamma} \frac{2}{z_i+z_j}\,. \tag{6.1.9}$$

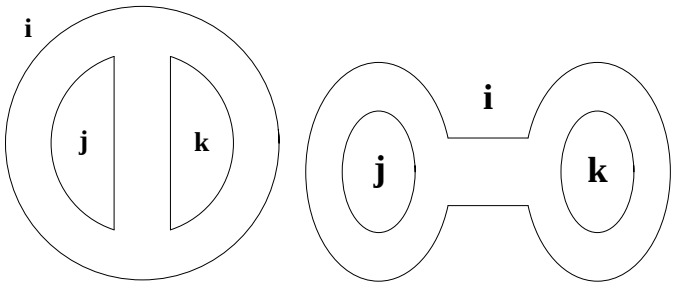

Figure 6.2: The two fatgraphs with $g = 0$ and $h = 3$. The indices i, j, k are Chan-Paton labels ranging from 1 to N. The sum of the two graphs is $g_s/(z_i z_j z_k)$. Upon summing over the Chan-Paton labels, this gives $t_1^3/(6g_s^2) \longrightarrow \langle \mathcal{O}_1\mathcal{O}_1\mathcal{O}_1\rangle_{g=0} = 1$.

Individual Feynman diagrams give complicated rational expressions in the parameters $\{z_i\}$, but remarkably the total answer can always be expressed as

$$\mathcal{F}_{g,n,N} = g_s^{2g-2} \sum_{\{k_1\cdots k_n\}}^{k_i\ \mathrm{odd}} \frac{C_{\{k_1\cdots k_n\}}}{\#\,\mathrm{Aut}(k_1\cdots k_n)} \prod_{i=1}^{n} g_s \frac{\mathrm{Tr} Z^{-k_i}}{k_i}\,. \tag{6.1.10}$$

We see from the definition (6.1.7) that the parameters t_k play the role of generalized 't Hooft couplings. From (6.1.4), we recognize

$$\langle \mathcal{O}_{k_1} \cdots \mathcal{O}_{k_n} \rangle_g = C_{\{k_1 \cdots k_n\}} \,. \tag{6.1.11}$$

The selection rule (6.1.5) is a simple consequence of Euler's theorem,

$$3(2-2g) = 3(\#V - \#P + n) = -\#P + 3n = -\sum_i k_i + 3n \,, \tag{6.1.12}$$

where $\#V$ and $\#P$ are the numbers of vertexes and propagators, and we used that $2(\#P) = 3(\#V)$.

In this computation, the rank N can be kept generic, as long as it is big enough to guarantee that the traces $\mathrm{Tr} Z^{-k}$ are functionally independent (otherwise the expression (6.1.10) is not uniquely defined); $N > \max(k_i)/2$ suffices. If instead we are interested in the full partition function $\mathcal{Z}^{closed}(g_s, t_k)$ for some fixed values of the infinitely many sources t_k, it is necessary to send $N \to \infty$ in order for the relation (6.1.7) to be invertible. So in particular we need infinite N to compute the correlators of the higher $(2, 2k+1)$ models, $k > 0$. Nevertheless, it makes perfect sense to keep N finite; the finite N Kontsevich model covers an N-dimensional submanifold in the moduli space of the closed string theory.

6.1.3 The Kontsevich model is cubic open string field theory

As we have just reviewed, the correlator of n closed string operators at genus g is computed in the Kontsevich model by the fatgraph vacuum amplitude of genus g and n boundaries. We propose that this is an exact open/closed duality: the Kontsevich model is to be interpreted as an open string field theory, dual to the $(2,1)$ bosonic closed string theory. The Kontsevich integral is to $(2,1)$ string theory as $\mathcal{N} = 4$ SYM is[7] to IIB on $AdS_5 \times S^5$. The duality works just as explained in section 1.1. The closed string partition function $\mathcal{Z}^{closed}(g_s, t_n)$ is identified with the vacuum partition function $\mathcal{Z}^{open}(g_s, z_i)$ of the open

[7] An apparent difference is that in AdS/CFT the SYM theory is obtained only in the low-energy limit of the theory on the D3 branes in flat space, whereas the Kontsevich model is the full open string field theory. We take this as a small hint that a better way to understand AdS/CFT should exist, where the SYM theory *is* the full open string field theory of some appropriate branes. See Section 7.

string field theory. Each hole in the open description is replaced by the insertion of a closed string puncture, indeed, as we have emphasized in our review of the Kontsevich model, powers of the generalized 't Hooft couplings t_k count insertions of the closed string operator $\mathcal{O}_k$.

The reasoning that led Kontsevich to (6.1.6) uses the decomposition of the moduli space of Riemann surfaces [162, 188, 189, 190, 191] that arises naturally in open string field theory [6] (OSFT), but so far this had not been given a direct physical interpretation. Here we are saying that in the Kontsevich model *is* OSFT. With the advantage of modern insight into the physics of D-branes, we can give a string theory "proof" of Kontsevich result. The logic is summarized by the following claims:

1. One can construct a family of stable D-branes in the $(2,1)$ string theory, labeled by a continuous parameter z.

2. Insertion of the boundary state $|\mathcal{B}(z)\rangle$ for any one such brane in a string amplitude is fully equivalent to the insertion of a closed string puncture, as in (6.1.2). In this case, the precise correspondence is
$$\int d\rho\, \rho^{L_0}\, |\mathcal{B}(z)\rangle_P \leftrightarrow \sum_{k\,\mathrm{odd}} \frac{\mathcal{O}_k(P)}{k\, z^k}\,. \tag{6.1.13}$$

3. The full cubic OSFT [6] on a collection of N of these D-branes, reduces precisely to the Kontsevich action (6.1.6). The parameters labeling the branes, $\{z_i\}$, $i = 1 \cdots N$, are the same as the parameters appearing in the quadratic term of the matrix integral.

These claims are sufficient to establish Kontsevich result. We just have to evaluate the string theory vacuum amplitude $\mathcal{Z}$ in the presence of N branes. We do this in two equivalent ways. Evaluating $\mathcal{Z}$ in the open channel, we have (claim 3) the sum of vacuum amplitudes of the Kontsevich integral, $\mathcal{Z}^{open}(g_s, z_i)$. Evaluating $\mathcal{Z}$ in the closed channel, we can replace each hole by a sum of closed string operators (claim 2), and obtain the generating function $\mathcal{Z}^{closed}(g_s, t_n)$ of closed string correlators. This identifies the vacuum amplitude of the Kontsevich integral with the closed string partition function,
$$\mathcal{Z}^{closed}(g_s, t_n) \equiv \mathcal{Z}^{open}(g_s, z_i)\,, \tag{6.1.14}$$

which is what Kontsevich showed by more abstract and rigorous methods. The dictionary (6.1.2) between the "open parameters" $\{z_k\}$ and the "closed parameters" $\{t_k\}$ has its microscopic explanation in the rule (6.1.13) to replace a boundary with a specific closed string operator.[8]

6.1.4 Extended Liouville D-branes in topological string theory

Our goal is now to justify these claims by standard worldsheet methods. The $(2,1)$ string theory is strictly speaking outside the range of the definition given at the beginning of section 1.2, since the Kac table is empty and there is no $(2,1)$ minimal model. A possible definition is formal analytic continuation to $k \to 0$ of the double-scaling results [184], but this is unsatisfactory for our purposes. Fortunately, there are several other more intrinsic formulations, appearing to all yield the same results.

Since $c_{2,1} = -2$, the simplest choice for the matter CFT is a pair of free, Grassmann odd scalars Θ^1 and Θ^2. This provides a continuum definition of the $(2,1)$ model as $c = -2$ matter coupled to $c = 28$ Liouville, and it is the set-up that we shall use in this chapter. The "topological point" $\{t_k = 0\}$ corresponds to taking the bulk cosmological constant $\mu \equiv t_1 = 0$.[9]

Claim 1 is established by taking Dirichlet boundary conditions for the Θ^α and FZZT boundary conditions in the Liouville direction. The FZZT boundary state depends on a continuous parameter μ_B, the boundary cosmological constant, which can be thought of as the vev of the open string tachyon living on the brane. We identify $\mu_B = z$. The full boundary state is then

$$|\mathcal{B}(z)\rangle = |\mathcal{B}_\Theta^{\text{Dirichlet}}\rangle \otimes |\text{FZZT}(\mu_B = z) \otimes |\mathcal{B}_{ghost}\rangle \,. \tag{6.1.15}$$

FZZT boundary conditions are closely related to the notion of macroscopic loop operator $w(\ell)$ in two-dimensional quantum gravity [193]. $w(\ell)$ is the operator that creates a hole of

[8] It makes sense to consider open string vacuum amplitudes at fixed values of $\{z_i\}$ because these are superselection parameters that do not fluctuate. This statement is dual to the statement that the closed string background $\{t_k\}$ is superselected [192].

[9] It may be useful to recall that in this theory (unlike the generic (p,q) model, $q \neq 1$) amplitudes depend analytically on μ and it makes sense to treat μ perturbatively.

length ℓ in the Riemann surface, where the length is measured with the metric obtained by taking the Liouville field as the conformal factor. Then[10]

$$\int d\rho\, \rho^{L_0}\, |\mathcal{B}(z)\rangle \sim \int_0^\infty \frac{d\ell}{\ell}\, e^{-\ell\, z}\, w(\ell)\,. \tag{6.1.16}$$

To obtain claim 2, we appeal to a standard bit of lore in non-critical string theory [193]. Under rather general conditions, the macroscopic loop operators can be expanded as $\ell \to 0$ as a sum of local closed string operators,

$$w(\ell) \sim \sum \ell^{x_k}\, \mathcal{O}_k\,, \tag{6.1.17}$$

where $x_k \geq 0$. A simple argument based on conservation of the Liouville momentum (section 3.1), fixes the exponents to be $x_k = 2k + 1$. The $\ell \to 0$ expansion of $w(\ell)$ translates after Laplace transform (6.1.16) into a $z \to \infty$ expansion of $|\mathcal{B}(z)\rangle$ as a sum of terms $\sim z^{-2k-1}\mathcal{O}_k$. This gives claim 2, modulo fixing the precise normalization of the operators $\mathcal{O}_k$. In principle these normalization coefficients could be obtained by a very careful analysis of the boundary state, but it it easiest to determine them indirectly by consistency, as we explain in section 5. This replacement of a boundary with a sum of closed string insertions is a generic fact in low-dimensional string theory, and does not appear to depend on the topological nature of the $(2, 1)$ model.

By contrast, claim 3 is based on a mechanism of topological localization, closely reminiscent of the way the open topological A-model reduces to Chern-Simons theory [170]. The worldsheet boundary CFT admits a nilpotent scalar supercharge Q_S [194], anti-commuting with the usual BRST operator Q_B. The open string (first-quantized) Hamiltonian is a Q_S anti-commutator, so it can be rescaled by an overall constant without changing the physics. As in the case of the open topological A-model [170], the only contributions to open string amplitudes come from the region of moduli space where the Riemann surfaces degenerate to ordinary Feynman graphs. In the usual OSFT decomposition of moduli space in terms of trivalent vertices and propagators (strips) of length $t^{(\alpha)}$, this is the limit in which each

[10] Here we are just tensoring the well-known relation between FZZT branes and macroscopic loops [193, 158] with the (trivial) Dirichlet b.c. for the Θ^α.

$t^{(\alpha)} \to \infty$. In this limit, the full cubic OSFT collapses to a cubic matrix integral for the open string "tachyon". A detailed analysis of Liouville BCFT correlators (section 4.3 and appendix) shows that this matrix integral is exactly the Kontsevich model, provided we identify the boundary cosmological constants $\{\mu_B^i\}$, $i = 1, \cdots, N$, with the parameters $\{z_i\}$.

6.2 Closed bosonic strings in D = −2

We define the $(2,1)$ closed string theory by choosing the total worldsheet action to be

$$S = S_{matter}^{c=-2} + S_{Liou}^{c=28} + S_{ghost}^{c=-26} \,. \tag{6.2.1}$$

The matter CFT is that of a pair of real, *Grassmann odd* scalar fields $\Theta^1(z,\bar{z})$ and $\Theta^2(z,\bar{z})$, with the free action

$$S_{matter}^{c=-2} = \frac{1}{2\pi} \int d^2z \, \epsilon_{\alpha\beta} \partial\Theta^\alpha \bar{\partial}\Theta^\beta \,, \qquad \alpha,\beta = 1,2 \,. \tag{6.2.2}$$

There is some freedom as to which CFT with $c = -2$ one should pick. Another possibility [194] would be to take the more familiar $\xi\eta$ ghost system, related to the Θ^α system as follows:

$$\eta(z) = \partial\Theta^2(z,\bar{z}) \,, \qquad \xi(z) + \xi(\bar{z}) = \Theta^1(z,\bar{z}) \,. \tag{6.2.3}$$

The two theories differ only in the treatment of the zero-modes. $\Theta^1(z,\bar{z})$ has only one *non-chiral* zero-mode (the same is true for $\Theta^2(z,\bar{z})$), so the mode expansion reads

$$\Theta^\alpha(z,\bar{z}) = \theta_0^\alpha + \frac{1}{2} d_0^\alpha \ln|z|^2 + \frac{1}{\sqrt{2}} \sum_{n=-\infty, n\neq 0}^{\infty} \left(\frac{d_n^\alpha}{n z^n} + \frac{\bar{d}_n^\alpha}{n \bar{z}^n} \right) . \tag{6.2.4}$$

This is a rather subtle difference, but we believe that the choice of the Θ^α is the correct one. First, this is the most obvious choice to describe "strings in minus two dimensions". It is indeed the choice singled out by defining the theory from double-scaling of a matrix model for random surfaces embedded in minus two dimensions [195, 196, 197, 198, 199]. Second, the treatment of closed string correlators is simpler, as unlike the $\xi\eta$ system, the Θ^α system

does not require the introduction of screening charges. We come back to this point in the next subsection. Finally, this is the choice that will naturally lead to the Kontsevich model.

The Θ^α system has of course properties very similar to those of a pair of free bosons, one need only keep track of Grassmann minus signs. The OPE reads

$$\Theta^1(z,\bar{z})\Theta^2(0) \sim -\frac{1}{2}\log|z|^2\,, \tag{6.2.5}$$

and the stress tensor is

$$T_\Theta = \epsilon_{\alpha\beta}\partial\Theta^\alpha\partial\Theta^\beta\,. \tag{6.2.6}$$

(Note that in this chapter we set $\alpha' = 1$). The Θ^α CFT as an obvious global SL(2) invariance that rotates the fields. This symmetry does not extend to an affine symmetry but to a W_3 algebra [200].

It is amusing to check the modular invariance of the Θ^α system. The vacuum amplitude on the torus can be easily found by explicit computation of the trace,[11]

$$\mathrm{Tr}\left[(-1)^F\,\theta_0^1\theta_0^2\,q^{L_0+1/12}\,\bar{q}^{\bar{L}_0+1/12}\right] = 2\pi\tau_2\,|q|^{1/6}\prod_{n=1}^{\infty}|1-q^n|^4 = 2\pi\tau_2\,|\eta(\tau)|^4\,, \tag{6.2.7}$$

and is indeed modular invariant. The unusual factor of τ_2 is a consequence of the zero-mode insertions, while the $(-1)^F$ factor follows from odd-Grassmanality. As it should be, this is the inverse of the torus vacuum amplitude for two free bosons. We should also mention that (orbifolds of) Θ^α systems have been studied in detail [200] as prototypes of logarithmic CFTs [201, 202].

Liouville CFT has been well-understood in recent years (see *e.g.* [159, 158, 152] and references therein), and it is largely thanks to this progress that we shall be able to carry

[11] To obtain a non-zero amplitude, we must of course insert the two zero modes θ_0^1 and θ_0^2.

our analysis. We collect here some standard facts:

$$S_{Liou} = \frac{1}{2\pi}\int d^2z\left(\partial\phi\bar{\partial}\phi + Q\,R\,\phi + \mu\, e^{2b\phi}\right) \tag{6.2.8}$$

$$c_{Liou} \equiv 1 + 6Q^2\,, \quad Q = b + \frac{1}{b} \tag{6.2.9}$$

$$\phi(z,\bar{z})\phi(0) \sim -\frac{1}{2}\log|z|^2 \tag{6.2.10}$$

$$T^{Liou} = -\partial\phi\partial\phi + Q\partial^2\phi \tag{6.2.11}$$

$$\mathcal{V}_\alpha \equiv e^{2\alpha\phi}\,, \quad h_\alpha = \alpha(Q-\alpha)\,. \tag{6.2.12}$$

Specializing to $c_{Liou} = 28$, we have $Q = 3/\sqrt{2}$, $b = 1/\sqrt{2}$. We shall keep the symbol b in many formulas to facilitate future generalizations; unless otherwise stated, it is understood that $b \equiv 1/\sqrt{2}$.

6.2.1 Remarks on closed string observables

In this subsection we offer some side remarks about closed string amplitudes. Our main interest is in the *open* string sector, indeed the essential point is that one can bypass the closed string theory altogether and compute everything using open string field theory (the Kontsevich model), which is structurally much simpler. The subject of closed string amplitudes in topological gravity is notoriously subtle [166, 187, 203, 204, 205, 206]. Here we attempt to make contact with some of the previous work and suggest that the action (6.2.1,6.2.2) may offer a different and simpler starting point.

A model very similar to (6.2.1, 6.2.2) (but with the $\xi\eta$ system instead of the Θ^α system) was considered by Distler, who observed that by an elegant change of variables (see (6.3.12) below) the bosonic $(2,1)$ theory could be formally related to the topological gravity formulation of [185]. This is one of the several [166, 187, 203, 204, 205, 206] (closely related) field-theoretic formulations of topological gravity (see [207, 208] for reviews). They all have in common a sophisticated BRST machinery extending the ordinary moduli space to a (non-standard) super-moduli space, which in essence is just the space of differential forms over the bosonic moduli space. These formulations (as particularly transparent in Verlinde's set-up [187]) make it manifest that closed string amplitudes are intersection numbers on

the moduli space. In this chapter we will carry our analysis in the context of the bosonic $(2,1)$ theory, but we believe that an analogous derivation of the Kontsevich model must be possible in the BRST formulations of topological gravity.

A potential worry is the claim by Distler and Nelson [205] that the bosonic $(2,1)$ model (*with the $\xi\eta$ system*) does not correctly reproduce the topological gravity results, and that the full BRST machinery is necessary to obtain the correct measure of integration over the moduli space. It is quite difficult to compute topological gravity amplitudes from first principles using standard worldsheet methods, in any of the field-theoretic formulations. The difficulty stems from the very nature of the observables: amplitudes are naively zero before integration over the moduli space, and receive contributions only from "contact terms" (degenerations of the punctured surface). This is related to the fact that there are no non-trivial closed string states in the absolute BRST cohomology, the only observables being in the semi-relative cohomology.

However, the different zero-mode structure of the Θ^α system does certainly affect the calculation of these contact terms. We believe that a careful analysis using the action (6.2.2) would fully account for the correct contact term algebra. This is very plausible in light of the fact that using this worldsheet action we will obtain the Kontsevich model. More concretely, our derivation of the Kontsevich model suggests a "canonical" form for the closed string vertex operators,

$$\mathcal{O}_{2k+1} = e^{2(1-k)b\phi}\, \mathcal{P}_k(\partial\Theta^\alpha, \bar\partial\Theta^\beta)\, c\bar c\,. \tag{6.2.13}$$

Here $\mathcal{P}_k(\partial\Theta^\alpha, \bar\partial\Theta^\beta)$ is a primary of dimension $\left(\frac{k(k+1)}{2}, \frac{k(k+1)}{2}\right)$, and it should be invariant under the SL(2) symmetry. This follows from the fact that the D-branes which we use to obtain the Kontsevich model are SL(2) invariant. It turns out that there is a *unique* such operator in the Θ^α CFT. This can be seen from the results in [200]. In that paper it is proved that (in the chiral theory), for each $j \in \mathbf{N}/\mathbf{2}$, there is exactly one spin-j SL(2) multiplet of primaries, of conformal dimension $j(2j+1)$. Since there is only one way to combine the chiral and antichiral fields into an SL(2) singlet, this shows the uniqueness of $\mathcal{P}_k(\partial\Theta^\alpha, \bar\partial\Theta^\beta)$.

The operators (6.2.13) differ from the ones considered by Distler [194], which are not SL(2) invariant. In [194] a further operation of "picture changing" was necessary in order to obtain non-zero correlators. In that language, the operators (6.2.13) are already in the correct picture and in principle their correlators can be evaluated without any extra screening insertions. The only selection rule comes from anomalous conservation of Liouville momentum, and it is precisely (6.1.5).

6.3 Open string theory on stable branes

We now turn to the open string sector of the $(2,1)$ theory. The natural boundary conditions for the Θ^α system are either Neumann or Dirichlet. Boundary conditions for the Liouville CFT are either ZZ (unstable, localized at $\phi \to \infty$) or FZZT (stable, extended in the Liouville direction). The choice leading to the Kontsevich model is to combine Dirichlet b.c. for Θ^α and FZZT b.c. for Liouville,[12]

$$i(\partial\phi - \bar\partial\phi)|_\partial = 4\pi\mu_B\, e^{b\phi}\,, \qquad \Theta^\alpha|_\partial = 0\,. \tag{6.3.1}$$

The FZZT boundary conditions are generated by the adding to the Liouville action the boundary term

$$\mu_B \int_\partial e^{b\phi}\,. \tag{6.3.2}$$

One of the basic ingredients of our construction is the claim that amplitudes with boundaries can be reduced to amplitudes where each boundary is replaced by a specific closed string insertion. The same phenomenon was demonstrated for D-branes in imaginary time through a precise CFT analysis in the usual framework of (critical) string theory. In the present case it is easiest to use instead the language of two-dimensional quantum gravity (or non-critical string theory). This language gives a very useful geometric understanding of the FZZT boundary state, which we now review.

[12] Another interesting choice is Neumann for Θ^α and ZZ for Liouville, related to the double-scaled matrix model, see section 6.1.

6.3.1 Macroscopic loops

In critical string theory, we are instructed to integrate he appropriate CFT amplitudes over the moduli space of Riemann surfaces. In quantum gravity, we integrate over the two-dimensional metric (modulo diffeomorphisms). Of course the two points of view are completely equivalent, as the integral over metrics can be replaced by the Liouville path-integral followed by integration over the moduli. Schematically,

$$\int \frac{[\mathcal{D}g_{ab}]}{\text{Diff}} \int [\mathcal{D}X]\ (\mathcal{O}_1 \cdots \mathcal{O}_n\ ) \leftrightarrow \int_{\mathcal{M}_{g,n}} [d\,m] \int [\mathcal{D}X]\,[\mathcal{D}\phi]\,[\mathcal{D}b]\,[\mathcal{D}c]\ (\mathcal{O}_1 \cdots \mathcal{O}_n\ )\ . \quad (6.3.3)$$

Here $\mathcal{M}_{g,n}$ denotes the moduli space of closed Riemann surfaces of genus g and n punctures, ϕ the Liouville field, X a collective label for the matter fields, and $\{\mathcal{O}_k\}$ a generic assortment of local operators. To compute amplitudes in the presence of h boundaries, in the language of critical string theory we would of course integrate over the moduli space of $\mathcal{M}_{g,n,h}$ of Riemann surfaces with h holes, specifying appropriate boundary conditions for all the fields. In the language of quantum gravity, FZZT boundary conditions have the simple interpretation of introducing a 'weight' for each boundary length ℓ_i [193, 158],

$$\int \frac{[\mathcal{D}g_{ab}]}{\text{Diff}}\, e^{-\sum_{i=1}^{h} \mu_B^i\, \ell_i[g]} \int [\mathcal{D}X]\ (\cdots) \equiv \langle \prod_i \left[\int \frac{d\ell_i}{\ell_i}\, e^{-\mu_B^i \ell_i} w(\ell_i) \right] \cdots \rangle\,. \quad (6.3.4)$$

Here on the r.h.s. we have introduced the definition of the macroscopic loop operator $w(\ell)$, which is the operator creating a boundary of length ℓ in the two-dimensional universe. Note that we have also left implicit a choice of boundary conditions for the matter fields X. Another standard object is the Laplace transform of $w(\ell)$,

$$W(\mu_B) \equiv \int \frac{d\ell}{\ell}\, e^{-\mu_B \ell} w(\ell)\,. \quad (6.3.5)$$

In the presence of three or more boundaries, each loop operator $w(\ell)$ can be expanded in non-negative powers of ℓ [193], or equivalently, $W(\mu_B)$ can be expanded in inverse powers of μ_B [193]. Each term in this expansion represents a local disturbance of the surface, and is thus equivalent to the insertion of a local operator.

In our case, the expansion will take the general form

$$W^{Dirichlet}(\mu_B) = g_s \sum_k^{\infty} c_k \frac{\mathcal{O}_k}{\mu_B^{x_k}}. \quad (6.3.6)$$

The superscript on W is a reminder that we are imposing Dirichlet boundary conditions for the matter fields Θ^α. Recall that we are taking the bulk cosmological constant $\mu = 0$. For $\mu \neq 0$, the coefficients c_k would be replaced by functions $c_k(\mu_B^2/\mu)$. The operators $\{\mathcal{O}_{2k+1}\}$ are the matter primaries, appropriately dressed by the Liouville field,

$$\mathcal{O}_k = e^{2(1-k)b\phi}\mathcal{P}_k(\partial\Theta^\alpha, \bar\partial\Theta^\beta)\,. \tag{6.3.7}$$

To write this expression, we are using the information that the set of matter primaries $\{\mathcal{P}_k(\partial\Theta^\alpha, \bar\partial\Theta^\beta)\}$ of the Θ^α system have dimensions $\left(\frac{k(k+1)}{2}, \frac{k(k+1)}{2}\right)$. Their explicit expressions can be found in [200].[13] The value of the Liouville dressing follows as usual by requiring that the total dimension be $(1,1)$. It is then immediate to determine the powers of μ_B in (6.3.6) by conservation of the Liouville momentum. One has to recall that each boundary carries a Liouville momentum $Q/2$, and that each factor of μ_B carries momentum $b/2$. This fixes $x_k = 2k+1$. The normalization coefficients c_k could also be computed with some effort, but we shall ignore this here. Consistency of the contact term algebra (section 5) will be an easier route to fix normalizations.

Although this logic seems perfectly satisfactory, it would be nice to have a derivation of the same result using the language of *critical* string theory, treating the Liouville theory as an ordinary CFT, in the same spirit as the argument given for branes in imaginary time [177]. The FZZT boundary state can be written as an integral over the continuum spectrum of Liouville momenta $\frac{Q}{2} + iP$ of appropriate Ishibashi states,

$$|\mathrm{FZZT}(\mu_B)\rangle = \int_0^\infty dP\ \Psi(\mu_B, P)\,|\frac{Q}{2} + iP\rangle\,. \tag{6.3.8}$$

It is conceivable that the analyticity properties of the theory in the complex P plane may allow a contour deformation that would pick up only the poles corresponding to on-shell states in $\frac{b_0}{L_0}\left(|\mathrm{FZZT}(\mu_B)\rangle \otimes |\mathrm{matter}\rangle \otimes |\mathrm{ghost}\rangle\right)$. This should reduce the boundary state to the same sum of on-shell closed string insertions expected from the quantum gravity argument.

[13] There is in fact a whole SL(2) multiplet of primaries of dimension $\frac{k(k+1)}{2}$ in each chiral half of the theory. However the Θ^α boundary state is an SL(2) singlet (see (6.3.9)), and this fixes uniquely $\mathcal{P}_k(\partial\Theta^\alpha, \bar\partial\Theta^\beta)$ for each k, as remarked in section 2.1.

6.3.2 Boundary CFT

The next logical step is to determine the spectrum of open strings living on these stable branes.

In the open sector of the Θ^α system with Dirichlet boundary conditions, chiral and antichiral oscillators d_n and $\bar{d}_n$ are identified, and we find a single copy of the chiral current $\partial\Theta^1$ (the same for $\partial\Theta^2$) without any zero modes.[14] It is amusing to check this statement by a modular transformation of the annulus partition function. For this purpose we write the boundary state,

$$|\mathcal{B}_\Theta^{\text{Dirichlet}}\rangle = \exp\left(\sum_{n=1}^{\infty}\frac{1}{n}\,\epsilon_{\alpha\beta}d_{-n}^{\alpha}\bar{d}_{-n}^{\beta}\right)\theta_0^1\theta_0^2\,|0\rangle\,. \tag{6.3.9}$$

The annulus amplitude can be swiftly evaluated,

$$\langle\mathcal{B}_\Theta^{\text{Dirichlet}}|q^{L_0+1/12}\,\bar{q}^{\bar{L}_0+1/12}|\mathcal{B}_\Theta^{\text{Dirichlet}}\rangle = 2\pi\tilde{t}\,\eta(\tilde{t})^2\,,\quad q\bar{q}\equiv e^{-2\pi\tilde{t}}\,. \tag{6.3.10}$$

Modular transformation gives $\eta(t)^2$, which is indeed the same result obtained by tracing over the open string spectrum described above,

$$\text{Tr}_{open}\left[(-1)^F\,e^{-2\pi t(L_0+1/12)}\right] = \eta^2(t)\,. \tag{6.3.11}$$

The open string spectrum of the Liouville BCFT for FZZT boundary conditions is known to have the usual primaries $\{e^{\alpha\phi}\}$, of dimension $h_\alpha = \alpha(Q-\alpha)$ (note the factor of two difference with respect to the bulk primaries (6.2.12)). As usual in Liouville field theory, the continuum spectrum $\alpha = Q/2 + iP$ corresponds to delta-function normalizable states, while real exponents $\alpha \leq Q/2$ correspond to local operators and are used in the dressing of the matter primaries.

A crucial observation, due to Distler [194], is that Liouville and $c=-2$ matter can be formally combined into a $\beta\gamma$ bosonic ghost system of conformal dimensions $(2,-1)$,

$$\beta = \partial\Theta^1 e^{b\phi}\,,\qquad \gamma = \partial\Theta^2 e^{-b\phi}\,. \tag{6.3.12}$$

[14] Had we defined the $(2,1)$ string theory using a $\xi\eta$ system, a zero mode for ξ would survive on the boundary ($\xi_0 \equiv \bar{\xi}_0$, but *one* zero mode is still there). This would spoil our construction.

(Recall that for $c_{Liou} = 28$ the parameter $b \equiv 1/\sqrt{2}$). Distler applied this construction to each chiral half of the closed theory, where the Liouville CFT was taken to be a free linear dilaton ($\mu = 0$). The validity of the bosonization formulas (6.3.12) is then a simple consequence of the free OPEs. This commuting $\beta\gamma$ system has conformal dimensions $(2, -1)$, the same dimensions of the usual anticommuting bc ghost system. This makes the topological nature of the theory intuitively clear. In any open string vacuum amplitude, the oscillator parts of the bc and $\beta\gamma$ path-integrals will exactly cancel each other, and we should expect the only surviving contributions to arise from classical configurations. This expectation will be made more precise below. A basic ingredient is the scalar supersymmetry, or topological charge,

$$Q_S \equiv \oint J_S(z)\,, \quad J_S(z) \equiv b(z)\gamma(z) = \oint b(z)\partial\Theta^2(z)e^{-b\phi(z)}\,, \tag{6.3.13}$$

which obeys

$$Q_S^2 = 0\,. \tag{6.3.14}$$

The usual BRST operator of the bosonic string theory,

$$Q_B = \oint c(z)\left(T^{matter}(z) + T^{Liou}(z) + \frac{1}{2}T^{ghost}(z)\right), \tag{6.3.15}$$

turns out to be Q_S-exact,

$$Q_B = \{Q_S, \oint \frac{1}{2}\beta(z)c(z)\partial c(z)\}\,. \tag{6.3.16}$$

Turning on the bulk Liouville interaction ($\mu \neq 0$) is expected to preserve the topological nature of the theory, since the Liouville term is Q_S-closed; it is easy to check that Q_S is still nilpotent for non-zero μ. Even more crucially for our purposes, an FZZT brane with Dirichlet b.c. for the Θ^α will preserve the total charge $Q_S + \bar{Q}_S$. This is obvious for zero boundary cosmological constant, and holds also for $\mu_B \neq 0$ since the boundary interaction is killed by $Q_S^{boundary}$. Here we are defining an operator $Q_S^{bondary}$ acting on boundary vertex operators by integrating the current $J_S + \bar{J}_S$ on a semicircle around the boundary operator.

We are going to focus first on the case $t_1 = \mu = 0$ (recall that this was already assumed in the expression (6.3.6)). We shall comment on the more general case $\mu \neq 0$ at the end of section 5.

We devote the rest of this section to the computation of the cohomology of $Q_S^{boundary}$, a technical ingredient that we shall need in our analysis of the open string field theory. There is a slight complication due to the fact that for non-zero boundary cosmological constant μ_B, the BCFT is interacting and the action of $Q_S^{boundary}$ is non-trivial. Let us first consider the case $\mu_B = 0$. Then the action of $Q_S^{boundary}$ is just the same as for the chiral Q_S operator (6.3.13) and the cohomology may be readily evaluated. The task is simplified by the realization that the cohomology must lie in the kernel of L_0 and of J_0, the zero-mode of an appropriately defined current $J(z)$.

Consider the current[15]

$$J(z) \equiv J_{Liou}(z) - J_{bc}(z) = \frac{1}{b}\partial\phi + : b(z)c(z) : \ . \tag{6.3.17}$$

J_{Liou} is an anomalous current that counts the Liouville momentum in units of b, for example $e^{b\phi}$ has J_0 charge one. The linear combination $J(z)$ is non-anomalous and it is Q_S-exact,

$$J(z) = \{Q_S, c(z)\beta(z)\}\,. \tag{6.3.18}$$

This implies that the cohomology of Q_S is contained in the kernel of J_0. Indeed Q_S is invertible outside this kernel. Similarly, the total energy momentum tensor is Q_S exact. Indeed using (6.3.16)

$$T(z) = \{Q_B, b(z)\} = \{Q_S, G(z)\}\,, \quad G(z) \equiv 2\beta(z)\partial c(z) - \partial\beta(z)c(z)\,. \tag{6.3.19}$$

Hence the cohomology of Q_S is in the kernel of L_0. These two facts readily allow to identify the cohomology of Q_S as the states

$$e^{nb\phi(0)}c(0)\partial c(0)\cdots\partial^n c(0)|0\rangle\,, \qquad e^{-nb\phi(0)}b(0)\partial b(0)\cdots\partial^n b(0)|0\rangle\,. \tag{6.3.20}$$

When we turn on μ_B the BCFT becomes interacting and the action of $Q_S^{boundary}$ more complicated. Luckily the operator $e^{-b\phi(z)}$ that appears in Q_S is a degenerate field of level two for the Liouville CFT, and its OPEs truncate to two terms,

$$[e^{-b\phi}]\,[e^{\alpha\phi}] = [e^{(\alpha-b)\phi}] + C_-[e^{(\alpha+b)\phi}]\ . \tag{6.3.21}$$

[15]No confusion should arise between the parameter $b \equiv 1/\sqrt{2}$ and the antighost field $b(z)$!

Hence we can write

$$Q_S^{boundary} = Q_S^{(0)} + \mu_B^2 Q_S^{(2)} \,. \tag{6.3.22}$$

Note that for $\mu_B \neq 0$, $Q_S^{boundary}$ does not have definite J_0 charge, but it is a sum of the original charge zero term $Q_S^{(0)}$ plus a deformation of charge two $Q_S^{(2)}$. ($Q_S^{(2)}$ has charge two under J_0 becayse it has ghost number minus one and shifts the Liouville momentum of $+b$).

This is a mild deformation of $Q_S^{(0)}$. Nihilpotency of the total $Q_S^{boundary}$ for any μ_B implies

$$(Q_S^{(0)})^2 = 0 \quad \{Q_S^{(2)}, Q_S^{(0)}\} = 0 \,, (Q_S^{(2)})^2 = 0 \,. \tag{6.3.23}$$

As the J_0 charge of $Q_S^{(2)}$ is nonzero, this implies that $Q_S^{(2)} = \{Q_S^{(0)}, \cdots\}$ and hence it acts trivially on Q_S^0 cohomology.

We conclude that the cohomology of $Q_S^{boundary} = Q_S^{(0)} + \mu_B^2 Q_S^{(2)}$ has the same dimensionality as the one of $Q_S^{(0)}$: one operator for each ghost number. We will mainly be interested in the ghost number one operator, the open string "tachyon" $e^{b\phi(0)}c_1|0\rangle$. It is immediate to check that this state is in the cohomology for any μ_B. We can repeat the same reasoning also to the BCFT with different boundary cosmological constants μ_B^i and μ_B^j at the two endpoints of the open string. The only states of ghost number one in the cohomology of $Q_S^{boundary}$ are the open tachyons between brane i and brane j,

$$e^{b\phi(0)}c_1|0\rangle_{ij} \,. \tag{6.3.24}$$

6.4 Open string field theory and the Kontsevich model

It is our prejudice that open string field theory (OSFT) [6] must play a fundamental role in the understanding of open/closed duality. The Kontsevich model provides the prototypical example. In this section we construct the OSFT on N of the stable branes of the $(2,1)$ string theory, and show how it reduces to the Kontsevich matrix integral.

6.4.1 Generalities

The OSFT on N D-branes takes quite generally the familiar form

$$S[\Psi] = -\frac{1}{g_s}\left(\frac{1}{2}\sum_{ij}\langle\Psi_{ij}, Q_B\Psi_{ji}\rangle + \frac{1}{3}\sum_{ijk}\langle\Psi_{ij},\Psi_{jk},\Psi_{ki}\rangle\right) \,. \tag{6.4.1}$$

Let us briefly review the basic ingredients of this action, referring to [211] for background material. The string field $|\Psi_{ij}\rangle$, $i,j = 1,\cdots N$, is an element of the open string state space $\mathcal{H}_{ij}$ between D-brane i and D-brane j. This is the full state-space of the matter + Liouville + ghost BCFT. In classical OSFT, we restrict $|\Psi_{ij}\rangle$ to have ghost number one (in the convention that the SL(2,R) vacuum $|0\rangle$ has ghost number zero). In the BCFT language, which is the most natural for our purposes, one uses the state-operator map to represent string fields as boundary vertex operators. The string field $|\Psi_{ij}\rangle$ can be expanded as a sum over a complete set of vertex operators,

$$|\Psi_{ij}\rangle = \sum_{\alpha} c_\alpha \mathcal{V}^\alpha_{ij}(0)|0\rangle\,. \tag{6.4.2}$$

Here $\mathcal{V}^\alpha_{ij}(0)$ is a vertex operator inserted at the origin of the upper half plane, with boundary conditions for brane i on the negative real axis, and boundary conditions for brane j on the positive real axis.

The 2-point and 3-point vertices are then defined in terms of BCFT correlators on the boundary (real axis) of the upper half-plane,

$$\begin{aligned} \langle A, B\rangle &\equiv \langle I\circ A(0)\, B(0)\rangle_{\rm UHP}\,, \quad I(z)\equiv -\frac{1}{z} \\ \langle A, B, C\rangle &\equiv \langle f_1\circ A(0)\, f_2\circ B(0)\, f_3\circ C(0)\rangle_{\rm UHP}\,. \end{aligned} \tag{6.4.3}$$

Here $f\circ A(0)$ denotes the conformal transform of the operator $A(0)$ by the complex map f. The precise form of the maps $f_i(z)$, which implement the midpoint gluing of the three open strings, can be found in many places and will not be important for us.

We also recall that the string field obeys the reality condition

$$|\Psi_{ij}\rangle^* = |\Psi_{ji}\rangle\,, \tag{6.4.4}$$

where the $*$ involution is defined to be [46]

$$* = {\rm bpz}^{-1}\circ {\rm hc} = {\rm hc}^{-1}\circ {\rm bpz}\,. \tag{6.4.5}$$

The operation 'hc' is hermitian conjugation of the state (it sends bras into a kets, with complex conjugation of the coefficients). The operation 'bpz' sends a bra into a ket according to the rule

$${\rm bpz}(\mathcal{V}(0)|0\rangle) = \langle 0|I\circ\mathcal{V}(0)\,. \tag{6.4.6}$$

Definition of the quantum theory requires gauge-fixing. This is customarily accomplished by imposing Siegel gauge $b_0|\Psi\rangle = 0$. One must introduce Fadeev-Popov ghosts for this gauge fixing,

and in fact, since the gauge symmetry is reducible, one needs ghosts for ghosts, and ghosts for ghosts for ghosts, ad infinitum. It is a famous miracle [212] that the full second-quantized gauge-fixed action + ghosts can be written in the form

$$S_{Siegel} = -\frac{1}{g_s}\left(\frac{1}{2}\sum_{ij}\langle\Psi_{ij}, c_0 L_0 \Psi_{ji}\rangle + \frac{1}{3}\sum_{ijk}\langle\Psi_{ij}, \Psi_{jk}, \Psi_{ki}\rangle\right) , \tag{6.4.7}$$

where $|\Psi_{ij}\rangle$ is now a string field of *unrestricted* ghost number, obeying

$$b_0|\Psi_{ij}\rangle = 0\,. \tag{6.4.8}$$

The propagator

$$\frac{b_0}{L_0} = \int_0^\infty b_0\, dt\, e^{-t\, L_0} \tag{6.4.9}$$

has the geometric interpretation of building worldsheet strips of canonical width π and length t. The Feynman diagrams are fatgraphs built joining these flat strips at trivalent vertices (with the curvature concentrated at the common midpoint of the three open strings). This gives the famous decomposition of the moduli space of open Riemann surfaces [162, 188, 189, 190, 191] which plays a crucial role in Kontsevich construction as well.

6.4.2 Topological localization

The general OSFT action (6.4.7) is a very complicated object. In the critical bosonic string, explicit calculations are available for some simple perturbative amplitudes. Off-shell, non-perturbative calculations in the classical theory have so far been possible only using numerical methods (level truncation). In the present case, a drastic simplification occurs thanks to a mechanism of topological localization. A precedent of this phenomenon was discovered by Witten for the topological open A-model on the cotangent bundle $T^*(M)$, which reduces to Chern-Simons on the three-dimensional manifold M.

The localization works in the way familiar for topological theories of cohomological type. The nilpotent supersymmetry $Q_S^{boundary}$ (henceforth simply Q_S) induces a pairing of the states of the theory, such that in a vacuum amplitudes almost all states cancel pairwise; only unpaired states (the cohomology of Q_S) give a non-zero contribution. Let us demonstrate this in a more formal way. We are going to prove that Q_S is a symmetry of the gauge-fixed OSFT action (6.4.7); moreover the action is almost entirely Q_S-exact, except for the terms involving only the open string tachyons between the N branes. This reduces the OSFT action to an $N \times N$ matrix integral.

The topological symmetry is defined as

$$\delta_S|\Psi\rangle = Q_S|\Psi\rangle\,, \tag{6.4.10}$$

and it is an invariance of the gauge-fixed action.

$$\delta_S\, S_{Siegel} = 0\,. \tag{6.4.11}$$

The formal properties that ensure this invariance are

$$\begin{aligned}\langle V_2|\,(Q_S^{(1)} + Q_S^{(2)}) &= 0 \\ \langle V_3|\,(Q_S^{(1)} + Q_S^{(2)} + Q_S^{(3)}) &= 0\,.\end{aligned} \tag{6.4.12}$$

Here we are regarding the 2-point and 3-point vertices as elements of $\mathcal{H}^*\otimes\mathcal{H}^*$ and $\mathcal{H}^*\otimes\mathcal{H}^*\otimes\mathcal{H}^*$, i.e., as bilinear and trilinear functionals on the state space $\mathcal{H} = \oplus_{ij}\mathcal{H}_{ij}$. These properties are an immediate consequence of the fact that Q_S is the zero-mode of a conserved current. They are easily proved by contour deformations on the 2- and 3-punctured disks that define the vertices (see *e.g.* [210]).

We can now write

$$\langle V_2| \;=\; \langle V_2|^{Q_S\,\mathrm{coho}} + \langle W_2|\,(Q_S^{(1)} + Q_S^{(2)})\,, \tag{6.4.13}$$

$$\langle V_3| \;=\; \langle V_3|^{Q_S\,\mathrm{coho}} + \langle W_3|\,(Q_S^{(1)} + Q_S^{(2)} + Q_S^{(3)})\,. \tag{6.4.14}$$

Here we have defined a cohomology problem for Q_S in the spaces $\mathcal{H}^*\otimes\mathcal{H}^*$ and $\mathcal{H}^*\otimes\mathcal{H}^*\otimes\mathcal{H}^*$ in the natural way. Equ.(6.4.13) is simply the statement that since the 2-point and 3-point vertices are Q_S closed (6.4.12), they can be written as a sum of a term in the Q_S cohomology plus a Q_S-exact term. By Künneth formula the cohomology in the tensor product space is the tensor product of the cohomology. Thus, dropping Q_S-exact terms, we can restrict the whole OSFT action to the string fields in the cohomology of Q_S.

The cohomology of Q_S was computed in section 3.2 and consists of the states

$$e^{nb\phi(0)}c(0)\partial c(0)\cdots\partial^n c(0)|0\rangle_{ij}\,, \qquad e^{-nb\phi(0)}b(0)\partial b(0)\cdots\partial^n b(0)|0\rangle_{ij}\,. \tag{6.4.15}$$

Of these states, only the ones with bc ghost number ≥ 1 satisfy the Siegel gauge condition. Among them, only the open string "tachyons"

$$|T_{ij}\rangle \equiv e^{b\phi}c_1|0\rangle_{ij} \tag{6.4.16}$$

can give a contribution to the action, since all the other fields do not saturate the conservation of bc ghost number, which must add up to three. This concludes the argument that the OSFT action reduces to the terms containing only the open string tachyons.

6.4.3 Liouville BCFT and the matrix model

Writing the string field $|\Psi_{ij}\rangle$ as

$$|\Psi_{ij}\rangle = X_{ij}|T_{ij}\rangle + \cdots \tag{6.4.17}$$

for some coefficient X_{ij}, $i,j = 1,\cdots N$, the OSFT reduces to a matrix model for the $N \times N$ matrix X. The reality condition (6.4.4) for the string field implies that X is hermitian. The action for the matrix integral is

$$S[X] = -\frac{Volume}{g_s}\left(\frac{1}{2}\,X_{ji}X_{ij}\,\langle T_{ji}, c_0L_0T_{ij}\rangle + \frac{1}{3}\,X_{ij}X_{jk}X_{ki}\,\langle T_{ij}, T_{jk}, T_{ki}\rangle\right). \tag{6.4.18}$$

Here we are normalizing the inner products so that

$$\langle c_1, c_0c_1\rangle = 1\,, \tag{6.4.19}$$

and correspondingly we have extracted a factor of the (divergent) volume of the brane coming from the integration over the zero mode of the Liouville field.[16] It only remains to evaluate the 2- and 3-point vertices for the open string tachyons, which define the coefficients in this matrix action.

The structure of the result can be understood by a simple reasoning. It turns out that for the specific values of Liouville momenta that we are interested in, the effect of μ_B can be treated perturbatively. The Liouville anomaly on the disk is $Q = 3b$. A correlator in which the total Liouville momentum adds to three (in units of b) should then not get any correction from the presence of a boundary cosmological constant. Since the open string tachyon has Liouville momentum one, we expect that the cubic vertex can be evaluated as a free BCFT correlator,

$$\langle T_{ij}, T_{jk}, T_{ki}\rangle = 1\,. \tag{6.4.20}$$

Notice that the local coordinates $f_i(z)$ play no role since these are on-shell primary vertex operators. On the other hand, in the kinetic term we expect to need one insertion of the boundary cosmological constant to saturate the anomaly. This contribution can come from either side of the strip, so it is reasonable to guess

$$\langle T_{ij}, c_0L_0T_{ij}\rangle \sim \mu_B^{(i)} + \mu_B^{(j)}\,. \tag{6.4.21}$$

[16] This overall factor is present also in all the closed string correlation functions of the the $\mathcal{O}_k$ operators, and it will consistenly cancel out in all formulas.

With these values for the coefficients the OSFT action would then become

$$S[X] = -\frac{1}{g_s}\left(\frac{1}{2}X_{ij}X_{ji}(\mu_B^{(i)}+\mu_B^{(j)}) + \frac{1}{3}X_{ij}X_{jk}X_{ki}\right) \tag{6.4.22}$$

This is the Kontsevich model (6.1.6), after the identification $\mu_B^{(i)} \equiv z_i$.

One may raise an immediate objection to this reasoning: the kinetic term should actually be zero, since the open tachyon has conformal dimension zero and is thus apparently killed by L_0. Exactly at $c_{Liou} = 28$ there is a loophole in this objection, because the scalar product $\langle T_{ij}, c_0 T_{ji}\rangle$ is divergent. A more careful analysis is then called for, involving the full machinery of Liouville BCFT.

To regulate the divergence in the tachyon 2-point function, we can go slightly off-shell, considering the state $e^{(b+\epsilon)\phi}c_1|0\rangle_{ij}$. As we show in the appendix, the 2-point function in boundary (FZZT) Liouville theory has a pole as $\epsilon \to 0$, precisely with the expected residue,

$$\langle e^{(b+\epsilon)\phi} e^{(b+\epsilon)\phi}\rangle_{1,2} \sim \frac{\mu_B^{(1)}+\mu_B^{(2)}}{\epsilon}\,. \tag{6.4.23}$$

This pole cancels the zero from the action of L_0,

$$L_0\, e^{\alpha\phi}c_1|0\rangle = (\alpha-b)(\alpha-2b)e^{\alpha\phi}c_1|0\rangle = \epsilon\,(-b)\,e^{\alpha\phi}c_1|0\rangle\,, \tag{6.4.24}$$

giving the desired result. The careful computation of the 3-point function (see the appendix) is rather uneventful and confirms (6.4.20).

This resonant behavior of Liouville field theory correlators is related to the fact that the critical exponent $\gamma_{str} \equiv 1 - 1/b^2$ equals minus one. In general, a similar resonant behavior occurs when γ_{str} is a negative integer [196]. The corresponding values of the central charge $c_{Liou} = 1 + 6(p+1)^2/p$, with integer $p \geq 2$, are precisely the ones needed to dress the matter minimal models $(p, 1)$. These are also the models where the string theory is known to be topological and a matrix model *à la* Kontsevich exists.

6.4.4 Discussion

We have seen that only on-shell fields (the open string tachyons) give non-zero contributions. This can be given a geometric interpretation: the whole vacuum amplitude has support on the region of moduli space where all propagator lengths in the fatgraph diverge. The localization on such singular Riemann surfaces is again familiar from the Chern-Simons example [170]. In the language of [170], we can say that there are no ordinary instantons, and only virtual instantons at infinity contribute. It is well-known that in topological gravity closed string amplitudes are localized on singular surfaces

[166, 187]. Here we are seeing this phenomenon in the open channel. While in the closed channel contact terms are quite intricate, the open string moduli space is structurally much simpler, and open string contact terms arise only when boundaries touch each other or pinch. This geometric intuition could be used to streamline the combinatorial proofs [213, 214] of the Virasoro constraints for the Kontsevich model.

6.5 Open/closed duality and Ward identities

The main conclusion to draw is that in this theory, the effect of D-branes can be completely accounted for by turning on a simple source term for the closed strings,

$$\mathcal{Z}^{open}(g_s, z_i) = \mathcal{Z}^{closed}\left(g_s, t_k = g_s \sum_i \frac{1}{k\, z_i^k}\right) . \tag{6.5.1}$$

This conclusion can be strengthened by considering the partition function of the theory in the presence of both a D-brane and a non-trivial closed string background.

Recall that in the closed string theory, the partition function is completely determined by the Virasoro Ward identities [187, 215]

$$\begin{aligned}
\frac{\partial}{\partial t_1}\mathcal{Z} = \mathcal{L}_{-2}\mathcal{Z} &\equiv \frac{t_1^2}{2g_s^2}\mathcal{Z} + \sum_{k=0}^{\infty}(2k+3)t_{2k+3}\frac{\partial \mathcal{Z}}{\partial t_{2k+1}} \\
\frac{\partial}{\partial t_3}\mathcal{Z} = \mathcal{L}_{0}\mathcal{Z} &\equiv \frac{1}{8}\mathcal{Z} + \sum_{k=0}^{\infty}(2k+1)t_{2k+1}\frac{\partial \mathcal{Z}}{\partial t_{2k+1}} \\
\frac{\partial}{\partial t_{2n+5}}\mathcal{Z} = \mathcal{L}_{2n+2}\mathcal{Z} &\equiv \sum_{k=0}^{\infty}(2k+1)t_{2k+1}\frac{\partial \mathcal{Z}}{\partial t_{2k+2n+1}} + \frac{g_s^2}{2}\sum_{k=0}^{n}\frac{\partial^2 \mathcal{Z}}{\partial t_{2k+1}\partial t_{2n-2k+1}} .
\end{aligned} \tag{6.5.2}$$

Each of these equations details how a specific $\mathcal{O}_k$ operator, when integrated over the Riemann surface, picks contributions from collision with other operators or with nodes of the surface [187, 215]. The second term in the $\mathcal{L}_{-2}$ and $\mathcal{L}_0$ equations, and the first term in the $\mathcal{L}_{2n+2}$ equation, represent the collision of two operators. The last term in the $\mathcal{L}_{2n+2}$ equation represents the collision between an operator and a node. (The first term in the $\mathcal{L}_{-2}$ equation accounts for the conformal Killing vectors of the sphere, and similarly the first term in the $\mathcal{L}_0$ equation accounts for the CKV of the torus.) The structure of these equations is strongly constrained by self-consistency; it is only because the $\mathcal{L}_{2n}$ form (half) a Virasoro algebra that these equations have a solution.

To find the partition function when both D-brane sources and closed string sources are turned on, we will now extend these Ward identities by adding the contact terms that arise from the new ways the surface can degenerate: when an operator $\mathcal{O}_k$ collides with a boundary; and when a boundary

collides with a node. The collision of an operator with a boundary has the schematic aspect shown in Figure 6.3.

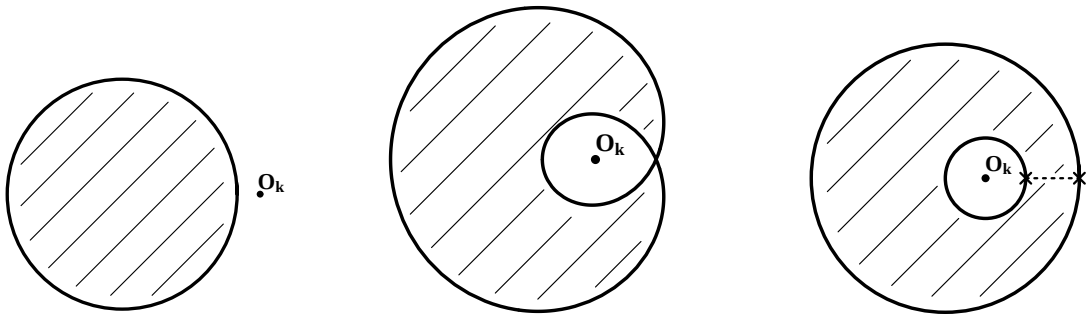

Figure 6.3: Degeneration of the Riemann surface as the closed string operator $\mathcal{O}_k$ approaches the boundary. The shadowed region represents the hole. As the short neck pinches, the surface factorizes into two surfaces, each with the extra insertion of an open string tachyon, indicated by a cross.

The short neck of the pinching surface is conformally equivalent to the insertion of a very long open string propagator; the collision leaves behind an open string tachyon insertion, with a power of z fixed by conservation of the Liouville momentum. This piece of knowledge, together with the requirement that we still have a Virasoro algebra, uniquely fixes the open + closed Ward identities. Considering for simplicity the case of a single D-brane with parameter z, they have the following form:

$$\begin{aligned}
\frac{\partial}{\partial t_1}\mathcal{Z} = \tilde{\mathcal{L}}^{(z)}_{-2}\mathcal{Z} &\equiv \mathcal{L}_{-2}\mathcal{Z} + (\frac{t_1}{z g_s} + \frac{1}{2z^2})\mathcal{Z} - \frac{1}{z}\frac{\partial \mathcal{Z}}{\partial z} \\
\frac{\partial}{\partial t_3}\mathcal{Z} = \tilde{\mathcal{L}}^{(z)}_{0}\mathcal{Z} &\equiv \mathcal{L}_{0}\mathcal{Z} - z\frac{\partial \mathcal{Z}}{\partial z} \\
\frac{\partial}{\partial t_{2n+5}}\mathcal{Z} = \tilde{\mathcal{L}}^{(z)}_{2n+2}\mathcal{Z} &\equiv \mathcal{L}_{2n+2}\mathcal{Z} - z^{2n+1}\frac{\partial \mathcal{Z}}{\partial z} - g_s\sum_{k=0}^{n} z^{2k+1}\frac{\partial \mathcal{Z}}{\partial t_{2n-2k+1}}\,.
\end{aligned} \tag{6.5.3}$$

The terms involving $\frac{\partial \mathcal{Z}}{\partial z}$ represent the collision of an operator with a boundary. The last term in the $\tilde{\mathcal{L}}^{(z)}_{2n+2}$ equation represents the collision of a boundary and a node. Finally the second term in the $\tilde{\mathcal{L}}^{(z)}_{-2}$ equation accounts for the CKV of the disk with two closed punctures and of the annulus with one closed puncture.

These identities are sufficient to completely determine the open + closed partition function $\mathcal{Z}^{open+closed}(g_s, t_k, z_i)$. Not surprisingly, one can easily verify that the solution is

$$\mathcal{Z}^{open+closed}(g_s, t_k, z_i) = \mathcal{Z}^{closed}\left(g_s, t_k + g_s\sum_i \frac{1}{k\, z_i^k}\right)\,. \tag{6.5.4}$$

This shows that even when there are non-trivial closed string sources to begin with, D-branes can still be re-absorbed into a shift of these sources. This argument also fixes the overall normalization in the relation between t_k and $\sum_i z_i^{-k}$. The closed operators $\mathcal{O}_k$ have an intrinsic normalization fixed by the algebra of closed contact terms. The algebra of open/closed contact terms can then be used to fix the coefficients of this canonically normalized $\mathcal{O}_k$ in the expansion of the boundary state. This ties a loose end in our derivation of the Kontsevich model.

We can also define an open partition function in a non-trivial closed background by subtracting the purely closed amplitudes,

$$\mathcal{Z}^{open}(g_s, z_i|t_k) = \frac{\mathcal{Z}^{open+closed}(g_s, t_k, z_i)}{\mathcal{Z}^{closed}(g_s, t_k)} \,. \tag{6.5.5}$$

An interesting question is whether this open partition function is computed by an appropriate generalization of the Kontsevich matrix model.

6.6 Future directions

There are many interesting directions in which the work of this chapter may be continued. In this section we mention some of them.

6.6.1 Relation with discretized random surface in D = −2

In this chapter we have focused on the Kontsevich model for the $(2,1)$ string theory. We have stressed that the finite N Kontsevich model There is also a double-scaled matrix model for this closed string theory, defined in terms of a matrix $M(\theta^1, \theta^2)$ that depends of two Grassmann-odd coordinates [195, 196, 197, 198, 199]. This model has a rich structure with many intriguing properties.

In the continuum limit, the coordinates θ^1 and θ^2 become precisely our fields Θ^α. This is one of the reasons why one should prefer the Θ^α system to the $\xi\eta$ system. Following the philosophy of [150], this doubled-scaled matrix model should be understood as the open string field theory on *unstable* D-branes of the theory. Indeed, if one considers in the continuum $(2,1)$ string theory ZZ boundary conditions for the Liouville direction, and Neumann b.c. for the Θ^α system, one finds that the tachyon dynamics is captured by a matrix $M(\theta_0^1, \theta_0^2)$, where θ_0^α are the zero-modes of Θ^α living on the Neumann boundary.

In [198], macroscopic loop operators for this matrix model are considered. The operators of topological gravity appear to be related to loop operators with Dirichlet boundary conditions on the

θ^α. This seems to agree with our construction, and it would be nice to understand this connection in detail.

More generally, it is of interest to see whether our approach can shed some light on open/closed duality [150] for the double-scaled matrix models. In the "old" approach, the doubled-scaled matrix model is thought of as a trick to discretize the Riemann surface, and it is essential to send N to infinity and $t \to t_c$ to recover the continuum theory. The modern approach starts instead from considering the worldvolume theory of a finite number N of ZZ branes in the continuum string theory. The precise relation between the old and the new approach is still a bit mysterious, as it seems that one cannot directly identify the finite N matrix model before double-scaling limit and the finite N open string field theory of the ZZ branes. The OSFT of N ZZ branes, with N finite, is presumably a unique and consistent continuum quantum theory, while the finite N matrix model has non-universal features, like the precise form of the potential. The OSFT on N ZZ branes may be expected [218] to be dual to a subsector of the full continuum closed string theory. This is in analogy with the finite N Kontsevich model.[17]

6.6.2 Generalizations

The most obvious generalization of this work that comes to mind is to the other (p, q) minimal string theories. (p, q) theories are solved by double-scaling of the $(p-1)$-matrix chain, where again q labels the order of criticality. $(p, 1)$ models represent the 'topological points', from which the (p, q) models with $q > 1$ are obtained by flows of the p-KdV hierarchy. There is a Kontsevich model for any $(p, 1)$ theory, it is a one-matrix integral with a potential of order $p + 1$. Our logic leads us to believe that the OSFT on the stable branes of the $(p, 1)$ theory will localize topologically to a matrix integral. Since OSFT is cubic, this process will lead to a cubic matrix integral involving several matrices (a matrix for each open topological primary). The simplest guess is that such cubic models are related to the known polynomial Kontsevich models by integrating out all matrices but one. A formulation in terms of a cubic multi-matrix integral may have the advantage of making more transparent the relation with a decomposition of moduli space, which has not been completly understood for the intersection numbers associated to the $(p, 1)$ models. Work is in progress along these lines.

Several other generalizations can be contemplated. $\hat{c} < 1$ theories admit topological points and to the best of our knowledge there is no known topological matrix model description; our procedure should give one. The case of $c = 1$ at the self-dual radius should also be attacked.

[17] We thank Ashoke Sen for pointing out this analogy.

6.7 Conclusions

In this chapter we have described an example of exact open/closed duality that should represent the simplest paradigm for a large class of similar dualities. The worldsheet picture of holes shrinking to punctures is not, we believe, an artifact of the simplicity of the model, and the same mechanism may be at work in more physical situations. We have found that at least in this example, open string field theory on an infinite number of branes is capable of describing the full string theory. This may contain a more general lesson.[18] Although here we have stressed the importance of open string field theory as a tool to understand open/closed duality, one of our original motivations was to learn about the structure of OSFT itself in the solvable context of low-dimensional string theories. The Kontsevich model is arguably the simplest imaginable OSFT - it is still a good question whether this and related examples can be used to sharpen our understanding of OSFT.

We would like to conclude with a speculation about how this may come about in the case of AdS/CFT. The example of the Kontsevich model suggests that the natural starting point is the closed string theory dual to free SYM ('t Hooft parameter $t = 0$). At the point $t = 0$, which in some sense must correspond to an infinitely curved AdS space, the closed string theory is expected to have an infinite dimensional symmetry group. This is analogous to the statement that $\{t_k = 0\}$ is the topological point of the Kontsevich model. If a a concrete description of this closed string theory were available, one may also hope to define D-branes. D-branes of a peculiar nature may exist, such that: 1)The open string field theory on these D-branes is precisely the SYM theory, with no extra massive open string modes. 2)When considered in the closed string channel, the presence of the D-brane can be completely re-adsorbed in a shift of the closed string background. Adding D-branes would then be equivalent to turning on a finite t, that is, to recovering a smooth AdS space. Statement 1) is analogous to the topological localization that we have described for the Kontsevich model, while statement 2) is the by now familiar mantra of replacing boundaries with punctures. This scenario would offer a derivation of AdS/CFT orthogonal to the usual one [1] that begins with D-branes in flat space and proceeds by "dropping the one" in the harmonic function.

[18] Open string field theory on an infinite number of branes has been conjectured [217] to be relevant for the issue of background independence in string theory.

6.8 Liouville BCFT correlators

In this appendix we give the technical details of the computation of 2- and 3-point vertices of open string tachyons.

We need the explicit expressions of 2- and 3-point functions of boundary primary operators in Liouville BCFT (with FZZT boundary conditions). The relevant formulas can be found in [158, 209]. We use the notations of [158]. The variable s is conventionally introduced[19]

$$\frac{\mu_B}{\sqrt{\mu}} = \cosh b\pi s\,. \tag{6.8.1}$$

Here μ is the bulk cosmological constant. We are interested in the limit $\mu \to 0$, since this is the topological point $t_k = 0$. Interestingly, the results for 2- and 3-point correlators of open string tachyon turn out to be independent of μ. We do not have a complete physical understanding of this fact. We suspect that turning on a non-zero μ would spoil our construction in other places.

An important ingredient is the special function $\mathbf{G}_b(x)$ defined in [158]. This function is entire-analytic and has zeros for $x = -nb - m/b$, with $m, n = 0, 1, 2, \cdots$; it is symmetric under $b \leftrightarrow 1/b$. A convenient combination of $\mathbf{G_b}$'s is the function $\mathbf{S}_b(x) = \mathbf{G}_b(Q-x)/\mathbf{G}_b(x)$, which obeys the shift relation

$$\mathbf{S}_b(x+b) = 2\sin(\pi b x)\mathbf{S}_b(x)\,. \tag{6.8.2}$$

The 2-point function of boundary primary fields is then [158]

$$\begin{aligned} d(\alpha,\mu_B^{(1)},\mu_B^{(2)},\mu) \equiv \langle e^{\alpha\phi}e^{\alpha\phi}\rangle = (\frac{\pi}{\sqrt{2}}\mu\gamma(\frac{1}{2}))^{\frac{3}{2}-\frac{\alpha}{\sqrt{2}}} \times \\ \times \frac{\mathbf{G}_{\frac{1}{\sqrt{2}}}(-2\alpha+\frac{3}{\sqrt{2}})\mathbf{S}_{\frac{1}{\sqrt{2}}}(\frac{3}{\sqrt{2}}+i(\,s_1+\,s_2)/2-\alpha\,)\mathbf{S}_{\frac{1}{\sqrt{2}}}(\frac{3}{\sqrt{2}}+i(\,s_1-\,s_2)/2-\alpha)}{\mathbf{G}_{\frac{1}{\sqrt{2}}}(-\frac{3}{\sqrt{2}}+2\alpha)\mathbf{S}_{\frac{1}{\sqrt{2}}}(i(\,s_1+\,s_2)/2+\alpha)\mathbf{S}_{\frac{1}{\sqrt{2}}}(i(\,s_1-\,s_2)/2+\alpha)}\,. \end{aligned} \tag{6.8.3}$$

We now take $\alpha = b + \epsilon$. As $\epsilon \to 0$ there is a pole arising from the zero of the first $\mathbf{G}_b$ in the denominator. The interesting residue is contained in the part of the expression, finite for $\alpha \to b = \frac{1}{\sqrt{2}}$, that contains the four $\mathbf{S}_{\frac{1}{\sqrt{2}}}$ functions,

$$\begin{aligned} &\frac{\mathbf{S}_{\frac{1}{\sqrt{2}}}(\frac{2}{\sqrt{2}}+i(\,s_1+\,s_2)/2)\mathbf{S}_{\frac{1}{\sqrt{2}}}(\frac{2}{\sqrt{2}}+(\,s_1-\,s_2)/2)}{\mathbf{S}_{\frac{1}{\sqrt{2}}}(i(\,s_1+\,s_2)/2+\frac{1}{\sqrt{2}})\mathbf{S}_{\frac{1}{\sqrt{2}}}(i(\,s_1-\,s_2)/2+\frac{1}{\sqrt{2}})} = \\ &4\sin(\frac{\pi}{2}+\frac{i\pi}{2\sqrt{2}}(s_1+s_2))\sin(\frac{\pi}{2}+\frac{i\pi}{2\sqrt{2}}(-s_1+s_2)) = \\ &2\cosh(\frac{\pi}{\sqrt{2}}s_1)+2\cosh(\frac{\pi}{\sqrt{2}}s_2) = 2\,\frac{\mu_B^{(1)}+\mu_B^{(2)}}{\sqrt{\mu}}\,. \end{aligned} \tag{6.8.4}$$

[19] The FZZT BCFT shows an interesting monodromy in the complex μ_B plane [219]. The physics is instead entire-analytic in terms of s.

The factor of $1/\sqrt{\mu}$ cancels against the $\sqrt{\mu}$ in the prefactor of (6.8.3). This proves the claim (6.4.23).

The three point function simplifies when one takes the three Liouville momenta to be equal to b. For generic b, this 3-point function is proportional to a rational function of μ, μ_B and the 'dual' cosmological constant $\tilde{\mu}_B$ [209],

$$\langle e^{b\phi}\, e^{b\phi}\, e^{b\phi}\rangle \sim \frac{\tilde{\mu}_B^{(1)}(\mu_B^{(2)}-\mu_B^{(3)})+\tilde{\mu}_B^{(2)}(\mu_B^{(3)}-\mu_B^{(1)})+\tilde{\mu}_B^{(3)}(\mu_B^{(1)}-\mu_B^{(2)})}{(\mu_B^{(2)}-\mu_B^{(3)})(\mu_B^{(3)}-\mu_B^{(1)})(\mu_B^{(1)}-\mu_B^{(2)})}. \tag{6.8.5}$$

For $c_{Liou}=28$, the dual cosmological constants obey

$$\tilde{\mu}_B^{(i)} \sim (2(\mu_B^{(i)})^2-\mu) \tag{6.8.6}$$

and the tachyon 3-point function is just a constant independent of μ and μ_B^i.

Here we have computed the Liouville correlators using analytic continuation in the Liouville momentum. Equally well, we could have use analytic continuation in b to regulate the expressions that become singular as $b \to 1/\sqrt{2}$. Indeed one of the achievements of the past few years has been the recognition that Liouville correlators have nice analytic properties with respect to all the parameters. If one insists in working strictly at $b=1/\sqrt{2}$ and with the on-shell vertex operators $e^{b\phi}$, an alternative way to phrase the results is the language of logarithmic CFT [201]. For generic b, the two operators $e^{\alpha\phi}$ and $e^{(Q-\alpha)\phi}$ are identified as

$$e^{\alpha\phi} = d(\alpha,\mu_B^{(1)},\mu_B^{(2)},\mu)\, e^{(Q-\alpha)\phi}\,. \tag{6.8.7}$$

The reflection coefficient $d(\alpha,\mu_B^{(1)},\mu_B^{(2)},\mu)$ has poles for $Q-2\alpha = nb+m/b$. For these cases, the identification becomes ill-defined. One way around this is that for these resonant values $\tilde{\alpha}$ we modify the identification as

$$(L_0-h_{\tilde{\alpha}})\, e^{\tilde{\alpha}\phi} = \Big[\lim_{\alpha\to\tilde{\alpha}}((h_\alpha-h_{\tilde{\alpha}})d(\alpha,\mu_B^{(1)},\mu_B^{(2)},\mu))\Big]\, e^{(Q-\tilde{\alpha})\phi}\,. \tag{6.8.8}$$

Notice that the term is in square brackets is just a finite coefficient. L_0 cannot be diagonalized in the subspace spanned by $e^{\tilde{\alpha}\phi}$ and $e^{(Q-\tilde{\alpha})\phi}$, which forms a non-trivial Jordan cell. In other terms, the two operators are a logarithmic pair. In our case, $\tilde{\alpha}=b$. Working at b strictly equal to $1/\sqrt{2}$, we can write

$$L_0\, e^{\phi(0)/\sqrt{2}} c_1|0\rangle_{ij} = (\mu_B^{(i)}+\mu_B^{(j)})\, e^{\sqrt{2}\phi(0)} c_1|0\rangle_{ij}\,. \tag{6.8.9}$$

This gives an alternative way to understand why the tachyon kinetic term in the OSFT action is $(\mu_B^{(i)}+\mu_B^{(j)})$.

References

[1] J. M. Maldacena, "The large N limit of superconformal field theories and supergravity," Adv. Theor. Math. Phys. **2**, 231 (1998) [Int. J. Theor. Phys. **38**, 1113 (1999)] [arXiv:hep-th/9711200].

[2] E. Witten, Adv. Theor. Math. Phys. **2**, 253 (1998) [arXiv:hep-th/9802150].

[3] S. S. Gubser and I. R. Klebanov, Phys. Rev. D **58**, 125025 (1998) [arXiv:hep-th/9808075].

[4] M. Green, J. Schwarz and E.Witten, "Superstring Theory Vol. 1" Cambridge University Press (1987).

[5] J. Polchinski, "String Theory Vol. 1" Cambridge University Press (1995).

[6] E. Witten, "Noncommutative Geometry And String Field Theory," Nucl. Phys. B **268**, 253 (1986).

[7] G. 't Hooft, "A Planar Diagram Theory For Strong Interactions," Nucl. Phys. B **72** (1974) 461.

[8] A. Sen, Int. J. Mod. Phys. **A14**, 4061 (1999) [hep-th/9902105];

[9] A. Sen, "Universality of the tachyon potential", JHEP **9912**, 027 (1999) [hep-th/9911116].

[10] V. A. Kostelecky and S. Samuel, "On A Nonperturbative Vacuum For The Open Bosonic String", Nucl. Phys. B **336**, 263 (1990);

[11] D. Gaiotto, L. Rastelli, A. Sen and B. Zwiebach, "Patterns in open string field theory solutions," JHEP **0203**, 003 (2002) [arXiv:hep-th/0201159].

[12] L. Rastelli and B. Zwiebach, "Tachyon potentials, star products and universality," JHEP **0109**, 038 (2001) [arXiv:hep-th/0006240].

[13] A. Sen and B. Zwiebach, "Tachyon Condensation in String Field Theory", JHEP **0003**, 002 (2000) [hep-th/9912249];

[14] N. Moeller and W. Taylor, Level truncation and the tachyon in open bosonic string field theory", Nucl. Phys. **B583**, 105 (2000) [hep-th/0002237];

[15] H. Hata and S. Shinohara, "BRST invariance of the non-perturbative vacuum in bosonic open string field theory," JHEP **0009**, 035 (2000) [arXiv:hep-th/0009105].

[16] M. Schnabl, "Constraints on the tachyon condensate from anomalous symmetries," Phys. Lett. B **504**, 61 (2001) [arXiv:hep-th/0011238].

[17] W. Taylor, "A perturbative analysis of tachyon condensation," arXiv:hep-th/0208149.

[18] V. A. Kostelecky and R. Potting, Phys. Rev. D **63**, 046007 (2001) [hep-th/0008252]. L. Rastelli, A. Sen and B. Zwiebach, Adv. Theor. Math. Phys. **5**, 393 (2002) [arXiv:hep-th/0102112]; JHEP **0111**, 035 (2001) [arXiv:hep-th/0105058]; JHEP **0111**, 045 (2001) [arXiv:hep-th/0105168]. D. J. Gross and W. Taylor, JHEP **0108**, 009 (2001) [arXiv:hep-th/0105059]; JHEP **0108**, 010 (2001) [arXiv:hep-th/0106036]. D. Gaiotto, L. Rastelli, A. Sen and B. Zwiebach, JHEP **0204**, 060 (2002) [arXiv:hep-th/0202151]. M. Schnabl, arXiv:hep-th/0201095; arXiv:hep-th/0202139. L. Bonora, D. Mamone and M. Salizzoni, Nucl. Phys. B **630**, 163 (2002) [arXiv:hep-th/0201060]; JHEP **0204**, 020 (2002) [arXiv:hep-th/0203188]. E. Fuchs, M. Kroyter and A. Marcus, JHEP **0209**, 022 (2002) [arXiv:hep-th/0207001].

[19] I. Bars, Phys. Lett. B **517**, 436 (2001) [arXiv:hep-th/0106157]. Bars and Y. Matsuo, Phys. Rev. D **65**, 126006 (2002) [arXiv:hep-th/0202030]; Phys. Rev. D **66**, 066003 (2002) [arXiv:hep-th/0204260].

[20] L. Rastelli, A. Sen and B. Zwiebach, "Star algebra spectroscopy," JHEP **0203**, 029 (2002) [arXiv:hep-th/0111281].

[21] M. R. Douglas, H. Liu, G. Moore and B. Zwiebach, "Open string star as a continuous Moyal product," JHEP **0204**, 022 (2002) [arXiv:hep-th/0202087].

[22] B. Feng, Y. H. He and N. Moeller, JHEP **0204**, 038 (2002) [arXiv:hep-th/0202176]; JHEP **0205**, 041 (2002) [arXiv:hep-th/0203175]. B. Chen and F. L. Lin, Nucl. Phys. B **637**, 199 (2002) [arXiv:hep-th/0203204]; arXiv:hep-th/0204233. D. M. Belov, arXiv:hep-th/0204164. T. G. Erler, arXiv:hep-th/0205107. D. M. Belov and A. Konechny, arXiv:hep-th/0207174; arXiv:hep-th/0210169. E. Fuchs, M. Kroyter and A. Marcus, arXiv:hep-th/0210155. D.M. Belov, arXiv:hep-th/0210199.

[23] L. Rastelli, A. Sen and B. Zwiebach, "String field theory around the tachyon vacuum," Adv. Theor. Math. Phys. **5**, 353 (2002) [arXiv:hep-th/0012251].

[24] D. Gaiotto, L. Rastelli, A. Sen and B. Zwiebach, "Ghost structure and closed strings in vacuum string field theory," arXiv:hep-th/0111129.

[25] Y. Okawa, "Open string states and D-brane tension from vacuum string field theory," JHEP **0207**, 003 (2002) [arXiv:hep-th/0204012].

[26] H. Hata and T. Kawano, JHEP **0111**, 038 (2001) [arXiv:hep-th/0108150]. L. Rastelli, A. Sen and B. Zwiebach, JHEP **0202**, 034 (2002) [arXiv:hep-th/0111153]. H. Hata, S. Moriyama and S. Teraguchi, JHEP **0202**, 036 (2002) [arXiv:hep-th/0201177]. H. Hata and H. Kogetsu, JHEP **0209**, 027 (2002) [arXiv:hep-th/0208067].

[27] K. Okuyama, JHEP **0201**, 043 (2002) [arXiv:hep-th/0111087]; JHEP **0201**, 027 (2002) [arXiv:hep-th/0201015]; JHEP **0203**, 050 (2002) [arXiv:hep-th/0201136]. T. Okuda, Nucl. Phys. B **641**, 393 (2002) [arXiv:hep-th/0201149]. Y. Imamura, JHEP **0207**, 042 (2002) [arXiv:hep-th/0204031].

[28] Presentation by L. Rastelli at Strings 2002, Cambridge, July 15-20 2002, on-line proceedings at `www.damtp.cam.ac.uk/strings02/avt/rastelli/`.

[29] J. Kluson, JHEP **0204**, 043 (2002) [arXiv:hep-th/0202045]; arXiv:hep-th/0209255. I. Kishimoto and K. Ohmori, JHEP **0205**, 036 (2002) [arXiv:hep-th/0112169]. T. Takahashi and S. Tanimoto, JHEP **0203**, 033 (2002) [arXiv:hep-th/0202133]. I. Kishimoto and T. Takahashi, arXiv:hep-th/0205275.

[30] W. Taylor, "D-brane effective field theory from string field theory," Nucl. Phys. B **585**, 171 (2000) [arXiv:hep-th/0001201].

[31] J. A. Harvey and P. Kraus, "D-branes as unstable lumps in bosonic open string field theory," JHEP **0004**, 012 (2000) [arXiv:hep-th/0002117].

[32] R. de Mello Koch, A. Jevicki, M. Mihailescu and R. Tatar, "Lumps and p-branes in open string field theory," Phys. Lett. B **482**, 249 (2000) [arXiv:hep-th/0003031].

[33] N. Moeller, A. Sen and B. Zwiebach, "D-branes as tachyon lumps in string field theory," JHEP **0008**, 039 (2000) [arXiv:hep-th/0005036].

[34] J. R. David, "U(1) gauge invariance from open string field theory," JHEP **0010**, 017 (2000) [arXiv:hep-th/0005085].

[35] A. Sen and B. Zwiebach, "Large marginal deformations in string field theory," JHEP **0010**, 009 (2000) [arXiv:hep-th/0007153].

[36] W. Taylor, Mass generation from tachyon condensation for vector fields on D-branes", JHEP **0008**, 038 (2000) [hep-th/0008033];

[37] R. de Mello Koch and J. P. Rodrigues, "Lumps in level truncated open string field theory," Phys. Lett. B **495**, 237 (2000) [arXiv:hep-th/0008053].

[38] N. Moeller, "Codimension two lump solutions in string field theory and tachyonic theories," arXiv:hep-th/0008101.

[39] H. Hata and S. Teraguchi, "Test of the Absence of Kinetic Terms around the Tachyon Vacuum in Cubic String Field Theory", hep-th/0101162;

[40] I. Ellwood and W. Taylor, "Open string field theory without open strings", hep-th/0103085;

[41] B. Feng, Y. He and N. Moeller, "Testing the uniqueness of the open bosonic string field theory vacuum", hep-th/0103103;

[42] P. Mukhopadhyay and A. Sen, "Test of Siegel gauge for the lump solution," JHEP **0102**, 017 (2001) [arXiv:hep-th/0101014].

[43] I. Ellwood, B. Feng, Y. H. He and N. Moeller, "The identity string field and the tachyon vacuum," JHEP **0107**, 016 (2001) [arXiv:hep-th/0105024].

[44] I. Ellwood and W. Taylor, "Gauge invariance and tachyon condensation in open string field theory," arXiv:hep-th/0105156.

[45] K. Ohmori, "Survey of the tachyonic lump in bosonic string field theory," JHEP **0108**, 011 (2001) [arXiv:hep-th/0106068].

[46] M. R. Gaberdiel and B. Zwiebach, "Tensor constructions of open string theories I: Foundations," Nucl. Phys. B **505**, 569 (1997) [arXiv:hep-th/9705038].

[47] B. Zwiebach, "Trimming the tachyon string field with SU(1,1)," arXiv:hep-th/0010190.

[48] H. G. Kausch, "Curiosities at c=-2," arXiv:hep-th/9510149.

[49] W. Taylor, "Perturbative diagrams in string field theory," arXiv:hep-th/0207132.

[50] J. A. Shapiro and C. B. Thorn, "Closed String - Open String Transitions And Witten's String Field Theory," Phys. Lett. B **194**, 43 (1987).

[51] B. Zwiebach, "Interpolating string field theories," Mod. Phys. Lett. A **7**, 1079 (1992) [arXiv:hep-th/9202015].

[52] A. Hashimoto and N. Itzhaki, "Observables of string field theory," JHEP **0201**, 028 (2002) [arXiv:hep-th/0111092].

[53] S. L. Shatashvili, "On field theory of open strings, tachyon condensation and closed strings," arXiv:hep-th/0105076.

[54] N. Drukker, "Closed string amplitudes from gauge fixed string field theory," arXiv:hep-th/0207266.

[55] A. Sen, JHEP **0204**, 048 (2002) [arXiv:hep-th/0203211]. arXiv:hep-th/0203265. Mod. Phys. Lett. A **17**, 1797 (2002) [arXiv:hep-th/0204143]. JHEP **0210**, 003 (2002) [arXiv:hep-th/0207105]. N. Moeller and B. Zwiebach, arXiv:hep-th/0207107.

[56] L. Rastelli, A. Sen and B. Zwiebach, "String field theory around the tachyon vacuum", hep-th/0012251.

[57] L. Rastelli, A. Sen and B. Zwiebach, "Classical solutions in string field theory around the tachyon vacuum," hep-th/0102112.

[58] L. Rastelli, A. Sen and B. Zwiebach, "Half-strings, Projectors, and Multiple D-branes in Vacuum String Field Theory", hep-th/0105058.

[59] L. Rastelli, A. Sen and B. Zwiebach, "Boundary CFT Construction of D-branes in Vacuum String Field Theory," hep-th/0105168.

[60] L. Rastelli, A. Sen and B. Zwiebach, "Vacuum string field theory," hep-th/0106010.

[61] D. J. Gross and W. Taylor, "Split string field theory. I," JHEP **0108**, 009 (2001) [arXiv:hep-th/0105059].

[62] D. J. Gross and W. Taylor, "Split string field theory. II," JHEP **0108**, 010 (2001) [arXiv:hep-th/0106036].

[63] T. Kawano and K. Okuyama, "Open string fields as matrices," JHEP **0106**, 061 (2001) [arXiv:hep-th/0105129].

[64] J. R. David, "Excitations on wedge states and on the sliver," JHEP **0107**, 024 (2001) [arXiv:hep-th/0105184].

[65] K. Furuuchi and K. Okuyama, "Comma vertex and string field algebra," JHEP **0109**, 035 (2001) [arXiv:hep-th/0107101].

[66] H. Hata and T. Kawano, "Open string states around a classical solution in vacuum string field theory," hep-th/0108150.

[67] I. Kishimoto, "Some properties of string field algebra," [arXiv:hep-th/0110124].

[68] P. Mukhopadhyay, "Oscillator representation of the BCFT construction of D-branes in vacuum string field theory," arXiv:hep-th/0110136.

[69] N. Moeller, "Some exact results on the matter star-product in the half-string formalism," arXiv:hep-th/0110204.

[70] H. Hata and S. Moriyama, "Observables as twist anomaly in vacuum string field theory," arXiv:hep-th/0111034.

[71] G. Moore and W. Taylor, "The singular geometry of the sliver," arXiv:hep-th/0111069.

[72] K. Okuyama, "Siegel gauge in vacuum string field theory," [arXiv:hep-th/0111087].

[73] V. A. Kostelecky and R. Potting, "Analytical construction of a nonperturbative vacuum for the open bosonic string," Phys. Rev. D **63**, 046007 (2001) [hep-th/0008252].

[74] D. Gross, http://online.itp.ucsb.edu/online/mtheory_01/gross/

[75] E. Witten, Phys. Rev. **D46**, 5467 (1992) [hep-th/9208027];

[76] D. Gaiotto, L. Rastelli, A. Sen, and B. Zwiebach, MISSING REFERENCE.

[77] D. Z. Freedman, S. B. Giddings, J. A. Shapiro and C. B. Thorn, Nucl. Phys. B **298**, 253 (1988).

[78] D. J. Gross and A. Jevicki, "Operator Formulation Of Interacting String Field Theory. 2," Nucl. Phys. **B287**, 225 (1987).

[79] A. LeClair, M. E. Peskin and C. R. Preitschopf, Nucl. Phys. B **317**, 411 (1989);

[80] B. Zwiebach, "Closed string field theory: Quantum action and the B-V master equation," Nucl. Phys. B **390**, 33 (1993) [arXiv:hep-th/9206084].

[81] B. Zwiebach, "Quantum Closed Strings From Minimal Area," Mod. Phys. Lett. A **5**, 2753 (1990).

[82] B. Zwiebach, "Minimal area problems and quantum open strings," Commun. Math. Phys. **141**, 577 (1991).

[83] S. B. Giddings, E. J. Martinec and E. Witten, Phys. Lett. B **176**, 362 (1986).

[84] B. Zwiebach, "A Proof that Witten's open string theory gives a single cover of moduli space," Commun. Math. Phys. **142**, 193 (1991).

[85] M. Saadi and B. Zwiebach, Annals Phys. **192**, 213 (1989).

[86] P. Yi, Nucl. Phys. B **550**, 214 (1999) [hep-th/9901159]; A. Sen, JHEP **9910**, 008 (1999) [hep-th/9909062]; O. Bergman, K. Hori and P. Yi, Nucl. Phys. B **580**, 289 (2000), [hep-th/0002223]; G. Gibbons, K. Hori and P. Yi, Nucl. Phys. B **596**, 136 (2001) [hep-th/0009061]; A. Sen, hep-th/0010240.

[87] A. A. Gerasimov and S. L. Shatashvili, JHEP **0101**, 019 (2001) [hep-th/0011009]; S. L. Shatashvili, "On field theory of open strings, tachyon condensation and closed strings," arXiv:hep-th/0105076.

[88] A. Sen, "Some issues in non-commutative tachyon condensation," JHEP **0011**, 035 (2000) [arXiv:hep-th/0009038].

[89] Y. Matsuo, "BCFT and sliver state," Phys. Lett. B **513**, 195 (2001) [arXiv:hep-th/0105175].

[90] L. Rastelli, A. Sen and B. Zwiebach, "A note on a proposal for the tachyon state in vacuum string field theory," hep-th/0111153.

[91] L. Rastelli, A. Sen and B. Zwiebach, "Star algebra spectroscopy," arXiv:hep-th/0111281.

[92] I. Kishimoto and K. Ohmori, "CFT description of identity string field: Toward derivation of the VSFT action," arXiv:hep-th/0112169.

[93] R. Rashkov and K. S. Viswanathan, "A note on the tachyon state in vacuum string field theory," arXiv:hep-th/0112202; "A proposal for the vector state in vacuum string field theory," arXiv:hep-th/0201229.

[94] I. Y. Arefeva, A. A. Giryavets and P. B. Medvedev, "NS matter sliver," arXiv:hep-th/0112214.

[95] I. Y. Arefeva, D. M. Belov and A. A. Giryavets, "Construction of the vacuum string field theory on a non-BPS brane," arXiv:hep-th/0201197.

[96] M. Marino and R. Schiappa, "Towards vacuum superstring field theory: The supersliver," arXiv:hep-th/0112231.

[97] K. Okuyama, "Ghost Kinetic Operator of Vacuum String Field Theory," arXiv:hep-th/0201015.

[98] L. Bonora, D. Mamone and M. Salizzoni, "B field and squeezed states in vacuum string field theory," arXiv:hep-th/0201060.

[99] K. Okuyama, "Ratio of tensions from vacuum string field theory," arXiv:hep-th/0201136.

[100] T. Okuda, "The equality of solutions in vacuum string field theory," arXiv:hep-th/0201149.

[101] H. Hata, S. Moriyama and S. Teraguchi, "Exact results on twist anomaly," arXiv:hep-th/0201177.

[102] M. Schnabl, "Anomalous reparametrizations and butterfly states in string field theory" arXiv:hep-th/0202139.

[103] D. J. Gross and A. Jevicki, "Operator Formulation Of Interacting String Field Theory," Nucl. Phys. **B283**, 1 (1987).

[104] I. Bars and Y. Matsuo, "Associativity Anomaly in String Field Theory," arXiv:hep-th/0202030.

[105] H. M. Chan, J. Bordes, S. T. Tsou and L. Nellen, Phys. Rev. D **40** (1989) 2620;
J. Bordes, H. M. Chan, L. Nellen and S. T. Tsou, Nucl. Phys. B **351** (1991) 441;
J. Bordes, A. Abdurrahman and F. Anton, Phys. Rev. D **49** (1994) 2966 [arXiv:hep-th/9306029];
A. Abdurrahman, F. Anton and J. Bordes, Nucl. Phys. B **411** (1994) 693;
A. Abdurrahman and J. Bordes, Phys. Rev. D **58** (1998) 086003;
T. Kawano and K. Okuyama, "Open string fields as matrices," JHEP **0106**, 061 (2001) [arXiv:hep-th/0105129].

[106] I. Bars, "Map of Witten's * to Moyal's *," Phys. Lett. B **517**, 436 (2001) [arXiv:hep-th/0106157].

[107] M. Schnabl, "Wedge states in string field theory," arXiv:hep-th/0201095.

[108] M. Gutperle and A. Strominger, "Spacelike branes," JHEP **0204**, 018 (2002) [arXiv:hep-th/0202210].

[109] A. Sen, "Rolling tachyon," JHEP **0204**, 048 (2002) [arXiv:hep-th/0203211].

[110] A. Sen, "Tachyon matter," JHEP **0207**, 065 (2002) [arXiv:hep-th/0203265].

[111] A. Sen, "Field theory of tachyon matter," Mod. Phys. Lett. A **17**, 1797 (2002) [arXiv:hep-th/0204143].

[112] A. Sen, "Time evolution in open string theory," JHEP **0210**, 003 (2002) [arXiv:hep-th/0207105].

[113] P. Mukhopadhyay and A. Sen, "Decay of unstable D-branes with electric field," JHEP **0211**, 047 (2002) [arXiv:hep-th/0208142].

[114] A. Strominger, "Open string creation by S-branes," arXiv:hep-th/0209090.

[115] A. Sen, "Time and tachyon," arXiv:hep-th/0209122.

[116] F. Larsen, A. Naqvi and S. Terashima, "Rolling tachyons and decaying branes," JHEP **0302**, 039 (2003) [arXiv:hep-th/0212248].

[117] M. Gutperle and A. Strominger, "Timelike boundary Liouville theory," arXiv:hep-th/0301038.

[118] A. Maloney, A. Strominger and X. Yin, "S-brane thermodynamics," arXiv:hep-th/0302146.

[119] N. Lambert, H. Liu and J. Maldacena, "Closed strings from decaying D-branes," arXiv:hep-th/0303139.

[120] B. Chen, M. Li and F. L. Lin, "Gravitational radiation of rolling tachyon," JHEP **0211**, 050 (2002) [arXiv:hep-th/0209222].

[121] S. J. Rey and S. Sugimoto, "Rolling tachyon with electric and magnetic fields: T-duality approach," arXiv:hep-th/0301049.

[122] N. Moeller and B. Zwiebach, "Dynamics with infinitely many time derivatives and rolling tachyons," JHEP **0210**, 034 (2002) [arXiv:hep-th/0207107].

[123] S. Sugimoto and S. Terashima, "Tachyon matter in boundary string field theory," JHEP **0207**, 025 (2002) [arXiv:hep-th/0205085].

[124] J. A. Minahan, "Rolling the tachyon in super BSFT," JHEP **0207**, 030 (2002) [arXiv:hep-th/0205098].

[125] T. Okuda and S. Sugimoto, "Coupling of rolling tachyon to closed strings," Nucl. Phys. B **647**, 101 (2002) [arXiv:hep-th/0208196].

[126] J. Kluson, "Exact solutions in open bosonic string field theory and marginal deformation in CFT," arXiv:hep-th/0209255.

[127] I. Y. Aref'eva, L. V. Joukovskaya and A. S. Koshelev, "Time evolution in superstring field theory on non-BPS brane. I: Rolling tachyon and energy-momentum conservation," arXiv:hep-th/0301137.

[128] A. Ishida and S. Uehara, "Rolling down to D-brane and tachyon matter," JHEP **0302**, 050 (2003) [arXiv:hep-th/0301179].

[129] L. Rastelli, A. Sen and B. Zwiebach, "String field theory around the tachyon vacuum," Adv. Theor. Math. Phys. **5**, 353 (2002) [arXiv:hep-th/0012251].

[130] C. G. Callan, I. R. Klebanov, A. W. Ludwig and J. M. Maldacena, "Exact solution of a boundary conformal field theory," Nucl. Phys. B **422**, 417 (1994) [arXiv:hep-th/9402113].

[131] J. Polchinski and L. Thorlacius, "Free Fermion Representation Of A Boundary Conformal Field Theory," Phys. Rev. D **50**, 622 (1994) [arXiv:hep-th/9404008].

[132] M. W. Choptuik, "Universality And Scaling In Gravitational Collapse Of A Massless Scalar Field," Phys. Rev. Lett. **70**, 9 (1993).

[133] R. Gregory and R. Laflamme, "Black Strings And P-Branes Are Unstable," Phys. Rev. Lett. **70**, 2837 (1993) [arXiv:hep-th/9301052].

[134] I. R. Klebanov and L. Thorlacius, "The Size of p-Branes," Phys. Lett. B **371**, 51 (1996) [arXiv:hep-th/9510200].

[135] A. Hashimoto and I. R. Klebanov, "Decay of Excited D-branes," Phys. Lett. B **381**, 437 (1996) [arXiv:hep-th/9604065].

[136] P. Di Vecchia, M. Frau, I. Pesando, S. Sciuto, A. Lerda and R. Russo, "Classical p-branes from boundary state," Nucl. Phys. B **507**, 259 (1997) [arXiv:hep-th/9707068].

[137] E. Witten, "Noncommutative Geometry And String Field Theory," Nucl. Phys. B **268**, 253 (1986).

[138] J. A. Shapiro and C. B. Thorn, "Brst Invariant Transitions Between Closed And Open Strings," Phys. Rev. D **36**, 432 (1987).

[139] J. A. Shapiro and C. B. Thorn, "Closed String - Open String Transitions And Witten's String Field Theory," Phys. Lett. B **194**, 43 (1987).

[140] N. Drukker, "Closed string amplitudes from gauge fixed string field theory," arXiv:hep-th/0207266.

[141] G. T. Horowitz and K. Maeda, "Fate of the black string instability," Phys. Rev. Lett. **87**, 131301 (2001) [arXiv:hep-th/0105111].

[142] S. S. Gubser, "On non-uniform black branes," Class. Quant. Grav. **19**, 4825 (2002) [arXiv:hep-th/0110193].

[143] B. Kol, "Topology change in general relativity and the black-hole black-string transition," arXiv:hep-th/0206220.

[144] S. R. Coleman and E. Weinberg, "Radiative Corrections As The Origin Of Spontaneous Symmetry Breaking," Phys. Rev. D **7**, 1888 (1973).

[145] R. Gopakumar and C. Vafa, "On the gauge theory/geometry correspondence," Adv. Theor. Math. Phys. **3**, 1415 (1999) [arXiv:hep-th/9811131].

[146] P. Di Francesco, P. Ginsparg and J. Zinn-Justin, "2-D Gravity and random matrices," Phys. Rept. **254**, 1 (1995) [arXiv:hep-th/9306153].

[147] I. R. Klebanov, "String theory in two-dimensions," arXiv:hep-th/9108019.

[148] P. Ginsparg and G. W. Moore, arXiv:hep-th/9304011.

[149] J. Polchinski, arXiv:hep-th/9411028.

[150] J. McGreevy and H. Verlinde, "Strings from tachyons: The c = 1 matrix reloated," arXiv:hep-th/0304224.

[151] I. R. Klebanov, J. Maldacena and N. Seiberg, "D-brane decay in two-dimensional string theory," JHEP **0307**, 045 (2003) [arXiv:hep-th/0305159].

[152] A. B. Zamolodchikov and A. B. Zamolodchikov, "Liouville field theory on a pseudosphere," arXiv:hep-th/0101152.

[153] T. Takayanagi and N. Toumbas, "A matrix model dual of type 0B string theory in two dimensions," JHEP **0307**, 064 (2003) [arXiv:hep-th/0307083].

[154] M. R. Douglas, I. R. Klebanov, D. Kutasov, J. Maldacena, E. Martinec and N. Seiberg, "A new hat for the c = 1 matrix model," arXiv:hep-th/0307195.

[155] I. R. Klebanov, J. Maldacena and N. Seiberg, "Unitary and complex matrix models as 1-d type 0 strings," arXiv:hep-th/0309168.

[156] E. J. Martinec, arXiv:hep-th/0305148.

I. R. Klebanov, J. Maldacena and N. Seiberg, JHEP **0307**, 045 (2003) [arXiv:hep-th/0305159].

N. R. Constable and F. Larsen, JHEP **0306**, 017 (2003) [arXiv:hep-th/0305177].

[157] J. McGreevy, J. Teschner and H. Verlinde, arXiv:hep-th/0305194.

V. Schomerus, JHEP **0311**, 043 (2003) [arXiv:hep-th/0306026].

A. Sen, Phys. Rev. Lett. **91**, 181601 (2003) [arXiv:hep-th/0306137].

S. Y. Alexandrov, V. A. Kazakov and D. Kutasov, JHEP **0309**, 057 (2003) [arXiv:hep-th/0306177].

D. Gaiotto, N. Itzhaki and L. Rastelli, Phys. Lett. B **575**, 111 (2003) [arXiv:hep-th/0307221].

M. Gutperle and P. Kraus, arXiv:hep-th/0308047.

A. Sen, arXiv:hep-th/0308068.

J. McGreevy, S. Murthy and H. Verlinde, arXiv:hep-th/0308105.

A. Giveon, A. Konechny, A. Pakman and A. Sever, JHEP **0310**, 025 (2003) [arXiv:hep-th/0309056].

J. L. Karczmarek and A. Strominger, arXiv:hep-th/0309138.

S. Ribault and V. Schomerus, arXiv:hep-th/0310024.

S. Dasgupta and T. Dasgupta, arXiv:hep-th/0310106.

S. Alexandrov, arXiv:hep-th/0310135.

J. Gomis and A. Kapustin, arXiv:hep-th/0310195.

[158] V. Fateev, A. B. Zamolodchikov and A. B. Zamolodchikov, "Boundary Liouville field theory. I: Boundary state and boundary two-point function," arXiv:hep-th/0001012.

[159] J. Teschner, "Remarks on Liouville theory with boundary," arXiv:hep-th/0009138. "Liouville theory revisited," Class. Quant. Grav. **18**, R153 (2001) [arXiv:hep-th/0104158].

[160] M. Kontsevich, Commun. Math. Phys. **147**, 1 (1992).

[161] S. Kharchev, A. Marshakov, A. Mironov, A. Morozov and A. Zabrodin, "Unification of all string models with $C < 1$," Phys. Lett. B **275**, 311 (1992) [arXiv:hep-th/9111037].

M. Adler and P. van Moerbeke, "A Matrix Integral Solution To Two-Dimensional W(P) Gravity," Commun. Math. Phys. **147**, 25 (1992).

L. Bonora and C. S. Xiong, "The (Nth, Mth) Kdv Hierarchy And The Associated W Algebra," J. Math. Phys. **35**, 5781 (1994) [arXiv:hep-th/9311070].

B. Dubrovin, "Geometry Of 2-D Topological Field Theories," arXiv:hep-th/9407018.

A. Morozov, "Matrix models as integrable systems," arXiv:hep-th/9502091.

S. Kharchev, "Kadomtsev-Petviashvili hierarchy and generalized Kontsevich model," arXiv:hep-th/9810091.

[162] R. Penner, "Perturbative series and the moduli space of Riemann surfaces". J. Diff. Geom. **27** (1988) 35.

[163] R. Dijkgraaf, G. W. Moore and R. Plesser, "The Partition function of 2-D string theory," Nucl. Phys. B **394**, 356 (1993) [arXiv:hep-th/9208031].

C. Imbimbo and S. Mukhi, "The Topological matrix model of c = 1 string," Nucl. Phys. B **449**, 553 (1995) [arXiv:hep-th/9505127].

[164] S. Y. Alexandrov, V. A. Kazakov and I. K. Kostov, "2D string theory as normal matrix model," Nucl. Phys. B **667**, 90 (2003) [arXiv:hep-th/0302106].

[165] S. Mukhi, "Topological matrix models, Liouville matrix model and c = 1 string theory," arXiv:hep-th/0310287.

[166] "On The Structure Of The Topological Phase Of Two-Dimensional Gravity," Nucl. Phys. B **340**, 281 (1990).

[167] R. Dijkgraaf and E. Witten, "Mean Field Theory, Topological Field Theory, And Multimatrix Models," Nucl. Phys. B **342**, 486 (1990).

[168] E. Witten, "The N matrix model and gauged WZW models," Nucl. Phys. B **371**, 191 (1992).

[169] E. Witten, "Two-Dimensional Gravity And Intersection Theory On Moduli Space," Surveys Diff. Geom. **1**, 243 (1991).

[170] E. Witten, "Chern-Simons gauge theory as a string theory," Prog. Math. **133**, 637 (1995) [arXiv:hep-th/9207094].

[171] H. Ooguri and C. Vafa, "Worldsheet derivation of a large N duality," Nucl. Phys. B **641**, 3 (2002) [arXiv:hep-th/0205297].

[172] M. Aganagic, R. Dijkgraaf, A. Klemm, M. Marino and C. Vafa, "Topological strings and integrable hierarchies," arXiv:hep-th/0312085.

[173] R. Dijkgraaf and C. Vafa, Nucl. Phys. B **644**, 3 (2002) [arXiv:hep-th/0206255]. Nucl. Phys. B **644**, 21 (2002) [arXiv:hep-th/0207106]. M. Aganagic, A. Klemm, M. Marino and C. Vafa, arXiv:hep-th/0305132.

[174] A. Strominger, "Closed String Field Theory," Nucl. Phys. B **294**, 93 (1987).

[175] M. B. Green and J. Polchinski, Phys. Lett. B **335**, 377 (1994) [arXiv:hep-th/9406012].

[176] S. L. Shatashvili, "On field theory of open strings, tachyon condensation and closed strings," arXiv:hep-th/0105076.

[177] D. Gaiotto, N. Itzhaki and L. Rastelli, "Closed strings as imaginary D-branes," arXiv:hep-th/0304192.

[178] R. Gopakumar, "From free fields to AdS," arXiv:hep-th/0308184.

[179] N. Berkovits, H. Ooguri and C. Vafa, "On the worldsheet derivation of large N dualities for the superstring," arXiv:hep-th/0310118.

[180] R. Dijkgraaf, H. Verlinde and E. Verlinde, "Notes On Topological String Theory And 2-D Quantum Gravity," PUPT-1217 *Based on lectures given at Spring School on Strings and Quantum Gravity, Trieste, Italy, Apr 24 - May 2, 1990 and at Cargese Workshop on Random Surfaces, Quantum Gravity and Strings, Cargese, France, May 28 - Jun 1, 1990*

[181] R. Dijkgraaf, "Intersection theory, integrable hierarchies and topological field theory," arXiv:hep-th/9201003.

[182] Nathan Seiberg and David Shih, "Branes, Rings and Matrix Models in Minimal (Super)string Theory", hep-th/0312170.

[183] A. A. Belavin, A. M. Polyakov and A. B. Zamolodchikov, "Infinite Conformal Symmetry In Two-Dimensional Quantum Field Theory," Nucl. Phys. B **241**, 333 (1984).

[184] E. Brezin and V. A. Kazakov, "Exactly Solvable Field Theories Of Closed Strings," Phys. Lett. B **236**, 144 (1990).

M. R. Douglas and S. H. Shenker, "Strings In Less Than One-Dimension," Nucl. Phys. B **335**, 635 (1990).

D. J. Gross and A. A. Migdal, "Nonperturbative Two-Dimensional Quantum Gravity," Phys. Rev. Lett. **64**, 127 (1990).

[185] J. M. F. Labastida, M. Pernici and E. Witten, "Topological Gravity In Two-Dimensions," Nucl. Phys. B **310**, 611 (1988).

[186] D. Montano and J. Sonnenschein, "Topological Strings," Nucl. Phys. B **313**, 258 (1989).

[187] E. Verlinde and H. Verlinde, "A Solution Of Two-Dimensional Topological Quantum Gravity," Nucl. Phys. B **348**, 457 (1991).

[188] J.L. Harer, "The cohomology of the moduli space of curves", in "Theory of Moduli", Lecture Notes in Mathematics, Springer-Verlag (1988)

[189] K. Strebel, "Quadratic differentials", Springer-Verlag (1984).

[190] S. B. Giddings, E. J. Martinec and E. Witten, "Modular Invariance In String Field Theory," Phys. Lett. B **176**, 362 (1986).

[191] B. Zwiebach, "A Proof That Witten's Open String Theory Gives A Single Cover Of Moduli Space," Commun. Math. Phys. **142**, 193 (1991).

[192] N. Seiberg and S. H. Shenker, "A Note on background (in)dependence," Phys. Rev. D **45**, 4581 (1992) [arXiv:hep-th/9201017].

[193] T. Banks, M. R. Douglas, N. Seiberg and S. H. Shenker, "Microscopic And Macroscopic Loops In Nonperturbative Two-Dimensional Gravity," Phys. Lett. B **238**, 279 (1990).

G. W. Moore, N. Seiberg and M. Staudacher, "From loops to states in 2-D quantum gravity," Nucl. Phys. B **362**, 665 (1991).

G. W. Moore and N. Seiberg, "From loops to fields in 2-D quantum gravity," Int. J. Mod. Phys. A **7**, 2601 (1992).

[194] J. Distler, "2-D Quantum Gravity, Topological Field Theory And The Multicritical Matrix Models," Nucl. Phys. B **342**, 523 (1990).

[195] V. A. Kazakov, A. A. Migdal and I. K. Kostov, "Critical Properties Of Randomly Triangulated Planar Random Surfaces," Phys. Lett. B **157**, 295 (1985).

D. V. Boulatov, V. A. Kazakov, I. K. Kostov and A. A. Migdal, "Analytical And Numerical Study Of The Model Of Dynamically Triangulated Random Surfaces," Nucl. Phys. B **275**, 641 (1986).

D. V. Boulatov, V. A. Kazakov, I. K. Kostov and A. A. Migdal, "Analytical And Numerical Study Of The Model Of Dynamically Triangulated Nucl. Phys. B **275**, 641 (1986).

F. David, "Randomly Triangulated Surfaces In Two-Dimensions," Phys. Lett. B **159**, 303 (1985).

I. K. Kostov and M. L. Mehta, "Random Surfaces Of Arbitrary Genus: Exact Results For D = 0 And -2 Dimensions," Phys. Lett. B **189**, 118 (1987).

[196] I. R. Klebanov and R. B. Wilkinson, "Matrix Model In Two-Dimensions And Its Effective Field Theory," Phys. Lett. B **251**, 379 (1990).

[197] I. R. Klebanov and R. B. Wilkinson, "Critical Potentials And Correlation Functions In The Minus Two-Dimensional Matrix Model," Nucl. Phys. B **354**, 475 (1991).

[198] J. D. Edwards and I. R. Klebanov, "Macroscopic boundaries and the wave function of the universe in the c = -2 matrix model," Mod. Phys. Lett. A **6**, 2901 (1991).

[199] J. C. Plefka, "Supersymmetric Generalizations of Matrix Models," arXiv:hep-th/9601041.

[200] H. G. Kausch, "Curiosities at c=-2," arXiv:hep-th/9510149.

[201] V. Gurarie, "Logarithmic operators in conformal field theory," Nucl. Phys. B **410**, 535 (1993) [arXiv:hep-th/9303160].

[202] M. A. I. Flohr, "On Fusion Rules in Logarithmic Conformal Field Theories," Int. J. Mod. Phys. A **12**, 1943 (1997) [arXiv:hep-th/9605151].

M. R. Gaberdiel and H. G. Kausch, "A rational logarithmic conformal field theory," Phys. Lett. B **386**, 131 (1996) [arXiv:hep-th/9606050].

H. G. Kausch, "Symplectic fermions," Nucl. Phys. B **583**, 513 (2000) [arXiv:hep-th/0003029].

[203] J. Distler and P. Nelson, "Topological Couplings And Contact Terms In 2-D Field Theory," Commun. Math. Phys. **138**, 273 (1991).

[204] J. Distler and P. Nelson, "Semirigid supergravity," Phys. Rev. Lett. **66**, 1955 (1991).

[205] J. Distler and P. Nelson, "The Dilaton equation in semirigid string theory," Nucl. Phys. B **366**, 255 (1991).

[206] C. M. Becchi, R. Collina and C. Imbimbo, "On the semirelative condition for closed (topological) strings," Phys. Lett. B **322**, 79 (1994) [arXiv:hep-th/9311097]. "A functional and Lagrangian formulation of two dimensional topological gravity," arXiv:hep-th/9406096.

C. M. Becchi and C. Imbimbo, "Gribov horizon, contact terms and Čech- De Rham cohomology in 2D topological gravity," Nucl. Phys. B **462**, 571 (1996) [arXiv:hep-th/9510003].

[207] S. Cordes, G. W. Moore and S. Ramgoolam, "Lectures on 2-d Yang-Mills theory, equivariant cohomology and topological field theories," Nucl. Phys. Proc. Suppl. **41**, 184 (1995) [arXiv:hep-th/9411210].

[208] M. Weis, "Topological aspects of quantum gravity," arXiv:hep-th/9806179.

[209] I. K. Kostov, B. Ponsot and D. Serban, "Boundary Liouville theory and 2D quantum gravity," arXiv:hep-th/0307189.

[210] L. Rastelli and B. Zwiebach, "Tachyon potentials, star products and universality," JHEP **0109**, 038 (2001) [arXiv:hep-th/0006240].

[211] C. B. Thorn, "String Field Theory," Phys. Rept. **175**, 1 (1989).

W. Taylor and B. Zwiebach, "D-branes, tachyons, and string field theory," arXiv:hep-th/0311017.

[212] M. Bochicchio, "String Field Theory In The Siegel Gauge," Phys. Lett. B **188**, 330 (1987).

C. B. Thorn, "Perturbation Theory For Quantized String Fields," Nucl. Phys. B **287**, 61 (1987).

[213] E. Witten, "On the Kontsevich model and other models of two-dimensional gravity," IASSNS-HEP-91-24

[214] C. Itzykson and J. B. Zuber, "Combinatorics Of The Modular Group. 2. The Kontsevich Integrals," Int. J. Mod. Phys. A **7**, 5661 (1992) [arXiv:hep-th/9201001].

[215] R. Dijkgraaf, H. Verlinde and E. Verlinde, "Loop Equations And Virasoro Constraints In Nonperturbative 2-D Quantum Nucl. Phys. B **348**, 435 (1991).

[216] J. A. Shapiro and C. B. Thorn, Phys. Rev. D **36**, 432 (1987). J. A. Shapiro and C. B. Thorn, Phys. Lett. B **194**, 43 (1987). B. Zwiebach, Mod. Phys. Lett. A **7**, 1079 (1992) [arXiv:hep-th/9202015]. A. Hashimoto and N. Itzhaki, JHEP **0201**, 028 (2002) [arXiv:hep-th/0111092]. D. Gaiotto, L. Rastelli, A. Sen and B. Zwiebach, Adv. Theor. Math. Phys. **6**, 403 (2003) [arXiv:hep-th/0111129].

[217] E. Witten, "Overview of K-theory applied to strings," Int. J. Mod. Phys. A **16**, 693 (2001) [arXiv:hep-th/0007175].

[218] A. Sen, "Open-closed duality: Lessons from matrix model," arXiv:hep-th/0308068.

[219] J. Teschner, "On boundary perturbations in Liouville theory and brane dynamics in noncritical string theories," arXiv:hep-th/0308140.